

# **CORROSION INHIBITION EXPLORATION OF SYNTHESIZED CARBOXYLIC ACID AND AMINO ESTERS ON SELECTED METALS IN ACID MEDIUM**

*By*

TSHIMANGADZO NESANE  
(11627022)

Submitted in fulfilment of the requirements for the degree of  
Master of Science

in the  
Department of Chemistry

School of Mathematics and Natural Sciences  
University of Venda  
South Africa

*Supervisor*

Dr L.C. MURULANA

*Co-Supervisor*

Dr S.S. MNYAKENI-MOLEELE

## DECLARATION

---

I hereby declare that the work in this dissertation is my own and was done under the supervision of Dr L.C Murulana and Dr S.S Moleele as my co-supervisor. The information derived from literature have been duly acknowledged in text and a list of references provided. This work is being submitted for the degree of Master of Science in Chemistry at the University of Venda and has not been submitted before for any degree or examination at any other university.

Full Names: Tshimangadzo Nesane      Date: January 2020.....

Signature: .....

## DEDICATION

---

This dissertation is dedicated to my mother, **Alugumi Tshivhundo**, for her endless love and for seeing it that I get the best education and life possible.

## TABLE OF CONTENTS

---

NO	CONTENTS	PAGE NO
	Acknowledgements	i
	Abstract	ii
	List of Abbreviations	iv
	List of figures	vi
	List of tables	xvi
1	INTRODUCTION	1
1.1	Introduction	2
1.2	Problem Statement	6
1.3	Justification of the Study	6
1.4	Aims and Objectives of the Study	8
2	LITERATURE REVIEW	9
2.1	Definition of Corrosion	10
2.1.1	Theories and Basic Principles of Corrosion	11
2.1.1.1	Local Cell Theory	11
2.1.1.2	Wagner and Traud Theory	12
2.1.2	Classification of Corrosion	14
2.1.3	The Corrosion Cell	15
2.1.4	Different Forms of Corrosion	16
2.1.5	Thermodynamics and Kinetics of Corrosion	26
2.1.6	The Rate of Corrosion	30
2.1.7	Factors Affecting the Rate of Corrosion	30
2.1.8	Consequences of Corrosion	35
2.1.9	Cost Implication of Corrosion	36
2.2	Corrosion of Metals	38

2.2.1	Aluminium (Al)	38
2.2.2	Mild Steel (MS)	40
2.2.3	Zinc	41
2.3	Corrosion Prevention Methods	44
2.4	Corrosion Inhibitors and Inhibition Mechanism	48
2.4.1	Definition of Corrosion Inhibitors	48
2.4.2	Mechanism of Corrosion Inhibition	49
2.4.3	Adsorption and its Influence on Corrosion Inhibition	50
2.4.4	Classification of Corrosion Inhibitors	54
2.5	Environmentally friendly (green) corrosion inhibitors	59
2.6	Carboxylic Acids and Amino Esters	60
2.7	Carboxylic Acids and Amino Esters as Corrosion Inhibitors	61
2.8	Corrosion Monitoring Techniques	66
2.8.1	Introduction	66
2.6.2	Non-Electrochemical Methods	66
2.6.3	Electrochemical Methods	68
3	EXPERIMENTAL	72
3.1	Chemicals and Materials	73
3.2	Synthesis of Inhibitors	74
3.2.1	Synthesis of N-benzoyl-2-aminobutyric acid (2-NBABA)	74
3.2.2	Synthesis of 4-(benzyloxy)-4-oxobutan-1-aminium methylbenzenesulfonate (4-BOBAMS)	4- 74
3.2.3	Synthesis of 1-(benzyloxy)-1-oxopropan-2-aminium methylbenzenesulfonate (1-BOPAMS)	4- 74
3.3	Nuclear Magnetic Resonance (NMR) Spectroscopy	75
3.4	Metal Specimen	76
3.5	Preparation of Solutions	77
3.6	Electrochemical Techniques	77
3.6.1	Electrochemical Impedance (EIS)	77

3.6.2	Potentiodynamic Polarization (PDP)	78
3.7	Fourier Transform Infrared Spectroscopy (FT-IR)	78
3.8	Gravimetric Analysis	79
4	RESULTS AND DISCUSSION	81
4.1	Characterization of Inhibitors	82
4.1.1	Characterization of 2-NBABA	82
4.1.2	Characterization of 4-BOBAMS	88
4.1.3	Characterization of 1-BOPAMS	94
4.2	Mild Steel	100
4.2.1	Effect of Inhibitor Concentration	100
4.2.2	Effect of Temperature	107
4.2.3	Adsorption Isotherm and Thermodynamic Parameters	116
4.2.4	Adsorption Film Analysis	128
4.2.5	Potentiodynamic Polarization (PDP)	131
4.2.6	Electrochemical Impedance Spectroscopy (EIS)	135
4.2.7	Proposed Inhibition Mechanism on MS	144
4.3	Aluminium	146
4.3.1	Effect of Inhibitor Concentration	146
4.3.2	Effect of Temperature	153
4.3.3	Adsorption Isotherm and Thermodynamic Parameters	161
4.3.4	Adsorption Film Analysis	173
4.3.5	Potentiodynamic Polarization (PDP)	176
4.3.6	Electrochemical Impedance Spectroscopy (EIS)	180
4.3.7	Proposed Inhibition Mechanism on Al	188

4.4	Comparison of the Corrosion Inhibition Performance of the Synthesized Carboxylic Acid and Amino Esters on Al and MS	189
5	CONCLUSIONS	190
5.1	Conclusions	191
5.2	Recommendations for Future Studies	192
	REFERENCES	193

## ACKNOWLEDGEMENTS

---

First and foremost, with humility and reverence, I would like to thank the almighty God for the protection and guidance He bestowed on me throughout my study.

It can be an overwhelming, frustrating and isolating experience to pursue any project and would not be possible without the support and encouragement of several individuals. I take immense pleasure and a profound sense of gratitude to express my deepest, most heartfelt and sincere indebtedness to my supervisor and mentor, **Dr L.C. Murulana**, for his guidance, valuable suggestions, continuous moral support, constructive criticism and careful but thorough reading of all my writing in this project. With your in-depth knowledge and insight into the field of research, you were always there to assist me in difficult moments. You went far beyond the duty of a supervisor with your unwavering support, and under your par excellence, you made this project to become a success. Thank you for making sure that I was able to run all the techniques required for this project. You are one of the rare mentors and supervisors that any student would be grateful and wishes to have.

I want to take this opportunity to express my sincere appreciation and gratitude to my co-supervisor, **Dr S.S. Mnyakeni-Moleele**, for his knowledge of organic chemistry. Without you, this project would not have been possible, and your advice in the selection and synthesis of the compounds utilized in this study resulted in its successful completion. You were always available when I was stuck during the synthesis part. I value your advice and the patience that you had with me and will never forget your kindness. Your help and contribution with the analysis of the compound is invaluable. You are the best co-supervisor I could have asked for.

I want to thank **Mr Tsoeunyane Mofu George** from the University of Johannesburg for assisting me with the electrochemical impedance spectroscopy analysis. I am thankful for taking your time and showing me how the instrument works.

I want to thank the **NRF and SASOL Foundation** for funding me throughout the two years of this research. Your funding went a long way in helping me to complete my studies without any financial concerns.

Lastly, I express my thanks to the Corrosion Inhibition Research Group for their encouragements and advice. You guys are the best.



## ABSTRACT

---

In this study, carboxylic acid and two ionic liquids-based amino esters were used as corrosion inhibitors for aluminium and mild steel. These compounds were selected because they are said to be non-toxic and environmentally friendly. The non-toxicity of these compounds is essential due to the increasing implementation of strict environmental regulations. The investigated compounds as corrosion inhibitors in this study include a carboxylic acid, namely, N-benzoyl-2-aminobutyric acid (2-NBABA), and two amino esters which are 1-(benzyloxy)-1-oxopropan-2-aminium 4-methylbenzenesulfonate (1-BOPAMS) and 4-(benzyloxy)-4-oxobutan-1-aminium 4-methylbenzenesulfonate (4-BOBAMS) for aluminium and mild steel corrosion in 1.0 M hydrochloric solution (HCl) at 303-333 K. The three compounds were synthesized and characterized by spectroscopic methods (FT-IR,  $^{13}\text{C}$ -NMR and  $^1\text{H}$ -NMR). Their anti-corrosive properties, inhibition mechanism, inhibitor-metal adsorption behaviour and corrosion inhibition efficiency were investigated by employing several techniques such as the gravimetric, potentiodynamic polarization (PDP) and electrochemical impedance spectroscopy (EIS). Fourier transform infrared spectroscopy (FT-IR) was used to investigate the functional group responsible for the adsorption/desorption process of the inhibitor molecules and those that disappeared or formed on the surfaces of mild steel and aluminium. Gravimetric analysis exhibited an increase in the inhibition efficiency as the concentrations of the inhibitors were increased for all the three inhibitors studied. Amongst the several isotherms plotted, Langmuir adsorption isotherm was found to be the best-fit isotherm for the three compounds on the metal surfaces. The isotherm provided a clear indication on the mechanism of adsorption which was mixed-type adsorption for both aluminium and mild steel. The impedance result showed an increase in the  $R_{ct}$  values as the concentration of the inhibitors was raised, resulting in an increase in the surface coverage by the inhibitor molecules. The adsorption of the inhibitor molecules on the aluminium and mild steel surface led to the decrease in the double-layer capacitance ( $C_{dl}$ ) as the molecules of the inhibitors replaced the water molecules at the metal/solution interface reducing the local dielectric constant while increasing the double layer thickness. The data gathered showed that the adsorption of the three inhibitors prevented the dissolution of the mild steel and aluminium in 1.0 M HCl without altering the corrosion mechanism of the metals. The PDP results obtained indicated that the three inhibitors affected both the anodic and cathodic half-reactions to a similar extent. The anodic and cathodic Tafel curves were both affected by the introduction of the inhibitors which revealed that the

investigated inhibitors act as mixed-type corrosion inhibitors. Fourier transform infrared spectroscopy studies showed that the corrosion process was reduced due to the interaction of the three inhibitors with mild steel and aluminium resulting in the formation of a Fe-inhibitor and Al-inhibitor complexes.

## LIST OF ABBREVIATIONS

---

<b>1-BOPAMS</b>	1-(benzyloxy)-1-oxopropan-2-aminium 4-methylbenzenesulfonate
<b>2-NBABA</b>	N-benzoyl-2-aminobutyric acid
<b>4-BOBAMS</b>	4-(benzyloxy)-4-oxobutan-1-aminium 4-methylbenzenesulfonate
<b>AC</b>	Alternating current
<b>Al</b>	Aluminum
<b>BSE</b>	Backscattered Electrons
<b>C<sub>dl</sub></b>	Double Layer Capacitance
<b>CorrISA</b>	Corrosion Institute of Southern Africa
<b>CPE</b>	Constant Phase Element
<b>DO</b>	Dissolved Oxygen
<b>E</b>	Electromotive force
<b>EIS</b>	Electrochemical Impedance Spectroscopy
<b>FHWA</b>	Federal Highway Administration
<b>FRA</b>	Frequency Response Analyzer
<b>FT-IR</b>	Fourier Transform Infrared Spectroscopy
<b>GDP</b>	Gross Domestic Product
<b>HCl</b>	Hydrochloric Acid
<b>IBP</b>	Intermediate Bode Plots
<b>IE</b>	Inhibition Efficiency
<b>ILs</b>	Ionic Liquids
<b>IR</b>	Infrared radiator
<b>IUPAC</b>	International Union of Pure and Applied Chemists
<b>LPR</b>	Linear Polarization Resistance
<b>MIC</b>	Microbial Corrosion
<b>MINTEK</b>	Council for Mineral Technology

<b>MS</b>	Mild Steel
<b>NACE</b>	National Association of Corrosion Engineers
<b>OCP</b>	Open Circuit Potential
<b>PCE</b>	Platinum Counter Electrode
<b>PDP</b>	Potentiodynamic Polarization
<b>PGSTAT302N</b>	Metrohm Autolab Potentiostat/Galvanostat
<b>PTSA</b>	p-toluenesulfonic acid monohydrate
<b><math>R_{ct}</math></b>	Charge Transfer Resistance
<b>RE</b>	Reference Electrode
<b><math>R_p</math></b>	Polarization Resistance
<b><math>R_s</math></b>	Solution Resistance
<b>SA</b>	South Africa
<b>SCC</b>	Stress Corrosion Cracking
<b>SCE</b>	Saturated Calomel Electrode
<b>WE</b>	Working Electrode
<b>SE</b>	Secondary Electrons
<b>SEM</b>	Scanning Electron Microscopy
<b>THF</b>	Tetrahydrofuran
<b>TME</b>	2-thiophenecarboxylic acid methyl ester
<b>USA</b>	United States of America
<b>VCI</b>	Volatile Corrosion Inhibitors
<b>WCO</b>	World Corrosion Organization
<b>Zn</b>	Zinc

## LIST OF FIGURES

No	DESCRIPTION	PAGE No
1.1	Pipeline corrosion failure (a) and a zoom in on the defect area (b)	3
1.2	Acid pickling in industries (a) and the transformation of the surface of steel before (b) after (a) pickling	4
2.1	Flow diagram showing the processes involved in metallurgy	10
2.2	Heterogeneous metal surface showing different types of imperfections	11
2.3	The reactions occurring during the corrosion of carbon steel	12
2.4	A schematic example of an electrochemical cell showing principles of corrosion	15
2.5	Atmospheric uniform corrosion attack of a steel bridge (a) and a pipeline (b) located on a concrete pier above the ocean water as highlighted	16
2.6	Intergranular corrosion on a stainless-steel nut	17
2.7	Dezincification of a bolt (a) in brass and high zinc content brass (b)	18
2.8	Crevice corrosion of stainless-steel flange and the mechanism of attack	18
2.9	Metals attacked by galvanic corrosion	19
2.10	Microbial induced corrosion in the pipeline (a) and rod-shaped Pseudomonas (b) bacteria	20
2.11	Illustration of the filament nature (a) and a worm or tentacles path (b) emanating from the point of attack of filiform corrosion	21
2.12	Erosion-corrosion of 115-mm API L-80 oil well tubing	22
2.13	Intergranular (a) stress-corrosion cracking in brass and trans-granular (b) stress-corrosion cracking in steel	23
2.14	Fretting corrosion on roller bearing race (a) and a sketch (b) illustrating the mechanism of attack	24
2.15	Diagram depicting the process occurring during pitting corrosion	25

2.16	The effect of oxygen concentration on the corrosion of low carbon steel in tap water at different temperatures	32
2.17	The effect of temperature on the corrosion rate of low carbon steel in tap water	33
2.18	Flow diagram illustrating the cost effects of corrosion	37
2.19	A schematic electrochemical mechanism of Al alloy corrosion	39
2.20	Schematic diagram of the corrosion process of the reinforcing steel rebar in concrete	41
2.21	Diagram of the zinc corrosion cycle in HCl	43
2.22	A poor (a) and good designs (b), for heating solutions	45
2.23	Organic inhibitor interaction with a metallic substrate in an acidic solution	50
2.24	Functional groups of amines (a) and carboxylates (b) adsorbed on the surface of the steel; the R-group may be a methyl or ethyl	62
2.25	Chemical (a) and physical (b) adsorption mechanism of amino acid	63
2.26	Typical electrochemical equivalent circuit commonly used to analyse EIS measurements in a corroding system	69
2.27	Evans polarization diagrams: (a) anodic control (b) cathodic control (c) mixed control	71
3.1	Synthetic schemes of 2-NBABA, 4-BOBAMS and 1-BOPAMS	75
3.2	Schematic illustration for the instrumentation used in the characterization of the inhibitors and the evaluation of corrosion of Al and MS metals	80
4.1	FT-IR spectrum of 2-NBABA compound	83
4.2	<sup>1</sup> H-NMR spectrum of 2-NBABA	83
4.3	<sup>1</sup> H-NMR first expansion spectrum of 2-NBABA	84

4.4	<sup>1</sup> H-NMR second expansion spectrum of 2-NBABA	85
4.5	<sup>1</sup> H-NMR third expansion spectrum of 2-NBABA	86
4.6	<sup>13</sup> C-NMR spectrum of 2-NBABA	87
4.7	FT-IR spectrum of 4-BOBAMS compound	89
4.8	<sup>1</sup> H-NMR spectrum of 4-BOBAMS	89
4.9	<sup>1</sup> H-NMR first expansion spectrum of 4-BOBAMS	90
4.10	<sup>1</sup> H-NMR second expansion spectrum of 4-BOBAMS	91
4.11	<sup>13</sup> C-NMR spectrum of 4-BOBAMS	92
4.12	<sup>13</sup> C-NMR spectrum expansion of 4-BOBAMS	93
4.13	FT-IR spectrum of 1-BOPAMS compound	95
4.14	<sup>1</sup> H-NMR spectrum of 1-BOPAMS	95
4.15	<sup>1</sup> H-NMR first expansion spectrum of 1-BOPAMS	96
4.16	<sup>1</sup> H-NMR second expansion spectrum of 1-BOPAMS	97
4.17	<sup>13</sup> C-NMR spectrum of 1-BOPAMS	98
4.18	<sup>13</sup> C-NMR spectrum expansion of 1-BOPAMS	99
4.19	The variations of the %IE with various concentrations of 2-NBABA, 1-BOPAMS and 4-BOBAMS corrosion inhibitors at 303 K	101
4.20	The variations of the %IE with various concentrations of 2-NBABA, 1-BOPAMS and 4-BOBAMS corrosion inhibitors at 313 K	102
4.21	The variations of the %IE with various concentrations of 2-NBABA, 1-BOPAMS and 4-BOBAMS corrosion inhibitors at 323 K	102
4.22	The variations of the %IE with various concentrations of 2-NBABA, 1-BOPAMS and 4-BOBAMS corrosion inhibitors at 333 K	103
4.23	Variation of C <sub>R</sub> of MS as a function of temperature for 1-BOPAMS	105
4.24	Variation of C <sub>R</sub> of MS as a function of temperature for 4-BOBAMS	105

4.25	Variation of $C_R$ of MS as a function of temperature for 2-NBABA	106
4.26	The variation of %IE with temperature for MS corrosion in 1.0 M HCl in the presence of a various concentrations of 1-BOPAMS	110
4.27	The variation of %IE with temperature for MS corrosion in 1.0 M HCl in the presence of a various concentrations of 4-BOBAMS.	110
4.28	The variation of %IE with temperature for MS corrosion in 1.0 M HCl in the presence of a various concentrations of 2-NBABA.	111
4.29	Arrhenius plots for the corrosion of MS in 1.0 M HCl in the absence and presence of different concentrations of 1-BOPAMS	111
4.30	Arrhenius plots for the corrosion of MS in 1.0 M HCl in the absence and presence of different concentrations of 4-BOBAMS	112
4.31	Arrhenius plots for the corrosion of MS in 1.0 M HCl in the absence and presence of different concentrations of 2-NBAB	112
4.32	The variation of the $E_a$ with various concentration of 2-NBABA, 1-BOPAMS and 4-BOBAMS corrosion inhibitors for MS	113
4.33	Transition state plots for the corrosion of MS in 1.0 M HCl in the absence and presence of different concentrations of 1-BOPAMS	114
4.34	Transition state plots for the corrosion of MS in 1.0 M HCl in the absence and presence of different concentrations of 4-BOBAMS	115
4.35	Transition state plots for the corrosion of MS in 1.0 M HCl in the absence and presence of different concentrations of 2-NBABA	115
4.36	Langmuir adsorption isotherm plot for the adsorption of different concentrations of 1-BOPAMS on the surface of MS in 1.0 M HCl at different temperatures	121
4.37	Langmuir adsorption isotherm plot for the adsorption of different concentrations of 2-NBABA on the surface of MS in 1.0 M HCl at different temperatures.	122



4.38	Langmuir adsorption isotherm plot for the adsorption of different concentrations of 4-BOBAMS on the surface of MS in 1.0 M HCl at different temperatures	122
4.39	Temkin adsorption isotherm plot for the adsorption of different concentrations of 1-BOPAMS on the surface of MS in 1.0 M HCl at different temperatures	123
4.40	Temkin adsorption isotherm plot for the adsorption of different concentrations of 2-NBABA on the surface of MS in 1.0 M HCl at different temperatures	123
4.41	Temkin adsorption isotherm plot for the adsorption of different concentrations of 4-BOBAMS on the surface of MS in 1.0 M HCl at different temperatures	124
4.42	Freundlich adsorption isotherm plot for the adsorption of different concentrations of 1-BOPAMS on the surface of MS in 1.0 M HCl at different temperatures	124
4.43	Freundlich adsorption isotherm plot for the adsorption of different concentrations of 2-NBABA on the surface of MS in 1.0 M HCl at different temperatures	125
4.44	Freundlich adsorption isotherm plot for the adsorption of different concentrations of 4-BOBAMS on the surface of MS in 1.0 M HCl at different temperatures	125
4.45	EL-Awady adsorption isotherm plot for the adsorption of different concentrations of 1-BOPAMS on the surface of MS in 1.0 M HCl at different temperatures	126
4.46	EL-Awady adsorption isotherm plot for the adsorption of different concentrations of 2-NBABA on the surface of MS in 1.0 M HCl at different temperatures	126

4.47	EL-Awady adsorption isotherm plot for the adsorption of different concentrations of 4-BOBAMS on the surface of MS in 1.0 M HCl at different temperatures	127
4.48	FT-IR spectra comparison of the frequencies for the pure compound and adsorption films formed on the MS in 1.0 M HCl by 2-NBABA corrosion inhibitor	129
4.49	FT-IR spectra comparison of the frequencies for the pure compound and adsorption films formed on the MS in 1.0 M HCl by 1-BOPAMS corrosion inhibitor	129
4.50	FT-IR spectra comparison of the frequencies for the pure compound and adsorption films formed on the MS in 1.0 M HCl by 4-BOBAMS corrosion inhibitor	130
4.51	Tafel plots for MS in 1.0 M HCl in the absence and presence of different concentrations of 2-NBABA inhibitor compound	132
4.52	Tafel plots for MS in 1.0 M HCl in the absence and presence of different concentrations of 1-BOPAMS inhibitor compound	133
4.53	Tafel plots for MS in 1.0 M HCl in the absence and presence of different concentrations of 4-BOBAMS inhibitor compound	133
4.54	Equivalent circuit used to fit the impedance spectra obtained for MS corrosion in 1.0 M HCl in the absence and presence of 2-NBABA 4-BOBAMS and 1-BOPAMS	135
4.55	Nyquist plots for MS in 1.0 M HCl in the absence and presence of different concentrations of 2-NBABA	137
4.56	Nyquist plots for MS in 1.0 M HCl in the absence and presence of different concentrations of 1-BOPAMS	137
4.57	Nyquist plots for MS in 1.0 M HCl in the absence and presence of different concentrations of 4-BOBAMS	138
4.58	Theoretical Bode plots of good, intermediate, poor quality coating	140

4.59	Bode diagrams of the impedance for MS in 1.0 M HCl without and with different concentrations of 2-NBABA at 303 K	141
4.60	Bode diagrams of the impedance for MS in 1.0 M HCl without and with different concentrations of 1-BOPAMS at 303 K	142
4.61	Bode diagrams of the impedance for MS in 1.0 M HCl without and with different concentrations of 4-BOBAMS at 303 K	143
4.62	The variations of the %IE with various concentrations of 2-NBABA, 1-BOPAMS and 4-BOBAMS corrosion inhibitors at 303 K	149
4.63	The variations of the %IE with various concentrations of 2-NBABA, 1-BOPAMS and 4-BOBAMS corrosion inhibitors at 313 K	149
4.64	The variations of the %IE with various concentrations of 2-NBABA, 1-BOPAMS and 4-BOBAMS corrosion inhibitors at 323 K	150
4.65	The variations of the %IE with various concentrations of 2-NBABA, 1-BOPAMS and 4-BOBAMS corrosion inhibitors at 333 K	150
4.66	Variation of $C_R$ of Al as a function of temperature for 1-BOPAMS	152
4.67	Variation of $C_R$ of Al as a function of temperature for 4-BOBAMS	152
4.68	Variation of $C_R$ of Al as a function of temperature for 2-NBABA	153
4.69	The variation of %IE with temperature for Al corrosion in 1.0 M HCl in the presence of a various concentrations of 1-BOPAMS	155
4.70	The variation of %IE with temperature for Al corrosion in 1.0 M HCl in the presence of a various concentrations of 4-BOBAMS	156
4.71	The variation of %IE with temperature for Al corrosion in 1.0 M HCl in the presence of a various concentrations of 2-NBABA	156
4.72	Arrhenius plots for the corrosion of Al in 1.0 M HCl in the absence and presence of different concentrations of 1-BOPAMS	157
4.73	Arrhenius plots for the corrosion of Al in 1.0 M HCl in the absence and presence of different concentrations of 4-BOBAMS	157

4.74	Arrhenius plots for the corrosion of Al in 1.0 M HCl in the absence and presence of different concentrations of 2-NBABA	158
4.75	The variation of the $E_a$ with various concentration of 2-NBABA, 1-BOPAMS and 4-BOBAMS corrosion inhibitors for Al	158
4.76	Transition state plots for the corrosion of Al in 1.0 M HCl in the absence and presence of different concentrations of 1-BOPAMS	161
4.77	Transition state plots for the corrosion of Al in 1.0 M HCl in the absence and presence of different concentrations of 4-BOBAMS	161
4.78	Transition state plots for the corrosion of Al in 1.0 M HCl in the absence and presence of different concentrations of 2-NBABA	162
4.79	Langmuir adsorption isotherm plot for the adsorption of different concentrations of 1-BOPAMS on the surface of Al in 1.0 M HCl at different temperatures	167
4.80	Langmuir adsorption isotherm plot for the adsorption of different concentrations of 4-BOBAMS on the surface of Al in 1.0 M HCl at different temperatures	167
4.81	Langmuir adsorption isotherm plot for the adsorption of different concentrations of 2-NBABA on the surface of Al in 1.0 M HCl at different temperatures	168
4.82	Temkin adsorption isotherm plot for the adsorption of different concentrations of 1-BOPAMS on the surface of Al in 1.0 M HCl at different temperatures	168
4.83	Temkin adsorption isotherm plot for the adsorption of different concentrations of 4-BOBAMS on the surface of Al in 1.0 M HCl at different temperatures	169
4.84	Temkin adsorption isotherm plot for the adsorption of different concentrations of 2-NBABA on the surface of Al in 1.0 M HCl at different temperatures	169

4.85	Freundlich adsorption isotherm plot for the adsorption of different concentrations of 1-BOPAMS on the surface of Al in 1.0 M HCl at different temperatures	170
4.86	Freundlich adsorption isotherm plot for the adsorption of different concentrations of 4-BOBAMS on the surface of Al in 1.0 M HCl at different temperatures	170
4.87	Freundlich adsorption isotherm plot for the adsorption of different concentrations of 2-NBABA on the surface of Al in 1.0 M HCl at different temperatures	171
4.88	EL-Awady adsorption isotherm plot for the adsorption of different concentrations of 1-BOPAMS on the surface of Al in 1.0 M HCl at different temperatures	171
4.89	EL-Awady adsorption isotherm plot for the adsorption of different concentrations of 4-BOBAMS on the surface of Al in 1.0 M HCl at different temperatures	172
4.90	EL-Awady adsorption isotherm plot for the adsorption of different concentrations of 2-NBABA on the surface of Al in 1.0 M HCl at different temperatures	172
4.91	FT-IR spectra comparison of the frequencies for the pure compound and adsorption films formed on the Al in 1.0 M HCl by 2-NBABA corrosion inhibitor	175
4.92	FT-IR spectra comparison of the frequencies for the pure compound and adsorption films formed on the Al in 1.0 M HCl by 1-BOPAMS corrosion inhibitor	175
4.93	FT-IR spectra comparison of the frequencies for the pure compound and adsorption films formed on the Al in 1.0 M HCl by 4-BOBAMS corrosion inhibitor	176
4.94	Tafel plots for Al in 1.0 M HCl in the absence and presence of different concentrations of 2-NBABA inhibitor compound	178

4.95	Tafel plots for Al in 1.0 M HCl in the absence and presence of different concentrations of 1-BOPAMS inhibitor compound	178
4.96	Tafel plots for Al in 1.0 M HCl in the absence and presence of different concentrations of 4-BOBAMS inhibitor compound	179
4.97	Equivalent circuit used to fit the impedance spectra obtained for Al corrosion in 1.0 M HCl in the absence and presence of 2-NBABA 4-BOBAMS and 1-BOPAMS	182
4.98	Nyquist plots for Al in 1.0 M HCl in the absence and presence of different concentrations of 2-NBABA	183
4.99	Nyquist plots for Al in 1.0 M HCl in the absence and presence of different concentrations of 1-BOPAMS	183
4.100	Nyquist plots for Al in 1.0 M HCl in the absence and presence of different concentrations of 4-BOBAMS	184
4.101	Bode diagrams of the impedance for Al in 1.0 M HCl without and with different concentrations of 2-NBABA at 303 K	186
4.102	Bode diagrams of the impedance for Al in 1.0 M HCl without and with different concentrations of 1-BOPAMS at 303 K	187
4.103	Bode diagrams of the impedance for Al in 1.0 M HCl without and with different concentrations of 4-BOBAMS at 303 K	188

## LIST OF TABLES

No	DESCRIPTION	PAGE No
3.1	The abbreviations, chemical formula and molecular structures of the carboxylic acids and amino ester compounds	76
4.1	Weight loss measurements of MS in 1.0 M HCl containing various concentrations of 1-BOPAMS, 4-BOBAMS and 2-NBABA at different temperatures	104
4.2	Kinetic and activation parameters (derived from the Arrhenius and transition-states plots) for MS in 1.0 M HCl in the absence and presence of various concentrations of 2-NBABA 4-BOBAMS and 1-BOPAMS	109
4.3	Thermodynamic and adsorption parameters (Langmuir adsorption isotherms) for Al in 1.0 M HCl at various temperatures for 2-NBABA, 1-BOPAMS and 4-BOBAMS	120
4.4	Thermodynamic and adsorption parameters obtained from various isotherms for MS in 1.0 M HCl at various temperatures for the utilized corrosion inhibitors	127
4.5	Potentiodynamic polarization (PDP) parameters such as corrosion potential ( $E_{corr}$ ), corrosion current density ( $i_{corr}$ ) and anodic and cathodic Tafel slopes ( $\beta_a$ and $\beta_c$ ) for MS corrosion in 1.0 M HCl in with and without different concentrations of 2-NBABA, 1-BOPAMS and 4-BOBAMS at 303 K	134
4.6	Electrochemical impedance (EIS) parameters such as the resistance of charge transfer ( $R_{ct}$ ), constant phase element ( $Y_o$ ), solution resistance ( $R_s$ ) and the CPE exponent ( $n$ ) for MS corrosion in 1.0 M HCl in absence and presence of different concentrations of 2NBABA, 1-BOPAMS and 4-BOBAMS at 303 K	139

4.7	Weight loss measurements of Al in 1.0 M HCl containing various concentrations of 1-BOPAMS, 4-BOBAMS and 2-NBABA at different temperatures	150
4.8	Kinetic and activation parameters (derived from the Arrhenius and transition-states plots) for Al in 1.0 M HCl in the absence and presence of various concentrations of 2-NBABA 4-BOBAMS and 1-BOPAMS	158
4.9	Thermodynamic and adsorption parameters (Langmuir adsorption isotherms) for Al in 1.0 M HCl at various temperatures for 2-NBABA, 1-BOPAMS and 4-BOBAMS	165
4.10	Thermodynamic and adsorption parameters obtained from various isotherms for Al in 1.0 M HCl at various temperatures for the utilized corrosion inhibitors	172
4.11	Potentiodynamic polarization (PDP) parameters such as corrosion potential ( $E_{\text{corr}}$ ), corrosion current density ( $i_{\text{corr}}$ ) and anodic and cathodic Tafel slopes ( $\beta_a$ and $\beta_c$ ) for Al corrosion in 1.0 M HCl in with and without different concentrations of 2-NBABA, 1-BOPAMS and 4-BOBAMS at 303 K.	178
4.12	Electrochemical impedance (EIS) parameters such as the resistance of charge transfer ( $R_{\text{ct}}$ ), constant phase element ( $Q_1$ ), solution resistance ( $R_s$ ) and the CPE exponent ( $n$ ) for Al corrosion in 1.0 M HCl in absence and presence of different concentrations of 2NBABA, 1-BOPAMS and 4-BOBAMS at 303 K	184
4.13	Comparison of the performance of 2-NBABA, 1-BOPAMS and 4-BOBAMS on the corrosion inhibition of Al and MS in 1.0 HCl solution	189



# CHAPTER 1

---

## INTRODUCTION

The work embodied in this dissertation entitled **“CORROSION INHIBITION EXPLORATION OF SYNTHESIZED CARBOXYLIC ACID AND AMINO ESTERS ON SELECTED METALS IN ACID MEDIUM”** is divided into four chapters.

This chapter provides a preliminary introduction on corrosion, the importance of corrosion management and the possibility of using organic compounds to control corrosion. It also states the motivation and reasons for conducting this research. The importance of using hydrochloric acid (HCl) as a corrosive solution (environment) is also highlighted. The aim and objectives of the study are also dealt with in this section.

## 1.1 INTRODUCTION

Metals have continued to be used in fields such as construction, mechanical, electrochemical, structural, etc., as raw materials for decades. This use stems from their properties, including flexibility, high melting and boiling points, lustre feature, durability, high density and good conductivity. Regrettably, metals/alloys continue to behave in a way that allows them to return to their more stable oxidized state, causing them to associate with different elements that recur in their surroundings. This process is referred to as corrosion [1, 2]. Metallic corrosion has been a serious problem facing humanity as it leads to metal decay, resulting in enormous economic loss, reduction in productivity and damage to the environment. The devastating effects of corrosion are a huge problem faced by many industries, as such, scientists are committed to finding ways to avoid or at best reduce the rate of corrosion to improve the lifetime of the metal surface, as the protection of metal against corrosion is a challenging task [1]. The economic costs of corrosion are enormous, and about 5% of a country's income such as South Africa (SA) is spent on corrosion prevention, maintenance and even replacement of destroyed or contaminated products as a result of corrosion [3, 4]. The deleterious effect of corrosion is mainly attributed to the deterioration of metallic products; however, this concept is not limited to them, it is also applicable to non-metallic materials such as plastics, concrete, and wood [5, 6]. Aqueous metallic corrosion is one of the most common forms of corrosion in which the material undergoing corrosion is a metal or alloy, and the corrosive environment is an aqueous solution such as hydrochloric acid (HCl). In everyday life, such type of corrosion is observed in different forms such as corroded nails, spots in car bodies, reddish-orange and hot-water tanks [7, 8]. Corrosion damage requires not only the replacement of the corroded material but like other environmental hazards such as severe weather disruptions, corrosion can cause severe and costly damage to electrical equipment, vehicles, home appliances, infrastructure, ports, railroads, ships, pulp and paper, hazardous materials storage, drinking water, sewer systems, waterways and telecommunications [9]. Corrosion is a universal natural phenomenon which cannot be eliminated, therefore has become an enduring problem. However, by applying proper strategies, it is practicable to decelerate the degenerative process so that equipment can perform their required tasks effectively for the predicted length of time they were manufactured for [10-14].

The following techniques and criteria are of paramount importance when looking for optimum equipment lifetime, minimal costs and maximum protection in many industries; such methods

involve the tracking, identification and control of corrosion. Effective management of corrosion requires first an understanding of the nature and process by which it occurs [15].

The effects of corrosion are also observed in industrial pipelines because of the ferociousness of the liquids carried through them (figure 1.1). Pipeline failures due to corrosion represent a significant concern for the oil and gas industry and society at large. Pipeline failure that results as a consequence of corrosion can cause hazards that involve several fatalities, significant environmental damage, dire economic implications and severe financial loss [16]. These failures lead to the reduction in annual profits margins that are borne by the pipeline operators due to infelicitous costly consequences of corrosion. As such, the need for awareness among operators to know how to look for and assess the consequences of pipeline failure due to corrosion and forecast its total cost has increased dramatically [17]. Even with the increase in education on the assessment of corrosion, most of the internal corrosion failures in pipelines are due to the lack of proper knowledge of the corrosion process and could be avoided if corrosion is predicted and mitigated on time. However, the lack of understanding of the corrosion process results in the use of incorrect remedy techniques. The liquids carried by these pipelines may be petroleum containing seawater, sulphur and water or high saline formation, containing a high concentration of ions such as chloride, sulphate and other ions of different metals. Due to this, introducing corrosion inhibitors through various sites of the pipes is vital [9].

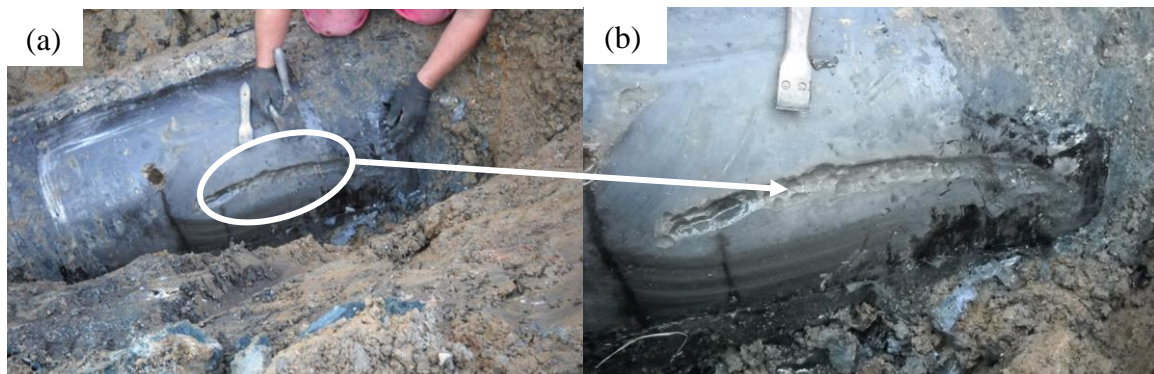


**Figure 1.1:** Pipeline corrosion failure (a) and a zoom in on the defect area (b) [18].

Aggressive acid solutions are extensively used in industries during the manufacturing processes and other applications like acid pickling, acid cleaning, acid de-scaling, and oil well cleaning [8]. Metals exposed to enamelling, cold rolling, electroplating, painting, galvanizing, phosphate coating, etc., should have a clean surface free from salt or oxide scaling. As such,

these metals are typically immersed in an acidic (HCl) solution known as a pickling acid bath to eliminate excessive scale such as rust in industrial plants. Pickling is a type of metal surface treatment used to remove impurities from ferrous metals, aluminium alloys and copper, such as inorganic contaminants, corrosion, stains or scales (figure 1.2) [19].

A pickle liquor or bath is a solution which contains strong acids and is used to clean or remove impurities on the surface of the metal. Acids like HCl, nitric acid, acetic acid, sulphuric acid, formic acid, hydrofluoric acid, etc., are the most widely used in the industrial processes. HCl is commonly used in the pickling baths due to its natural economic regeneration from the exhausted pickling solution. During pickling, the use of acids like, HCl leads to the corrosion of metal vessels and industrial pipelines and thereby reducing the production, resulting in economic loss. As such, acid-driven corrosion is one of the major concerns when it comes to metallic corrosion. Metals or alloys can be protected against acidic corrosion either by special treatment of the medium which reduces its aggressiveness or by the addition of minute concentration of different substances called corrosion inhibitors. The addition of a pickling inhibitor during the pickling process protects the surface of the metal from undergoing acidic corrosion while maintaining the pickling performance of the system. Therefore, adding an inhibitor increases the lifetime or durability of the pickling bath as well as reducing the acid consumption of the plant. If an inhibitor is not added, a significant amount of metal can be lost during the pickling process due to the aggressiveness of the acids. In pickling baths, hydrogen gas is evolved from the metal surface due to the interaction of the metal with the acid. This process creates a problem known as hydrogen embrittlement in which the diffusing of hydrogen through the metal makes it brittle [20, 21].

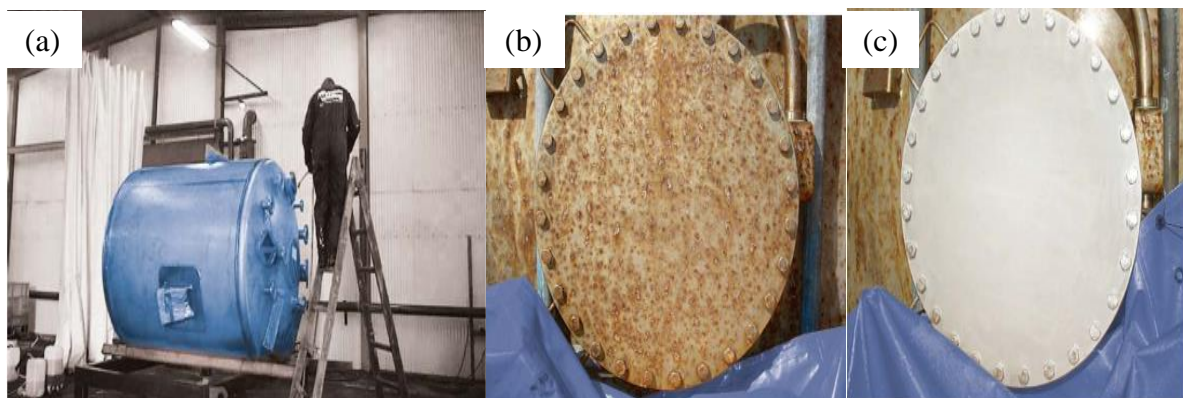


**Figure 1.2:** Acid pickling in industries (a) and the transformation of the surface of steel before (b) after (c) pickling [22].

According to Henthron Michael [23], “The secret of effective engineering lies in controlling corrosion rather than preventing corrosion because it is impossible to eliminate corrosion”. Therefore, research into corrosion is more of a subject of immense conceptual and practical concern. Reliable methods of control are, therefore required to manage the corrosion cycle. Polymer coatings can be used as the most effective and commonly used option for the protection of metals against corrosion; these coatings provide a layer that serves as a barrier against the spread of water, oxygen and electrolytes and thus avoiding the interaction of acid species with the metal surface. Unfortunately, the protection created by these coatings does not prevent the corrosion process from spreading on its own if the surface is disrupted by certain factors, such as atmospheric oxidation [24]. Certain methods can be employed to improve the performance of coatings, but they are mainly based on increasing the thickness of the coatings or increasing the contact of active metal powers which can be a bit costly [25, 26].

This limitations of coatings have for the past few years, motivated researchers to focus on developing a new generation of high-performance coatings which are referred to as ‘smart coating’, to achieve functionally acceptable performance by providing long-life protection against corrosion. Such coatings act by sensing changes that occur in the atmosphere surrounding the metal and interact with the metal surface in response to such changes, in addition to their protective function, they also have a decorating role, this are called corrosion inhibitors [27, 28].

The use of corrosion inhibitors is regarded as the most effective method for the protection of metals against corrosion in acidic environments amongst other methods such as coatings [29], anodic protection [30] and cathodic protection [31, 32]. The inhibitor(s) that are used to protect metals from attack by aggressive species must possess properties that are capable of adsorbing onto the metal surface and slow down the dissolution of metals. The resultant film of chemisorbed inhibitor provides protection by either retarding the electrochemical process or by acting as a barrier between the metal and the corrosive environment [33]. Even though several studies have been devoted to the subject of corrosion inhibitors, the selection of such an inhibitor remains a trial-and-error process largely both in the laboratory and in the fields [34]. This heuristic process is due to the limited mechanistic and molecular-scale knowledge; as such, a proper selection of an inhibitor is vital for different specific environment and metal. This selection of an inhibitor is crucial because an inhibitor that is capable of protecting certain metals may result in the acceleration of the dissolution of another metal(s) [35].

Various literature has demonstrated that N-heterocyclic compounds can be used as potential corrosion inhibitors for metals in acidic solutions and some of them include quinoline, [36] pyrimidine, [37] triazole [38] derivatives etc. The main functional groups of compounds that have been studied as corrosion inhibitors and are capable of forming chemisorbed bonds with the metal surfaces include, carboxyl (-COOH), phosphate (-PO<sub>3</sub>H<sub>2</sub>) and amino (-NH<sub>2</sub>) even though other functional groups or atoms can form coordinate bonds with metal surfaces [33]. The compounds used in the present study contain amino and carboxyl groups as some of the main functional groups hypothesized to be responsible for the adsorption of the compounds on the metal surface.

## **1.2 PROBLEM STATEMENT**

The process of corrosion progressively degrades limited mineral resources and the energy utilized in the processing and mining process altogether, and since these metals and products derived from them are very important in our day to day lives, their extraction and mining cannot be avoided making it a necessity to study their corrosion [39, 40]. The products made from these metals include, amongst others, cell phones, computers, construction structures and automobiles. Thus, due to corrosion affecting virtually all facet of contemporary development, the deterrence of corrosion is, therefore, of paramount importance for economic and safety reasons [14].

The biggest challenge with corrosion is that it is difficult to prevent from occurring altogether; however, it can be managed. When corrosion is managed, equipments can perform their required tasks effectively, and this can be achieved using inhibitors [13]. This, therefore, further advocates the increased need in the study of corrosion prevention mechanisms to prolong the lifespan of metals. The industrial costs of managing and controlling corrosion, hydrate deposition during gas and oil, scale, food, wax and transport is very high and as such corrosion causes tremendous harm to the national economy and more research is required in order to find practical solutions to control the problem [41].

## **1.3 JUSTIFICATION OF THE STUDY**

To promote the production and use of environmentally friendly, readily available, affordable and less toxic organic compounds that contain heteroatoms as corrosion inhibitors for applications requiring the use of metals/alloys in technology, further work on corrosion inhibition must be carried out. This study is founded on the premise that the protection of metals

from corrosion goes a long way to save a significant amount of money in the chemical, food, construction, manufacturing and oil and gas industries. This is important because the economy of a country is highly influenced by industrial products manufactured from metals and can be exported or sold locally. Yet, industrial equipments are corroded, which is of concern since these equipment are primarily made from metallic products. Corroded equipment results in the termination and contamination of metallic products such as computers, requiring a large amount of money for the decontamination of the products. Equipment or machinery also lose their efficiency when attacked by corrosion. The cost of remedying this is enormous. The World Corrosion Organization (WCO) state that the annual cost of corrosion in the world is about 2.2 trillion US dollars, which signifies the world Gross Domestic Product (GDP) [39]. If for a long time the consequences of corrosion are not properly attended to, then affected factories will shut down resulting in enormous amounts of money lost by the nation and business, as well as job losses. Therefore, large financial investment is being spent worldwide to offset the effects of corrosion. In SA, for instance, the study conducted by the Mineral Technology Council (MINTEK) group found that R130-billion per annum was spent in 2004 on corrosion costs and implications [42]. This implies that intensive studies need to be conducted concerning the prevention and control measures of corrosion in the industry and every area of human life. Findings from intensive studies conducted on the prevention and repairing of corrosion show that the prevention of corrosion is the most cost-effective measure of controlling corrosion instead of repairing the damage caused thereafter [12, 39, 43-47]. There are other significant reasons to justify studying the corrosion of metals, and some of them are listed in detail below [14]:

- a) Corrosion is a threat and can damage the environment. One example is when water is contaminated by corrosion products and becomes unsuitable for consumption; this shows how much the prevention of corrosion is integral to preventing the contamination of water, air and soil.
- b) Having knowledge of engineering is not complete without proper knowledge and understanding of corrosion since ships, automobiles, aeroplanes, and several other transport vehicles cannot be designed and manufactured without any measure of dealing with the corrosion behaviour of their materials.
- c) There have been reports in recent years on engineering disasters such as the explosion of oil pipelines and storage tanks, the crashing of naval, military and civil aircraft and passenger ships.

- d) Due to the application of metals as implants for the human body, there is a significant need for understanding corrosion science and engineering. This knowledge is required because human blood is very corrosive, and surgical implants have to be very resistant to corrosion.
- e) Materials such as copper, iron, aluminium, chromium, titanium, are precious, and their resources are dwindling fast, and shortly, there will be a shortage of these resources. The impending metal crisis is not just a remote possibility but an inevitable reality. The problem of corrosion is becoming enormous, and a challenging task, the collapse of bridges is one signal that shows that this problem has to be combated. To preserve and protect these valuable resources, there is a need to understand how the process of corrosion degrades them and how to preserve them by applying corrosion prevention protection measures.

#### **1.4 AIM AND OBJECTIVES OF THE STUDY**

The present study's main aim is intended in generating measurable and testable experimental data towards the control of corrosion of two metals, namely: mild steel and aluminium; which are in contact with the aggressive environment (HCl) by using inhibitors.

The specific objectives of this study are to:

- Synthesize, characterize and evaluate the anticorrosive properties of carboxylic acids and amino esters derivatives in acid media.
- Evaluate the inhibition efficiency of the organic synthesized inhibitors for mild steel and aluminium corrosion in the corrosive aqueous environment by gravimetric weight loss analysis at different temperatures and concentrations of the inhibitor compounds.
- Propose the type of adsorption mechanism and adsorption isotherm for corrosion inhibition.
- Evaluate the interaction of the inhibitor with the metal surface by electrochemical techniques such as electrochemical impedance spectroscopy (EIS) and potentiodynamic polarization (PDP).
- Use Fourier Transform Infrared spectrometry (FT-IR) to determine the functional groups which interacted between the compounds and the metal surface.



## CHAPTER 2

---

# LITERATURE REVIEW

This chapter deals with the literature review of the present study. In summary, it provides a general review on the basic principles of corrosion, its theories, forms and classification. This chapter also discusses factors that affect corrosion, consequences, cost implication and the thermodynamics and kinetics of corrosion. A general review on the corrosion of a few selected metals and the corrosion prevention techniques such as the use of organic compounds against metallic corrosion has been presented in this chapter. The mechanism, definition and classification of corrosion inhibitors and the use of carboxylic acids and amino acid esters as corrosion inhibitors is dealt on in this chapter. This chapter also addresses different monitoring techniques for corrosion with an emphasis on techniques utilized in this present study.

## 2.1 DEFINITION OF CORROSION

Corrosion is a ubiquitous costly phenomenon with detrimental impact for a variety of industries [48]. Despite having more than one definition [1], the process of corrosion is basically a result of the interaction between metals and their environment. Corrosion of materials (usually metals) can, therefore, be characterized as a spontaneous destructive chemical attack or an environmental electrochemical reaction. The latter process involves the transfer of electrons between the corrosion-affected metal surface and an aqueous solution to alter the properties of the material entirely [49].

For example, when a hard and ductile metal is long exposed to oxygen and humidity, this results in a complete shift from powder to rust of the metal. The proper definition of corrosion must, therefore, take into consideration both the material and the environment [14, 42, 50]. The process of corrosion is precisely the reverse of extraction of the metal from its minerals to its combined state in chemical compounds. This similarity is because when metals are manufactured from their ores, some amount of energy is provided during the refining process, and this leads to the metals being in a high energy state. As a consequence, metals tend to revert to their natural form under suitable corrosive environments by releasing this energy. This conversion phenomenon is referred to as corrosion. Thus, extractive metallurgy in reverse (figure 2.1) is being compared to the electrochemical process involved during corrosion of metals, in which a large amount of energy must be added in the refining process. The same amounts of energy required to extract metals from their ores are also lost during the corrosion chemical reactions. For example, in the case of corroding steel by oxygen and water there tend to be a tendency whereby the iron reverts to its natural and more thermodynamic stable state of hydrated iron oxide [51].

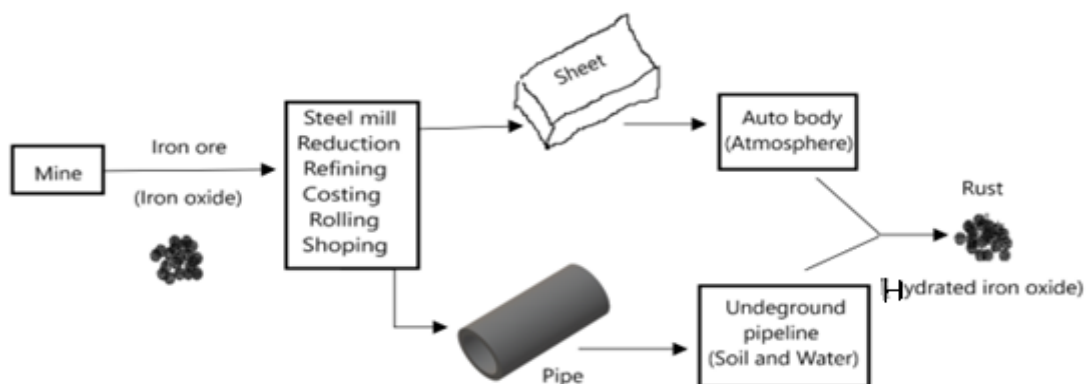


**Figure 2.1:** Flow diagram showing the processes involved in metallurgy [51].

## 2.1.1 THEORIES AND BASIC PRINCIPLES OF CORROSION

Different theories have been proposed to explain the principle and mechanism of corrosion. The local cell theory and the Wagner and Traud theory are some of those theories and are described in detail below.

### 2.1.1.1 Local cell theory

De la Rive [39-41] proposed an electrochemical mechanism of corrosion, which he based on his observation that impure metals tend to corrode much faster than pure metals in acidic solution. According to this theory, corrosion occurs as a result of the formation of a large amount of micro-local or electrochemical cells (figure 2.2) on the surface of the metal at heterogeneities (defects, impurities, non-uniform stress distribution, different phases, etc.). Since the process of corrosion is an electrochemical process, contaminants on the metal surface act like short-circuited cells in which the impurities play the role of the cathode, and the metal plays the role of the anode. This circuit enables an electrical potential difference to be established between two metals or different parts of a single metal. When the metal is electrically attached to a typical electrode, the voltage that arises can be determined. This potential can be more or less than that of the standard electrode where the voltage can either be expressed as negative or positive. The potential difference allows the current to pass through the metal and causes reactions to occur at the anodic and cathodic areas [42]. De la rive local cell theory of corrosion states that metals of the homogeneous surface (pure metals) do not corrode even in aqueous solution. However, anodic (metal dissolution) and cathodic (hydrogen evolution) processes can occur even on a homogenous metal surface at the same location and the same potential. Since the corrosion of homogenous surfaces is in contradiction with the local cell theory, Wagner and Traud came up with a new theory of corrosion [52, 53], which is described in detail in the section below.

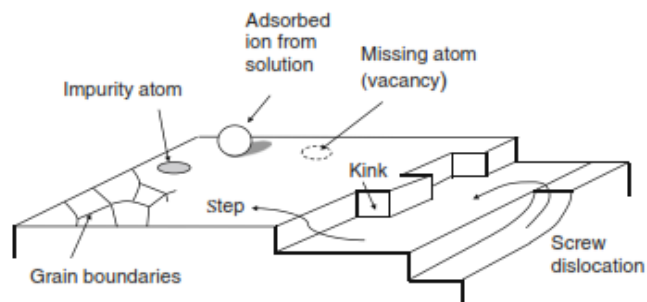


**Figure 2.2:** Heterogeneous metal surface showing different types of imperfections [54].

### 2.1.1.2 Wagner and Traud theory

To eliminate the contradiction of the local cell theory, Wagner and Traud [55] proposed that the dissolution of the metal and hydrogen evolution takes place even on homogenous materials exposed to homogenous environments simultaneously and alternatively at the same place and called this the Wagner and Traud theory. According to this theory, the corrosion of pure metals follows an electrochemical process regardless of the presence of impurities or any other heterogeneities. The corrosion process proceeds through the anodic and cathodic electrochemical reactions on the entire metal surface. The critical conditions required for the corrosion cycle are that metal dissolution, and electronation reaction co-occur at the metal-environment interface. When such conditions are met, this results in the corrosion of metals due to the load transfer reactions at the interface. Thus, it is paramount that the voltage of the system is more negative or more positive at the interface than the equilibrium potential for the anodic or cathodic reactions, respectively. The impurities that are found on the metal surface may result when the metals are molten during their formation, shaping and rolling operations. Even though the process of corrosion is complicated, it can be explained as an electrochemical reaction, as highlighted in figure 2.3. The processes taking place during the corrosion of carbon steel are also described detail below:

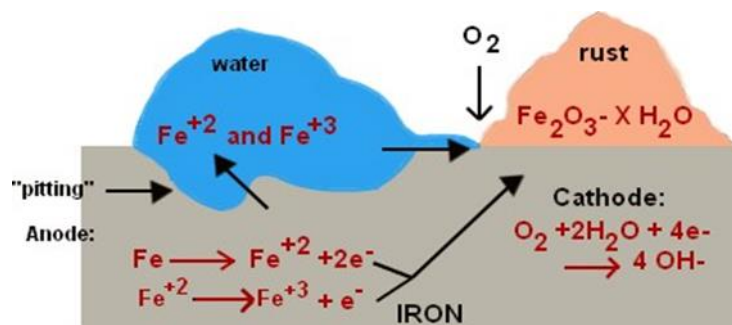
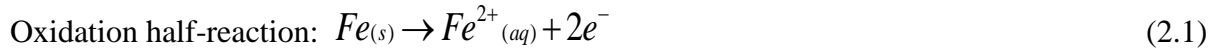


**Figure 2.3:** The reactions occurring during the corrosion of carbon steel [55].

#### The processes taking place when the corrosion cell is functioning:

- *At the anodic region of the metal:*

At the metal/electrode of the anodic area, metal dissolution takes place. Fe atoms oxidise into  $\text{Fe}^{2+}$  ions. They leave the steel surface and move into the water solution, leaving the released electrons on the anodic area of the metal. This process is known as oxidation. During the corrosion process of steel, the anodic reaction can/or proceeds in a two-step process.



The oxidation of iron into a ferrous ion is the first step and depending on the potential; the ferrous ion might be oxidized into a ferric ion.



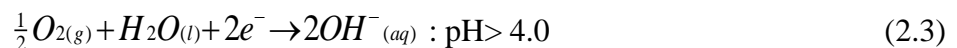
The process results in the release of electrons on the steel surface and an increase in the number of  $Fe^{2+}$  ions in the water solution.

- ***Along the steel surface:***

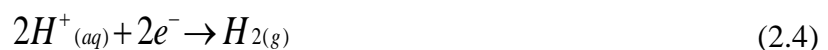
The processes at the steel surface generate a potential difference between the two ends of the metal. The released electrons flow from the anodic area through the steel surface to the cathodic area. This motion produces an electric current.

- ***At the cathodic region of the metal:***

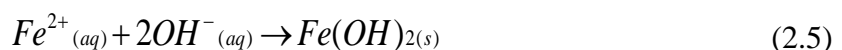
The released electrons produced at the anodic reaction are consumed at the cathodic region of the metal. This consumption process is known as reduction. This process balances the anodic reactions above. It should be noted that the anodes and cathodes can be either made up of two dissimilar metals or occur at different sites of the same metal surface. During the reduction reaction, oxygen in the aqueous solution takes up electrons at the cathodic area of the metal and forms hydroxyl ( $OH^{-}$ ) ions at the surface of the metal and completes the electric circuit.



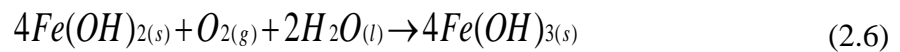
However, hydrogen ions are the ones that take part in the reaction in acidic solution in the absence of dissolved oxygen. Therefore, the main cathodic reaction is hydrogen evolution:



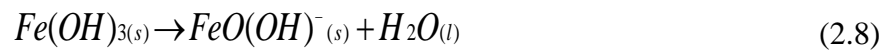
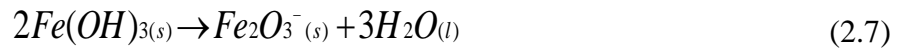
The  $OH^{-}$  ions combine with  $Fe^{2+}$  ions that are produced through the dissolution of the metal and may be deposited on the steel surface as follows:



The reaction produces ferrous hydroxide as a product. The ferrous hydroxide precipitates as loosely clumped mass of fine particles due to its low solubility and oxidises at a faster rate to form ferric hydroxide between the metal and water solution as follows:



The product formed is then broken down, leading to the formation of corrosion products on the steel surface, and this process is represented by equations (2.6) and (2.7).



At the anode, there is the precipitation of the solid corrosion products which may result in the precipitation of other ions of water solution. Therefore, the corrosion film on the metal surface may have traces of hardness salts, silt clay, sand, and microbiological slime. However, if the film formed on the metal surface that is porous, this can lead to the continuation of corrosion to a detrimental extent. This continuance of corrosion is due to the metal ions that keep on penetrating through the metal surface until they reach the interface between the metal and the water solution. However, if a tight and strong adherent film is formed then the movement of  $Fe^{2+}$  ions from the anodic area to the cathodic area (ionic diffusion) is prevented, and the corrosion of the metal is stopped [55]. It should be noted that all the process mentioned above should/or take place simultaneously; otherwise, the corrosion process will not occur.

### 2.1.2 CLASSIFICATION OF CORROSION

There are typically two different categories of corrosion based on the mechanism of corrosion: dry corrosion (chemical) and wet corrosion (electrochemical) [56]. These categories will be briefly explained in the following sub-headings.

*Wet corrosion (electrochemical):* Wet/aqueous corrosion result when an aqueous solution is present. For example, the corrosion of steel in seawater. It accounts for most of the metal deterioration and pertains to the corrosion of steel reinforcement in concrete [56].

*Dry corrosion (chemical):* Chemical corrosion is more concerned with the chemical kinetics of a heterogeneous reaction. The process of chemical corrosion does not require the presence of liquid phase nor dew point of the environment, but it is rather associated/linked with high-temperature metal gas or metal vapour iron which involves non-metals and atmospheric environment conditions such as, for example, air pollutants, high temperature and moist air [57]. This present study will be investigating the corrosion process in the presence of moisture (i.e., electrochemical corrosion).

### 2.1.3 THE CORROSION CELL

The process of wet/aqueous corrosion involves an electrochemical reaction and is realized in a corrosion cell. The main idea behind the electrochemistry of corrosion has been reported by Michael Faraday [58] in the early nineteenth century. A corrosion cell consists of two metallic conductors (electrodes) which are in contact with an electrolyte, that may be a liquid, a solid or a solution. The electrolyte generally consists of ions capable of conducting an electric current during the electrochemical reaction. An electrode and its electrolyte make up an electrode compartment. The electrode or area on the metal surface at which oxidation occurs is called the anode; while the electrode or area on the metal surface at which reduction occurs is called the cathode. The corrosion cell is complete when an electrical connection is established between the two electrodes [58]. The electrical conduction is realised by making use of a low resistance metallic wire that connects the two compartments or electrodes. If any component of the cell is removed, corrosion reaction does not occur. However, hastened attack of the metal (i.e., localized corrosion) can still happen if impurities are present at the anode. The impurities are capable of creating a local action cell that results in a slow corrosion reaction on the anode surface [1]. When the cell is closed, the anode electrode is corroded and loses the electron that migrates towards the cathode electrode. Thus, the anode is the positive electrode where the oxidation half-reaction takes place. The cathode electrode takes up the electron from the anodic area. The cathode is the negative electrode where the reduction half-reaction takes place. To complete the corrosion reaction, cations (positively charged ions) migrate towards the cathodic area while anions (negatively charged ions) migrate towards the anodic area. Below is a figure depicting the corrosion cell.

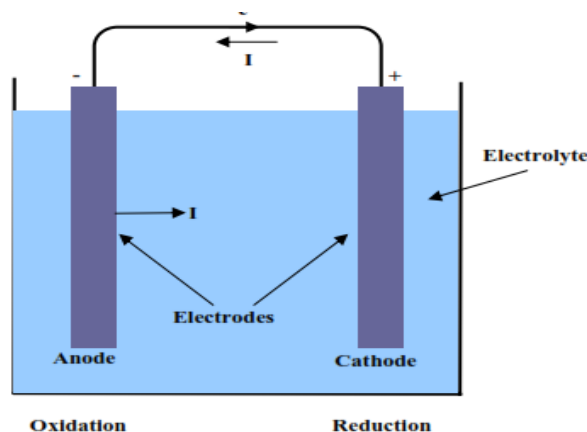


**Figure 2.4:** A schematic example of an electrochemical cell showing principles of corrosion [59].

## 2.1.4 DIFFERENT FORMS OF CORROSION

Corrosion manifests as damages on the surface of corroding metals and has antagonistical effects associated with it and in this context, it becomes imperative to classify corrosion by physical appearance as this is the most reliable, accurate and most convenient way of identifying it. The substances/materials that remain on the surface of the metal when it is/was in contact with a corrosive or aggressive environment in the presence of oxygen is what mostly results in the degradation (i.e., corrosion) of the metals [60]. The morphology of the attack of corrosion and where it is occurring can also be used to classify and differentiate various forms of corrosion. A selection of the most common types of corrosion are reviewed below:

**Atmospheric uniform or general corrosion:** Uniform or general corrosion is a form of corrosion that occurs when an exposed surface area of a metal decays at a similar rate [61, 62]. As the name implies, uniform corrosion results in the regular uniform removal or penetration of the entire exposed metal surface. Uniform corrosion (figure 2.5) is the most expected mode of corrosion in metals. For uniform corrosion to occur, the corrosive environment species must have full access to all parts of the metal surface and the metal itself be compositionally and metallurgically uniform. The best examples used for this type of corrosion are uniform corrosion of steel in acid solutions, atmospheric corrosion of ferrous and non-ferrous metals [63-66].

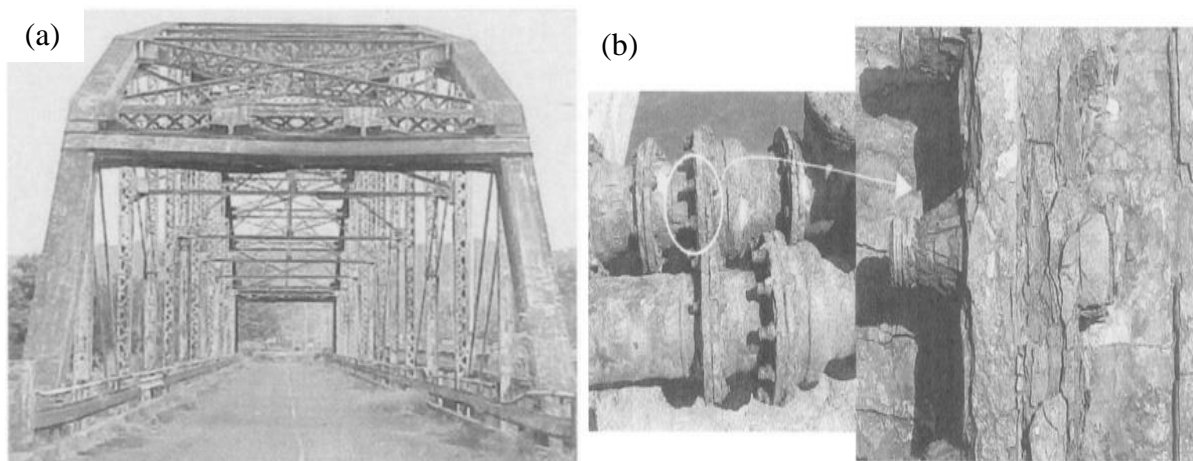


**Figure 2.5:** Atmospheric uniform corrosion attack of a steel bridge (a) and a pipeline (b) located on a concrete pier above the ocean water as highlighted [67].



**Intergranular corrosion:** This is a form of corrosion that occurs with alloys when there is a difference in potential between the grain boundary and grain itself. The emphasis of intergranular corrosion is that it makes use of the very acidic or basic environment to corrode the grain boundaries of different materials. Figure 2.6 below represent the intergranular corrosion on a stainless-steel nut. Any commercially manufactured alloy contains a highly augmented cross that shows the granular metal structure. Alloys possess individual grains with a well-defined boundary as compared to grains within the metal, which further possesses different chemical characteristics. During the corrosion process, the grain boundary acts as the anode whereas the cathode is the grain centre, and when they come into contact with the electrolytic solution, they undergo corrosion (i.e., they react). Intergranular corrosion of alloys can be prevented from occurring by subjecting the alloys to sufficient heat before they are exposed to an acidic environment. The 7075 and 2014 aluminium alloys are usually the ones that suffer the most from this type of corrosion [68].

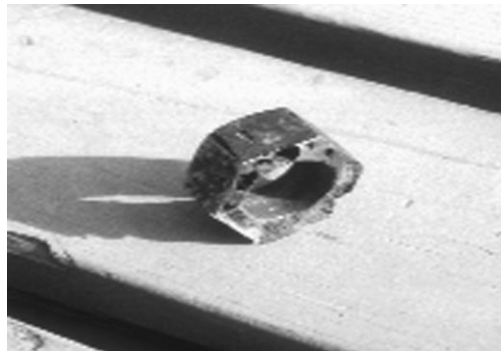


**Figure 2.6:** Intergranular corrosion on a stainless-steel nut [69].

**Dealloying:** Is a term that is usually assigned to the corrosion process in which the constituent of an alloy is removed preferentially from the alloy, leaving behind the modified residual structure. This particular type of corrosion is also named “selective leaching”, which occurs as a result of selective corrosion of a phase or elements. The most known form of this type of corrosion, as explained below, are dezincification and graphitization.

Dezincification (figure 2.7a and b) occurs in the copper-zinc alloy, where zinc is more susceptible to dezincification, and the dealloying occurs as zinc is always removed first from alloys. While when brass is considered, zinc is removed first leaving copper and even copper oxide behind which makes the brass weak. As a result, dealloying eventually destroys and penetrates the metal, making it susceptible to gas or liquids leakages.

Graphite corrosion or graphitization is the ejection of ferrite from grey iron. Graphitization occurs mostly in grey cast irons in mild environments where the selectively leaching of iron leaves the network of graphite. In this type of corrosion, the metallic properties and strength of metal are lost, and no dimensional change occurs [70].

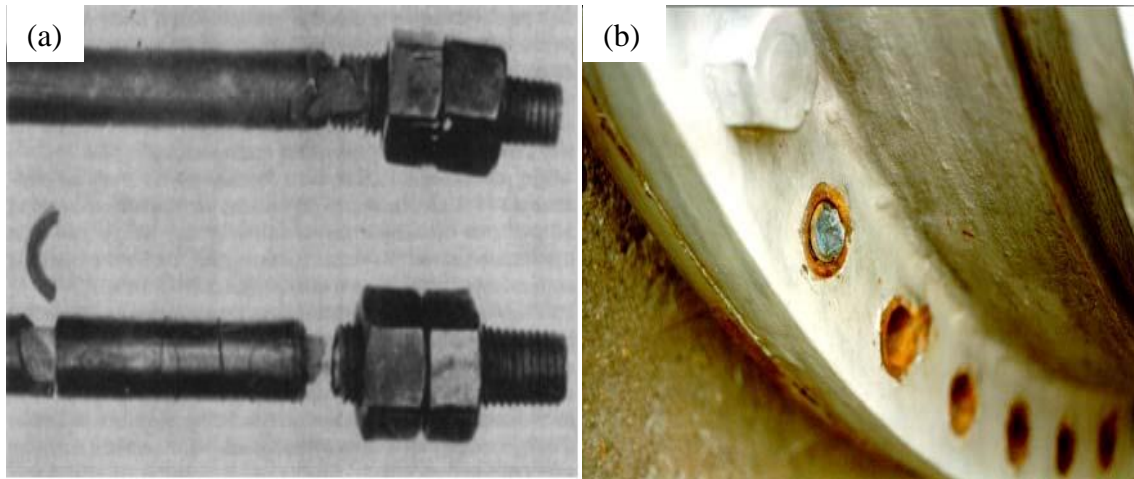


**Figure 2.7:** Dezincification of a bolt (a) in brass [8] and high zinc content brass (b) [59].

**Crevice corrosion:** Crevice corrosion refers to corrosion occurring in conditions where there is limited access from the atmosphere to the working fluid. Such spaces are called crevices. Crevices are defined as gaps and contact areas resulting from gaskets, within cracks, between sections, under piles of sludge, and even in deposit-filled spaces. They also form surface deposits of corrosion products, scratches in paint films, amongst other facts. This type of attack is called deposit corrosion, gasket corrosion or preferably crevice corrosion [63-66, 71]. Figure 2.8 shows the crevice corrosion of stainless-steel flange and the mechanism of attack.

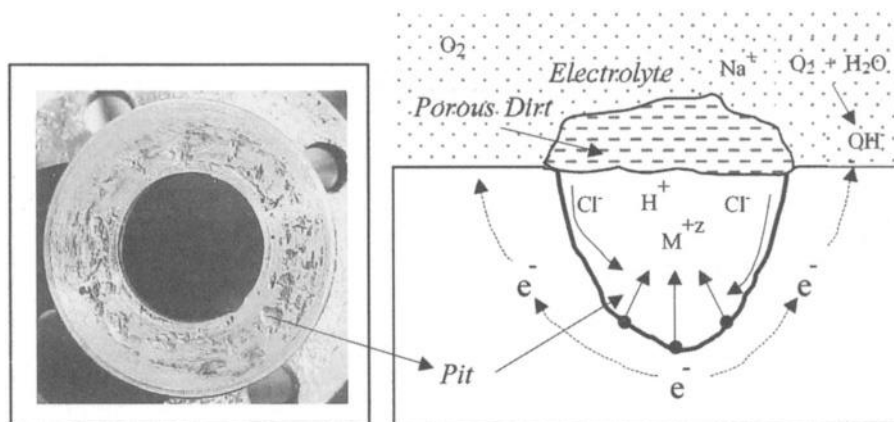


**Figure 2.8:** Crevice corrosion of stainless-steel flange and the mechanism of attack [51].

**Galvanic or general corrosion:** Galvanic corrosion is observed in the presence of an electrolyte and an electron conductive path when two dissimilar metals are in contact with each other under electrochemical action (figure 2.9). It occurs when the dissimilar metals are mixed electrically in a solution; the more positive (noble) metal acts as the corrosion cell cathode and its level of corrosion decreases and can be detectable by a build of corrosion products at the joints between the two dissimilar metals. Whereas, the more negative (active) metal functions as the anode and its corrosion rate will increase. For instance, when steel (stainless or carbon steel) is in contact with magnesium or aluminium alloys, galvanic corrosion can result and accelerate the corrosion of magnesium or aluminium [72-74].

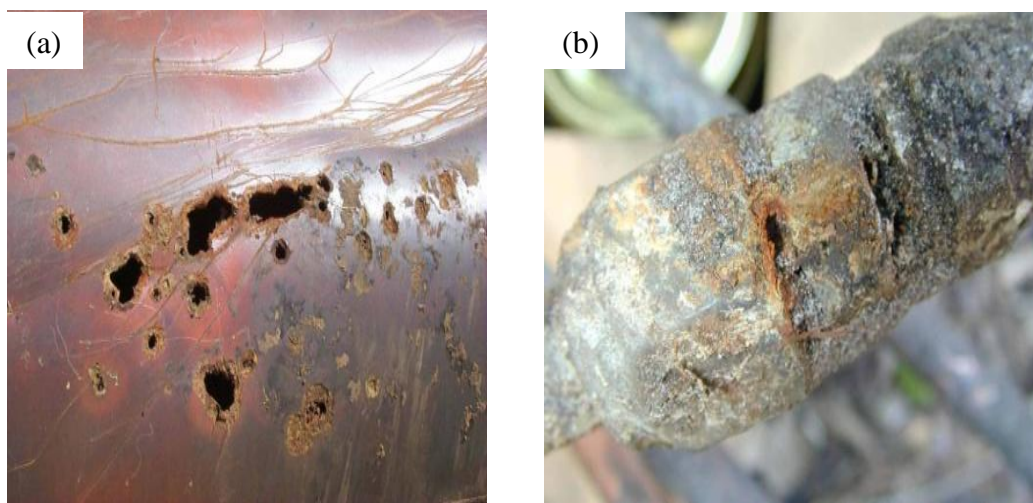


**Figure 2.9:** Metals attacked by galvanic corrosion [75].

**Microbiologically influenced corrosion (MIC):** Is a type of corrosion influenced by the activities and presence of microorganisms such as bacteria, fungi, and their metabolites. The aerobic bacterium produces very corrosive species as part of their metabolites. Most materials such as metals, polymers, ceramics and glass can be corroded in this manner [76]. This form of corrosion may occur in both cold and hot water systems, especially in large buildings like hospitals with long pipe runs. Through inspection, MIC materialize as nodules of copper carbonate that forms predominately at the bottom of horizontal pipe runs or as large irregular shaped carbonate moulds along the bottom of the pipes. The surface of the pipes attacked by microbes is usually covered by a black layer of copper (II) oxide (cupric oxide). An example of a microbe that attacks the metal through this type of corrosion is pseudomonas, which is capable of creating biofilms containing polysaccharides above the metal surface [77]. Figure 2.10 shows an example of MIC occurring in the pipeline that can be seen after the surface of

the metal is cleaned (a) as well as rod-shaped pseudomonas bacteria (b) that causes microbial corrosion.

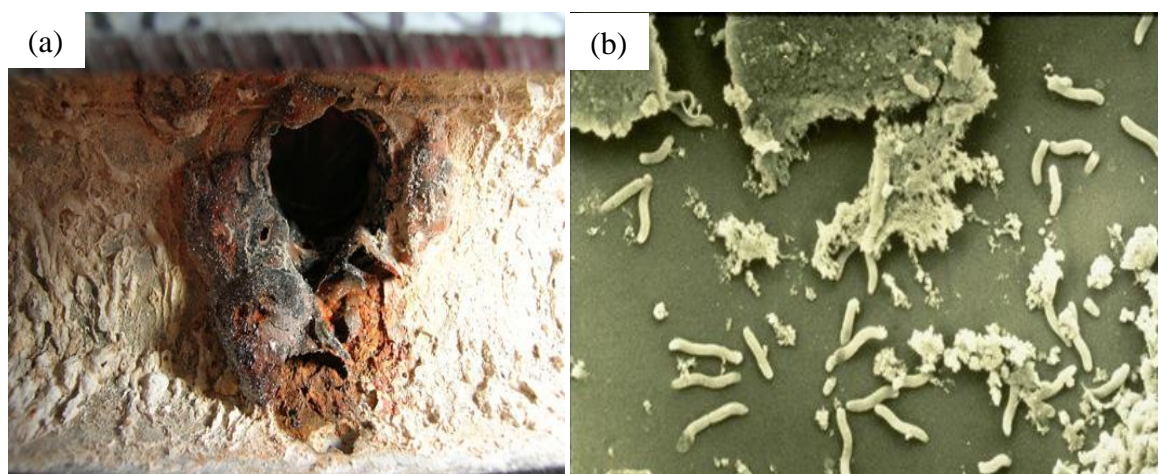


**Figure 2.10:** Microbial induced corrosion in the pipeline (a) and rod-shaped *Pseudomonas* (b) bacteria [78].

**Filiform corrosion:** Filiform corrosion is a unique form of corrosion resulting in the formation of irregular hair-fine filaments of rubber, paint, glass, lacquer, enamel, etc., undercoatings of corrosion materials. This form of corrosion tends to follow grinding and polishing points, regardless of metallurgical factors [76, 79]. This is a particular type of corrosion of the crevice that is sometimes referred to as ‘under film corrosion’. Filiform corrosion usually happens under the painted skin of used cars as blisters. The filament stretches under the film in direct lines and appears as stretched or unified. Some of the filaments focus on the film's surface because of obstacles such as sticky sections of the organic film or sub-coating and become trapped in narrow places [80]. Corrosion of filaments is found on metals that are coated with organic films, and due to some discontinuity in the film, water and air may penetrate through the paint or film and damage the metal surface. The region next to the relatively high oxygen and the water level is saturated with soluble salt corrosive ions and produces an area that serves as the filament face. The rate of dissolution of the metal decreases as the solubility of oxygen rises [81, 82]. An illustration of the filament nature of filiform corrosion (figure 2.11a) shows the direction of the propagation mechanism and section of the tail. Figure 2.11b shows the propagation of filiform corrosion that is spreading under the paint from the point of attack like a worm.

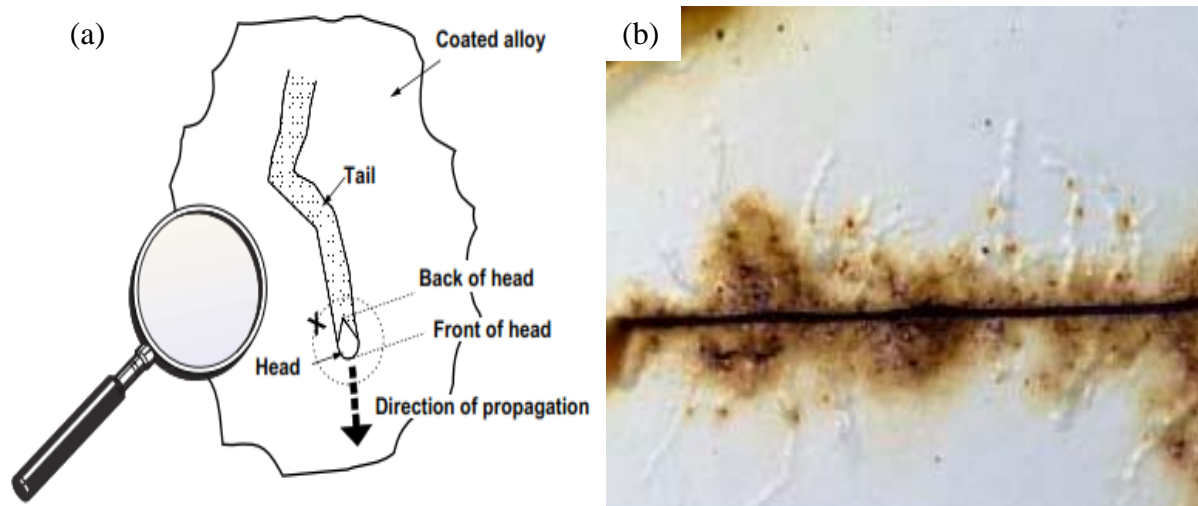


**Figure 2.11:** Illustration of the filament nature (a) [61] and a worm or tentacles path (b) [59] emanating from the point of attack of filiform corrosion.

**Erosion or impingement corrosion:** Erosion corrosion is a type of material degradation involving mechanical wear and electrochemical corrosion [83]. According to Zeng et al., [84], it is generally perceived that the total material weight loss exceeds the amount of pure mechanical erosion and electrochemical corrosion throughout the erosion-corrosion cycle. This concept is because the erosion cycle augments the corrosion process, and vice versa; this is commonly referred to as a synergistic effect. Although extensive research has been carried out, the synergy mechanism between corrosion and erosion is very complex and not fully understood [85]. Erosion (figure 2.12) can increase the rate of corrosion by removing the roughening part of the metal surface, increasing the process of mass transport, passive film; while corrosion can promote erosion by increasing surface roughness, weakening the grain and phase boundaries and dissolving the work-hard protective layer [84]. The start of corrosion can be particularly dangerous if the alloy protective layer is unable to regenerate rapidly and continuously [3]. Also, erosion-corrosion is a standard mode of failure in power plants, oil and gas and petrochemical industries. Typical examples of failures have been reported that have occurred inflow handling equipment where the fluid varies direction, or the flow becomes turbulent, such as valves, pipelines and various rotating equipment [86].

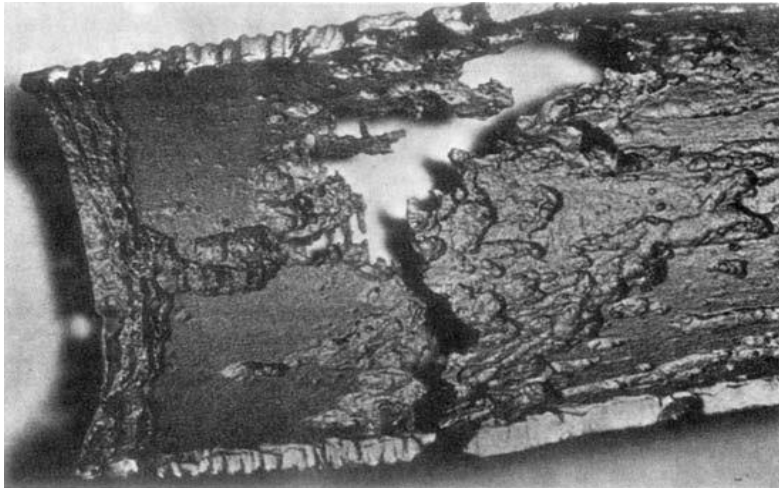


**Figure 2.12:** Erosion-corrosion of 115-mm API L-80 oil well tubing [87].

***Stress-corrosion cracking (SCC):*** SCC refers to an insidious form of cracking that is induced by a conjoint action of sustaining tensile stress and a specific corrosive medium. Throughout SCC, most of the metal surface is practically unattached, but fine filaments propagate through the metal in transgranular mode [88]. Cracks formed by this type of corrosion on the metal surface are highly branched, as illustrated in figure 2.13. The morphology of the crack may be affected by various factors like stress level, type of environment and the metal structure. Three important factors must be met for this type of damage to occur:

- The presence of corrosive species: some ionic compounds can act as the corrodent. Stress-corrosion cracking is often initiated by the availability of aggressive ions like  $\text{Cl}^-$ . The potential of hydrogen (pH) also plays a role in the initiation of SCC and the lower the pH, the greater the propensity of SCC.
- The presence of tensile stress: this may either be a result of residual or applied stress caused by fabrication or operation conditions of equipment, respectively.
- Temperature: for stress-corrosion cracking to occur, the temperature of the environment must be in the temperature range of around  $60\text{ }^\circ\text{C}$  [68].

The troubling issue with SCC is that almost no metal loss occurs, and this makes it challenging to inspect this type of corrosion. SCC is visible or evident after prefoliation has occurred and this is after the metal has been damaged already. The three described factors required for SCC to take place are, to a certain extent, synergistic and complementary. The pits formed at the early stage of the development of SCC function as a local stress riser which results in the

opening of the pits. Such an opening promotes the penetration of new electrolytes which alternatively reaches the anodic area of the pit. This penetration leads to perceptible corrosion that occurs initially at the tip of the pit. After a certain period, the corrosion branches out further to other areas of the pit and eventually progress to the entire metal surface [68].

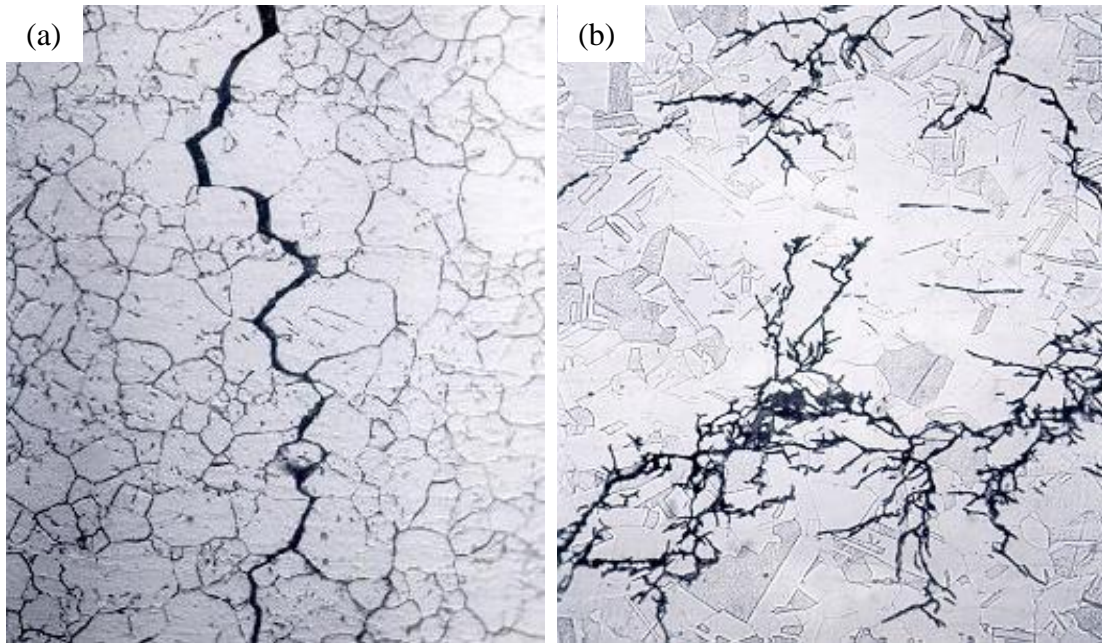


**Figure 2.13:** Intergranular (a) stress-corrosion cracking in brass and trans-granular (b) stress-corrosion cracking in steel [59].

***Fretting corrosion:*** A form of corrosion that manifests at the interface between two closely fitting components and there is a relatively small but significant motion between them. The type of movement may vary from less than a nanometer to several micrometres in amplitude [20, 89]. It is thought to act in conjunction with wear and the presence of oxygen. Even though fretting is said to occur in materials that are in motion with one another, it is usually observed in materials that are designed not to be in motion with each other. The nature of fretting corrosion makes it difficult to detect since it occurs in hidden locations of material interfaces. The best way to deal with this type of corrosion is to be knowledgeable on the ideal material combinations and applications that it attacks and the techniques that can be utilized to combat it. Fretting corrosion (figure 2.14a and b) is influenced by several factors, which include environmental conditions, materials properties, and contact conditions [90].

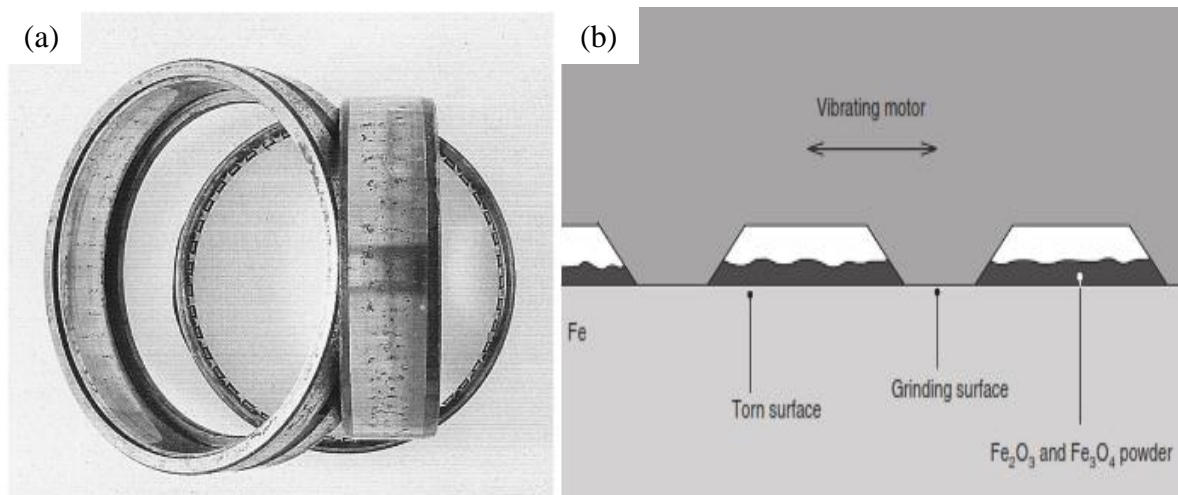
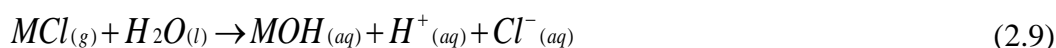


**Figure 2.14:** Fretting corrosion on roller bearing race (a) [14] and a sketch (b) illustrating the mechanism of attack [91].

**Pitting corrosion:** Pitting is a form of localized corrosion considered to be one of the most destructive and produces holes in the metal or alloy. The pits are small holes or cavities with a depth greater than or equal to the metal surface of diameter. They drill through the metal, triggering the collapse of equipment due to preformation with negligible weight loss [51, 92-94]. It is a self-sustaining type of corrosion process in which the metal dissolution occurs at a relatively small area. Compared to uniform corrosion, pitting is considered to be more dangerous and causes more damage. This is because failure can occur all of a sudden without any visual warning since significant amounts of corrosion can occur before any cracks and spalls become visible in the concrete. Thus, it is more difficult to predict, detect and prevent pitting corrosion. For instance, the immersion of metal M in an aerated sodium chloride solution (NaCl) (figure 2.15) leads to the dissolution of the metal and the formation of a pit at a localized area. The dissolution process creates an abundance of positively charged ions ( $M^+$ ) in the pit, subsequently attracting negatively charged ions ( $Cl^-$ ) in massive amounts, which result in an increase of metal salts ( $MCl$ ) in the pit. The solution in the pit becomes oxygen-depleted, and the reduction of oxygen ceases in the pit. The metal dissolution process continues in the pit which is fuelled by oxygen reduction that is occurring on the surface area outside the pit (figure 2.15), which then becomes cathodically protected from corrosion while the pit is active. The metal salts hydrolyze in the pit by a process called hydrolysis:





The solution in the pit ends up becoming acidic (i.e., pH is reduced) due to the increase of hydrogen ions ( $H^+$ ). As a result, the dissolution process increases rapidly and becomes autocatalytic; this is because of the migration and hydrolysis reaction of the chloride [51, 92-94].

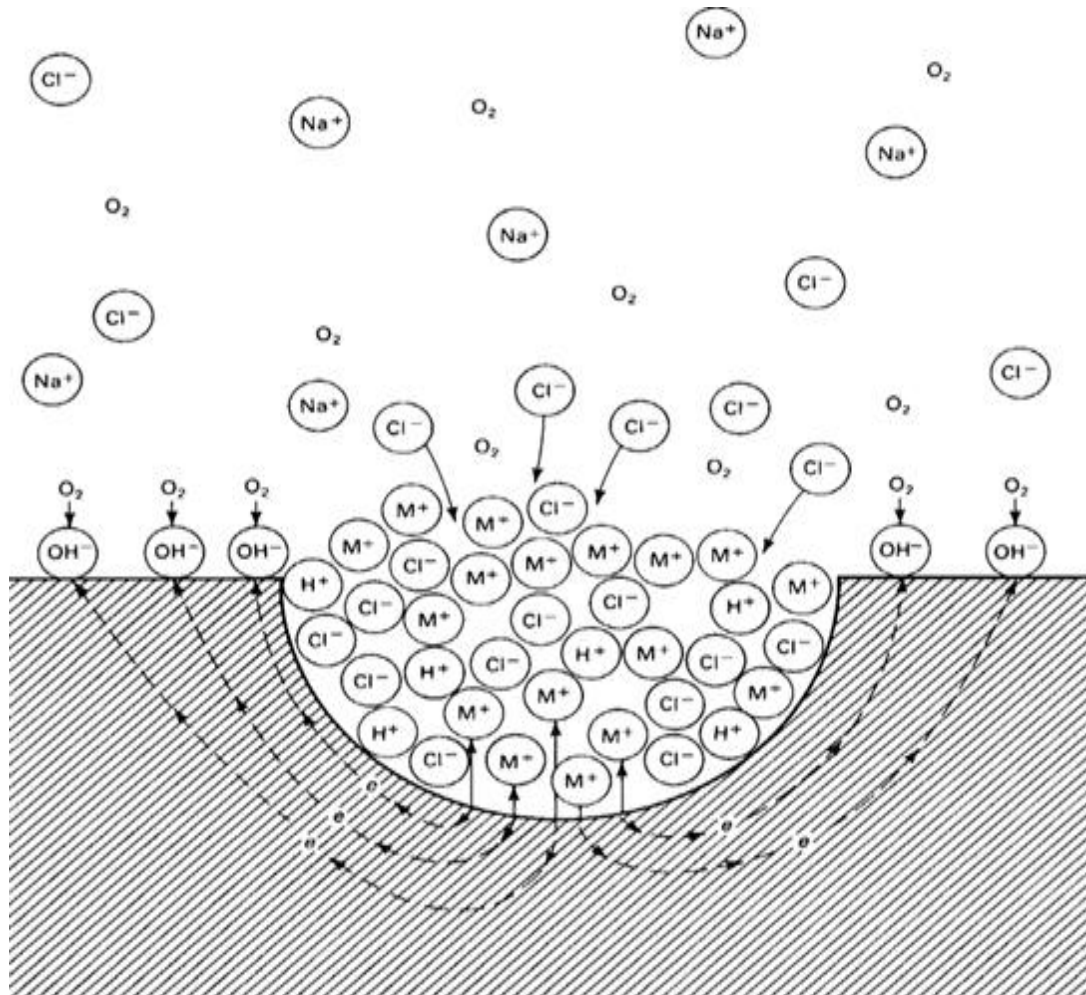


**Figure 2.15:** Diagram depicting the process occurring during pitting corrosion [51].

### 2.1.5 THERMODYNAMICS AND KINETICS OF CORROSION

When it has been ascertained that corrosion of metal will occur then the next feasible step is to find out how fast it will occur (i.e., corrosion rate), which is the objective of corrosion kinetics.

#### Kinetics of Corrosion

Corrosion kinetics is of paramount importance because it reflects the speed of the cycle of corrosion, how rapidly it happens at a particular time and place. Corrosion kinetics shows the form of reactions involved in the process of corrosion and the electrons absorbed. The electrons involved in the reactions can further be quantified as current [95, 96]. Even though the initial rate of corrosion can be distractive on metals, it often decreases over time as protective corrosion products are formed. This makes studying corrosion kinetics of paramount importance. Not only is it essential knowing if the corrosion process will occur, but it is vital also to know how fast it occurs and how the metal environment components influence the process of corrosion [97].

Further data can be produced in the corrosive environment by the electrochemical behaviour of metallic materials by the impact that temperature has on the corrosion kinetic cycle. The Arrhenius law below can be used to provide data on the relationship between the temperature dependence of the constant corrosion rate of chemical reactions [95, 96].

$$K = \frac{Ae^{-E_a}}{RT} \quad (2.10)$$

Where:

K is the rate constant

A is the pre-exponential factor or the pre-factor

R is the gas constant

E<sub>a</sub> is the activation energy

T is the absolute temperature

Equation (2.9) indicates that the corrosion rate of a certain metals increases as the temperature increases and that the activation energy (E<sub>a</sub>) and the pre-exponential factor or the pre-factor (A) usually varies with the temperature of the environment. Depending on the type of analysis,

the rate of corrosion can be evaluated by different methods, and when gravimetric methods are employed, then the equation (2.11) below can be used directly.

$$\rho = \left( \frac{\Delta W}{St} \right) \quad (2.11)$$

Where:

$\rho$  is the corrosion rate

$\Delta W$  is the average weight loss of the material

S is the total area of the material of interest

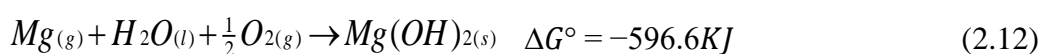
T is the immersion time

### **Thermodynamics of Corrosion**

The occurrence of corrosion is best explained in terms of the reaction that it involves and the stability of chemical species. As such, the thermodynamic control concept may be of paramount importance in grasping the process of corrosion, although thermodynamic calculations cannot foretell the corrosion rate. Thermodynamic has one huge advantage of calculating the theoretical activities of a particular metal when the composition of the environment is distinguished. When studying the corrosion processes, it is important to pay attention to the spontaneous and non-spontaneous reactions occurring [95, 96]. The Gibbs free energy can be used to provide more information on corrosion as discussed below:

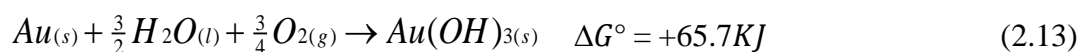
#### *Gibbs free energy*

Studies of corrosion need some insight into Gibbs free energy, which gives an idea of a chemical reactions ability to occur. The corrosion cycle is an electrochemical reaction requiring the use of free energy from the Gibbs to determine whether a spontaneous corrosion reaction may occur. Generally, the Gibbs free energy change value must be negative for a spontaneous reaction [98].



Gibbs free energy value is significant and negative, suggesting that the aerated aqueous medium has a high potential to destroy Mg. A lower negative value of  $\Delta G^\circ$ , however, would have meant a lower propensity for the reaction to occur. The thermodynamic studies reveal that metals are found in nature at their lowest energy level. This makes them to exist as complexes (i.e., combined) with other elements in nature since at this point, they are at the low, stable energy level.

For example, iron is found in nature as Fe-ores mainly because it has low energy oxides or ores. In order to separate the iron from its ore and reduce it, heat is applied. Noble metals like gold (Au) can exist alone, and this can be seen from their Gibbs free energy value, as shown below:



The Gibbs free energy for gold is positive in the above reaction to react in aerated aqueous solution. This shows that the above reaction is non-spontaneous and that in normal conditions, gold does not corrode. Also, a zero  $\Delta G^\circ$  value would imply that the reaction is in a state of equilibrium. It is important to note that a high value of  $\Delta G^\circ$  implies that the reaction will quickly occur but does not mean that the corrosion rate will be high. For example, aluminium, which has a high negative  $\Delta G^\circ$  undergoes corrosion at a slower rate as compared to iron with a lower negative  $\Delta G^\circ$  value [98]. The standard free energy of the cell reaction  $\Delta G^\circ$  under standard conditions can be calculated by the equation below:

$$\Delta G^\circ = -nF\Delta E^\circ \quad (2.14)$$

Where:

$\Delta G^\circ$  is the standard Gibbs free energy change

N is the number of electrons exchanged in the reactions

F is the Faraday constant

$\Delta E^\circ$  is the standard energy change in the reaction

Studies have shown that  $\Delta G^\circ$  values around  $40 \text{ kJ.mol}^{-1}$  or higher show chemisorption (chemical) type of adsorption and those that are around  $20 \text{ kJ.mol}^{-1}$  or lower implies physisorption (physical) type of adsorption [96].

Other thermodynamics parameters can also be used to fully grasp the spontaneity of the adsorption process of the inhibitor on the metal surface. Such parameters include the  $\Delta H^\circ_{\text{ads}}$  and entropy of adsorption ( $\Delta S^\circ_{\text{ads}}$ ). The  $\Delta H^\circ_{\text{ads}}$  can be deduced from the Van't Hoff equation below [99]:

$$\ln K = -\frac{\Delta H^\circ_{\text{ads}}}{RT} + \text{Constant} \quad (2.15)$$

Where  $K$  is the adsorption equilibrium constant,  $R$  is the universal gas constant and  $T$  is the absolute temperature.

The Gibbs-Helmholtz equation below can also be used to calculate the enthalpy of adsorption [100]:

$$\left[ \frac{\partial(\Delta G^\circ_{\text{ads}} / T)}{\partial T} \right]_P = -\frac{\Delta H^\circ_{\text{ads}}}{T^2} \quad (2.16)$$

The Gibbs-Helmholtz equations (2.16) can be arranged to give the following equation:

$$\frac{\Delta G^\circ_{\text{ads}}}{T} = \frac{\Delta H^\circ_{\text{ads}}}{T} + k \quad (2.17)$$

The  $\Delta S^\circ_{\text{ads}}$  can be calculated from the parameters of Gibbs free energy of adsorption ( $\Delta G^\circ_{\text{ads}}$ ) and  $\Delta H^\circ_{\text{ads}}$ , using the following thermodynamic basic equation (13).

$$\Delta S^\circ_{\text{ads}} = \frac{\Delta H^\circ_{\text{ads}} - \Delta G^\circ_{\text{ads}}}{T} \quad (2.18)$$

The equilibrium constant ( $K_{\text{eq}}$ ) for the reaction can be calculated using equation (2.19) below:

$$RT \ln K_{\text{eq}} = -\Delta G^\circ = nF\Delta E^\circ \quad (2.19)$$

### 2.1.6 THE RATE OF CORROSION

As previously mentioned in section 2.1.1.2 by the Wagner and Traud theory [55], three essential steps form part of the foundation required for corrosion to proceed and if one of these steps is prevented from occurring, it stops the process of corrosion or reduces the rate at which it occurs. Among these steps, the slowest step is the rate-determining step for the overall corrosion process. During the corrosion of steel, of the three steps involved, the cathodic reaction is the slowest step. Therefore, the cathodic reaction is the rate-determining step for steel corrosion. When the cathodic surface area is large compared to the anodic area, this then allows more electrons, oxygen and water to react thereby increasing the rate at which electrons flow from the anodic area to the cathodic area resulting in the rapid increase of the corrosion rate. Nevertheless, the rate of corrosion increases as the cathodic region becomes smaller compared to the anodic area. This ratio affects the corrosion rate and is critical in the choice of an active corrosion inhibitor [101].

### 2.1.7 FACTORS AFFECTING THE RATE OF CORROSION

There are several factors that affect the rate of corrosion of metals, either by speeding up or slowing it down. Factors that are of significant interest in this present study will be briefly discussed in the following sub-headings.

***Chemical deposits:*** These are deposits introduced onto the surface of the metal in the form of coatings left through the process of evaporation and electrolysis. This factor is one that has received less interest amongst the other factors affecting the corrosion rate even though it results in the most destructive damage on the metal surface. The use of chemicals as a means of inhibiting corrosion usually result in their deposits that lead to harsh corrosion problem on the material they are protecting or inhibiting [102, 103].

***Galvanic effects:*** These are effects observed during galvanic corrosion when two different metals are in contact or joined together when developing cooling systems to be exposed to water. The galvanic series shows that lower metals tend to have a high tendency to undergo corrosion (i.e., corrode), while the upper metals have a lower tendency of being corroded. In the galvanic series, magnesium is the most active metal while gold; on the other hand, is the least active. The galvanic series is based upon gauging the potential of different metals compared to the hydrogen electrode (i.e., reference electrode). When metals far from each other on the series are coupled together, in the presence of an electrolyte, the rate of galvanic

corrosion is very fast; regardless, however, metals can still be carefully selected from the series in such a manner that results in the reduction of corrosion rate [104].

***Effect of dissolved oxygen:*** The amount of dissolved oxygen (DO) in water plays a complicated but significant role in the corrosion of metals. Since the cathodic process of corrosion involves the presence of oxygen on the metal surface in alkaline, acidic and neutral solutions, in the absence of DO in the water, the process of corrosion is reduced almost to zero in neutral and alkaline solution. However, as the concentration of DO increases, the process of corrosion occurs at a faster rate due to the involvement of oxygen in the cathodic process. The depolarization process of the cathodic products occurs when oxygen is present as depicted in equation (2.1) and (2.3). In most circumstances, the depolarization by oxygen tends to control the rate at which iron is corroded, but the rate at which equation (2.3) occurs is mostly at a faster rate to the point that the concentration of oxygen approaches zero at the cathodic surface. The rate of oxygen depolarization is, therefore, dependent on the rate at which oxygen is diffused through the resistant film formed on the metal surface. The process of oxidation converts ferrous iron into a ferric state, and most normal rust is made up of the hydrated ferric oxide. Rust film that is formed as a result of corrosion is generally composed of three layers of iron oxide in various oxidation states, and this is because a black layer of magnetic hydrous ferrous ferrite  $[\text{Fe}_3\text{O}_4 \cdot n\text{H}_2\text{O}]$  is frequently formed between  $\text{FeO}$  and  $\text{Fe}_2\text{O}_3$ . When the concentration of oxygen has passed a critical point, the rate of corrosion drops again to an even lower value even though an increase in the concentration of oxygen at first result in the acceleration of corrosion of iron. The rate of corrosion usually decreases if a large amount of oxygen is introduced into high purity water at a high temperature and specific conditions resulting in the formation of a protective passive dense film that consists of metal oxides present on the surface of the metal [105]. The injection of water is used as one of the measures for controlling corrosion in a power station. Cohen [106] reported that in the presence of oxygen, the rate of corrosion occurs 65 times than it would when oxygen is absent. The rate of corrosion increased at a higher velocity as reported by Whitman [107] as a result of an increase in the diffusion and breaking down of protective films on the metal surface. Frese [108, 109] presented that iron becomes passive in the presence of high oxygen concentration. Figure 2.16 below shows the effect of oxygen concentration on the corrosion of low carbon steel in tap water at different temperatures.

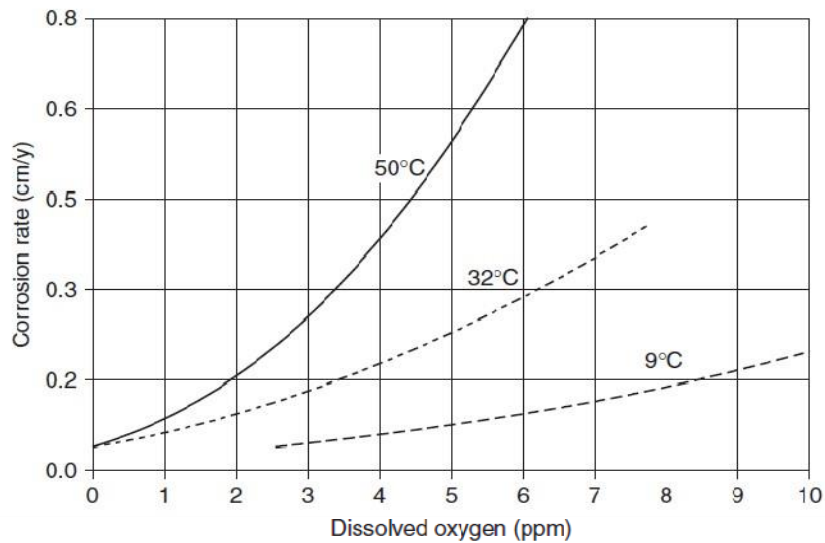


**Figure 2.16:** The effect of oxygen concentration on the corrosion of low carbon steel in tap water at different temperatures [68].

**The temperature of the medium:** The process of corrosion is an activation-controlled chemical reaction, and its rate is highly influenced by temperature. When the temperature increases, it frequently increase the corrosion rate. The process of corrosion being controlled by diffusion of oxygen is an essential criterion that the corrosion rate doubles for every 30 °C rise in temperature at a given oxygen concentration. When the corrosion process is occurring in an open vessel that permits dissolved oxygen to escape, the rate of corrosion increase as the temperature is increased, to a high temperature of 80 °C and decreases after that to a lower boiling point value. The lower corrosion rate that occurs above 80 °C is linked to a decrease in the solubility of oxygen in the water as the temperature is raised, and this eventually overshadows the accelerating effect of temperature alone. In a closed system, however, since oxygen cannot escape, the rate of corrosion increases with temperature until all the oxygen is consumed. The rate of corrosion doubles for every 30 °C rise in temperature when the process is followed by hydrogen evolution [110]. The depolarization by hydrogen evolution generally results in the increase in temperature, increase in diffusion, and decreases in both the viscosity and over-voltage. When the diffusion increases, this allows more dissolved oxygen to react with the cathodic surface resulting in the depolarizing of the corrosion cell. In a domestic water system, an increase in temperature from 25 °C to 75 °C, as shown in figure 2.17, may result in an increase in the corrosion process to as much as 400 percent. The temperature increase of the system usually causes the chemical reaction to speed up, as stated by the thermodynamic considerations [111].



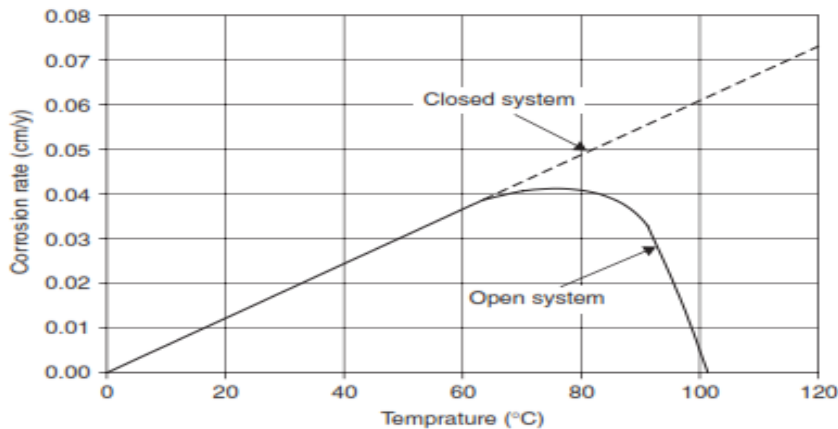


**Figure 2.17:** The effect of temperature on the corrosion rate of low carbon steel in tap water [68].

**The availability of a corrosion inhibitor:** Inhibitors are classified as substances that are introduced in minimal concentration into a corrosive environment and affects the rate at which corrosion takes place for a given metal. As recorded in literature, the higher the concentration of an inhibitor, the slower the rate of corrosion would be [60, 112, 113].

**Hydrogen ion concentration of the solution:** The rate of corrosion increases as the concentration of hydrogen ion for a given environment increases. This process occurs when the pH of the medium is decreased [114]. The alkaline environments are less corrosive than the acidic environment and contain a lower concentration of hydrogen ions and high pH values. The movement of metal ions in the alkaline environment from the anode towards the cathode results in a slow corrosion rate as opposed to those of acidic environments [60, 114].

**The nature of the metal:** The electrochemical series shows that metals with more positive potential are more stable as compared to those of more negative potential [47, 115]. One can predict whether a metal would undergo corrosion or not by making use of the electrode potential of the metals in some electrolyte. The electromotive force (E) is defined as the difference between the electric potentials of the cathodic and anodic reaction and is related to the Gibbs free energy equation (2.13):

$$E = E_{cathodic} - E_{anodic} \quad (2.20)$$

When the process of corrosion occurs, hydrogen is evolved during the cathodic reaction, and its overpotential affects the process. When a metal is being corroded in a particularly corrosive environment, it has a unique hydrogen potential. As a result, a metal with low hydrogen overpotential undergoes external corrosion. However, when alloys are considered, entities added in minute quantities will change the hydrogen overpotential affecting the corrosion process as a result [47, 115].

**pH:** Is defined as the hydrogen ion ( $H^+$ ) concentration in a solution. A higher pH suggests a low number of hydrogen ions, but a low pH indicates more hydrogen ions in solution. Acidic solution (low pH) increases the rate of corrosion since there is a high supply of hydrogen ions. For closed-loop systems, the pH of water is maintained at 8.5 to 9 and 11 for boiler systems. The primary type of corrosion that occurs in an acidic medium (i.e., pH 5 and below) is called uniform corrosion. When the pH is increased above 4, iron oxides precipitate from the solution forming deposits which blocks the diffusion of oxygen towards the surface of the metal, decreasing the rate of corrosion as a result. Moreover, the nature of the iron oxide deposits transforms from loosely adhering at pH 6 to hard and persistent form at pH 8 with an increase in temperature [116].

**Microbial activity:** Microbes affect and accelerate the rate of corrosion by adhering to the metal surface forming a biofilm. This type of microbial action is referred to as biofouling and has detrimental effects associated with it. Most engineering alloys, except titanium along with high nickel-chromium alloy, are damaged due to corrosion caused by microbial activity. Microorganisms like bacteria, fungi and algae, grow and propagate ideally in recirculating water systems environments and can break the continuous flow of water that occurs through heating equipment like heat exchangers and other similar conduits. Biofouling process interferes with the transfer of heat by reducing the transfer efficiency contributing to the internal corrosion and damaging the entire water circulating system [1, 116].

### 2.1.8 CONSEQUENCES OF CORROSION

The outcomes of corrosion vary, and their effects are more severe than the mere loss of metal mass; such effects compromise the safety, efficiency and reliability of the equipment made up of these metals. The burden placed on the economy by corrosion is enormous and expensive as it results in unnecessary mining and replacement of the corroded metal. Various harmful effects of corrosion are discussed briefly below:

*Nuclear effects:* Corroded radioactive products can be transported to water streams and become detrimental to plants, animals and humans. The Chernobyl disaster is one example of this kind of nuclear effect [56].

*Health effects:* The easy use of metals make it possible for their application in the health sector. Metals have been used as prosthetic devices to aid in hip joints and pacemakers in recent years, and their corrosion in human bodies may result in harmful effects on human health [68, 102].

*Contamination effects:* Corrosion can lead to the contamination of soils and groundwater as a consequence of pipes bursting, resulting in the leakages and contamination of vessel fluids. This effect does not only affect the liquids carried by these pipes but can also have a significant impact on the quality of agricultural land that the leakages seeps in for decades. The rupturing and leakages of fuel gases can result in explosion and fire, which can cause great harm, particularly within urban areas [117, 118]. An example of the contamination effect is beer going cloudy when a small amount of corroded heavy metals is released. Corrosion can also result in the contamination of dyes, chemicals, packed food, water and pharmaceuticals [56].

*Cultural effects:* Artefacts that are precious, valuable and carry historical value to communities and countries can/are severely deteriorated because of corrosion. When this artefact (metal) is destroyed, the history that connects and defines generations of humans is cut short [68, 102].

*Safety effects:* Metals are found in almost everything that humans use in their everyday life. Human beings are subjected to injuries and loss of lives in instances of metal failure due to corrosion. For example, metals find application in the construction and transportation industries. Thus, human safety is of priority concern [68, 102].

### 2.1.9 COST IMPLICATION OF CORROSION

It is essential to pay a keen interest in corrosion as it results in substantial economic loss and is inescapable. Even though advanced and developing countries tackle the issues of corrosion at different degrees, the effort they put into preventing the corrosion menace is vital and the key to combating corrosion [119-124]. In 1949, Uhlig [125] pioneered the research in the economic cost of corrosion; he estimated the annual cost of corrosion in the United States of America (USA) to be 2.1% of the country total Gross Domestic Product (GDP). His research was followed by several studies on the economic cost of corrosion around the world, including countries such as the United Kingdom, Kuwait, Sweden, Japan, China, Australia, Finland, and India. The characteristic finding from all these studies was the fact that the annual cost of corrosion ranged roughly between 1 to 5% of each nation GDP [126]. In the late 1970s, the USA embarked on a significant study of the economic effects of corrosion. The study revealed that the total loss as a result of corrosion in the year 1975 was \$70 billion, approximately 5% of the country GDP of that particular year [127].

The USA Federal Highway Administration (FHWA) published an important discovery in 2002, which estimated the direct cost of corrosion associated with the metallic corrosion in the USA industrial sector. The study was established by the National Association of Corrosion Engineers (NACE). The total annual direct cost of corrosion was found to be \$276 billion, approximately 3.1% of the nation's GDP [39]. This figure could be even more since it does not include the direct cost of corrosion during the replacement of damaged components or materials. The indirect cost of corrosion such as environmental damage, injuries, transportation disruption and loss of production was roughly calculated to be equal to the direct costs of corrosion [128].

In recent papers, the worldwide economic loss due to corrosion was reported to be \$2.5 trillion as estimated in 2016 by NACE international [129, 130]. In SA, the research conducted by the University of Witwatersrand in association with the Corrosion Institute of Southern Africa (CorrISA) showed that R154 billion per annum is spent on combating the effects of corrosion in industrial areas, which supports the research findings of MINTEK which found that the direct cost of corrosion to the economy of SA in 2004 was R130 billion per annum. [42]. Flow diagram in figure 2.18 illustrates the cost effects of corrosion.

Recent data on the cost of corrosion in SA is limited and not readily available in the literature. The absence of such data can be interpreted as demonstrating the lack of the country viewing

the issue of corrosion as a significant problem. Thus, the present study is very significant in SA and can show how devastating corrosion can be and how to tackle it.

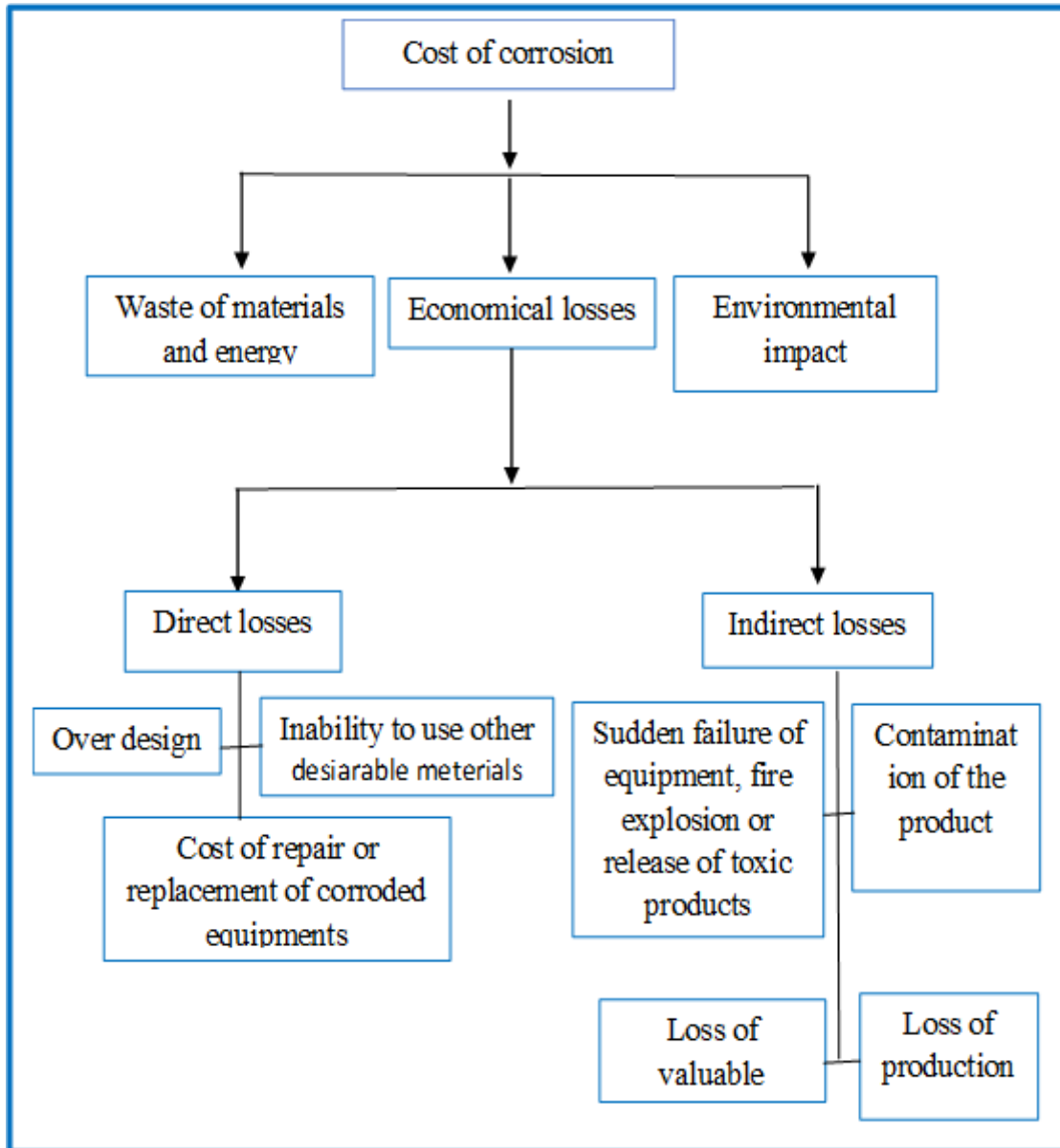


**Figure 2.18:** Flow diagram illustrating the cost effects of corrosion [128].

## 2.2 CORROSION OF METALS

### 2.2.1 ALUMINIUM (Al)

Aluminium has excellent thermal and electrical conductivity with the density lightweight of  $2.71 \text{ g.cm}^{-3}$  [131]. It is used in many industries to manufacture equipment used in construction, automotive, food handling, heat exchange, aerospace and electrical transmission [132-134]. This metal differs from mild steel in a manner that the oxide formed in mild steel by oxygen attaches loosely to the metal surface and does not stay bound to the metal, while in Al the coating formed by the oxide bonds with the metal surface. Aluminium is consequently less disposed to corrosion than mild steel [135, 136].

Moreover, Al is highly reactive and withstands most corrosive conditions, although it may undergo corrosion if exposed directly to corrosive environments. The corrosion resistance of this metal is due to the Al oxide film inert and protective nature, which forms on the metal surface when exposed to moisture [137-140]. The thickness of an oxide layer that helps prevent corrosion is affected by several factors, and amongst others, this includes elements present in the alloy, the environment and temperature. The oxide layer is thinner than the one that can result in high temperatures. Nevertheless, when corrosion damages the old oxide film, a new one rapidly forms [135]. Sadly, the Al metal suffers from corrosion in acidic or alkaline environments (i.e., pH 4 or 9) as the passivation layer is lost. The oxide layer is attacked usually by fluoride or chloride ions, causing the metal to corrode. This metal is resistant to most forms of corrosion, but the most common type of corrosion it undergoes is pitting corrosion resulting from reactive species such as chlorides. Researchers are paying more attention to the corrosion studies of Al and Al alloys due to their technological and industrial applications [141-145].

The corrosion process of Al is an electrochemical reaction where the Al metal disintegrates, and electrons move from the anode to the cathode where they are taken up. The corrosion reactions taking place in aqueous solutions involves the reduction and oxidation of species in the solution due to the transfer of the electron between both the reactants. Oxygen undergoes reduction at the cathode where the  $\text{OH}^-$  is formed while  $\text{Al}^{3+}$  ions are released from the anode through an oxidation process.  $\text{Al}(\text{OH})_3$  deposits are formed by Al and  $\text{H}_2\text{O}$  converting into ions  $\text{Al}^{3+}$  and  $\text{OH}^-$  and reacting together. This is because of a gel, or white powder that is formed on the surface of Al metal alloy, and any further damage to the protective oxide film on the metal surface is from the release of  $\text{H}_2$ . Electrochemical reactions that take place during the process of corrosion of Al metal are shown below:



The cathodic reaction exemplifies corrosion in a natural environment where the corrosion occurs at near-neutral pH values. The cathodic reaction in acidic solution is [146]:

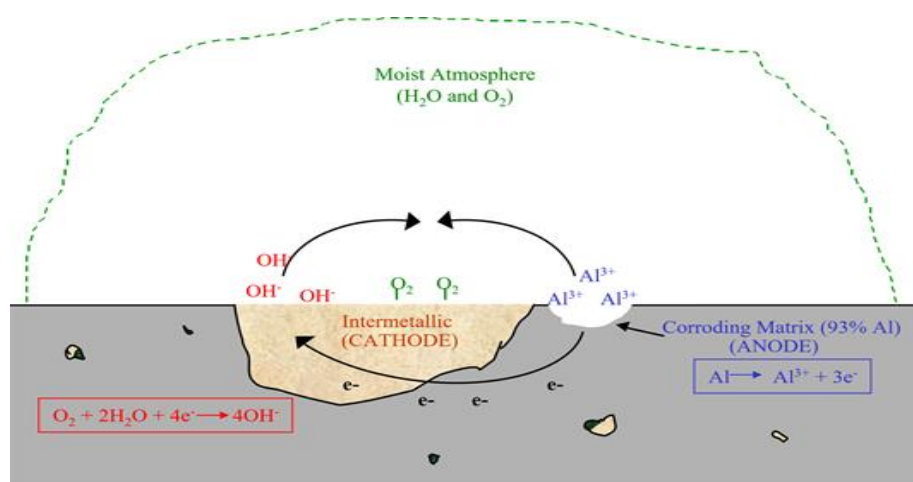
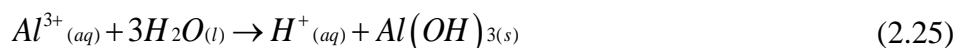


**Figure 2.19:** A schematic electrochemical mechanism of Al alloy corrosion [147].

The electrons are transferred through the metal to the cathode. When the Al cation combines with the hydroxyl anion in the liquid, this produces a solid precipitate, as shown in figure 2.19 and when both the cathodic and anodic partial reaction mix, then an Al hydroxide is produced (equation 2.22 and 2.23). Thus, a white crystalline product of corrosion is formed on the surface of the Al metal.



The process involves the consumption of hydrogen ions and the pH of the droplet rises as the corrosion of Al takes place. Instead, as the concentration of hydrogen ions decreases, the hydrogen ions emerge in the solution (water) and then combine with the Al ions and create insoluble hydroxide or green rust [148].

### 2.2.2 MILD STEEL (MS)

Mild steel is an alloy that is comprised of iron with a low quantity of carbon and other elements such as sulphur, Al, silicon, phosphorus, magnesium and silicon. The quality of steel, hardness, strength and ductility differ with the amount of the alloying element [149]. Due to its low carbon content, MS has interesting mechanical properties and the higher the amount of carbon, the stronger, stiffer and harder the steel is. Therefore, carbon is an alloying element that increases the hardness of the steel [150].

Mild steel is inexpensive, readily available, mechanically durable, thermally and electrically conductive, weldable and malleable. As such, it is used for both domestic and industrial applications. It is used in different areas such as boilers, petrochemical industry, oil and gas industry, marine applications automobiles, medical prosthetic implants, heat exchangers, electrical appliances, agricultural implants, cookware, and so on. However, it readily undergoes rusting when exposed to corrosive environments containing humidity, acids etc [151].

The compositions of MS vary due to its applications, and the maximum limit of carbon content in all acceptable forms is around/at 0.29% with the proportions of copper, silicon and magnesium fixed at 0.6%, 0.6% and 1.65%, respectively. The percentages of molybdenum, cobalt, niobium, chromium, titanium, zirconium, tungsten, vanadium and nickel are varied. However, the composition of iron is consistent at approximately 99% [105]. When metals corrode, the oxide layer formed on the surface of the metal has specific characteristics and colour. The colour that result is from the amount of water available in the oxide. The rate of corrosion is prolonged in environments with low water content as compared with high water content environments or alkaline and acidic conditions. When MS is exposed to extreme acidic environments, iron is corroded forming rust. The name rust is commonly used to describe iron oxides and hydroxides. For example, the iron compounds such as  $\text{Fe}(\text{OH})_3$ ,  $\text{FeO}(\text{OH})$ ,  $\text{Fe}_2\text{O}_3 \cdot \text{H}_2\text{O}$  and  $\text{Fe}(\text{OH})_2$ , are all forms of rust that result from the corroded iron [106]. When steel deteriorates in various environments, they resist corrosion in a quick manner and reagents that are frequently used such as  $\text{HCl}$  and  $\text{H}_2\text{SO}_4$  are vital and essential for economic consideration in many industries [149].



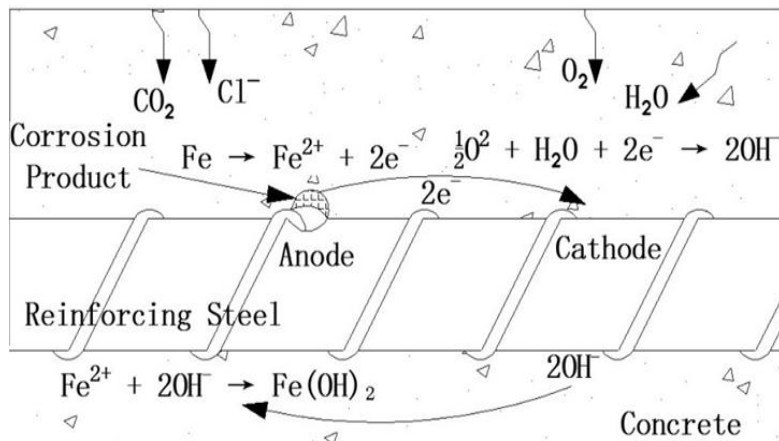


**Figure 2.20:** Schematic diagram of the corrosion process of the reinforcing steel rebar in concrete [152].

The corrosion mechanism process of steel takes place, as described in section 2.1.1 under the Wagner and Traud theory of corrosion.

### 2.2.3 ZINC

Zinc is a precious metal used in steel and iron coating. This usage is because it has several features that make it suitable for metal coating and improves iron and steel resistance to corrosion [153]. Thus, zinc is mostly used in the protection (galvanization) of iron by cathodic protection since it is higher than iron on the electrochemical scale, reducing it to the metal and destroying the rust in the process [20]. Zinc can also be used to coat and protect other metals that are linked to the electrochemical series which accounts for its employment in galvanizing industries, consequently making galvanizing one of the most crucial method for the protection of machines and building structures [154]. Zinc is the most important metal coated on steel structures to resist corrosion in atmospheric environments, due to its ability to produce a protective oxide layer of zinc carbonate that decreases the rate of corrosion in the same way as Al in the atmospheric environment [155].

Pure zinc does not react with dilute acids or even water since it forms a thin hydrogen gas layer on the surface of the metal. This metal creates hydroxide ( $\text{Zn}(\text{OH})_2$ ) that can dehydrate producing anhydrous oxide ( $\text{ZnO}$ , that is critical in ceramics, ink and rubber industries) and zinc salt in an acidic solution or zincate in alkaline solution. Zinc compounds such as zinc chloride ( $\text{ZnCl}_2$ ) and zinc sulphate ( $\text{ZnSO}_4$ ) are required in massive amounts worldwide, as they are used as deodorants in many fluids and also to treat a zinc deficiency in textile and soil industries respectively [20, 154, 156]. Zinc is non-toxic and essential to plant and human

growth in comparison to metals like lead and cadmium, which are toxic [154, 156]. Also, zinc is less damaged by corrosion compared to MS since it can form insoluble essential carbonate films that have the ability to stick to the surface of metal-reducing the rate of corrosion as a result. Zinc corrosion depends on the type of environment in which corrosion is taking place. The lowest corrosion rate has been observed in environments that have a pH of 6.5 to 12. The corrosion rate of zinc is accelerated by conditions such as marine, acidic or alkaline to the point that it becomes useless and cannot be used in such environments, making it vital to protect zinc against corrosion [155]. When zinc is exposed to aggressive ions (chloride ions), it suffers from pitting corrosion.

Below are the half-reactions that the corrosion of zinc follows [157].

Anodic reaction: Zinc firstly undergoes oxidation and is oxidized into  $Zn^{2+}$  ions as in the reaction equation (2.24).



Cathodic reaction: Then hydrogen ion is reduced to hydrogen gas by gaining two electrons from the oxidized zinc metal.



The overall reaction: The anodic and cathodic reaction can be combined to form the final reaction, as indicated in equation (2.26).

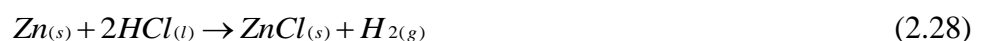
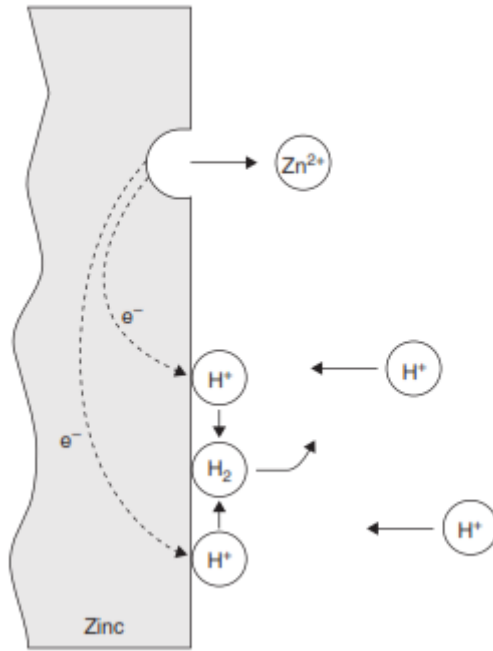


Figure 2.21 below elaborates the process of corrosion on the surface of zinc metal schematically.



**Figure 2.21:** Diagram of the zinc corrosion cycle in HCl [68].

## 2.3 CORROSION PREVENTION METHODS

Metals such as Al and MS are prone to corrosion as they strive to return to their most stable oxidation state (i.e., natural state). However, specific mitigation procedures can be applied, which may result in the minimization of the corrosion effects. These measures reduce the corrosion rate to an economically sustainable level. The mitigation procedures amongst others include inspection, dehumidify, plating, cathodic and anodic protection, protective coatings, design improvement and most importantly, the use of inhibitors. Inhibitors are employed as a form of corrosion control in this study to protect Al and MS in a corrosive environment of HCl. Below is a brief explanation of some of the methods of corrosion prevention:

**Protective coatings:** Coatings are described as thin materials that are applied to provide a barrier between the materials and the corrosive environment. The barrier created protects the material by depriving it from oxygen or by resistance inhibition. The inhibitive coatings protect against corrosion by altering the chemistry occurring at the surface of the metal substrate [158]. Coatings such as paints are used mostly to protect metallic surfaces of vehicles from corrosion. There are several other types of coatings in addition to paints, and some of them include auto-deposition, wax, powder, inorganic, electroplating and metallic coatings. All the coatings mentioned here impede corrosion by preventing direct interaction between the metal surface and the corrosive environment [159]. Coatings generally have two important purposes; one is the cosmetic purposes while the other is corrosion protection. The latter purpose is of interest to engineers, and they can choose the proper coat for metal from a wide range of coatings. However, as far as corrosion control is concerned the most widely used coating for corrosion are protective coatings. These special coatings work by means of separating the surface that is vulnerable to corrosion from the corrosive environment. The downside of protective coatings is that they cannot provide 100% protection to the surface of metals/materials. This drawback is observed mostly in the localized form of corrosion and causes a rapid catastrophic failure; thus, additional corrosion control measures must be put in place. For example, corrosion control coatings are useful when coupled with other techniques such as galvanic or cathodic protection [61].

**Design Improvement:** Proper design considerations can also extenuate corrosion. Applying acceptable engineering techniques to reduce the effects of corrosion is important to the control of corrosion. When designing for corrosion control, there is one crucial factor to consider, and that is to avoid crevices in places that are not accessible to maintenance and where water-soluble deposits can accumulate. A crevice site can be any region where two surfaces are joined to come into proximity with one another. Other crevice corrosion problems can also be avoided by combining the geometries of two surfaces. Examples include back-to-back angles, intermittent welding, weld spatter, bolting, rough welds, sharp edges, discontinuities, and corners [160]. Applying a rational design principle can significantly decrease the cost and time associated with repairing and maintaining damage caused by corrosion, as shown in figure 2.22 [161].

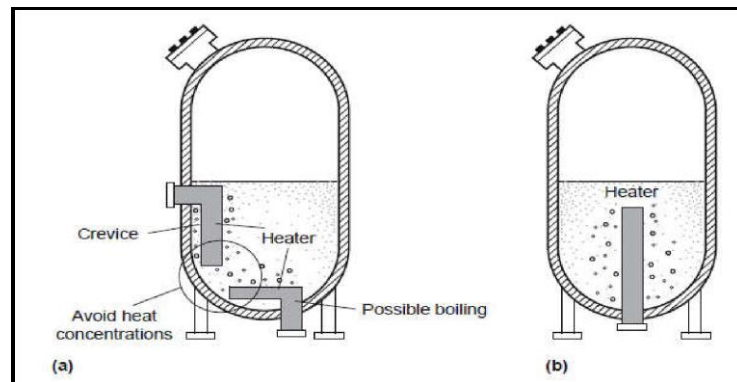


**Figure 2.22:** A poor (a) and good designs (b), for heating solutions [162].

In the poor design (a) there are gaps known as hot spots as shown by the circled area; the hot spots can induce boiling at the bottom of the vessel walls under the heater, trapping fluids and eventually leading to crevice or gasket corrosion. In functional design (b); however, the model can be constructed so that the formation of pockets and hot spots where a small volume of liquids can be trapped is avoided.

**Cathodic and anodic protection:** Cathodic and anodic protection is the type of methods that involve the alteration of a metal potential. The potential of the metal of interest can be altered or shifted into a region of passivity or immunity, either by the galvanic action that occurs due to the connection of dissimilar metals or by the application of direct current from a power supply. Shifting the potential to more oxidizing conditions (positive) within a region of

passivity is referred to as anodic protection. Whereas, the shift to a more reducing (negative) potential favours immunity of the metal and is referred to as cathodic protection.

Cathodic protection is described as a technique that can be applied to structures that are exposed to a continuous electrolyte. The technique applies virtually to all types of metals and has been used for more than 175 years. Some of the typical application includes protection from marine corrosion and soil corrosion. Cathodic protection is frequently applied in conjunction with organic coatings. Below are some of the limitations of cathodic protection [163]:

- (a) Results in stray-current corrosion in a neighbouring unprotected buried structure.
- (b) Materials can remain exposed to the corrosive environment and remain unprotected if the polarization is too weak.
- (c) Applying the cathode current can result in the destruction of passivity in certain passive alloys such as stainless steel.
- (d) If polarization is too high, certain metals such as lead, and tin can be attacked by gasification forming gaseous hydrides, which results in the weakening and consequently disintegration of articles.

Anodic protection is the most recent method for corrosion protection available. The technique was first applied in the late 1950s but became commercially successful in early 1970s and is now being used on a smaller scale when compared to other corrosion protection techniques. This type of protection is realized by maintaining an active-passive alloy or metal in the passive region by an externally applied anodic current [162]. Anodic protection has advantages and disadvantages associated with it, and some of them are described in the sub-headings below [164-167]:

Advantages:

- It can be conducted in the presence of acids.
- It can be applied in fertilizer industries and other chemical industries.

Limitations:

- It requires expensive instruments like a potentiostat.
- This technique applies to limited types of metals which can be passive in specific environments only.

- The metal cannot be protected above the waterline.
- The technique cannot be applied for metals exposed to an aggressive environment containing anions such as chlorides.

***Corrosion inspection and monitoring:*** Most of the damage caused by corrosion is related to inadequate monitoring and management of equipment by humans. Corrosion attack is also initiated by a lack of attention to technical shortcomings and insufficient review of the design. Thus, it is essential to make sure that issues of technical corrosion are appropriately managed, and the proper human response is provided to tackle them. To ensure unabated operations of industrial processes occurs at minimum cost, the inspection of corrosion should be conducted during the period that equipment is designed until they shut down. Inspections must be conducted from time to time by corrosion engineers to ensure that equipment are working under proper conditions. Methods that can be used to evaluate the corrosion rate include weight loss analysis and other modern electrochemical techniques like linear polarization resistance (LPR) and electrochemical impedance spectroscopy (EIS), and such methods must be used to inspect changes in physical dimensions and properties of the materials [168-170].

***Proper selection of materials:*** It is paramount to know the type of corrosion that is attacking a specific metal. This knowledge is vital because there is no material in existence that is immune to corrosion in all environments. As such, materials must be frequently matched with the type of environment they are to be utilised in. The selection of materials to be utilized in a particular environment is usually done during the stages of design and relies on factors like the cost of material, chemical, physical and visual properties. For instance, titanium would be the ideal material choice in most situations since it is exceptionally resistant to corrosion. However, steel is often used due to its low cost and flexibility as opposed to titanium. Steel is used in the oil industry to manufacture equipment such as vessels, pipes, tanks, and wells as results of its mechanical property and low cost. However, in other situations, there is a need to use a more corrosive resistance material(s). Thus, other alternative metals such as cobalt, chromium and stainless steel may also be used [1].

***Modification of the Corrosive Environment:*** This is usually done with the use of corrosion inhibitors. A detailed discussion of corrosion inhibitors is presented in the next section.

## 2.4 CORROSION INHIBITOR AND INHIBITION MECHANISM

### 2.4.1 DEFINITION OF CORROSION INHIBITORS

Corrosion inhibitors are chemical substances that are introduced into a corrosive (medium) environment in minute concentration with the sole purpose of depressing the aggressiveness of the environment without reacting significantly with the environmental components. Depending on the specification, the concentrations of inhibitors can range from 1 to 15,000 ppm (0.0001 to 1.5 wt percent). Inhibitors for oxidation process (corrosion) can be oils, solids, and fluids that can be used in water, solid, and gas materials. An atmosphere or water vapour can be the gaseous medium. Coal slurries, asphalt or natural coatings can be solid media. Liquids can be an aqueous, organic or liquid solution. Depending on their dispersibility or solubility in fluids to be inhibited, inhibitors are picked.

To suppress hydrocarbon processes, for example, inhibitors that are soluble in hydrocarbons are used. In two-phase systems composed of both hydrocarbons and water, oil-soluble water-dispersible inhibitors are utilized. An active inhibitor is one that is environmentally friendly, cheap, and produces the desired effect when used in low concentrations. A significant number of scientific studies have been devoted to the subject of corrosion inhibitors [160, 171-183]. Inhibitors are used mainly to ensure adequate regulated concentrations in closed environments with good circulation. These conditions can be used in oil refining, water recirculation systems for cooling, oil production, and steel component acid pickling. The selection of an inhibitor for a particular system must be made cautiously; this is because an inhibitor that provides excellent protection for one metal in that system can aggravate the corrosion for other metals in the same system [174]. Inhibitors can be inorganic or organic compounds usually dissolved in aqueous environments. Heterocyclic nitrogen compounds, amines, sulfur compounds such as thioethers, thioalcohols, thiourea, thioamides, and hydrazine are some of the most efficient organic inhibitors. Silicates, carbonates, chromates, phosphate nitrites, and arsenates are some of the examples of inorganic inhibitors. Nowadays, the use of chromates and zinc salts has increasingly decreased because of their toxicity and have been replaced by organic inhibitors. Therefore, practical criteria for choosing corrosion inhibitors from the great variety of organic and inorganic substances with inhibiting properties should not only be based on their inhibition efficiency but also economic constraints, safety, and compatibility with other chemicals in the system and environmental concerns [174].



To be an efficient corrosion inhibitor, the inhibitor must at least satisfy the following requirements [183, 184]:

- a) It should be capable of protecting the entire exposed surface of materials from attack by an aggressive solution.
- b) The inhibitor molecules should possess strong electron donor or acceptor properties or even both.
- c) When an insufficient concentration of the inhibitor is used, the rate of corrosion should not increase drastically. The same condition should apply in the case of an overdose of the inhibitor.
- d) It must provide excellent inhibition efficiency even at a deficient concentration.
- e) It should be soluble enough to be saturated rapidly in the corroding area without being leached at the same rate.
- f) It should be capable of suppressing both localized and uniform corrosion.
- g) It must be active at the specific pH and temperature of the environment of interest.
- h) It should not cause any toxicity or pollution problems.
- i) It must be compatible and capable with the proposed system so that adverse side effects are not produced.

#### **2.4.2 MECHANISM OF CORROSION INHIBITION**

Corrosion inhibitors protect against corrosion by forming protective films on the metal surface, diminishing any possible contact of the metal surface with the aggressive environment. For inhibitors to be able to protect the metal from corrosion, they must first reach the metal and react with the products of electrochemical reactions or get adsorbed (adsorption) to the metal surface [171, 175, 181, 185]. As such, substances used as corrosion inhibitors must have centres or functional groups in their molecule, with a high electron density from which they could donate electrons to the metal surface, resulting in the coordination of the inhibitor to the metal surface [142, 185]. The mechanism of protection by inhibitors is not general but varies depending on whether the inhibitor is cathodic, anodic or adsorption inhibitor. The cathodic inhibitors protective mechanism depends on their reaction with products of the electrochemical cathodic response ( $\text{OH}^-$ ). While, anodic inhibitors like molybdate, phosphate, nitrites and carbonate act by forming passive oxide, hydroxide or salt layer. For example,  $\text{Zn}^{2+}$  ions react with  $\text{OH}^-$  ions forming an insoluble  $\text{Zn}(\text{OH})_2$  layer at cathodic sites of metallic surfaces. Organic inhibitors are adsorbed on the metal surface and the presence of electrons in

conjugated double or triple bonds and electronegative functional groups, promote their adsorption on a metallic surface and as such, function as an exceptional corrosion inhibitor. The structure of the corrosion inhibitor compound must contain several numbers of heteroatoms like oxygen, sulphur, phosphorus and nitrogen to provide a high inhibition efficiency [142, 171, 175, 181, 185].

### 2.4.3 ADSORPTION AND ITS INFLUENCE ON CORROSION INHIBITION

The adsorption process is defined as a surface phenomenon that is encountered or exhibited by solid materials which consist of adhesion in very thin layers of molecules, gases, dissolved substances and liquids that are in contact with the materials. The mutual interactions of species present at the boundary stage, such as the adsorbent electrostatic and chemical interactions with the surface, adsorbate-adsorbate and adsorbate-solvent interactions, are used to determine the adsorption of ions or neutral molecules on the metal surface immersed in the aggressive solution [186, 187]. The potential energy of surface adsorbing an inhibitor or molecule decreases as the inhibitor approaches the surface. The nature of the solid and of the molecules being adsorbed significantly influences the degree of adsorption, and it is a function of pressure (or concentration) and temperature [188]. An adsorbate is a substance that is adsorbed on a thin layer of another substance which can be of solid surface. An adsorbent is a condensed phase at the surface of which adsorption may occur [189]. In acidic solution, the adsorption of an inhibitor onto the metal surface through their functional group(s) forming a 2-D monolayer/sub-monolayer (figure 2.23) is assumed to be the first step in the mechanism of corrosion inhibition [190].

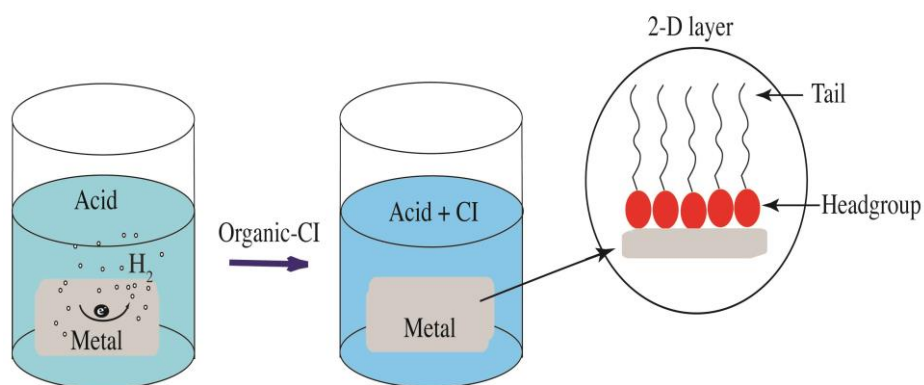


**Figure 2.23:** Organic inhibitor interaction with a metallic substrate in an acidic solution [190].

Depending on the nature of forces involved, two kinds of mechanism of adsorption are possible, physical (or physisorption) and chemical (or chemisorption) adsorption as briefly described below:

**Physisorption (electrostatic):** A type of adsorption that is triggered by the attractive electrostatic force between ionic species or dipoles of inhibitor molecules in solution and the charge on the surface of the metal. The forces involved in the electrostatic adsorption are generally weak. The adsorption process is easy, and no direct physical contact occurs between the inhibitor and the metal. Ions are separated from the metal by a solvent layer of molecules. Physical adsorption is a process characterised by low activation energy and is relatively independent of temperature [106].

**Chemisorption:** This type of adsorption process involves the transfer or sharing of charges from the inhibitor molecules to the surface of the metal, forming a coordinate bond. It is slower than electrostatic sorption and has higher activation energy. The temperature dependence shows higher inhibition efficiency at higher temperatures [8]. However, as opposed to electrostatic adsorption, chemisorption is particular for specific metals and is not entirely reversible [106]. Below is a brief description of factors that influence the adsorption of inhibitors on the surface of the metal [191-195]:

- a) **The concentration of inhibitors:** Inhibitors utilized during corrosion inhibition are supposed to be above a certain minimum concentration level. In a system with an insufficient amount of the inhibitor, the rate of corrosion may be accelerated to an even higher level than in the case without an inhibitor. The concentration of the inhibitor usually drops dramatically during the initial formation of the protective film on the metal surface or due to its reaction with the impure metal surface. This reaction/film is the reason why the initial concentration of the inhibitor is always higher than the one maintained during the inhibition process.
- b) **The interaction between adsorbed inhibitor species (antagonism and synergism):**  
The adsorbed species can form different types of interactions on the electrode surface, which can end up influencing their mechanism and inhibitive properties.
- c) **The pH of the System:** Different inhibitors have their specific pH range at which they exhibit excellent inhibition efficiency. Beyond this range, the inhibition efficiency decreases, and in some cases, the inhibitor molecules become ineffective.

- d) **The metal surface charge:** The adsorption of an inhibitor may result from the attractive electrostatic forces that occur between the electric charge on the metal at the metal-solution interface and the ionic charges or dipoles on the adsorbed inhibitor.
- e) **Synergistic Effect:** 'Synergism' refers to the reinforcement of the inhibiting action of one inhibitor by the addition of small amounts of a second inhibitor, to produce a combined effect that is more significant than the sum of the individual effects. However, the reinforcing inhibitor effect is less effective when used alone. For instance, tetraisoamyl ammonium sulphate has little impact on the corrosion of iron in 4 N sulphuric acid. However, when the small concentration of KI (0.005 M) is added, the organic cation is adsorbed, reducing the double layer capacity, and the dissolution of iron is very much decreased.
- f) **The reaction of adsorbed inhibitors:** An electrochemical reaction of the adsorbed inhibitor may result in forming an inhibitive product of corrosion. The added substance and the inhibition function of the product formed is referred to as primary and secondary inhibition, respectively.
- g) **The functional groups, availability of  $\pi$  electron density and structure of inhibitor:** Inhibitors can bind strongly on the surface of the metal through the transfer of electron and coordinate bonds thereby creating an effective inhibition of corrosion. Effective corrosion inhibition is due to inhibitors or species that contain anion atoms, lone pair of electrons and organic ring structures of somewhat loosely electrons. Functional groups of elements belonging to group V or VI of the periodic table that support stronger bonding and simpler electron transfer or triple bonding due to  $\pi$ -electron systems also play a role in the inhibitor effectiveness. The tendency for inhibitors to form a strong coordinate bond(s) increases with decreasing electronegativity in the order  $O < N < S < P$ .

Typically, adsorption isotherms are used to describe the metal surface adsorption of the inhibitors. This explanation is because adsorption isotherms have been proven to provide vital information and clues on the thermodynamics of inhibitors which can be used to provide useful insights on the mechanism inhibition of corrosion and the nature of the interactions between the metal surface and the inhibitor [183, 196]. An adsorption isotherm is a mathematical expression which relates the bulk concentration of an adsorbing species to its surface concentration at a constant temperature. An adsorption isotherm provides information on the relationship between the coverage of an interface with the adsorbed species (i.e., the amount adsorbed) and the concentration of species in solution. The metal surface area that is not

covered by corrosion inhibitors is said to be of zero appropriateness for inhibitor adsorption [197]. It should be noted, however, that, the prediction provided by these isotherms cannot give sufficient priori predictions of the inhibitor performance [198]. Various adsorption isotherms have been used to describe the adsorption of inhibitors on the metal surface, and this includes the Freundlich isotherm [199], Langmuir isotherm [172, 173, 180], Flory- Huggins isotherm [200-202], Temkin isotherm [203-205], Frumkin isotherm [206-208], Dhar-Flory-Huggins and Bockris-Swinkels [209].

#### 2.4.4 CLASSIFICATION OF CORROSION INHIBITORS

The various types of inhibitors are classified based on their mechanism and mode of action and mostly rely on effects such as the type of environment in which corrosion is occurring, the nature of the inhibitor and that of the metal. Some of the types of inhibitors are discussed below:

**Anodic corrosion inhibitors:** These are types of inhibitors that stifle the anodic reactions, thereby reducing the rate at which corrosion takes place. They generally form insoluble thick films (i.e., by reacting with the corrosion product initially) which then adheres tightly to the surface of the metals preventing the corrosive/acidic solution from entering into contact with the surface of the metal. As a result, the rate of corrosion is slowed down or prevented. Nitrite ( $\text{NO}_2^{2-}$ ), molybdate ( $\text{MoO}_4^{2-}$ ), orthophosphate ( $\text{PO}_4^{3-}$ ) and chromate ( $\text{CrO}_4^{2-}$ ) are among the examples of anodic inhibitors [35.23, 16]. They are mainly employed in solutions that are at near-neutral pH levels and where corrosion products are soluble such as salts, hydroxides and oxides [35.23, 17]. For example, the nitrite inhibitors seem to act by oxidizing the products of corrosion to compounds with lower solubility, forming protective films on the metal surface more quickly. The anodic types of inhibitors are commonly referred to as passivation inhibitors [210-212].

**Mixed corrosion inhibitors:** Inhibitors that inhibit corrosion by simultaneously reducing the rate at which the cathodic and anodic reactions of the corrosion process takes place are known as mixed-type inhibitors [185, 213]. The mixed-type inhibitors account for 80% of all types of inhibitors that are not classified as cathodic nor anodic types [214]. Mixed-type inhibitors are much less dangerous as compared to the pure anodic inhibitors and in many cases, do not lead to an increase in corrosion intensity [187, 215-220]. These inhibitors adsorb and form stable, protective film bonds which limit the rate of corrosion as the adsorption surface process goes to completion [218]. In this type of inhibition, the rate of corrosion reactions is decreased by reducing the number of surface sites available [214]. Thus, mixed-type inhibitors are also referred to as adsorption inhibitors due to this mode of inhibition. Certain factors influence the process of adsorption, and these include, the type of electrolyte, the type of inhibitor and the charge on the surface of the metal [211]. The inhibition efficiency of the protective film that is formed by the corrosion inhibitor depends on its concentration and the contact time that it has on the metal surface. The degree to which the inhibitor is effective is dependent on the extent to which it is absorbed and the coverage on the metal surface [211].

***Volatile corrosion inhibitors (VCIs):*** Corrosion inhibitors can be volatile or non-volatile. VCIs are chemical compounds that are transported by the process of volatilization from the source through a closed environment to the site where corrosion is occurring. In boilers, for example, critical VCIs such as hydrazine or morpholine are transported with steam to prevent corrosion in the condenser tubes by neutralizing acid carbon dioxide or by changing the pH of the surface to less acidic corrosive values [221]. Hydrazine has replaced morphine in the boiler system due to having superior performance and its availability at a low cost. Even though hydrazines are excellent corrosion inhibitors, they come with drawbacks such as toxic effects to humans, especially if ingested in/with food. Other volatile corrosion inhibitors that can be used for corrosion control include solids such as salts of cyclohexylamine, hexamethylene-amine and dicyclohexylamine, which are used in closed vapour spaces like shipping containers. Koehan [222] and his colleagues came up with materials that have an ambient temperature vapour pressure by using organic compounds and their derivatives, which were used as VCIs. Dicyclohexylamine and oleylamine were used as VCIs for MS in the CO<sub>2</sub> environment [223]. Wood bark oils of *Strychnos nux-vomica*, *Cassia siamea-gonrai*, *Crataeva religiosa* and *Cassia auriculata*, were used as vapour phase corrosion inhibitors for copper and MS in sulphur dioxide and sodium chloride environments [224].

***Natural products as corrosion inhibitors:*** Most corrosion inhibitors are hazardous organic chemicals, and this limits their application in specific areas such as in cooling and aqueous heating systems. Over the years there has been considerable interest in naturally occurring substances as corrosion inhibitors, otherwise referred to as green inhibitors because they are non-toxic, readily available, cheap and biodegradable. Plant-based inhibitors such as *Xylopiya ferruginea* [225], *Citrus paradise* [226], *Myristica frangans* [227], *Nicotiana tobacum* [228], *Parthenium hystophrous* [229] and *Cyamopsis tetragonaloba* [230] have been used in recent years as corrosion inhibitors for different metals and alloys. The parts of the plant that were used as corrosion inhibitors include; stems, leaves or seeds in which specific chemical compounds were extracted and isolated using organic solvents or acids. Dahmani et al., [231] isolated piperine from black pepper and compared its corrosion inhibition property with that of black pepper extract with both of them providing an inhibition efficiency of above 95%. Rajendran [232] extracted and isolated flavonoids from *Tecoma stans* and *Nerium oleander* flowers which he used for the inhibition of MS corrosion in sulphuric acid.

***Precipitation corrosion inhibitors:*** Precipitation inhibitors are compounds that form precipitates onto the surface of the metal, creating a protective film that is capable of blocking both the cathodic and anodic sites indirectly from corrosion. Hard water that contains a high amount of magnesium and calcium is less corrosive than soft water due to the tendency of salts in hard water capable of precipitating on the metal surface, forming a protective film. Phosphates and silicates are the most common types of inhibitors in this category. Sodium silicates, for example, is used in various domestic water softeners to prevent the development of rust water and in aerated hot water systems, sodium silicate protects copper, brass and steel. However, protection is not always guaranteed and relies mostly on pH and a saturation index that is influenced by temperature and water composition. Phosphates provide effective inhibition when oxygen is present. Phosphates and silicates do not offer the degree of protection that nitrites and chromates are capable of delivering; however, they are instrumental in situations where non-toxic additives are required [61].

***Cathodic corrosion inhibitors:*** Cathodic inhibitors are compounds that reduce the corrosion rate indirectly by stifling the corrosion reactions. This process involves the divalent cations reacting with the hydroxyl anions forming precipitates over the cathodic sites, avoiding cathodic reaction [233]. There are two main types of cathodic inhibitors, which are the cathodic precipitators and cathodic poisons. Cathodic precipitators function in a way that the alkalinity at the cathodic site is increased and they selectively precipitate as insoluble compounds, resulting in the formation of a film barrier [211]. Therefore, the rate of corrosion decreases as the area that is available for cathodic reactions decreases. Examples of cathodic precipitators include magnesium salts, zinc salts, polyphosphate and calcium salts [210].

In contrast, cathodic poisons deter the rate of reduction of the corrosion reaction due to different types of poisons by reducing the rate of corrosion through several mechanism processes. Selenides and sulphides are some of the examples of poisons that adsorb onto the metal surface while others such as antimony and arsenic compounds create a metallic layer by undergoing reduction at the cathode. Compounds such as borates, silicates and phosphate additionally decrease the rate of corrosion by forming a protective film which reduces the diffusion of oxygen to the surface of the metal [211]. Some other types of inhibitors remove reducible species from the corrosive environment. The removal of oxygen from the aggressive environment significantly decreases the corrosion rate. This removal can be achieved by either one of the mechanisms such as, oxygen scavengers like hydrazine and sodium sulphate which



react with oxygen and remove it from the solution, boiling to reduce the dissolved oxygen concentration and vacuum deaeration [187, 215-220].

***Inorganic corrosion inhibitors:*** These are corrosion inhibitors used in neutral to alkaline environments. They act by forming a protective film on the metal surface and inhibits mostly anodic reactions. The most common inorganic inhibitor is chromate, which also inhibits the cathodic reaction and is capable of forming a protective film. Inorganic inhibitors are used as an alternative to organic inhibitors since organic inhibitors can degrade with time and temperature [234]. Inorganic compounds such as antimony trioxide ( $\text{Sb}_2\text{O}_3$ ) and aluminium oxide ( $\text{Al}_2\text{O}_3$ ) have been reported as effective inhibitors of corrosion in an acid medium [19]. The effectiveness of these inhibitors can be improved by merely adding salts of electropositive metals into a corrosive medium. The metal of interest is then protected from the aggressive medium due to the reduction of electropositive ions and the deposition of the ions on the surface of the metal. As a result, the ions are reducing the overvoltage of the main cathodic depolarization reaction [235]. The resistance of corrosion for titanium is improved based on the electrode potentials of ions like platinum (Pt), copper (Cu), rhodium (Rh), mercury (Hg) and iridium (Ir) and is mostly observed for platinum because of its low hydrogen overvoltage [236]. Nickel ions are also capable of reducing the rate of corrosion of titanium [237], even at 0.2 ppm nickel ions render passivity of titanium in 3.5% NaCl, this is because it can lower the overvoltage of hydrogen on titanium in strongly acidic solutions. Chromates are widely used for the treatment of ferrous and non-ferrous materials since they can be applied over a wide range of pH. Chromates are capable of “self-healing” and whenever the protective film breaks its relocated to another site of breakage and re-creates the film. However, its usage has decreased due to its carcinogenic properties, and in some countries, it is forbidden [116, 238, 239]. Polyphosphates are the other types of inorganic inhibitors that are non-toxic and inhibits the corrosion of iron alloys even at low concentrations. They are extensively used for the inhibition of corrosion in water circulating systems. Their drawback, however, is that at high concentration they might enhance the corrosion reaction by forming soluble complexes with metal cations, activating local corrosion of steel, especially in the alkaline environment [238].

**Organic corrosion inhibitors:** Organic corrosion inhibitors are widely used in industry due to their compatibility with protected materials, excellent solubility, effectiveness at various temperature ranges and relatively low toxicity [240, 241]. These characteristics of organic inhibitors are fundamental to researchers which is confirmed by the increasing number of research papers published. Both cathodic and anodic effects can be observed with organic inhibitors. Anodic corrosion inhibitors act by reacting with the metal cation to form an insoluble hydroxide on the metal surface which blocks the active site and move the corrosion potential towards positive values. This prevents any further dissolution (oxidation) of the metal, thus reducing the rate of corrosion.

In contrast, cathodic inhibitors move the corrosion potential towards negative (lower) values and delay the reaction occurring at the cathodic site (oxygen reduction and hydrogen evolution). With anodic corrosion inhibitors, it is imperative to use the right amount of the inhibitor; this is because an insufficient amount of the inhibitor which does not cover the entire active site can result in localized corrosion which is difficult to detect [242, 243]. Due to organic inhibitors being capable of forming hydrophobic films on the surface of the metal, they are called ‘film-forming’ inhibitors. Most of these organic inhibitors compounds inhibit corrosion by adsorbing onto the surface of the metal (i.e., adsorption mechanism). The chemisorbed inhibitors create a film on the surface of the metal that protects the metal from corrosion by either blocking the surface of the metal physically from the corrosive environment or by retarding the electrochemical process. Main organic functional groups that are capable of forming chemisorbed bonds on the metal surface include carboxyl (-COOH), phosphonate (-PO<sub>3</sub>H<sub>2</sub>) and amino (NH<sub>2</sub>) groups. Other functional groups or atoms, however, are also capable of forming coordinate bonds with the metal surface. Organic inhibitors are adsorbed onto the metal surface due to their ionic charge and charge on the metal surface. For example, anionic and cationic inhibitors such as sulfonates/phosphonate and amines respectively are adsorbed preferentially depending on whether the metal is positively or negatively charged. The effectiveness of organic inhibitors depends on their molecular structure, their affinities for the metal surface and their composition. Since the formation of a film on the metal surface occurs through adsorption process factors such as pressure and temperature of the system play an important role. However, the most significant or dominant factor is the strength of the adsorbed bond for soluble organic inhibitors [61].

## 2.5 ENVIRONMENTALLY FRIENDLY (GREEN) CORROSION INHIBITORS

Organic compounds serve as efficient inhibitors of corrosion, but some of them are incredibly toxic and non-biodegradable in some situations. This is a problem because it can lead to the emission of industrial wastewaters with a vast amount of toxic material to waterways. Due to their toxicity, most organic compounds do not meet entirely the required environmental protection standards [234]. Even though there is no specific definition for green corrosion inhibitors, a large number of recent studies have been devoted to finding eco-friendly organic corrosion inhibitors. The amino esters used in this study contains both the positively and negatively charged groups (zwitterions) and can be referred to as amino ester (amino ester-based ionic liquids). Ionic liquids (ILs) are usually referred to as molten salts at room temperature and have enjoyed more employment as corrosion inhibitors to solve the toxicity problem. The reason for the use of ILs as inhibitors is because they are characterised by properties such as excellent thermal stability, non-toxicity, intrinsic ionic conductivity, non-flammability, large electrochemical potential windows, negligible vapour pressure, and low melting point [244-246]. They also have many physiochemical properties, such as non-flammability and high ionic conductivity, and excellent thermal and chemical stability [245, 247, 248]. The carboxylic acids are suitable to be used as corrosion inhibitors for metals because they are very effective, bio-degradable and non-toxic. They have the capabilities of inhibiting the dissolution of both ferrous and non-ferrous alloys [238, 249]. Therefore, the present study will make use of amino esters and carboxylic acids as corrosion inhibitors for MS and Al in HCl.

## 2.6 CARBOXYLIC ACIDS AND AMINO ESTERS

Carboxylic acids are molecules which occupy a principal place among carbonyl compounds and serves as the starting materials in the synthesis of various carboxylic acid derivatives such as esters, thioesters, amides and acid chlorides. They can be found in nature in different forms, and this includes butanoic acid, which is responsible for the rancid odour of sour butter, an acetic acid which is the principal organic component of vinegar, etc., and is also involved in major biological pathways. The International Union of Pure and Applied Chemists (IUPAC) name of the simplest carboxylic acids is derived from that of the longest carbon chain that contains the carboxyl group and replacing the terminal -e of the corresponding alkene name with the suffix -oic followed by “acid”. During the naming of carboxylic acids, the carbon atom to which the carboxyl group ( $\text{-COOH}$ ) is attached to, is numbered first and substituents are numbered relative to that number. Many simple carboxylic acids are often named according to the sources they were derived from. This is because at the time their structural formulas were unknown, for example, butyric acid ( $\text{CH}_3\text{CH}_2\text{CH}_2\text{COOH}$ ), is named after the Latin name “butyrum” which is a name for butter because it was first obtained from butter [250].

Carboxylic acids are useful ligands in coordination chemistry that can bind to various metals [251]. These are known to bind iron (III) ions and iron (III) oxide structures and include, in addition to this property, an electronegative oxygen atom as well as donors and acceptors of hydrogen bonds. They are strongly associated with their solid-state and solutions, and the 8-membered dimers demonstrate the characteristics of forming intermolecular hydrogen bonding between ligands [252]. The interest in carboxylic acids as corrosion inhibitors is due to their ability to create hydrogen bonds with each other. The existence of these hydrogen bonds has been previously confirmed by spectroscopy [253]. Some carboxylic acids contain an amine group (amine-carboxylic acid interactions). Amines are compounds that contain a basic nitrogen atom with lone pairs of electrons. These are ammonia derivatives with one hydrogen atom that is replaced by a substituent, like an alkyl group. Amines are divided into three groups, primary, a secondary and tertiary amine. Primary amines have one of the three hydrogen atoms in ammonia being replaced by an alkyl substituent, secondary amines contain two substituents bound to the nitrogen atom together with one hydrogen atom, and tertiary amines are referred to when all the three hydrogen atoms are replaced by the alkyl group [250].

Many kinds of carboxylic acid derivatives are known, but this study primarily focuses on esters derivatives, namely amino esters. Amino esters are organic functional groups that contain amine ( $\text{-NH}_2$ ) and carboxyl ( $\text{-COOH}$ ) as functional groups, along with a side chain that is

specific to each amino ester. Esters are derivatives of carboxylic acids that are named by firstly identifying the alkyl group that is attached to the oxygen atom and the carboxylic acid after that, with the -ic acid end being replaced by -ate. For the most naturally occurring compounds, esters are one of the most prevalent compounds. The simplest useful esters include anisole, a pleasant-smelling aromatic ester responsible for the fragrant odours of flowers and fruits, and tetrahydrofuran (THF) which is a cyclic ether often used as a solvent for organic synthesis [250].

## 2.7 CARBOXYLIC ACIDS AND AMINO ESTERS AS CORROSION INHIBITORS

The exploration of organic compounds as acid corrosion additive is a subject of interest for researchers due to numerous industrial applications like descaling, oil well cleaning and pickling [254-260]. The anticorrosive properties of these organic compounds depend on the specific interaction that occurs between certain functional groups in their molecules and the active centres on the metal surface [160, 261-263]. Most organic inhibitors are adsorbed on the surface of the metals by displacing water molecules away from the surface and forming a compact barrier film on the surface of the metals [202, 264]. As a result, organic compounds with heteroatoms such as oxygen, sulphur, nitrogen and multiple bonds have been investigated as corrosion inhibitors for metals such as zinc and MS in acidic medium and found to behave as efficient corrosion inhibitors due to the availability of  $\pi$ -electrons for interaction with the metal surface [265].

Amines and alkanolamines are typical examples of commercial organic inhibitor compounds. Their adsorption mechanism can be explained more specifically. The lone pair electrons of the nitrogen atom found mainly in the amino groups functions as the adsorption centres on the MS surface. The Fe ions ability to accept electrons from the nitrogen atom indicate that they act as Lewis acid. The amines functional groups (R-groups) bound to the nitrogen atom (figure 2.24a) may influence their adsorption owing to their electronic properties (i.e., electron acceptor or electron donor). The same inhibition mechanism of amines also applies to alkanolamines, but with the hydroxyl more likely to form a chelate on the metal surface [266].

Organic carboxylate compounds (carboxylic acids) have the delocalizing effect on the electrical charge of carboxylate anion ( $-\text{COO}^-$ ) responsible for the adsorption of the molecules on the metal surface, thereby forming a thin organic layer on the surface of the metal. Carboxylic acids are distinguished by one or more proton donating carboxylic group ( $-\text{COOH}$ ).

The adsorption is affected by the presence of a functional electron-donor/acceptor, R-groups connected to the carboxylate ion [266], as shown in figure 2.24b. The amino esters inhibiting properties are connected to the capability of the amino groups to adsorb on the metal surfaces and metal oxides by sharing their unshared pair of electrons of the nitrogen atom with the metal (oxide) substrate. This adsorption forms a film on the surface of the metal, thereby protecting it from being corroded. Amino esters are said to act as a mixed inhibitor capable of suppressing both the anodic and cathodic corrosion reactions [267-269]. Amino groups are also capable of displacing water molecules at the metal surface and forming a hydrophobic film which protects against corrosion [270].

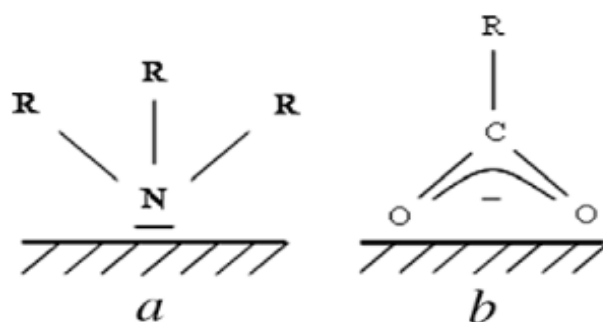


**Figure 2.24:** Functional groups of amines (a) and carboxylates (b) adsorbed on the surface of the steel, the R-group may be a methyl or ethyl [266].

Amino acids and their derivatives are well-established as effective corrosion inhibitors due to their functional groups. Various researches have confirmed the adsorption capabilities of amino acids on the metal surface through the formation of a protective film. Amino acids adsorption on metal surface plays a vital but controversial role since the degree of protection of the metal relies on the adsorption process [271]. The adsorption process of amino acids could be chemical (figure 2.25a) similar to that of amines explained above. Even physical adsorption is a possibility in the case where the metal surface undergoes oxidation due to the presence of dissolved oxygen. The ability of amino acids to protect the metal from attack by an aggressive solution can be attributed to their tendency to form hydrogen bonds with the oxide or hydroxide species present on the metal surface. The oxide film presence on the metal surface may promote amino acids adsorption through hydrogen bonding, which accounts for most of the inhibitory action of these compounds. The formation of hydrogen bonds between the oxidised surface species and the amino acids is said to be responsible for the physical adsorption of amino acids (figure 2.25b) [272].

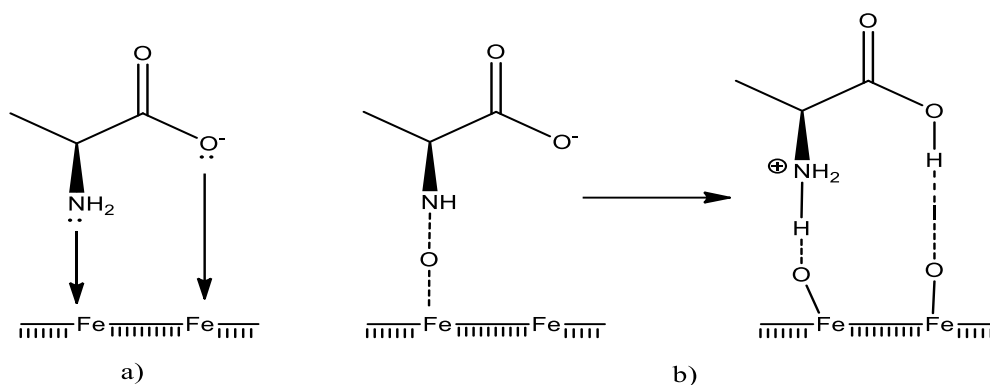


**Figure 2.25:** Chemical (a) and physical (b) adsorption mechanism of amino acid [272].

Amines, carboxylic acids and their mixtures have been used as VCLs to inhibit against atmospheric corrosion of steel and ferrous metals during storage and transportation [72, 273-276]. The use of amines and carboxylic acid mixtures as corrosion inhibitors requires a suitable combination of the two, which has shown a synergetic effect that is attributed to the formation of a thicker film barrier on the metal surface that prevents the penetration of the corrosion-causing contaminants [277]. Kohler et al., [278, 279] have comprehensively investigated amine-carboxylic acid interactions. They found that carboxylic acids have a strong tendency to dimerise, as each pair can form two hydrogen bonds in a pair ring formation.

A classic example of carboxylic acid corrosion inhibitor that has been used for decades to protect metals from attack by corrosive environments is benzoic acid like sodium salt ( $C_6H_5COOH$ ). Sodium benzoate nitrile is another example of such an inhibitor and is used in automobiles radiators. Benzoate is among one of the known anodic inhibitors. Salts of benzoic acid are among the most widely investigated carboxylic acid for the protection of steel concrete against corrosion [268, 280-283]. In the early 1970s, Gouda and Halaka [283] discovered that sodium benzoate could function as effective corrosion inhibitors for steel-concrete being attacked by chlorides. The molecules of benzoic acid with an additional carboxylic group such as phthalic acid have been reported to show a more efficient corrosion inhibition compared to nitrites for eco-rapid hardening Japanese cement [281].

Andreev et al., [284] studied the corrosion inhibiting effect of salts of substituted benzoic acids in chloride-containing calcium hydroxide solutions. They found that such salts inhibit steel depassivation while elevating the potential of pit formation and extending its induction period. The corrosion inhibition efficiency was found to be dependent on the hydrophilic/hydrophobic nature of the substituents. The efficiency decreases when both hydrophilic and hydrophobic substituents are introduced in the aromatic benzoic nucleus.

Zerjav et al., [285] investigated the inhibition of corrosion in the simulated urban rain by carboxylic acids namely, hexanoic, stearic decanoic, and myristic acids as inhibitors for Zn, Cu, Cu<sub>40</sub>Zn and Cu<sub>10</sub>Zn by electrochemical techniques. The study was conducted through the immersion of the metals zinc, copper and brasses in ethanol solution in the presence of carboxylic acids as the inhibitors if concentration 0.01 M to 0.1 M for 1 minute to 6 days. Surface etching effect was also studied by making use of these carboxylic acids. From the results, longer carbon chains carboxylic acids were found to be better corrosion inhibitors. The formation of a self-assembled film on the metal surface was found to be a rapid process with high inhibition values being observed after a short period of immersion (i.e., one minute). Carboxylic acids inhibitors were found to have an excellent inhibition efficiency towards copper and myristic and especially, stearic acids, towards brasses showing an inhibition efficiency of greater than 95% even at low molarities. However, both inhibitors were less effective when it came to the inhibition of Zn, with up to 60% effectiveness.

Khaled et al., [286] used electrochemical methods such as electrochemical impedance spectroscopy, PDP and electrochemical frequency modulation techniques to intensively report the effect of 2-thiophenecarboxylic acid methyl ester (TME) on iron corrosion in 1.0 M HCl solution. Using quantum calculations and molecular dynamics, the adsorption process of TME on the iron surface was investigated. Methods for simulating molecular dynamics were used to measure the binding energy and the energy of adsorption resulting between the TME molecule and the iron surface. Also, the Metropolis Monte Carlo method measured the adsorption strength of the inhibitor molecules on the iron surface. The experimental results showed that the thiophene derivative reduces the corrosion rate of iron remarkably as its concentration increases. Polarization studies show that TME molecules act as a cathodic-type inhibitor. The presence of sulphur and oxygen atoms as well as  $\pi$ -electrons in the inhibitor molecule permits the interaction and bonding between TME and the iron surface.

Hammouti et al., [287] studied pure iron corrosion in physiological 9 g/L NaCl solution by electrochemical technique under different hydrodynamic conditions which were simulated by using a rotating disc electrode. The inhibition of corrosion using methionine, amino acid and some amino esters, namely methionine methyl ester and methionine ethyl ester, on the electrochemical behaviour of iron. The results showed that the criterion of Levich is proved. The results showed that ethyl 2-amino-4-(methylthio) butanoate or methionine ethyl ester (MetOC<sub>2</sub>H<sub>5</sub>) is the best inhibitor of series and its effectiveness attains 80 % inhibition efficiency in 10<sup>-2</sup>M. The MetOC<sub>2</sub>H<sub>5</sub> acts on the iron surface according to the Frumkin model.



Madram et al., [288] investigated the corrosion behaviour of Al in 1 M NaOH solution, the absence and presence of some aromatic carboxylic acids. This investigation was done using PDP techniques, scanning electron microscope (SEM) and electrochemical impedance spectroscopy (EIS). The results showed that 4-bromomethyl, 3-bromo and 3-hydroxybenzoic acid among the investigated aromatic carboxylic acids, were more effective inhibitors for Al in alkaline medium. Thermodynamic parameters which included the  $\Delta G^{\circ}_{\text{ads}}$  and the adsorption equilibrium constant ( $K_{\text{ads}}$ ) were calculated and discussed. The results obtained showed that the adsorption process of the studied corrosion inhibitors on Al surface obeys the Langmuir adsorption isotherm.

Agarwal and Landolt [289] investigated the influence of the nature and concentration of electrolyte anions on the efficiency of carboxylic acid-based inhibitors for steel in neutral solution was by using anodic and cathodic polarization method. The N-ethyl-morpholine salts of a  $\omega$ -benzoyl alkanolic acid model compound and benzoic acid were used as inhibitors. The compounds were both found to inhibit the anodic partial reaction. The results showed that the corrosion inhibition effect was more noticeable at low electrolyte concentration in the potential active region, signifying an adsorption mechanism. Because of both inhibitors capability to function as a buffer in the diffusion layer, they both favoured the passivation of the electrode. The inhibition effects of the inhibitor molecules are attributed to their ability to block the metal surface sites for anodic dissolution. The type of adsorption mechanism was proven to depend on the concentration and nature of the electrolyte anion and followed Langmuir adsorption isotherm. The model predicts a stronger corrosion inhibition effect for low electrolyte concentration, which was in agreement with experimental observations made with N-ethyl-morpholine salts of two aromatic carboxylic acids.

## 2.8 CORROSION MONITORING TECHNIQUES

### 2.8.1 INTRODUCTION

Corrosion measurement involves the application of various quantitative techniques to estimate and evaluate the effectiveness of corrosion control and prevention, providing feedback on the proper prevention and control methods that can be optimized. The results obtained after evaluation can be used to enhance and improve the different techniques.

Corrosion monitoring techniques can be divided into two kinds, the electrochemical and non-electrochemical methods as described in the sub-headings below:

### 2.8.2 NON-ELECTROCHEMICAL METHODS

Several non-electrochemical methods can be utilized to study the corrosion rate; these include gasometric analysis, surface analysis, gravimetric analysis, etc. In this study, the surface and gravimetric analysis will be employed.

**Gravimetric/weight loss analysis:** The gravimetric technique has been documented as the most preferred method to study corrosion by observing the inhibitive action of different compounds in various medium. This technique is a simple, reliable, precise and accurate method that provides appropriate quantitative data. Weight loss can be used to measure corrosion of specimens if they are of the same size and tested for the expression as a loss in weight per unit area per unit time [290-293]. The technique involves immersing a specimen of interest into a corrosion environment/medium for a given period, then removing the specimen for analysis. The necessary data obtained from this measurement is weight loss that takes place during the immersion period and is expressed as the corrosion rate. Some of the factors that make the weight loss method the most popular for corrosion studies are described below:

- a) **It is simple:** It does not require any sophisticated instruments to obtain results.
- b) **It is versatile:** It can be applied to all corrosive environments, providing information on all various forms of corrosion.
- c) **It is direct:** Direct measurements are obtained with no theoretical assumptions or approximations.

**Surface Analysis:** Surface analysis techniques have immense success in enlightening almost all facets of the corrosion phenomenon. Surface analysis of metals is conducted in both the absence and presence of an inhibitor contributing to the understanding of the mechanism of inhibition. It is conducted to gain more knowledge of the type of adsorption process (morphology) that takes place on the surface of the metal. Methods such as the X-Ray Diffraction (XRD), Scanning Electron Microscope/Electron Dispersive Spectroscopy (SEM/EDS) are the most common and valuable methods. Surface analyses of an MS specimen in the acids have been studied by Fourier transform infrared (FT-IR) Spectroscopy.

**Fourier transform infrared (FT-IR) Spectroscopy:** Infrared spectroscopy is exceptionally supportive for the confirmation of the functional group in the sample. It detects the irrational characteristics of chemical functional groups present in the sample. This method is only applicable to molecules with a permanent dipole moment in them. Homonuclear molecules like O<sub>2</sub>, H<sub>2</sub> and N<sub>2</sub> etc. do not interact with infrared (IR) radiation because they have zero dipole moment, whereas the heteronuclear molecules such as HCl can interact with IR radiation. When infrared radiation (4000-400cm<sup>-1</sup>) interact with matter, the chemical bonds experience changes in rotation, bending, twisting, stretching or rocking vibration modes. This interaction leads to chemical functional groups exhibiting changes in the specific wavenumber range. By examining the absorption of IR radiation vibration mode can be detected [294]. The advantage of using FT-IR over the conventional IR spectroscopy is its speed and that it provides a better signal to noise ratio [227]. The FT-IR spectrum is a plot of transmittance versus wavenumber. A transmittance spectrum is obtained as,  $%T = I \setminus I_o$ .

Here, % T is the transmittance; I is the intensity measured with the sample and I<sub>o</sub> is the intensity measured from the background. The absorbance spectra calculated from the transmittance spectra can be written as follows  $A = -\log_{10} T$ .

**Scanning electron microscopy (SEM):** SEM is an electron microscope that produces images of a sample by scanning it with a focused beam of electrons [295]. Scanning electron microscopy is one of the most multipurpose instruments used for chemical composition and microstructure morphology. The image produced is due to the acquisition of interacting signals from the specimen of interest and the electron beam; which can either be elastic or inelastic interactions. The elastic interactions result in the loss of a small amount of energy being lost during the collision and is typified by a wide-angle directional change of scattered electron,

otherwise known as backscattered electrons. Backscattered electrons (BSE) are electron beams reflected from the sample during elastic scattering. Inelastic scattering generates secondary electrons (SE) and results from the interaction between incident electrons and atoms near or at the surface of the sample (metal) causing the primary beam electron to transfer a considerable amount of energy to the atom. The specimen electrons (which may be excited singly or collectively) and the binding energy of the electron to the atom are the two factors that the amount of energy lost depends on. Electron emitter such as field emission gun, tungsten wire or lanthanum hexaboride filament is always the primary source of electrons. The disintegration process linked to the incident electron ejecting a core-shell electron always leads to the emission of an x-ray with energy that can be used to identify the excited atom. The x-rays can be analysed by an energy dispersive spectrometer (EDS), thus identifying and determining the elemental composition of the sample surface [296].

### **2.8.3 ELECTROCHEMICAL METHODS**

Electrochemical techniques and its instrumentation can be made use of to study the phenomenon of corrosion; this is because corrosion is an electrochemical process itself. This study has been proven by several electrochemical measurements of corrosion that have been developed over the years. These types of techniques are famous for studying the rate of corrosion because they are, sensitive, versatile, accurate, fast, and can be used to study a wide range of corrosion-related phenomenon. Electrochemical measurements can also be used to measure the tendency of a metal to exhibit localized (pitting or crevice) corrosion and the rate of uniform corrosion, to study the passivation behaviour of a corroding system and the sensitization effects., to quantify galvanic corrosion. The method(s) can be used in the field or the laboratory. Different types of electrochemical techniques have been developed for explicitly studying corrosion. These techniques are referred to as "DC Techniques". These techniques, amongst others, include Tafel plots, polarization Resistance, cyclic polarization, and electrochemical impedance spectroscopy [160]. Electrochemical impedance spectroscopy and polarization techniques are explained thoroughly below as they are employed in this study.

**Electrochemical impedance spectroscopy (EIS):** EIS is a technique that is used to evaluate the resistive properties of materials at various frequencies. The EIS measurements for studies of corrosion are thought to be non-destructive because of the magnitude of polarization that is inflicted on the type of materials that are being characterised, a signal of less than 30mV peak to peak is usually used [297]. EIS method built on alternating currents can be employed to find more insights on the corrosion mechanism and to ascertain how effective a specific corrosion hindering method such as inhibition and coatings is. Impedance is used to determine for a given voltage the amplitude of the current in an alternating current circuit and is the proportionality factor between current and voltage. The interface between the solution and metal can be characterised by a simple model (figure 2.26) which includes three essential parameters, which are, the capacitance of the double layer ( $C_{dl}$ ), the polarization resistance ( $R_p$ ) and the solution resistance ( $R_s$ ) [298].

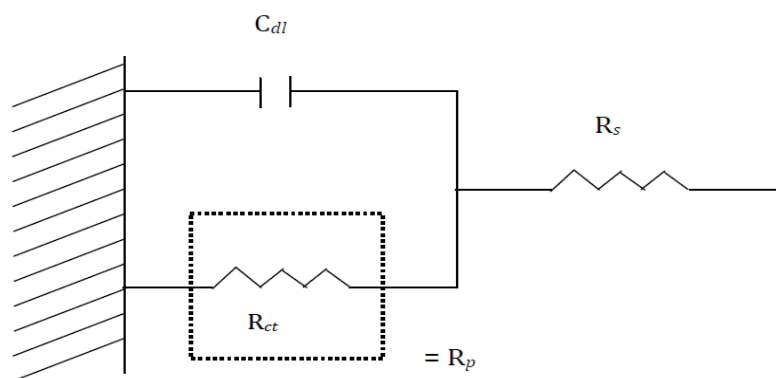


**Figure 2.26:** Typical electrochemical equivalent circuit commonly used to analyse EIS measurements in a corroding system [299].

$C_{dl}$  is an electrical phenomenon that is observed at the interface between the electrolyte and the metal surface. The double-layer is developed by a charged interface due to the interaction of polar water molecules on the surface of the corroding metal and reflects similar behaviour to that of a charged capacitor.

$R_p$  is a measure of resistance to reaction kinetics and the diffusion towards and away from the corroding surface of the reactants. The polarisation resistance value is obtained by taking the inverse of the slope of the potential current curve around the open circuit or corrosion potential and is inversely proportional to the corrosion rate.

$R_s$  is the resistance experienced to the flow of ionic current between the reference electrode and the working electrode. Solution resistance value decreases with an increase in the electrolyte conductivity [300].

When the frequency is zero, direct currents are measured, and the impedance of the capacitor goes to infinity. In parallel electrical circuits, circuits with the smallest impedance dominate and the data obtained can be used for the measurement of the sum of  $R_s$  and  $R_p$  [298]. EIS has several advantages when compared to other techniques that are used to evaluate the corrosion of metals and this includes [298]:

- a) It provides mechanical information that is based on using an equivalent electronic circuit which response similar to cells being investigated.
- b) It provides more information on the kinetic data on the corrosion process.
- c) It provides information on the properties of coatings that are applied to the metal such as the capacitance and resistance. The changes that occur on the properties of the coatings are associated with the loss of their protective properties.

**Polarization:** Polarization [298] is defined as the movement of electrode potential from their equilibrium values which is from an open circuit potential (OCP) resulting in a decrease of the current density. When two metal surfaces are in contact, current can flow from the anodic site to the cathodic site leading to the corrosion of the two metals. The potential difference of the open circuit that results between the anodic and cathodic areas controls the current flow direction. However, the magnitude of the current is controlled by the polarization characteristics of the electrodes. One of the important factors that control the polarization is the corrosive species concentration, which changes or gets consumed at the cathode and can be accumulated at the anode when the process of corrosion progresses near each electrode. The greater the polarization of the cathodic and anodic electrodes, the smaller the corrosion current even though the OCP difference is higher. If the anode is polarized alone, then the corrosion rate is controlled by polarization, as shown in figure 2.27a, where the anode mostly determines the corrosion rate. If the cathode is polarized alone, then the cathodic polarization curve is steeper, and the corrosion current is under cathodic control, as shown in figure 2.27b. However, when both electrodes undergo polarization at the same time, then this is under mixed controls, as shown in figure 2.27c [199].

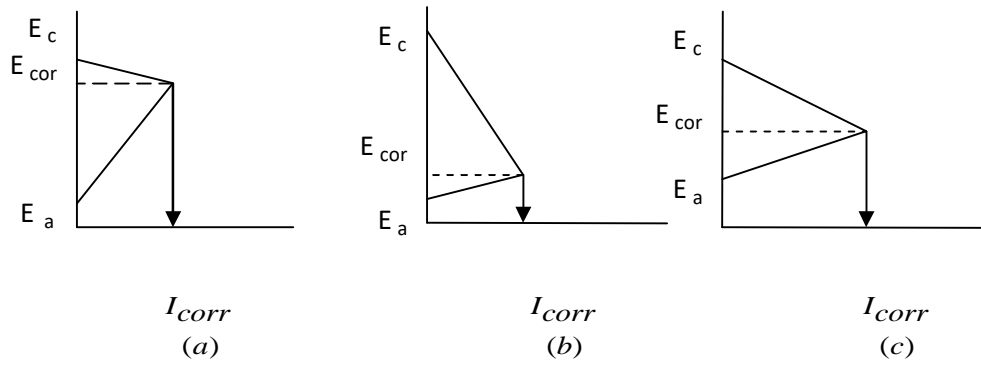


**Figure 2.27:** Evans polarization diagrams: (a) anodic control (b) cathodic control (c) mixed control [199].

## CHAPTER 3

---

# EXPERIMENTAL

This chapter describes the materials and methods used, which includes:

- a) Chemicals and materials
- b) Metal specimens
- c) Synthesis of inhibitors
- d) Nuclear magnetic resonance (NMR) spectroscopy
- e) Preparation of solutions
- f) Corrosion inhibition studies using, Gravimetric analysis and Electrochemical techniques; Electrochemical impedance spectroscopy (EIS) and Potentiodynamic polarization (PDP)



### 3.1 CHEMICALS AND MATERIALS

All the chemicals that were used for the synthesis of the three inhibitors were purchased from Sigma Aldrich Chemicals Pvt Ltd (SA). All of them were of analytical grade and used without any further purification. Below is a list for the materials and chemicals used in this study:

- Benzoyl alcohol ( $C_6H_5CH_2OH$ ),  $D = 1.045 \text{ g/ml}$ ,  $M = 108.14 \text{ g/mol}$
- Benzoyl chloride ( $C_6H_5COCl$ ),  $D = 1.211 \text{ g/ml}$ ,  $M = 140.57 \text{ g/mol}$
- Carbon tetrachloride ( $C_6H_5COCl$ ),  $D = 1.594 \text{ g/ml}$ ,  $M = 153.82 \text{ g/mol}$
- Chloroform ( $HCCL_3$ ),  $D = 1.48 \text{ g/ml}$ ,  $M = 119.38 \text{ g/mol}$
- Chloroform-d ( $CDCl_3$ ),  $D = 1.500 \text{ g/ml}$ ,  $M = 120.384 \text{ g/mol}$
- Diethyl ether ( $Et_2O$ ),  $D = 0.706 \text{ g/ml}$ ,  $M = 74.120 \text{ g/mol}$
- Dimethyl sulfoxide-d<sub>6</sub> (DMSO),  $D = 1.100 \text{ g/ml}$ ,  $M = 78.130 \text{ g/mol}$
- Hydrochloric acid (HCl),  $D = 1.161 \text{ g/ml}$ ,  $M = 36.460 \text{ g/mol}$
- L-alanine ( $C_3H_7NO_2$ ),  $D = 1.400 \text{ g/ml}$ ,  $M = 89.090 \text{ g/mol}$
- Methanol ( $CH_3OH$ ),  $D = 0.0791 \text{ g/ml}$ ,  $M = 32.040 \text{ g/mol}$
- p-toluenesulfonic acid monohydrate (PTSA),  $D = 1.240 \text{ g/ml}$ ,  $M = 190.220 \text{ g/mol}$
- Sodium hydroxide (NaOH),  $D = 2.130 \text{ g/ml}$ ,  $M = 40.000 \text{ g/mol}$
- Toluene (PhMe),  $D = 0.865 \text{ g/ml}$ ,  $M = 92.740 \text{ g/mol}$
- $\alpha$ -aminobutyric acid ( $C_2H_5CH(NH_2)CO_2H$ ),  $D = 1.100 \text{ g/ml}$ ,  $M = 103.120 \text{ g/mol}$
- $\gamma$ -aminobutyric acid ( $NH_2(CH_2)_3CO_3H$ ),  $D = 1.110 \text{ g/ml}$ ,  $M = 103.120 \text{ g/mol}$
- Aluminium (Al) sheets
- Distilled water
- Filter papers
- Mild steel (MS) sheets

## 3.2 SYNTHESIS OF INHIBITORS

### 3.2.1 Synthesis of N-benzoyl-2-aminobutyric acid (2-NBABA)

The general method for the synthesis of carboxylic acid derivatives is shown in figure 3.1. N-benzoyl-2-aminobutyric acid was synthesized by dissolving 2.5089 g (24.3299 mmol) of  $\alpha$ -aminobutyric acid in 10% NaOH (50 ml) solution in a 250 ml conical flask. To this, 4.5 ml (5.4315 g, 38.6391 mmol) of benzoyl chloride in four portions was added, the solution was then transferred to a 250 ml beaker. Then, small crushed ice was added into the solution as well as concentrated HCl until the solution was acidic. The solid product was collected by filtration, washed with water and drained well until dry. The solid was then placed in a 100 ml conical flask containing 20 ml of carbon tetrachloride. The mouth of the flask was covered with a watch glass and heated gently on a boiling water bath for 5 minutes. The mixture was allowed to cool and the solid product decanted. The pure acid was recrystallized in boiling water, dried and washed with chloroform (1 ml). FT-IR,  $^1\text{H-NMR}$  and  $^{13}\text{C-NMR}$  were used for the characterization of the chemical structure of the compound, 2-NBABA ( $\text{C}_{11}\text{H}_{13}\text{NO}_3$ , Mol. Wt. 207,23): Yield: 3.8898 g, 78 %.

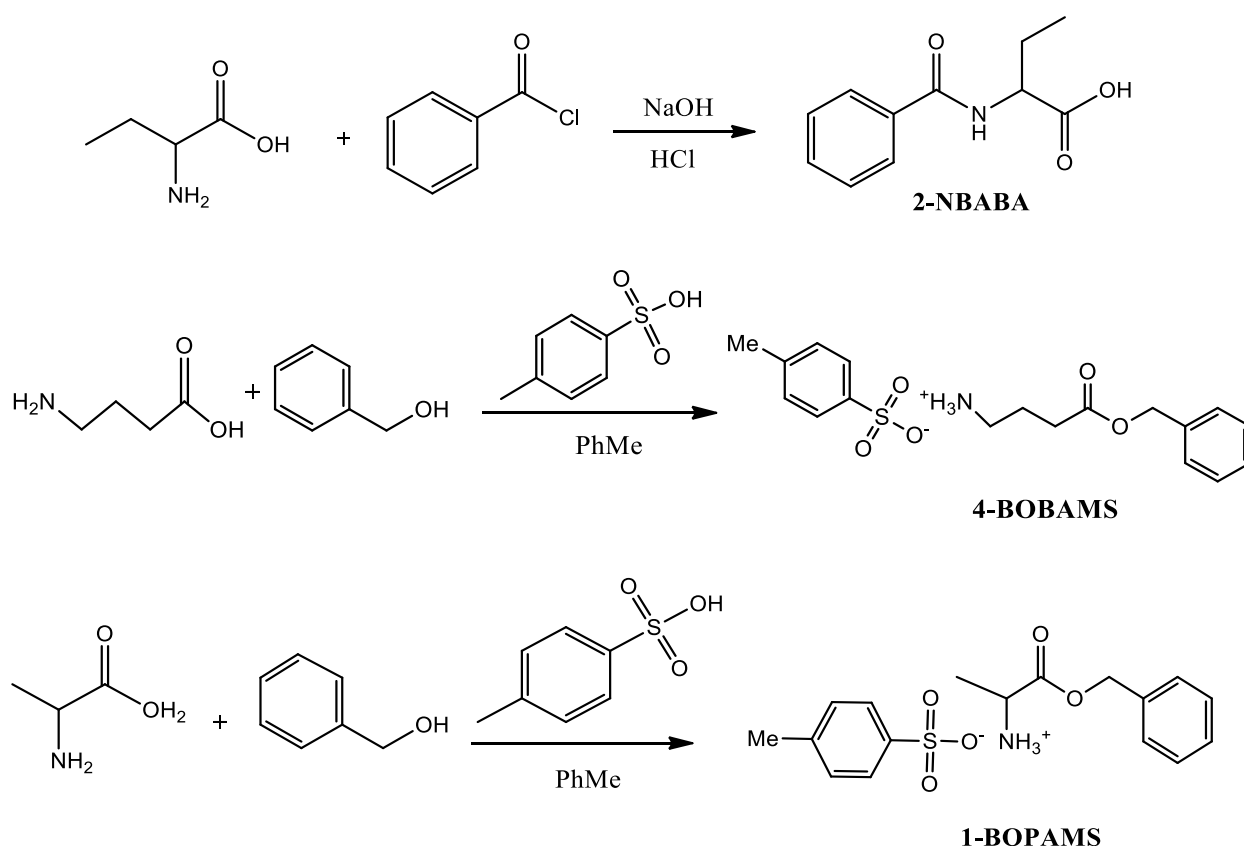
### 3.2.2 Synthesis of 4-(benzyloxy)-4-oxobutan-1-aminium 4-methylbenzenesulfonate (4-BOBAMS)

The general method for the synthesis of amino esters derivatives is shown in figure 3.1. Benzyl 4-aminobutanoate 4-methylbenzenesulfonate was synthesized by the suspension of  $\gamma$ -amino butanoic acid (7.0164 g, 68.0411 mmol), 10 ml benzoyl alcohol (10.4 g, 96.1716 mmol) and p-toluenesulfonic acid monohydrate (PTSA) (14.5821 g, 84.6812 mmol) in PhMe (200 ml). The mixture was then heated to reflux for 10 h with azeotropic removal of water. The product was precipitated by the addition of  $\text{Et}_2\text{O}$  (100 ml). The precipitate was then filtered, dissolved in  $\text{CH}_3\text{OH}$  (60 ml), and again precipitated by addition of  $\text{Et}_2\text{O}$  (100 ml), giving after filtration and drying the benzyl ester product (23.0146 g, 93%) as white crystals. 4-BOBAMS ( $\text{C}_{18}\text{H}_{23}\text{NO}_5\text{S}$ , Mol. Wt. 365,44): Yield: 23.0146 g, 93%.

### 3.2.3 Synthesis of 1-(benzyloxy)-1-oxopropan-2-aminium 4-methylbenzenesulfonate (1-BOPAMS)

Benzyl 2-aminopropanoate 4-methylbenzenesulfonate (figure 3.1) was synthesized by the suspension of 6.2124 g (69.7395 mmol) of L-alanine, 10.4 g (96.1716 mmol) of benzoyl

alcohol and p-toluenesulfonic acid monohydrate (PTSA) 14.5821 g (84.6812 mmol) in PhMe (200 ml). The mixture was then stirred for 10 minutes with stirring rod. The reaction solution was heated to reflux for 10 h with azeotropic removal of water. The product was precipitated by the addition of Et<sub>2</sub>O (100 ml). The precipitate was filtered, dissolved in CH<sub>3</sub>OH (60 ml) and again precipitated by addition of Et<sub>2</sub>O (100 ml), giving after filtration and drying the benzyl ester product (25.3816 g) as white crystals. 1-BOPAMS (C<sub>17</sub>H<sub>21</sub>NO<sub>5</sub>S, Mol. Wt. 351,42): Yield: 25.3816 g, 91%.

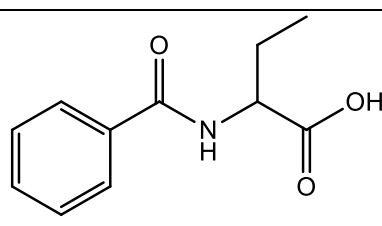
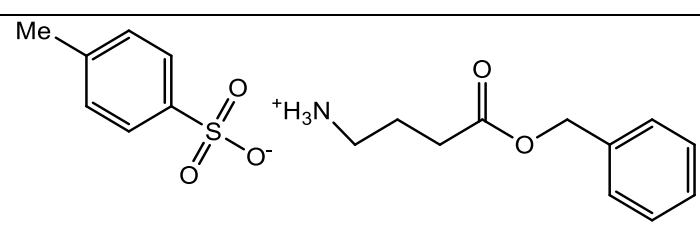
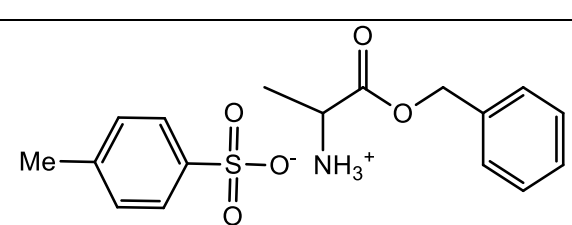


**Figure 3.1:** Synthetic schemes of 2-NBABA, 4-BOBAMS and 1-BOPAMS.

### 3.3 NUCLEAR MAGNETIC RESONANCE (NMR) SPECTROSCOPY

The synthesized compounds were characterized by using NMR (<sup>1</sup>H-NMR and <sup>13</sup>C-NMR) spectroscopy to validate their structures. The characterization was done by using a Bruker NMR spectroscopy, and about 10-30 mg of each compound (2-NBABA, 1-BOPAMS and 4-BOBAMS) was dissolved in the appropriate NMR solvent (DMSO and/or chlorofom) in a clean NMR tube. The <sup>13</sup>C-NMR and <sup>1</sup>H-NMR chemical shifts obtained were then assigned to different carbons and hydrogens.

**Table 3.1:** The abbreviations, chemical formula and molecular structures of the carboxylic acids and amino ester compounds.

Abbreviation	Chemical formula	Molecular structure
2-NBABA	$C_{11}H_{13}NO_3$	
4-BOBAMS	$C_{18}H_{23}NO_5S$	
1-BOPAMS	$C_{11}H_{13}NO_3$	

### 3.4 METAL SPECIMEN

The specimens used for corrosion tests were MS and Al coupons with a dimension of 3 cm length  $\times$  2 cm breadth and contained a small hole of 2 mm diameter for hanging on a glass rod. The chemical composition (wt %) of the MS used in all experimental procedures are: (Mn = 0.37), (Ni = 0.039), (P = 0.02), (S = 0.03), (C = 0.21) (Fe = 99.32) and (Mo = 0.01). Al coupons of approximately 99 (wt %) composition were also used. Before the electrochemical measurements, the surfaces of all the specimens were polished under running water by different grades emery paper and rinsed with doubly distilled water.

### 3.5 PREPARATION OF SOLUTIONS

Approximately 1.0 M HCl aggressive solution was carefully prepared by diluting the appropriate amount of analytical grade 32% HCl with doubly distilled water. Stock solutions of  $10.0 \times 10^{-4}$  M and  $10.0 \times 10^{-3}$  M for the corrosion inhibitors were carefully prepared by weighing appropriate amounts of the inhibitors and by the addition of doubly distilled water to the mark of 1000 ml volumetric flask. From the two stock solutions, a series of concentrations ( $1.0 \times 10^{-4}$ - $5.0 \times 10^{-4}$  M) were prepared through the use of appropriate amounts of doubly distilled water as indicated in the results section. The stock solution of  $10.0 \times 10^{-4}$  M was used to prepare inhibitor concentration range used for Al metal and that of  $10.0 \times 10^{-3}$  M was used to prepare concentration of the inhibitors for MS.

### 3.6 ELECTROCHEMICAL TECHNIQUES

For the electrochemical experiments, PDP was carried out using a Metrohm Autolab Potentiostat/Galvanostat (PGSTAT302N), and EIS was carried out using Bio-Logic ASA Potentiostat. Both the analyzers were equipped with a three-electrode cell that consisted of a saturated calomel with Ag/AgCl as a reference electrode (RE), the platinum counter electrode (CE) and the working electrode (WE) was the metal specimen of interest. For EIS, a bridge tube was used to place the working electrode near the reference electrode to minimize IR contribution/Ohmic drop from the electrolyte solution. During the PDP and EIS measurements, the Al and MS samples were allowed to corrode in open circuit potential (OCP) freely for 30 minutes; this was done to reach a stable corrosion potential ( $E_{\text{corr}}$ ) for the two working electrodes (Al and MS). OCP was run before the electrochemical (PDP and EIS) measurements because the two techniques rely on the stability of the OCP. An equivalent circuit was then drawn by using the EC-lab software with the use of the Z-fit method and the best-fit circuit was obtained/chosen for a particular system (Al and MS). The circuit fitting was done for both the uninhibited as well as the inhibited solution.

#### 3.6.1 Electrochemical impedance spectroscopy (EIS)

The electrochemical impedance curves were obtained by using a frequency response analyzer (FRA) that is connected to the Potentiostat at a frequency range of 100 kHz to 0.00001 kHz under conditions of potentiodynamic that has an amplitude of 5 mV peak to peak by using an AC signal at  $E_{\text{corr}}$ . The metal specimens that were used had a  $1 \text{ cm}^2$  surface area subjected to

the aggressive/acid solution. The measurements were all conducted at atmospheric conditions without any stirring. The obtained Nyquist and bode plots from the EIS measurements were analyzed to interpret the dissolution of Al and MS.

EIS was used to evaluate the corrosion of Al and MS in 1.0 M HCl. Electrochemical parameters were then obtained, and their data were used to calculate the percentage inhibition efficiency from the equation below:

$$\% IE_{EIS} = \left( 1 - \frac{R_{ct}^{\circ}}{R_{ct}} \right) \times 100 \quad (3.1)$$

where;  $R_{ct}^{\circ}$  is the charge transfer resistance in the absence of the inhibitor and  $R_{ct}$  is the charge transfer resistance in the presence of the inhibitor.

### 3.6.2 Potentiodynamic polarization (PDP)

The PDP studies were performed at a potential range of -250 to +250 mV (SCE), and at a scan rate of 1 mV.s<sup>-1</sup>, Tafel curves were obtained. The PDP measurements were done for Al and MS specimen in the presence and absence of inhibitors. Relevant electrochemical parameters such as the corrosion current density ( $i_{corr}$ ), corrosion potential ( $E_{corr}$ ), anodic ( $\beta_a$ ) and cathodic ( $\beta_c$ ) Tafel slopes were determined by utilizing the PDP method. The inhibition efficiencies (IE) based on corrosion current density values were calculated using the equation given below:

$$\% IE_{PDP} = \left( \frac{i_{corr}^{\circ} - i_{corr}^i}{i_{corr}^{\circ}} \right) \times 100 \quad (3.2)$$

where  $i_{corr}^{\circ}$  and  $i_{corr}^i$  are values of corrosion current density in the absence and the presence of inhibitor, respectively.

### 3.7 FOURIER TRANSFORM INFRARED SPECTROSCOPY (FT-IR)

FT-IR was used on the adsorption films on the surface of electrochemically tested samples, namely, Al and MS, in 1.0 M HCl in the presence and absence of corrosion inhibitors at 303 K. The films were scratched off the surface of the specimen with care by using sharp scissors, and FT-IR was used to analyze the powders. The technique was also used to characterize and determine the functional groups of the synthesized inhibitors.

### 3.8 GRAVIMETRIC ANALYSIS

Al and MS were first weighed and then completely immersed in 100 ml of 1.0 M HCl in the absence and presence of the inhibitor at different concentrations and various temperatures ranging from 303-333K for a total immersion time of 8 h. The method was performed in a thermostatic water bath to maintain the heat during the immersion period. Then after the immersion period has passed, the specimens were removed, rinsed/washed with doubly distilled water then dried, and the final weights of the specimens were noted. The results obtained were used to calculate the percentage inhibition efficiency (%IE), corrosion rate ( $\rho$ ) and surface coverage ( $\theta$ ) in  $\text{g.cm}^2.\text{h}^{-1}$  using the equations below:

$$\%IE = \left(1 - \frac{\rho_1}{\rho_2}\right) \times 100\% \quad (3.3)$$

where IE is the inhibition efficiency,  $\rho_1$  is the corrosion rate of metal in the presence of inhibitor and  $\rho_2$  is the corrosion rate of metal in the absence of inhibitor.

The following equation gives the degree of surface coverage:

$$\theta = \left(1 - \frac{\rho_1}{\rho_2}\right) \quad (3.4)$$

where  $\theta$  is the degree of surface coverage,  $\rho_1$  is the corrosion rate of metal in the presence of inhibitor and  $\rho_2$  is the corrosion rate of metal in the absence of inhibitor.

The rate of corrosion can be calculated from equation (2.11).

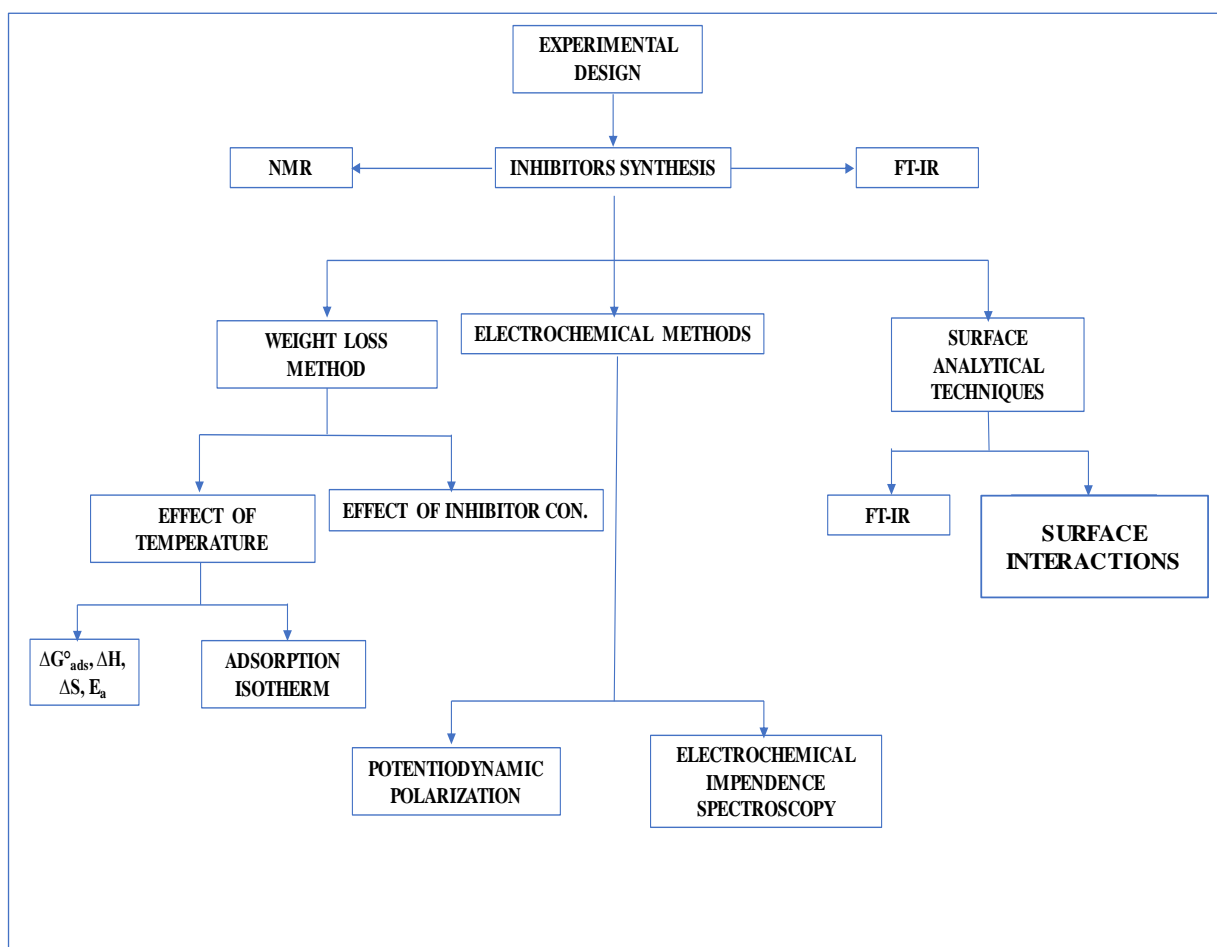


**Figure 3.2:** Schematic illustration for the instrumentation used in the characterization of the inhibitors and the evaluation of corrosion of Al and MS metals.



## CHAPTER 4

---

# RESULTS AND DISCUSSION

This chapter is divided into three sections. In the first section, the three synthesized organic compounds are characterized by FT-IR,  $^1\text{H-NMR}$  and  $^{13}\text{C-NMR}$  spectroscopies and their percentage yield obtained for each compound are stated. The second and third section describes the corrosion inhibition behaviour of 2-NBABA, 1-BOPAMS and 4-BOBAMS on MS and Al respectively, in 1.0 M HCl medium. These two sections discuss the effect of temperature and inhibitor concentration, the adsorption isotherms and thermodynamic parameters, adsorption film analysis. They also discuss the results obtained via the PDP and EIS techniques. Inhibition mechanisms for both MS and Al are also highlighted. They end with the comparison of the inhibition performance of the synthesized carboxylic acid and amino esters on Al and MS.

## 4.1 CHARACTERIZATION OF INHIBITORS

### 4.1.1 Characterization of 2-NBABA

2-NBABA was purified as white crystal product and characterized by IR,  $^1\text{H-NMR}$  and  $^{13}\text{C-NMR}$ . The FT-IR spectra (figure 4.1) of carboxylic acids are recognized by noting the O-H and C=O stretch. The synthesized 2-NBABA compound showed a C=O stretching bands around 1711 and around  $1632\text{ cm}^{-1}$ . The N-H (secondary amine) stretching absorption band was observed at the frequency around  $3032\text{-}3281\text{ cm}^{-1}$ , with a spike at  $3280\text{ cm}^{-1}$ . The O-H group overlaps along with the N-H vibration. The C-N vibration is located around  $1166\text{ cm}^{-1}$ . There are multiple absorption bands located at around  $1246\text{-}1352\text{ cm}^{-1}$ , representing the C-O absorption band. The  $\text{CH}_3$ ,  $\text{CH}_2$  and CH absorption bands are observed at around  $2578\text{ cm}^{-1}$ ,  $2900\text{ cm}^{-1}$  and  $2976\text{ cm}^{-1}$  respectively. The  $^1\text{H-NMR}$  spectra of 2-NBABA is shown in figures 4.2-4.5. The  $^1\text{H-NMR}$  spectrum of 2-NBABA showed a triplet at  $\delta$ , 0.96 accounting for three protons ( $\text{CH}_3$ ). This triplet is due to the methylene protons which themselves are confirmed by multiplet at 1.74-1.91 ppm since the two protons are non-equivalent because of a neighbouring chiral centre. A methine proton is confirmed by a multiplet peak at 4.28-4.31 ppm. The presence of multiplet around 7.47, a triplet of triplet around 7.64, and multiplet around 7.89 ppm is due to the presence of aromatic protons. The presence of a doublet around 8.57 (-N-H group) is due to the methylidyne group. The presence of a singlet around 12.59 (-O-H group). The  $^{13}\text{C-NMR}$  spectra of 2-NBABA is shown in figure 4.6. The  $^{13}\text{C-NMR}$  frequencies represent the correct number of carbon atoms (nine peaks) at the appropriate chemical shift values. A methyl carbon peak was observed at 11.38 ppm. A methylene carbon peak at around 24.42 ppm. Four methine peaks at approximately 54.62 ppm, 127.93 ppm (2xCH), 128.67 ppm (2xCH) and at 131.79 ppm (1xCH). Three quaternary carbons at around 134.48 ppm, 167.09 ppm (C=O) and 174.18 ppm (C=O). The spectral data (IR,  $^1\text{H-NMR}$ ,  $^{13}\text{C-NMR}$  and mass) of all the synthesized compounds are in full agreement with the proposed structures.

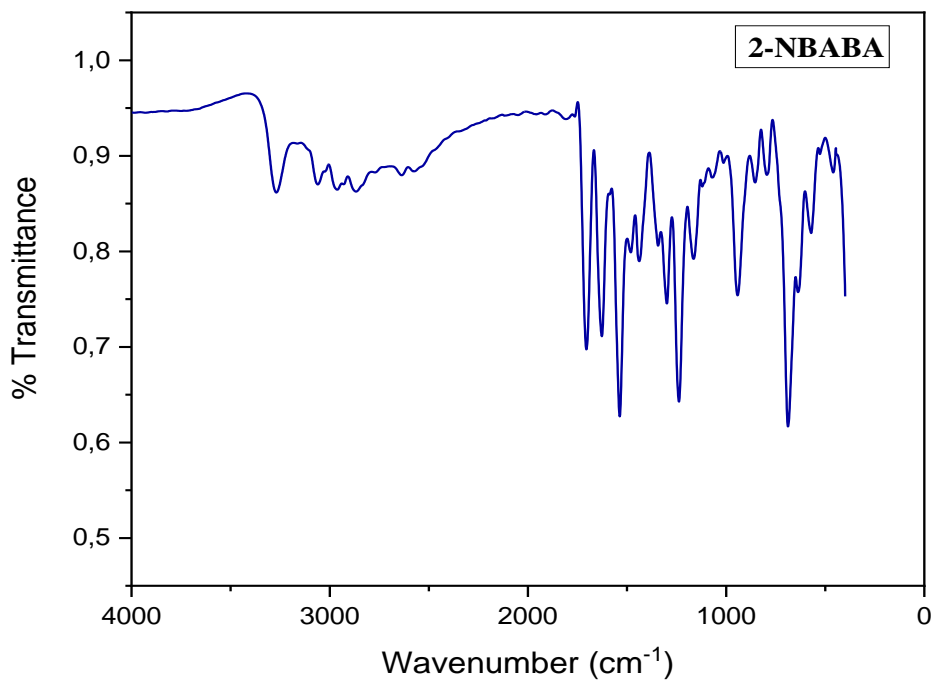


**Figure 4.1:** FT-IR spectrum of 2-NBABA compound.

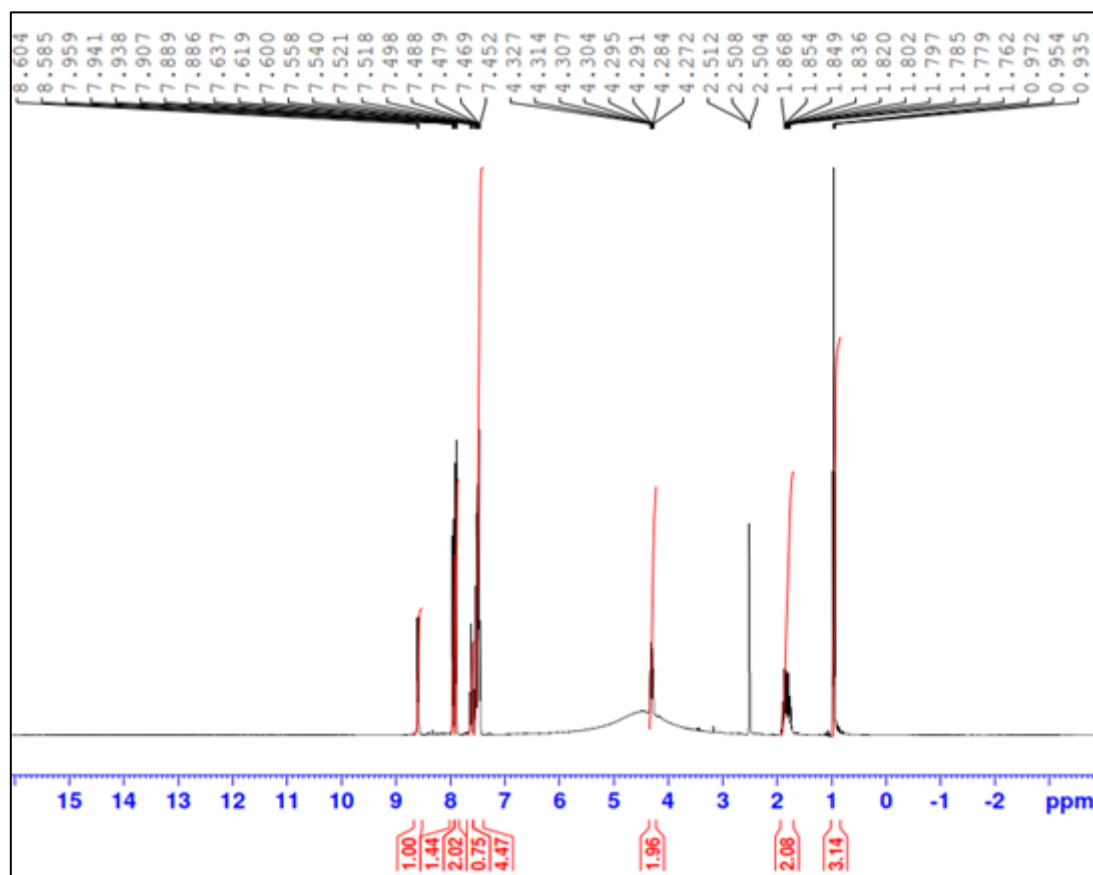


**Figure 4.2:** <sup>1</sup>H-NMR spectrum of 2-NBABA.

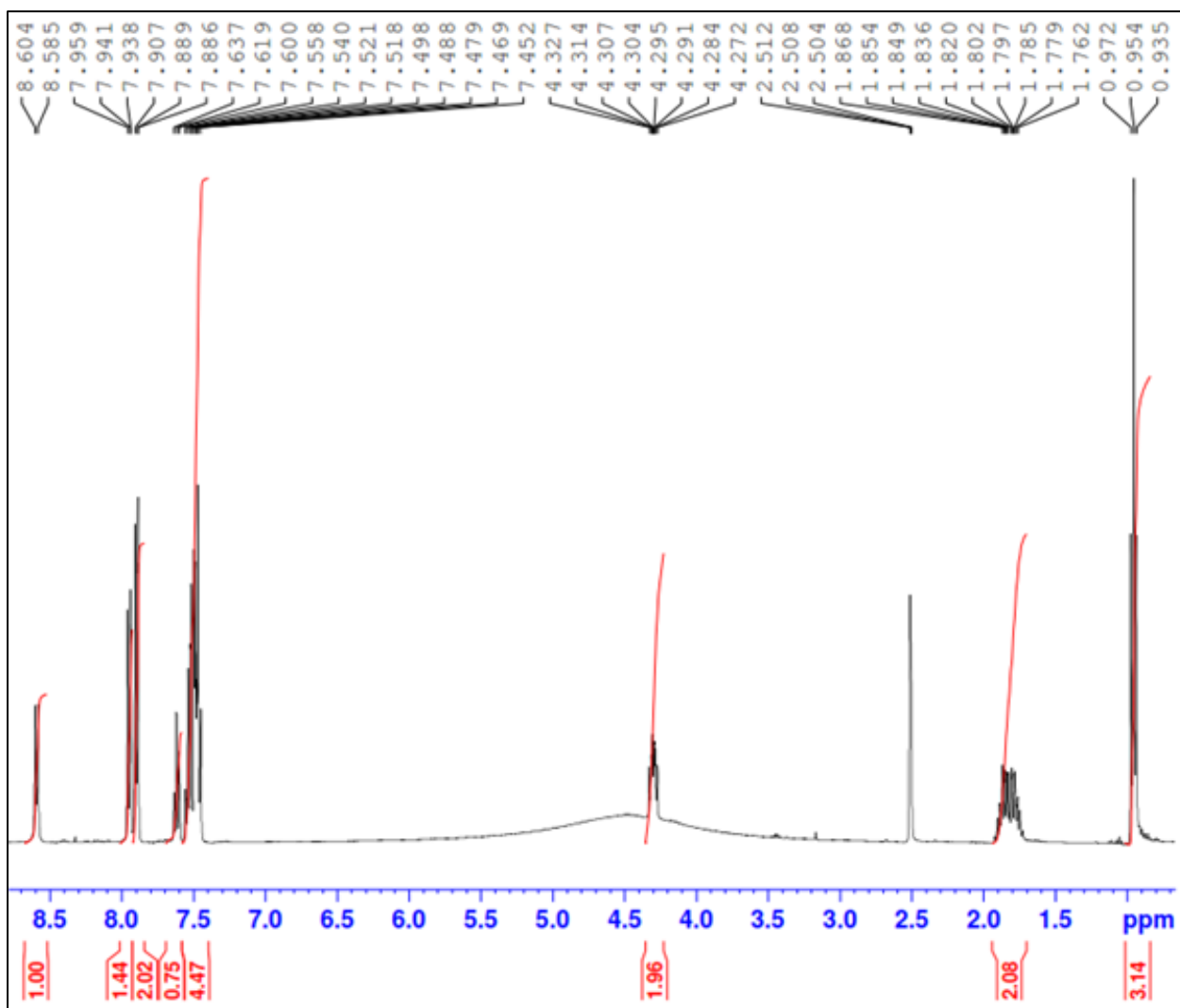


**Figure 4.3:** <sup>1</sup>H-NMR first expansion spectrum of 2-NBABA.

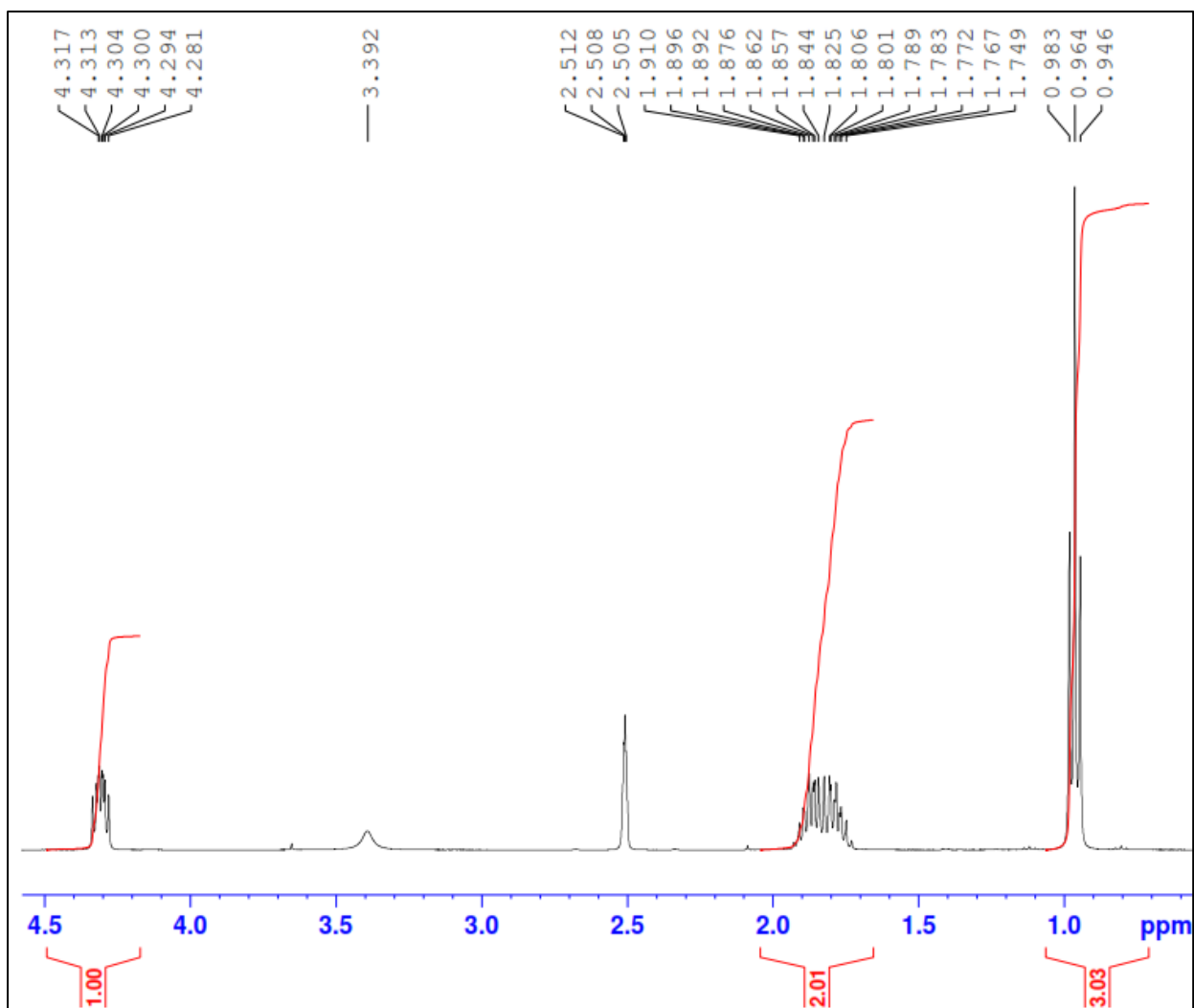


**Figure 4.4:**  $^1\text{H}$ -NMR second expansion spectrum of 2-NBABA.

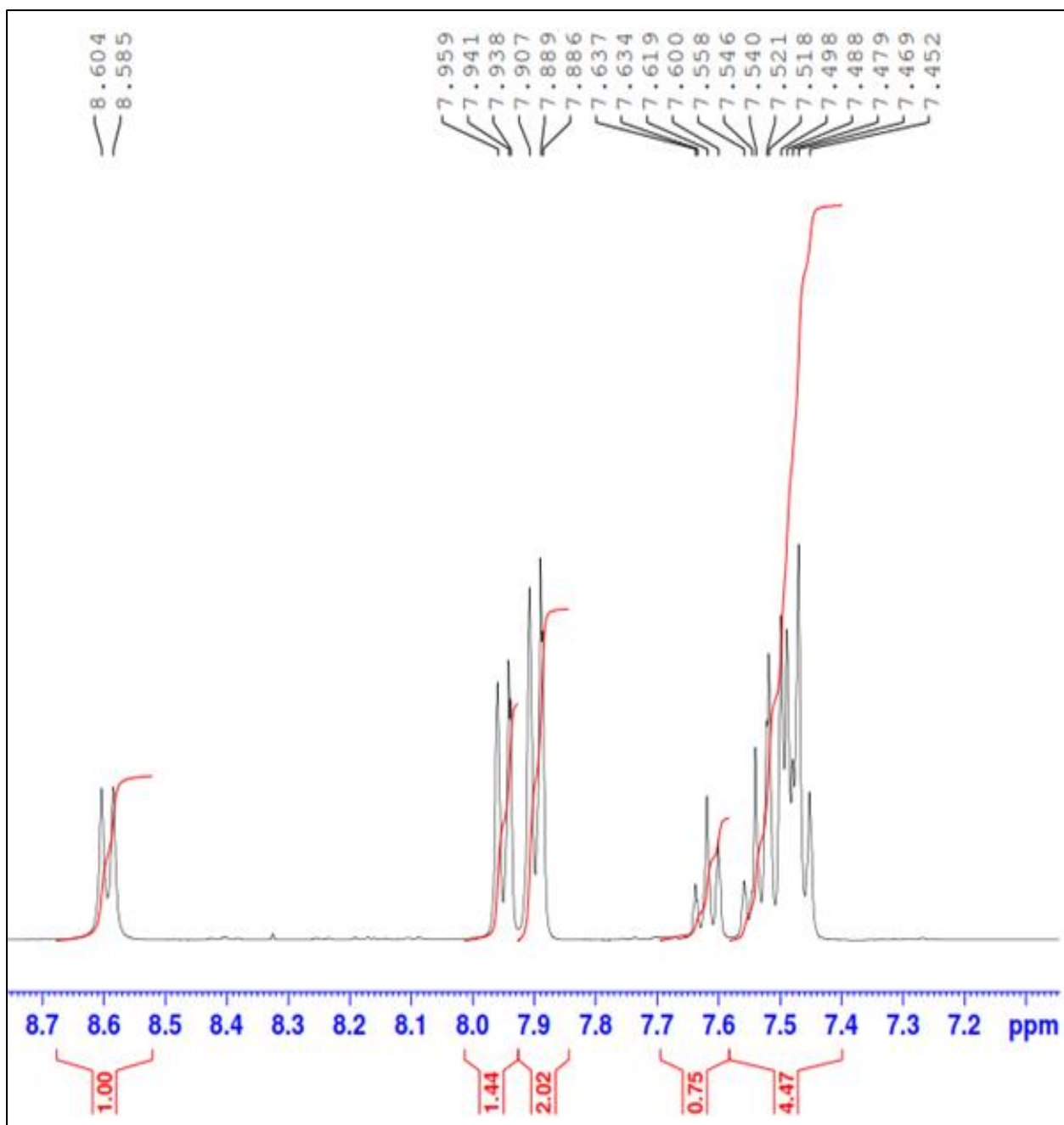


**Figure 4.5:**  $^1\text{H}$ -NMR third expansion spectrum of 2-NBABA.

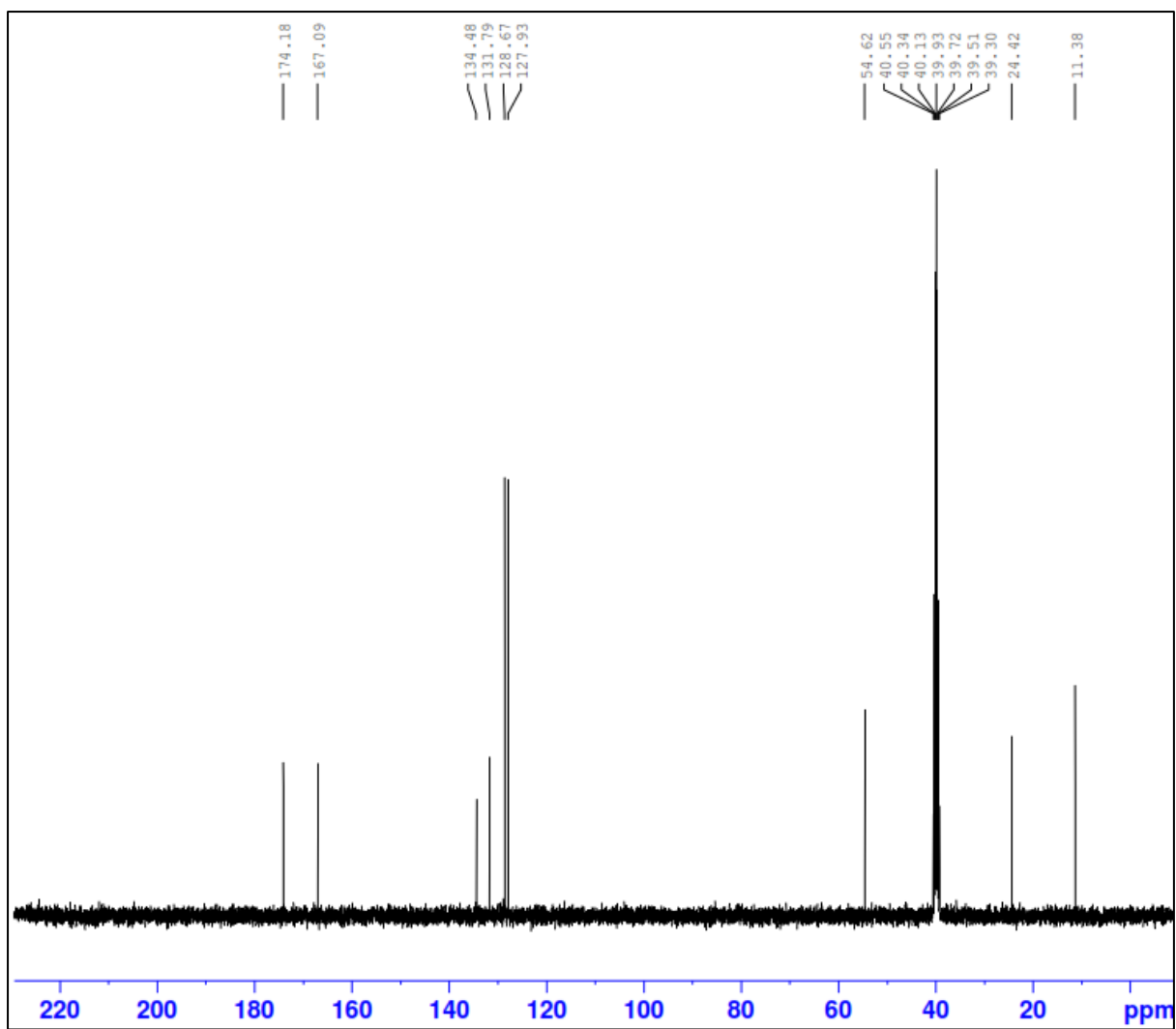
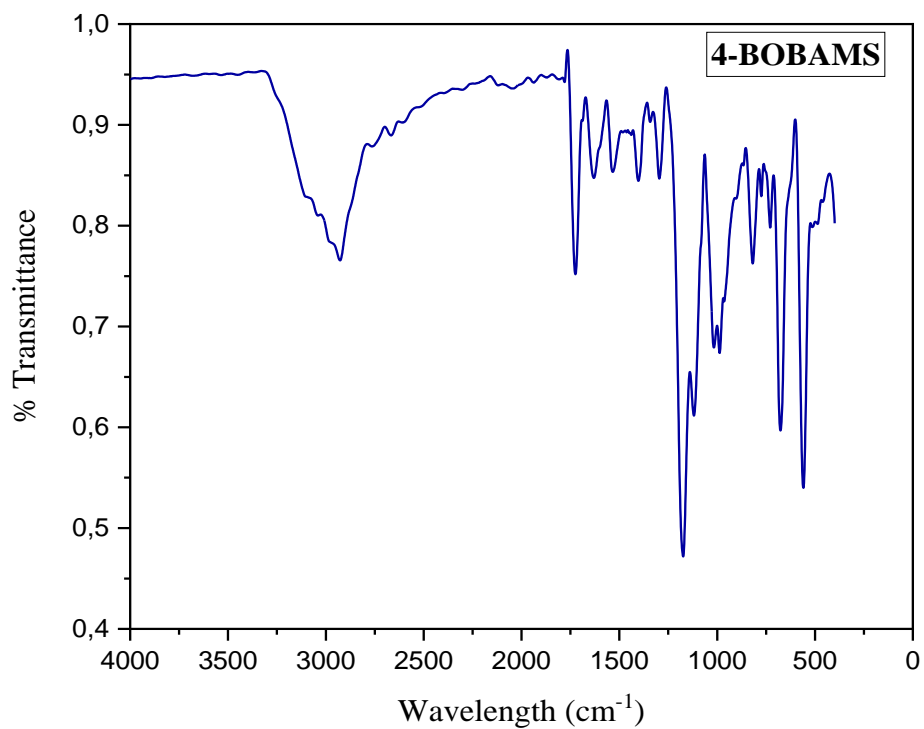


Figure 4.6:  $^{13}\text{C}$ -NMR spectrum of 2-NBABA.

#### 4.1.2 Characterization of 4-BOBAMS

4-BOBAMS was purified as white crystal product and characterized by IR,  $^1\text{H-NMR}$  and  $^{13}\text{C-NMR}$ . The 4-BOBAMS inhibitor molecules exist as zwitterions since they contain both positively and negatively charged groups. The FT-IR spectra (figure 4.7) of the synthesized compounds showed an ammonium salt ( $^+\text{NH}_3$ ) which gave a strong, broad absorption band at around  $3095\text{ cm}^{-1}$ . The absorption bands with the wavenumber range  $1345\text{-}1539\text{ cm}^{-1}$  correspond to the  $\text{O}=\text{S}=\text{O}$  group. An intense  $\text{C}=\text{O}$  stretching absorption band was located at approximately  $1730\text{ cm}^{-1}$ . The  $\text{S-O}^-$  absorption band, is found at around  $1644\text{ cm}^{-1}$ , and  $\text{C-O}$  stretching is located at  $1032\text{ cm}^{-1}$ . The  $\text{C-N}$  stretch was observed at around  $1121\text{-}1194\text{ cm}^{-1}$ . The aromatic  $\text{C}=\text{C}$  peaks are observed at around  $1456\text{-}1528\text{ cm}^{-1}$ . The  $\text{CH}_3$ ,  $\text{CH}_2$  and  $\text{CH}$  absorption bands are found at about  $2927\text{-}2983\text{ cm}^{-1}$ ,  $2875\text{ cm}^{-1}$  and  $2607\text{-}2742\text{ cm}^{-1}$  respectively. The broad, intense peak at around  $2875\text{-}3095\text{ cm}^{-1}$  is due to the partial  $\text{O-H}$  bond. The  $^1\text{H-NMR}$  spectra of 4-BOBAMS is shown in figure 4.8-4.10. The  $^1\text{H-NMR}$  spectra of 4-BOBAMS showed quintet in the region of  $\delta$ , 1.81 ( $\text{H}_2\text{C}(3)^{\text{GABA}}$ ) due to the four protons of the two methylene group. The presence of singlet around 2.29 ppm ( $\text{H}_3\text{C}^{\text{PTSA}}$ ). There are two triplets at around 2.48 and 2.83 ppm of ( $\text{H}_2\text{C}(2)^{\text{GABA}}$ ) and ( $\text{H}_2\text{C}(4)^{\text{GABA}}$ ) respectively. A singlet peak at approximately 5.11 ppm ( $\text{H}_2\text{C}^{\text{Bn}}$ ). Two doublets at around 7.14 and 7.51 ppm respectively, due to the equivalent aromatic protons of the p-toluenesulfonic acid ring. The aromatic protons of the product gave a signal of multiplet at around 7.32-7.41 ppm ( $\text{HC}^{\text{Ar}}$ ). A singlet at approximately 7.74 ppm was observed ( $^+\text{NH}_3$ ). The  $^{13}\text{C-NMR}$  spectra of 4-BOBAMS is shown in figure 4.11-4.12. The  $^{13}\text{C-NMR}$  spectra represent the correct number of carbon atoms at the appropriate chemical shifts. A methyl carbon peak at around 21.24 ppm ( $\text{CH}_3^{\text{PTSA}}$ ). There are four methylene carbon peaks at about 22.87 ( $\text{CH}_2(3)^{\text{GABA}}$ ), 30.71 ( $\text{CH}_2(2)^{\text{GABA}}$ ), 38.67 ( $\text{CH}_2(4)^{\text{GABA}}$ ) and 66.07 ( $\text{CH}_2^{\text{Bn}}$ ) ppm. The aromatic protons of the benzene rings were observed at around 125.94-128.92 ppm ( $\text{C}^{\text{Ar}}$ ). There are four quinary peaks at about 136.56, 138.37, 145.75, and 172.50 ppm ( $\text{CO}_2^{\text{Bn}}$ ).





**Figure 4.7:** FT-IR spectrum of 4-BOBAMS compound.

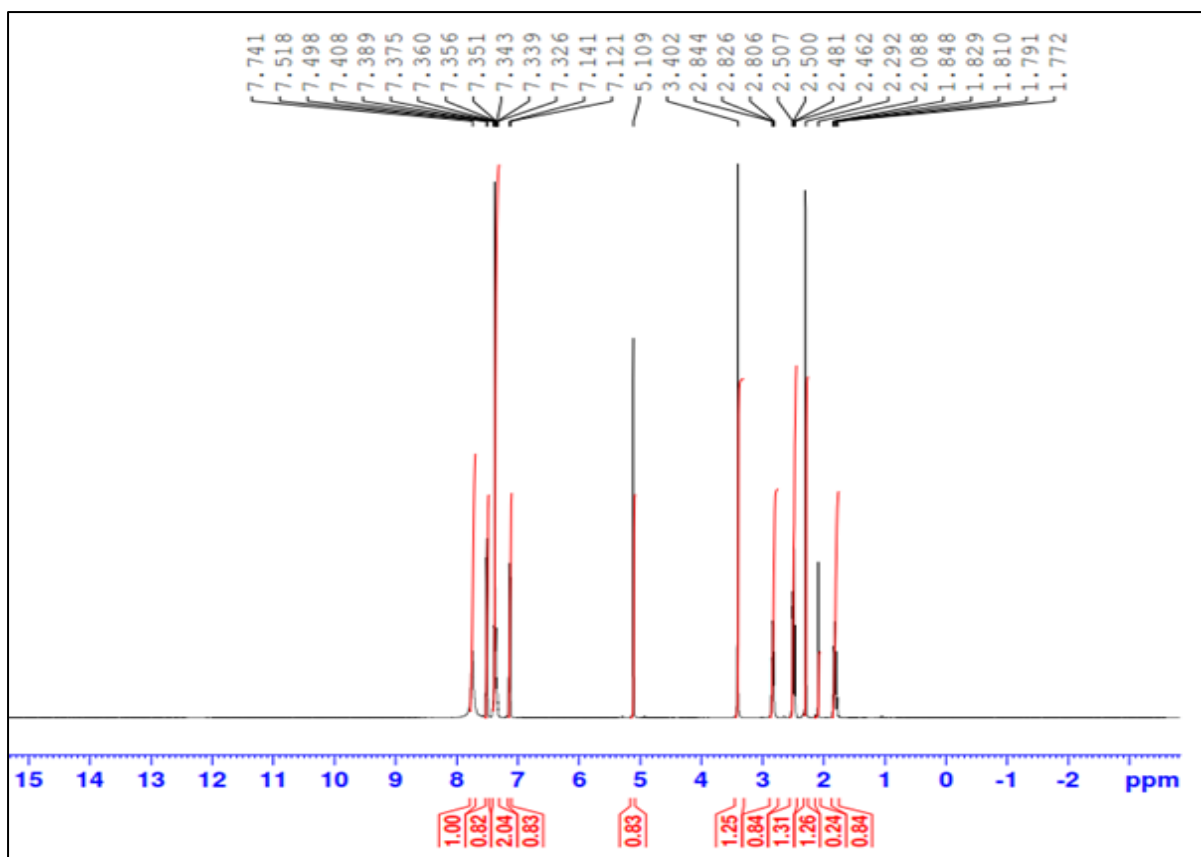


**Figure 4.8:** <sup>1</sup>H-NMR spectrum of 4-BOBAMS.

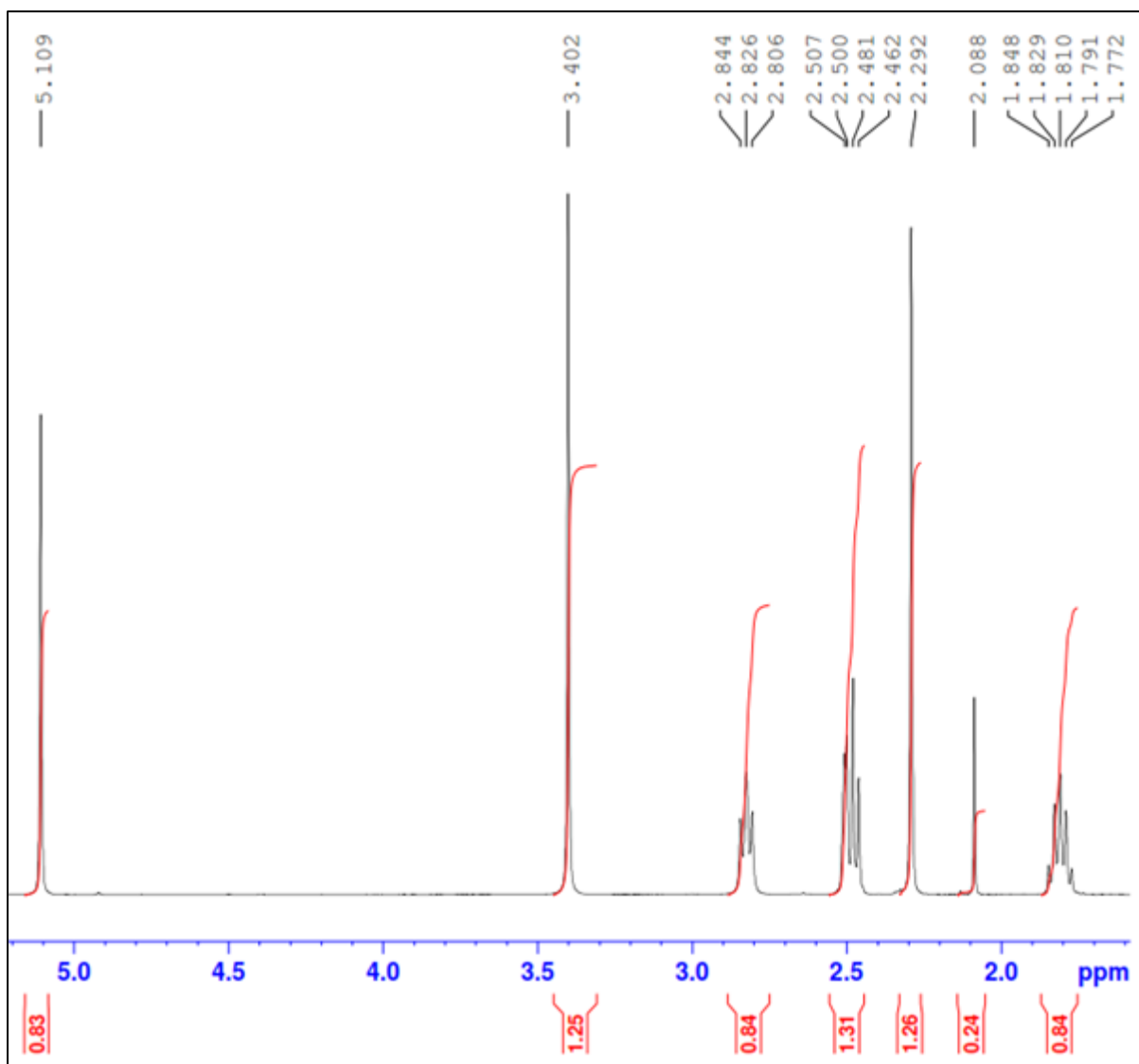


**Figure 4.9:** <sup>1</sup>H-NMR first expansion spectrum of 4-BOBAMS.

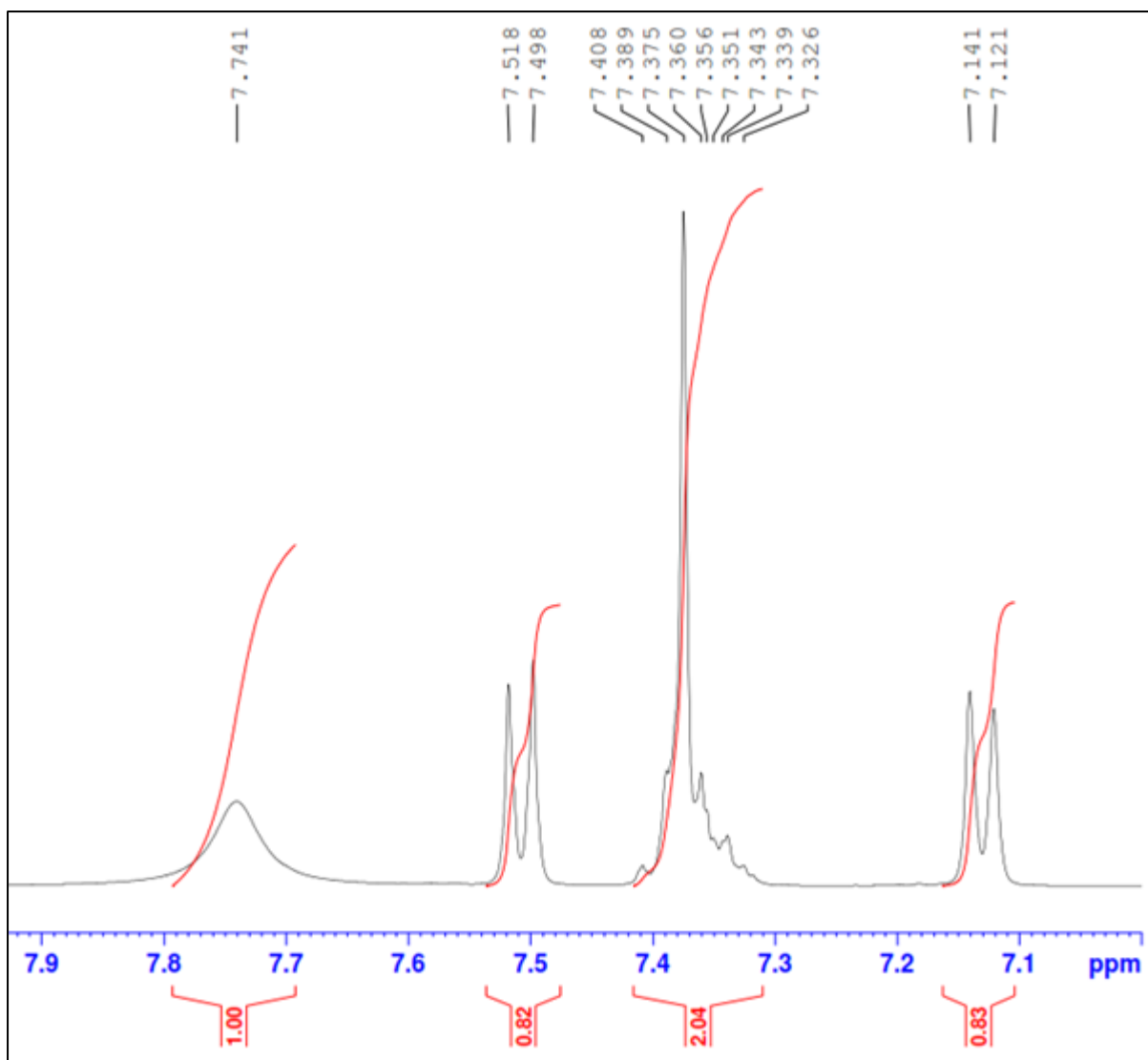


**Figure 4.10:**  $^1\text{H}$ -NMR second expansion spectrum of 4-BOBAMS.

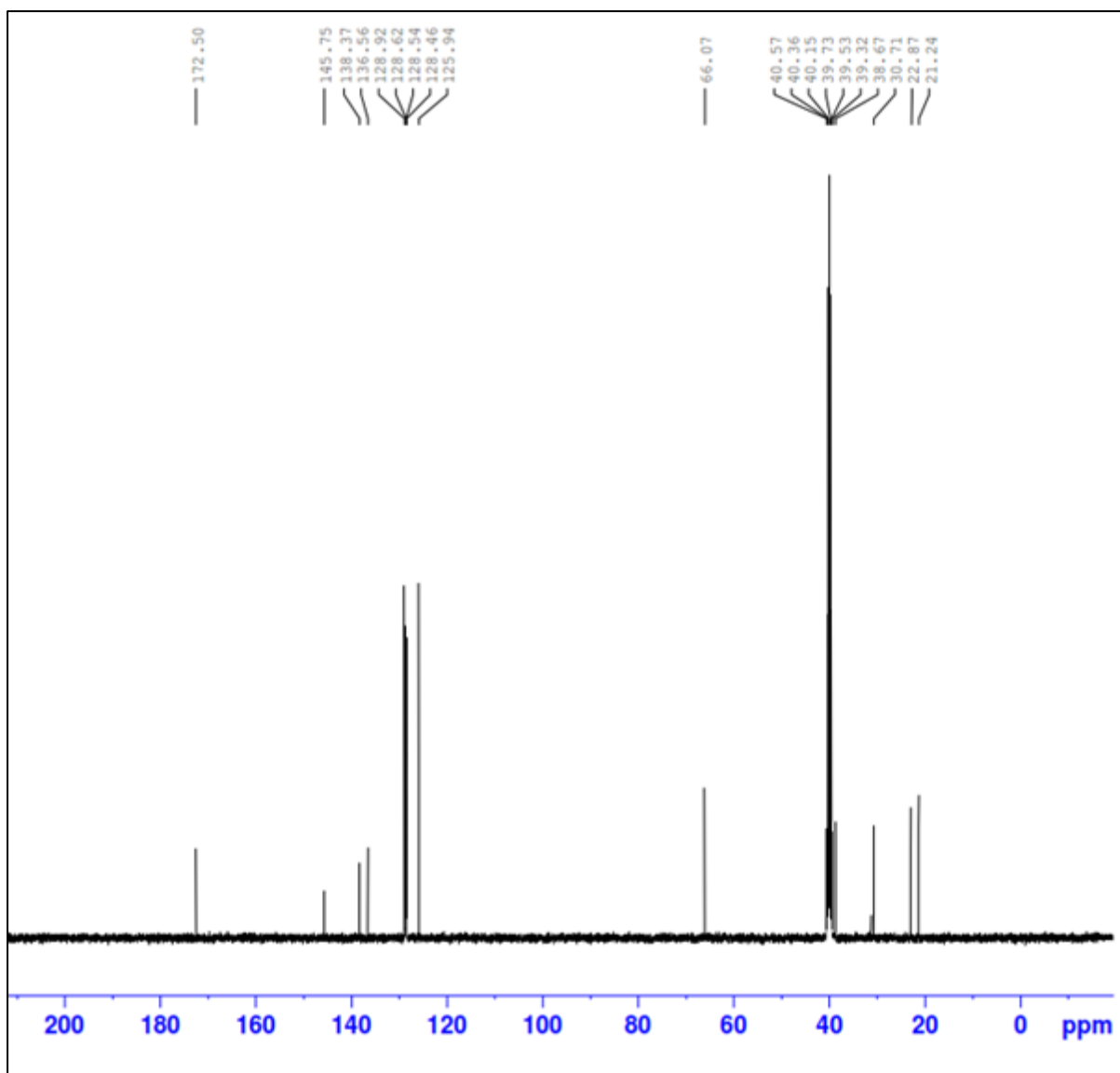
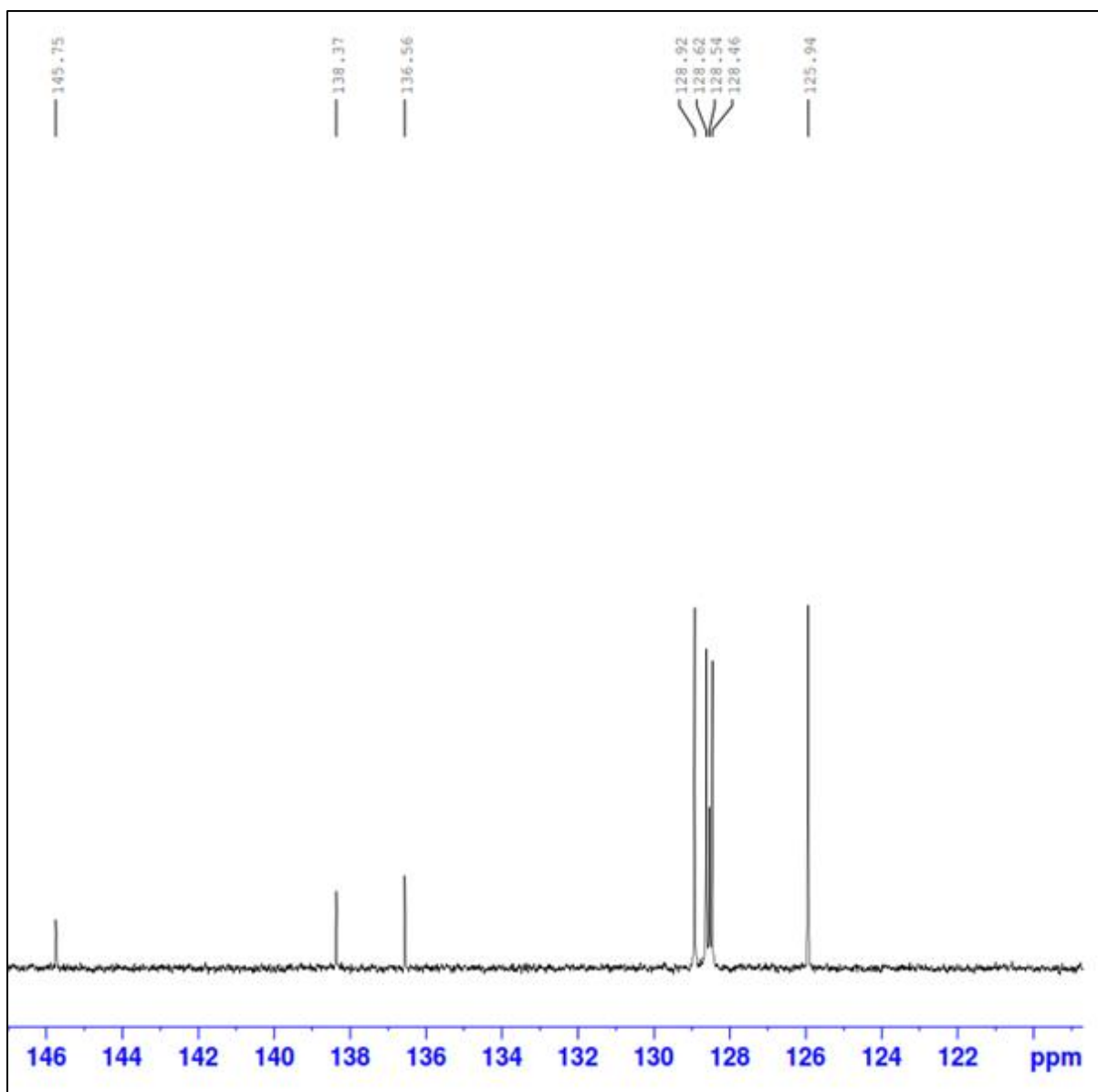


Figure 4.11:  $^{13}\text{C}$ -NMR spectrum of 4-BOBAMS.



**Figure 4.12:**  $^{13}\text{C}$ -NMR spectrum expansion of 4-BOBAMS.

### 4.1.3 Characterization of 1-BOPAMS

1-BOPAMS was purified as white crystal product and characterized by IR,  $^1\text{H-NMR}$  and  $^{13}\text{C-NMR}$ . The 1-BOPAMS inhibitor molecules also exist as zwitterions since they contain both positively and negatively charged groups. The FT-IR spectra (figure 4.13) of the synthesized compounds showed an ammonium salt ( $^+\text{NH}_3$ ) which gave a strong, broad absorption band at around  $3066\text{ cm}^{-1}$ . The absorption bands with the wavenumber range  $1367\text{-}1452\text{ cm}^{-1}$  correspond to the  $\text{O}=\text{S}=\text{O}$  group. An intense  $\text{C}=\text{O}$  stretching absorption band was located at approximately  $1740\text{ cm}^{-1}$ . The  $\text{S}-\text{O}^-$  absorption band, is found at around  $1613\text{ cm}^{-1}$ , and  $\text{C}-\text{O}$  stretching is situated at  $1100\text{-}1124\text{ cm}^{-1}$ . The  $\text{C}-\text{N}$  stretch was observed at around  $1171\text{-}1278\text{ cm}^{-1}$ . The aromatic  $\text{C}=\text{C}$  peaks are observed at about  $1513\text{ cm}^{-1}$ . The  $\text{CH}_3$ ,  $\text{CH}_2$  and  $\text{CH}$  absorption bands are found at about  $3016\text{ cm}^{-1}$ ,  $2954\text{ cm}^{-1}$  and  $2532\text{-}2653\text{ cm}^{-1}$  respectively. The broad, intense peak at around  $2730\text{-}3232\text{ cm}^{-1}$  is due to the partial  $\text{O}-\text{H}$  bond. The  $^1\text{H-NMR}$  spectra of 1-BOPAMS is shown in figures 4.14-4.16. The  $^1\text{H-NMR}$  spectra of 1-BOPAMS showed doublet in the region of  $\delta$ , 1.41 ( $\text{H}_3\text{C}(1)^{\text{Aln}}$ ) due to the one protons ( $\text{HC}$ ) of the alanine group. The presence of singlet around 2.29 ppm ( $\text{H}_3\text{C}^{\text{PTSA}}$ ). The presence of quintet at around 4.18 ppm of ( $\text{HC}(2)^{\text{Aln}}$ ). A singlet was observed at approximately 5.24 ppm ( $\text{H}_2\text{C}^{\text{Bn}}$ ). Two doublets at around 7.14 and 7.51 ppm ( $\text{H}^{\text{PTSA}}$ ) respectively, due to the equivalent aromatic protons of the p-toluenesulfonic acid ring. A multiplet signal was observed due to aromatic protons at around 7.35-7.43 ppm ( $\text{HC}^{\text{Ar}}$ ). A singlet at approximately 7.74 ppm was observed ( $^+\text{NH}_3$ ). The  $^{13}\text{C-NMR}$  spectra of 1-BOPAMS is shown in figure 4.17-4.18. The  $^{13}\text{C-NMR}$  spectra represent the correct number of carbon atoms at the appropriate chemical shift values. Two methyl carbon peaks at around 16.16 ppm ( $\text{H}_3\text{C}(3)^{\text{Aln}}$ ) and 21.25 ppm ( $\text{H}_3\text{C}(3)^{\text{PTSA}}$ ). A methine carbon at approximately 31.16 ppm ( $\text{HC}(2)^{\text{Aln}}$ ). A methylene carbon peak was observed at around 67.49 ppm ( $\text{H}_2\text{C}^{\text{Bn}}$ ). The aromatic protons of the benzene rings were found at around 125-128.97 ppm ( $\text{C}^{\text{Ar}}$ ). There are four quinary peaks at about 135.71, 138.31, 145.82, and 170.31 ppm ( $\text{CO}_2^{\text{Bn}}$ ).

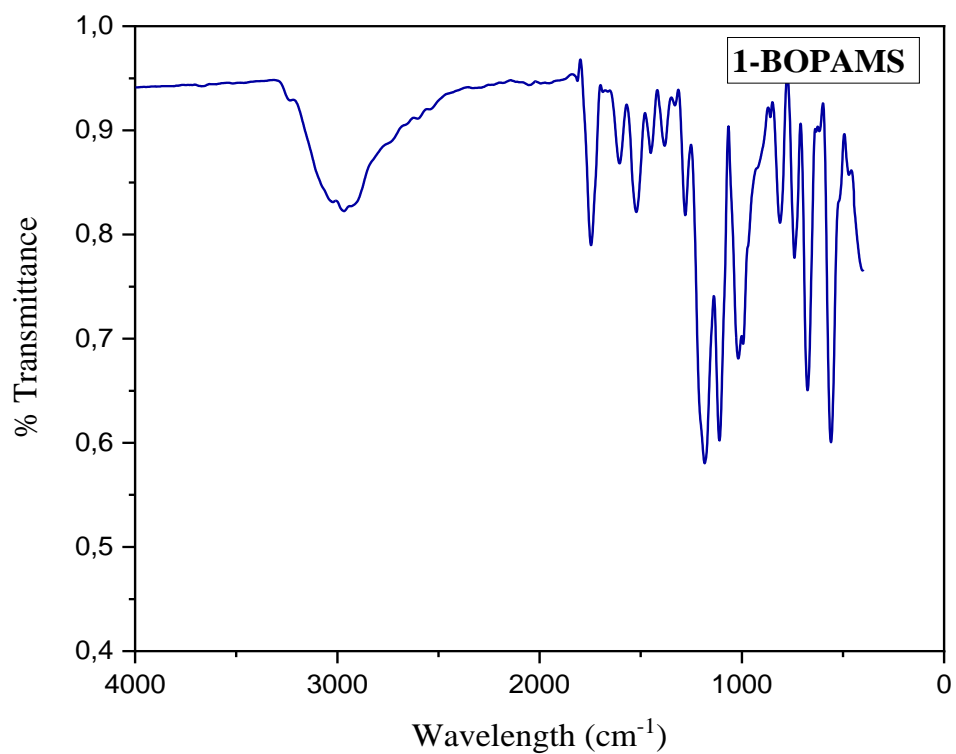


**Figure 4.13:** FT-IR spectrum of 1-BOPAMS compound.

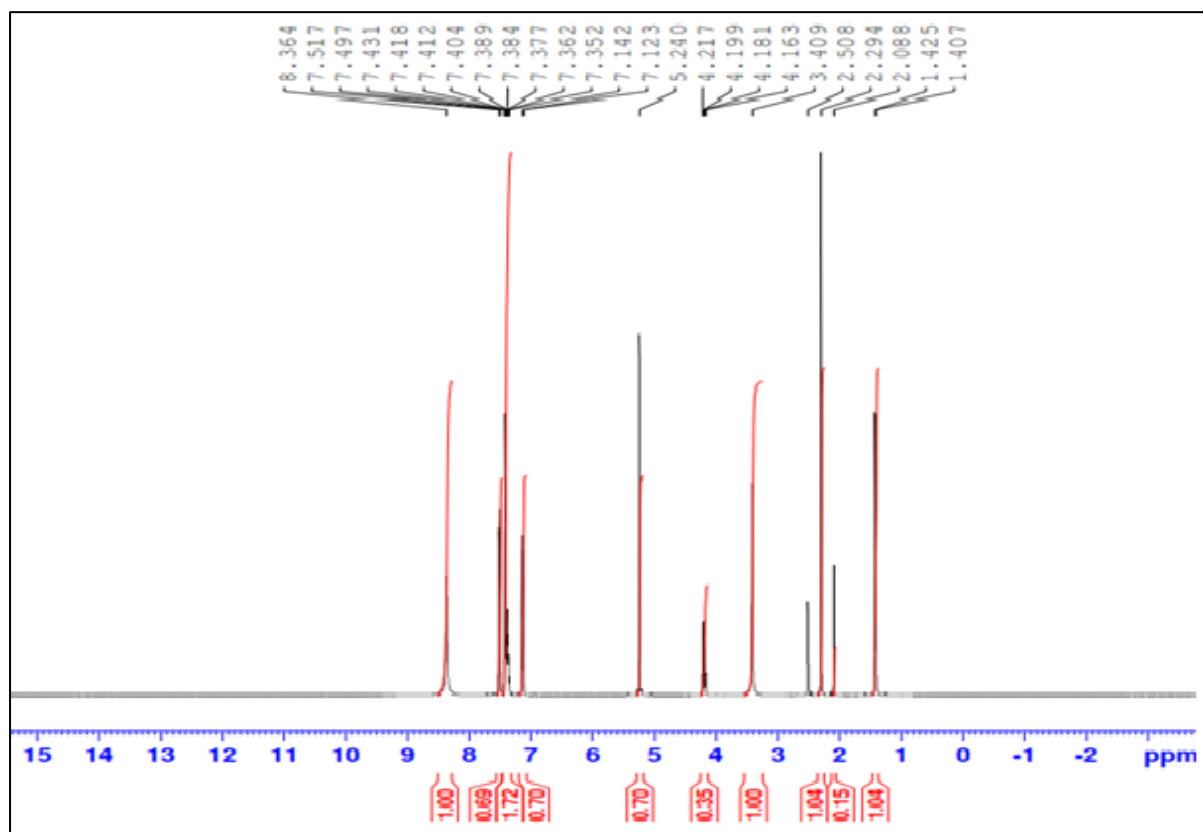


**Figure 4.14:**  $^1\text{H-NMR}$  spectrum of 1-BOPAMS.

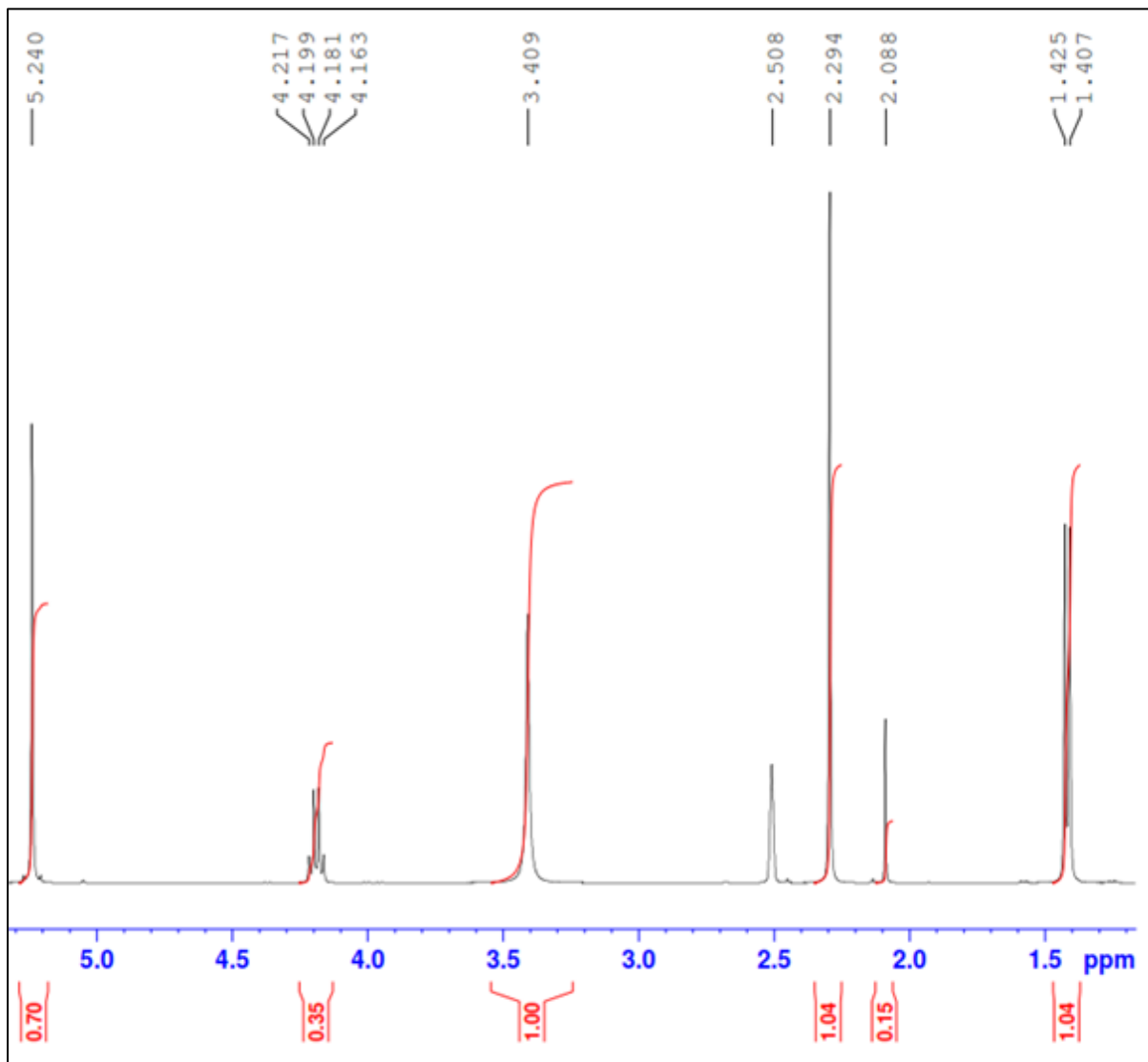
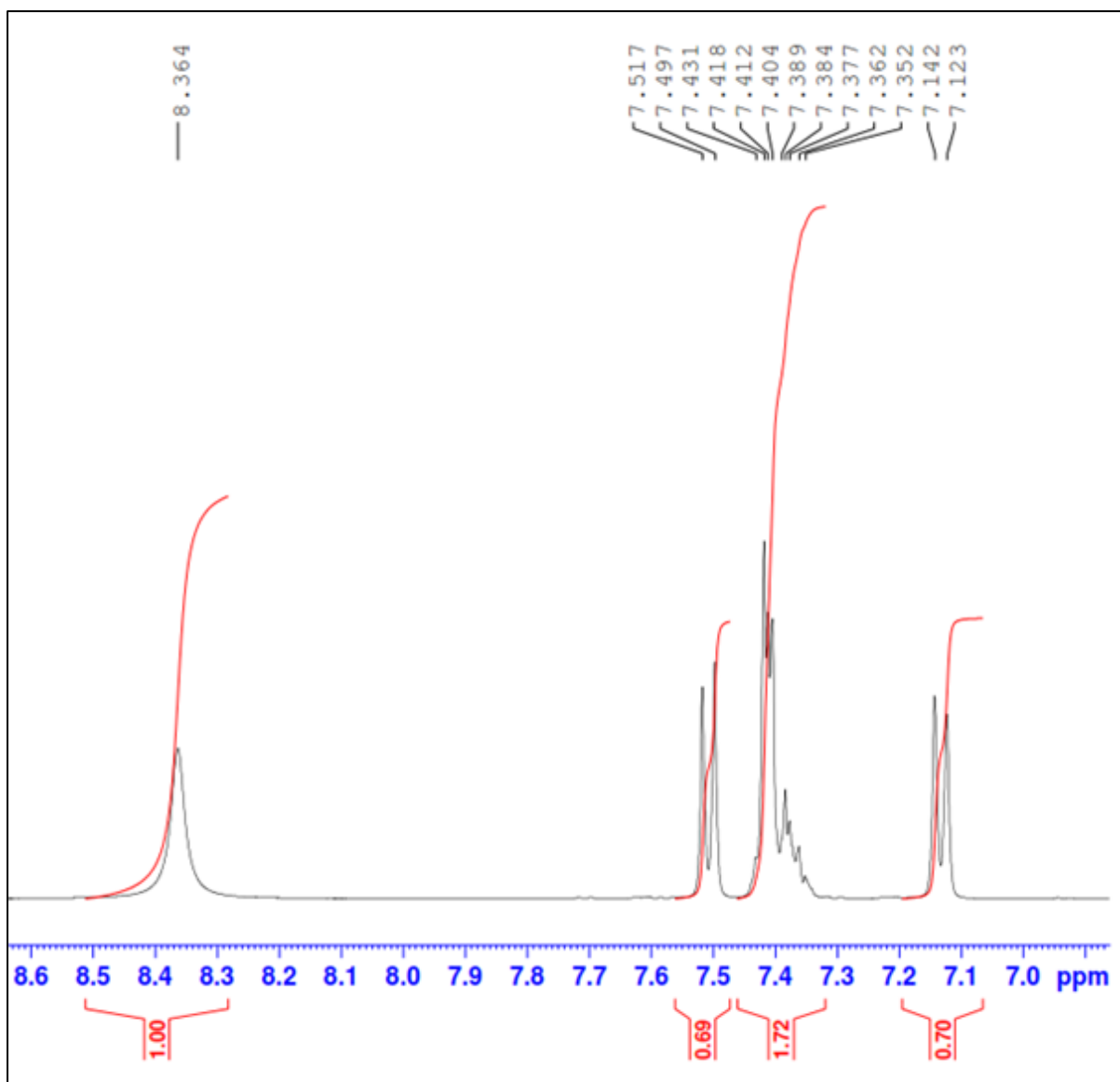


Figure 4.15: <sup>1</sup>H-NMR first expansion spectrum of 1-BOPAMS.





**Figure 4.16:**  $^1\text{H}$ -NMR second expansion spectrum of 1-BOPAMS.

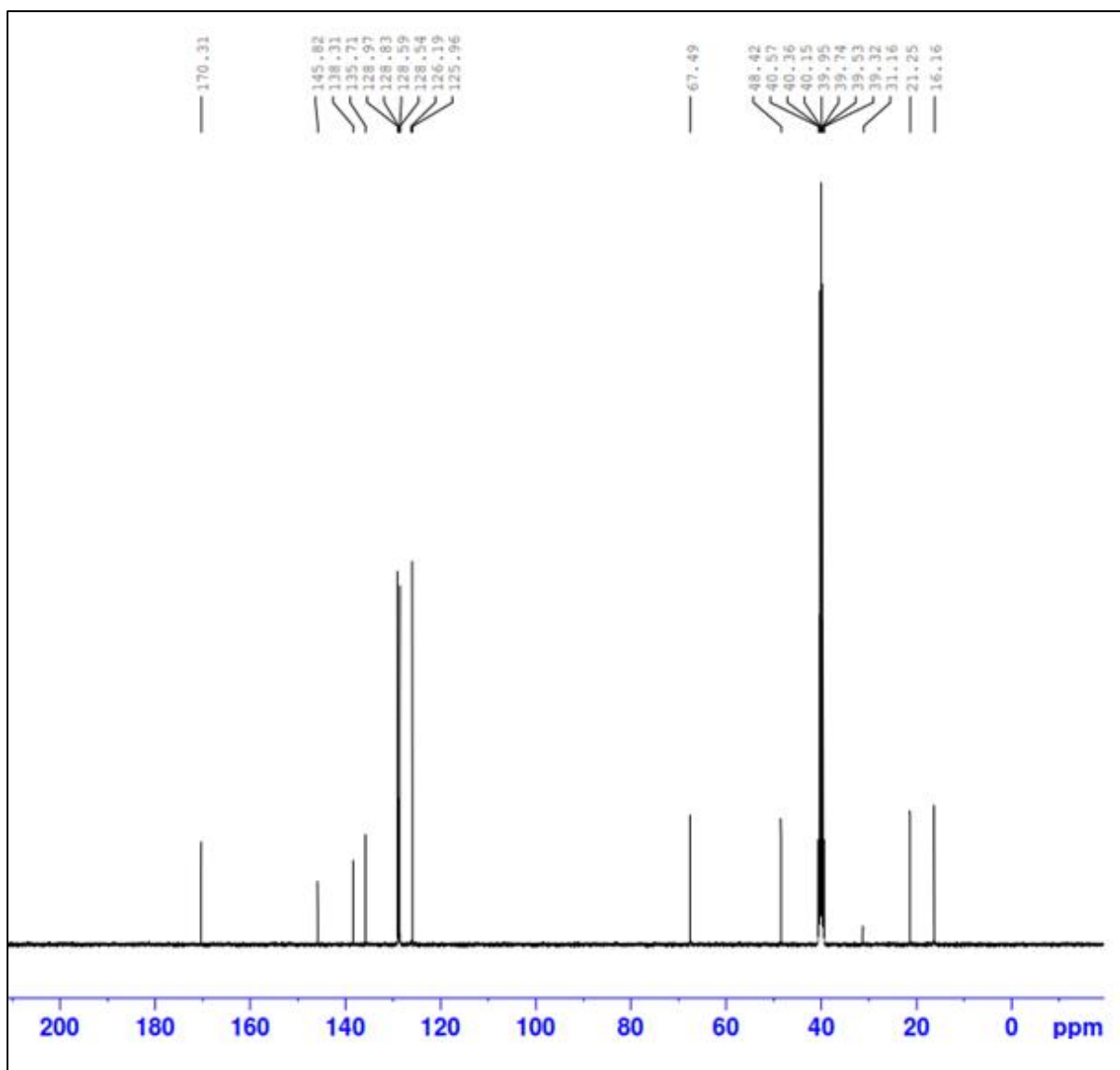
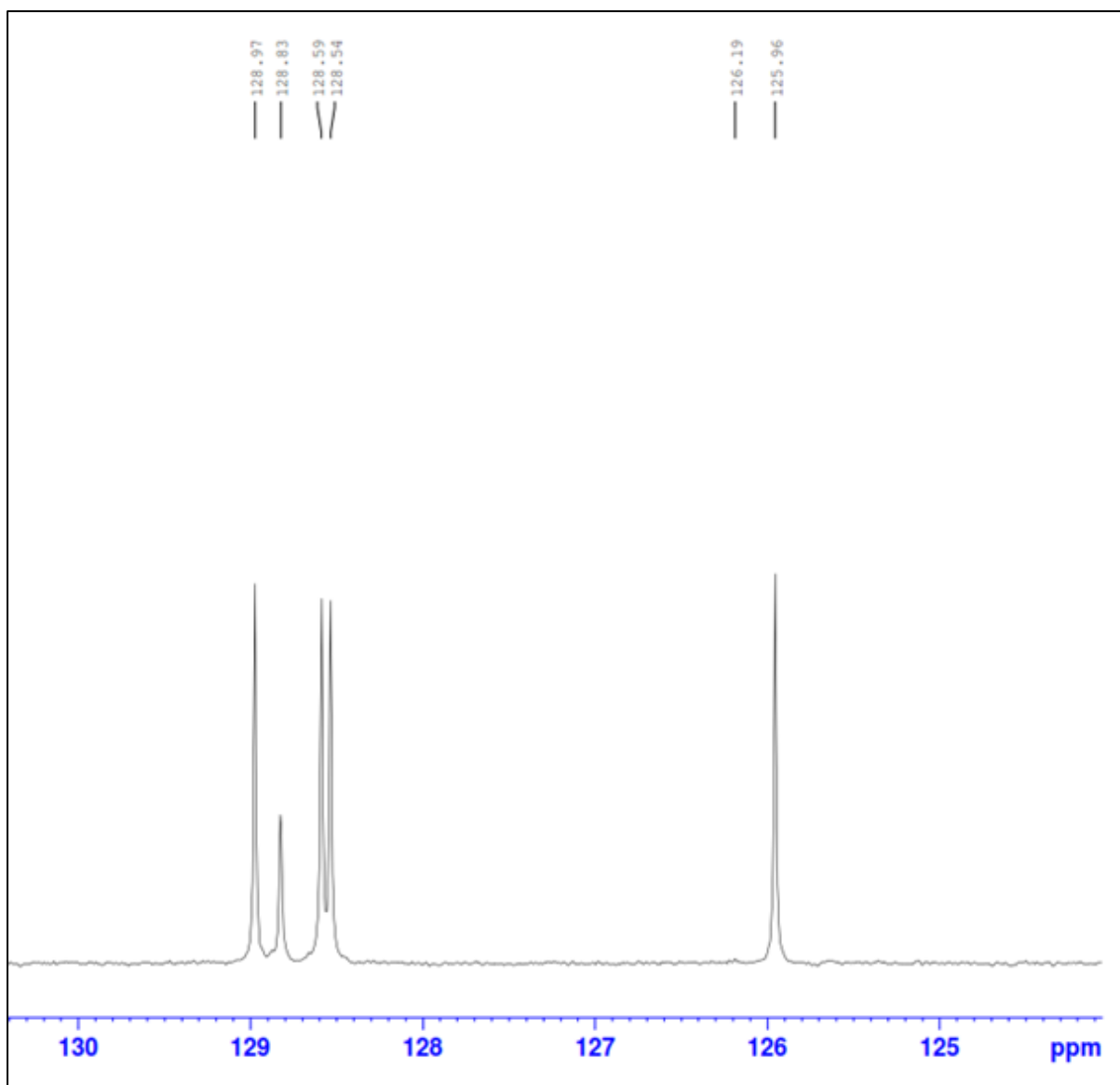


Figure 4.17:  $^{13}\text{C}$ -NMR spectrum of 1-BOPAMS.



**Figure 4.18:**  $^{13}\text{C}$ -NMR spectrum expansion of 1-BOPAMS.

## 4.2 MILD STEEL

### 4.2.1 EFFECT OF INHIBITOR CONCENTRATION

The corrosion rate ( $C_R$ ) and %IE in the absence and presence of various concentrations of 2-NBABA and 4-BOBAMS and 1-BOPAMS in 1.0 M HCl solution and at different temperatures (303-333 K) are presented in Table 4.1. The inspection of the data reveals that the addition of 2-NBABA 4-BOBAMS and 1-BOPAMS markedly decreases the corrosion rate of MS and the decrease is proportional to the increase in the concentration of the inhibitors. The variation of the %IE with the concentrations of the inhibitors at various temperatures (figure 4.19-4.22) shows that the %IE increases as the concentration of all three inhibitors are increased. These figures reveal that, at the lowest concentration of the inhibitors ( $1.0 \times 10^{-3}$  M) and temperature (303 K) the inhibition efficiency for 2-NBABA, 1-BOPAMS and 4-BOBAMS was found to be 76.10, 78.63 and 92.73% respectively. But when the inhibitor concentration was increased to  $5.0 \times 10^{-3}$  M at the same temperature the %IE for 2-NBABA, 1-BOPAMS and 4-BOBAMS reached the highest values of 76.10, 90.32 and 97.91%, signifying excellent inhibitive properties of these inhibitors. The high inhibitive properties of the amino ester and carboxylic acids at  $5.0 \times 10^{-3}$  M is because the adsorption and the degree of surface coverage of all inhibitors on MS increases as there is greater availability of inhibitor molecules as compared to  $1.0 \times 10^{-3}$  M, this results in the effective separation of the MS surface from the HCl solution which slows down the dissolution process [301]. The studied carboxylic acid and amino ester attained the maximum inhibition efficiency at  $5.0 \times 10^{-3}$  M at all temperatures investigated. In the uninhibited system, the weight loss was higher and found to decrease at a faster rate as the temperature of the solution was increased from 303 to 333 K. The acceleration in the weight loss can be attributed to the increase in the collision of the HCl molecules with the surface of MS. However, when an inhibitor is introduced into the solution, the weight loss decreased significantly, this is due to the formation of film by the adsorption of the inhibitor molecules which acts as a barrier between the aggressive HCl molecules and MS surface. Even in the presence of the inhibitors in solution, the %IE decreased as the temperature was increased and this might be because of the desorption of the inhibitors on the MS surface. For instance, the %IE of 1-BOPAMS at 303 K is 90.32% and decreases to 61.73% at 333 K for the highest concentration of  $5.0 \times 10^{-3}$  M. This is observed for all the inhibitors studied. The protective properties of the inhibitors are possible as a result of the interaction between  $\pi$ -electrons and heteroatoms with the positively charged MS surface [302]. The results obtained from the gravimetric measurements are in good correlation with those of electrochemical studies.

Among the investigated inhibitors, the amino ester provided the highest inhibition efficiency for MS as compared to the carboxylic acid. This high inhibition may be due to the presence of an extra benzene ring, presence of sulphur, and two additional oxygen groups in the amino ester. The trend of the inhibition efficiency follows the order: 2-NBABA > 1-BOPAMS > 4-BOBAMS, with 4-BOBAMS exhibiting the highest inhibition efficiency at almost all temperatures and concentrations used.

The  $C_R$  in the absence of the inhibitors was considerably higher at all temperatures investigated. The highest  $C_R$  was observed was at the highest temperature (333 K) of the solution which was the temperature at which the lowest %IE was observed. However, immediately when the inhibitor was introduced in the acid solution, it led to the reduction of the corrosion rate. For instance, the  $C_R$  in the absence of the inhibitors for MS at 303 K, was  $0.00717 \text{ g.cm}^2.\text{h}^{-1}$ . At the same temperature, it is clear that the introduction of different concentrations of the inhibitors resulted in a decrease of the  $C_R$ ; this trend is observed in all the temperature studied. For 2-NBABA at 303 K, the  $C_R$  decreased significantly to  $0.00171 \text{ g.cm}^2.\text{h}^{-1}$  at the lowest concentration of the inhibitors and to  $0.000998 \text{ g.cm}^2.\text{h}^{-1}$  at the highest concentration of the inhibitors utilized.

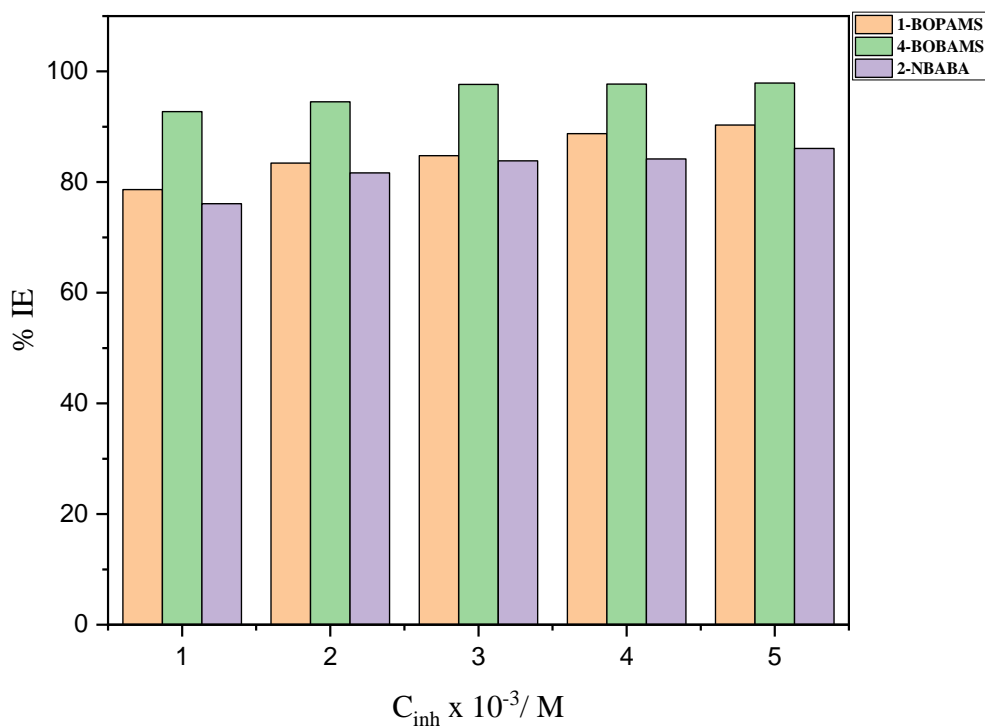


**Figure 4.19:** The variations of the %IE with various concentrations of 2-NBABA, 1-BOPAMS and 4-BOBAMS corrosion inhibitors at 303 K.

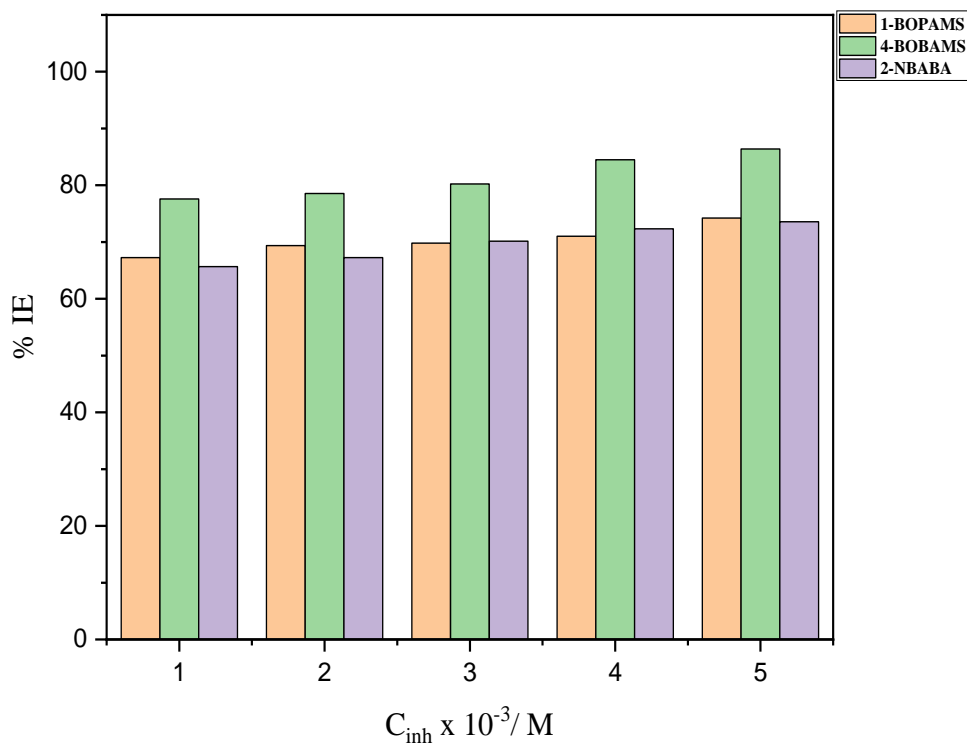


**Figure 4.20:** The variations of the %IE with various concentrations of 2-NBABA, 1-BOPAMS and 4-BOBAMS corrosion inhibitors at 313 K.

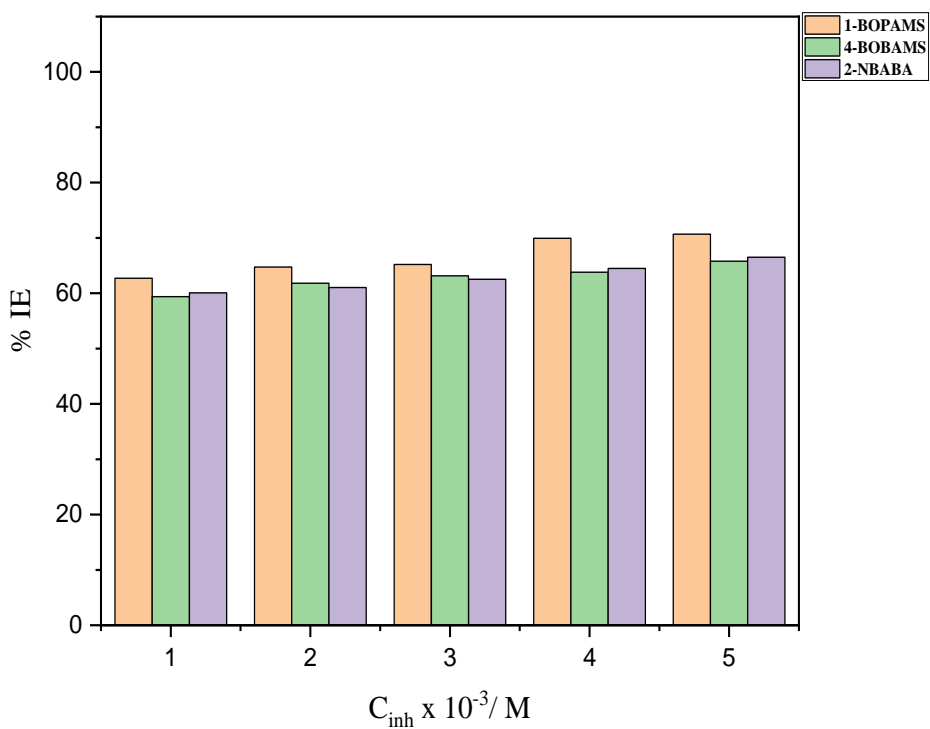


**Figure 4.21:** The variations of the %IE with various concentrations of 2-NBABA, 1-BOPAMS and 4-BOBAMS corrosion inhibitors at 323 K.

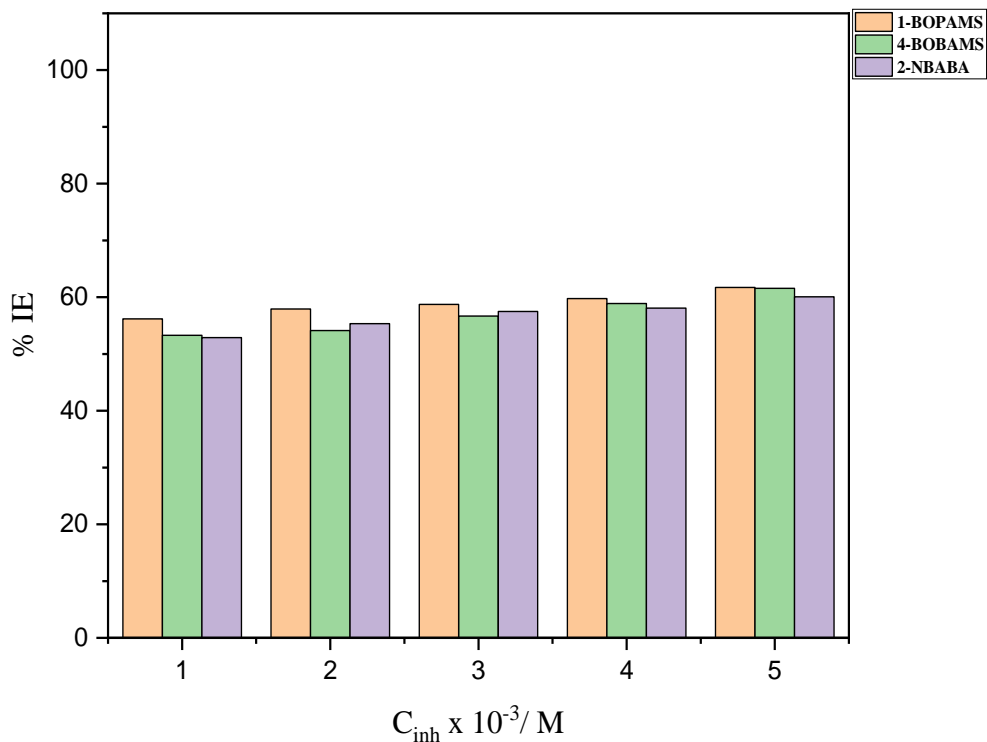


**Figure 4.22:** The variations of the %IE with various concentrations of 2-NBABA, 1-BOPAMS and 4-BOBAMS corrosion inhibitors at 333 K.

**Table 4.1:** Weight loss measurements of MS in 1.0 M HCl containing various concentrations of 1-BOPAMS, 4-BOBAMS and 2-NBABA at different temperatures.

Inhibitor	C <sub>inh</sub> (M)	303 K		313 K		323 K		333 K	
		C (g.cm <sup>-2</sup> .h <sup>-1</sup> )	IE (%)	C (g.cm <sup>-2</sup> .h <sup>-1</sup> )	IE (%)	C <sub>R</sub> (g.cm <sup>-2</sup> h <sup>-1</sup> )	IE (%)	C <sub>R</sub> (g.cm <sup>-2</sup> .h <sup>-1</sup> )	IE (%)
Blank	-	0.00717	-	0.01320	-	0.02437	-	0.04099	-
1-BOPAMS	1.0×10 <sup>-3</sup>	0.00153	78.63	0.00432	67.27	0.00909	62.72	0.01797	56.17
	2.0×10 <sup>-3</sup>	0.00189	83.43	0.00404	69.37	0.00860	64.73	0.01725	57.93
	3.0×10 <sup>-3</sup>	0.00109	84.77	0.00399	69.80	0.00848	65.19	0.01692	58.73
	4.0×10 <sup>-3</sup>	0.000806	88.75	0.00383	71.01	0.00733	69.92	0.01650	59.75
	5.0×10 <sup>-3</sup>	0.000694	90.32	0.00340	74.23	0.00715	70.68	0.01569	61.73
4-BOBAMS	1.0×10 <sup>-3</sup>	0.000521	92.73	0.00296	77.59	0.00990	59.38	0.01880	53.28
	2.0×10 <sup>-3</sup>	0.000394	94.51	0.00283	78.54	0.00931	61.81	0.01899	54.13
	3.0×10 <sup>-3</sup>	0.000169	97.65	0.00261	80.24	0.00898	63.14	0.01776	56.68
	4.0×10 <sup>-3</sup>	0.000165	97.70	0.00205	84.49	0.00882	63.80	0.01686	58.88
	5.0×10 <sup>-3</sup>	0.00015	97.91	0.00180	86.40	0.00833	65.81	0.01576	61.56
2-NBABA	1.0×10 <sup>-3</sup>	0.00171	76.10	0.00453	65.68	0.00973	60.07	0.0193	52.88
	2.0×10 <sup>-3</sup>	0.00131	81.66	0.00432	67.26	0.00949	61.05	0.0183	55.33
	3.0×10 <sup>-3</sup>	0.00116	83.84	0.00394	70.16	0.00913	62.54	0.0174	57.48
	4.0×10 <sup>-3</sup>	0.00113	84.19	0.00365	72.34	0.00864	64.50	0.0172	58.07
	5.0×10 <sup>-3</sup>	0.000998	86.08	0.00349	73.57	0.00816	66.52	0.0164	60.08



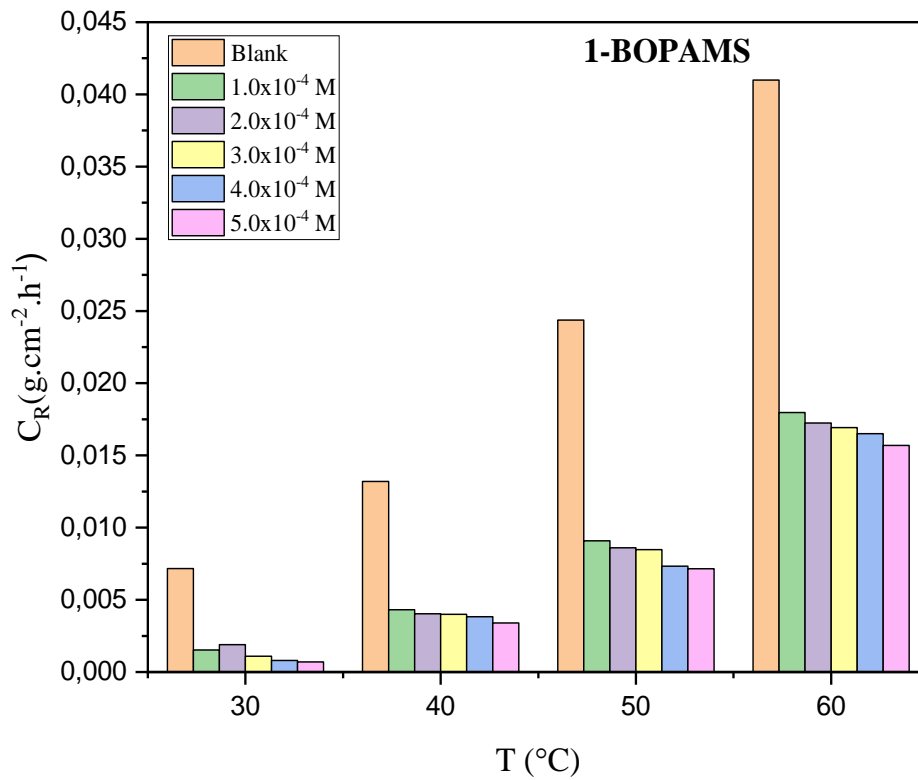


**Figure 4.23:** Variation of  $C_R$  of MS as a function of temperature for 1-BOPAMS.

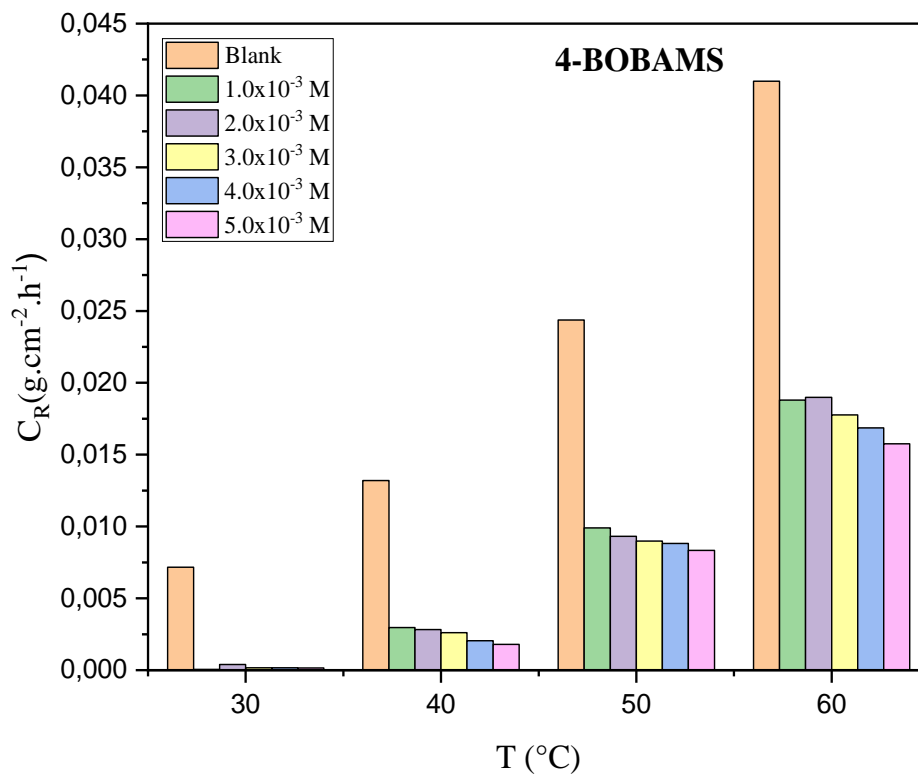


**Figure 4.24:** Variation of  $C_R$  of MS as a function of temperature for 4-BOBAMS.

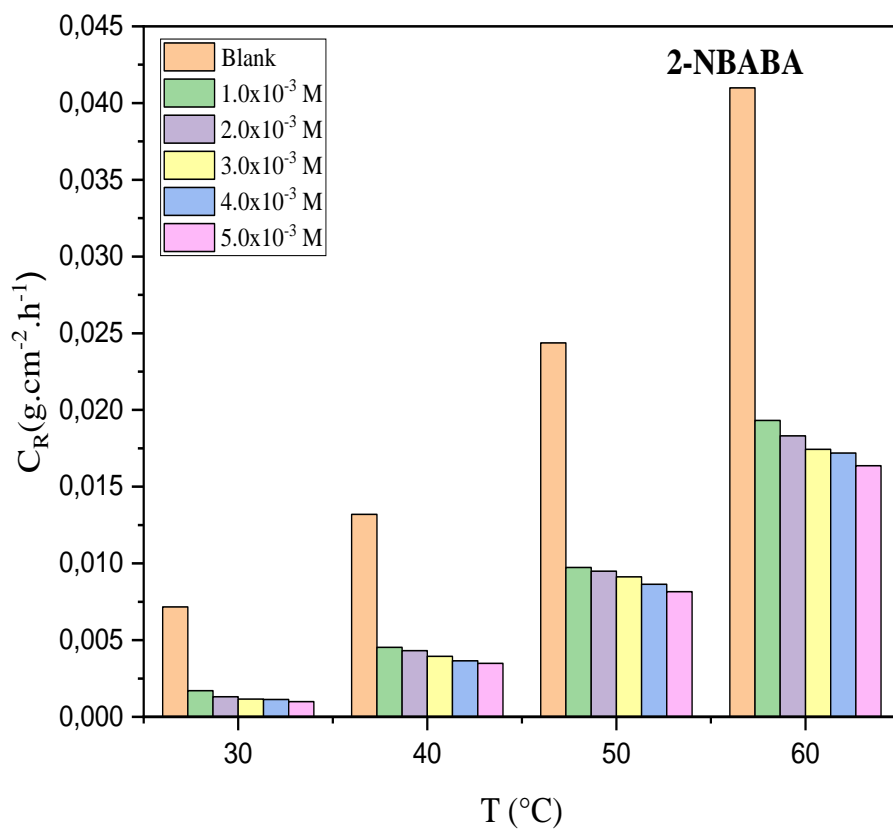


**Figure 4.25:** Variation of  $C_R$  of MS as a function of temperature for 2-NBABA.

#### 4.2.2 EFFECT OF TEMPERATURE

The temperature has a considerable role in understanding the inhibitive mechanism of the corrosion process. The rate of corrosion increases exponentially with temperature in acid solution due to the decrease in the hydrogen evolution overpotential [303]. To investigate the effect of temperature on the anticorrosion properties of the synthesized carboxylic acids and amino esters derivatives on MS in 1.0 M HCl, weight loss measurements were carried out in the temperature range 303-333 K in the absence and presence of various concentrations of the inhibitors during 8h of immersion time. The maximum %IE for all the inhibitors was reached at 303 K and decrease gradually with increasing temperature from 303-333 K. This indicates that the studied compounds are more efficient at lower temperatures, which is a result of physical interaction. The rate of corrosion increases with the rise in temperature in the uninhibited solution but gets highly reduced in the presence of inhibitors (figure 4.23-4.25). As a consequence of the increase in temperature, the %IE decreases, and this may be because higher temperatures accelerate the hot-movement of the organic molecules which weakens the adsorption capacity of the inhibitor on the metal surface [96, 304] and also increases the collision frequency of the oxygen and chlorine molecules with the MS surface. Since corrosion is a thermodynamic process, thermodynamic parameters such as the activation energy ( $E_a$ ) can be used to study the dependence of corrosion rate on temperature and in understanding the inhibition mechanism of corrosion. The activation energy of MS corrosion is referred to as the minimum quantity of energy which MS components (mainly Fe), acidic medium components, oxygen and moisture must possess to produce corrosion products such as rust. The effect of temperature on the adsorption and determination of activation parameters for MS corrosion was evaluated from the Arrhenius-type plot according to the following equation (4.1) below [290, 293]:

$$\log C_R = \log A - \frac{E_A}{2.303RT} \quad (4.1)$$

where  $E_a$  is the apparent activation energy for the corrosion process which represents the energy necessary for a molecule to react,  $C_R$  is the corrosion rate in  $\text{g.cm}^{-2}.\text{h}^{-1}$ ,  $A$  is the Arrhenius pre-exponential factor,  $T$  is the absolute temperature, and  $R$  is the universal gas constant. The values of  $E_a$  for MS in 1.0 M HCl in the absence and presence of inhibitors were calculated from the slope of the plots of  $\log C_R$  versus  $1/T$  (figure 4.23-4.25) and are recorded in Table 4.2.

The dependence of the %IE of an inhibitor and  $E_a$  on temperature can be classified into three various categories according to temperature effects listed below [305]:

1. The decrease of the %IE with an increase in temperature,  $E_a$  (inhibited solution)  $>$   $E_a$  (uninhibited solution).
2. The increase of the %IE with an increase in temperature,  $E_a$  (inhibited solution)  $<$   $E_a$  (uninhibited solution).
3. The %IE does not change with temperature,  $E_a$  (inhibited solution)  $=$   $E_a$  (uninhibited solution).

It is clear from Table 4.2 that  $E_a$  values were found to be higher for the inhibited systems compared to those for the uninhibited systems which imply that dissolution of MS is slow due to the formation of the inhibitor-Fe complex. This suggests a physical adsorption phenomenon of the inhibitors [306]. The  $E_a$  higher values of the inhibited systems can be linked with the increasing thickness of the double layer, which enhances the  $E_a$  of the corrosion process [307]. The increase in the  $E_a$  values with the rise of the inhibitor molecules concentrations suggests that inhibitors induce an energy barrier for the corrosion reaction, which increases as the inhibitor concentration increases [308]. This also highlights the electrostatic nature of the adsorption of the inhibitors on the MS surface [309].

An alternative formulation of the Arrhenius equation can be used to plot  $\log(C_R/T)$  versus  $(1/T)$  (figure 4.33-4.35) and provide further data on the effect of temperature on the inhibition efficiency from thermodynamic parameters like the entropy of activation ( $\Delta S_a^*$ ) and the enthalpy of activation ( $\Delta H_a^*$ ) from the slope ( $-\Delta H_a^* / 2.303R$ ) and an intercept of  $[\log (R/Nh) + \Delta S_a^* / 2.303R]$  as recorded in Table 4.2. The alternate form of the Arrhenius equation can be written as [310, 311]:

$$\log\left(\frac{C_R}{T}\right) = \left[ \log\left(\frac{R}{Nh}\right) + \left(\frac{\Delta S^*}{2.303R}\right) \right] + \left(\frac{-\Delta H^*}{2.303R}\right)\left(\frac{1}{T}\right) \quad (4.2)$$

where  $R$  is the universal gas constant,  $h$  is the Plank`s constant,  $T$  is the absolute temperature, 2.303 is a conversion factor from natural log to log10 and  $N$  is the Avogadro`s number.

**Table 4.2:** Kinetic and activation parameters (derived from the Arrhenius and transition-states plots) for MS in 1.0 M HCl in the absence and presence of various concentrations of 2-NBABA, 4-BOBAMS and 1-BOPAMS

Inhibitor	$C_{inh}$ (M)	$E_a$ (kJ.mol <sup>-1</sup> )	$\Delta H_a^*$ (kJ.mol <sup>-1</sup> )	$\Delta S_a^*$ (J.mol <sup>-1</sup> .K <sup>-1</sup> )
Blank	-	48.6079	45.9904	-193.8214
1-BOPAMS	1.0 x10 <sup>-3</sup>	67.6165	65.0004	-191.1797
	2.0 x10 <sup>-3</sup>	73.0278	70.4121	-190.3347
	3.0 x10 <sup>-3</sup>	74.6554	72.0378	-190.0814
	4.0 x10 <sup>-3</sup>	80.7164	78.1001	-189.1401
	5.0 x10 <sup>-3</sup>	83.9768	81.3573	-188.6415
4-BOBAMS	1.0 x10 <sup>-3</sup>	99.9776	97.3633	-185.9978
	2.0 x10 <sup>-3</sup>	106.3423	103.7225	-184.9954
	3.0 x10 <sup>-3</sup>	126.4505	123.8320	-181.7983
	4.0 x10 <sup>-3</sup>	127.6307	124.9579	-181.6500
	5.0 x10 <sup>-3</sup>	128.8801	126.2696	-181.4718
2-NBABA	1.0 x10 <sup>-3</sup>	66.8065	64.1755	-191.2830
	2.0 x10 <sup>-3</sup>	72.2561	69.6180	-190.4299
	3.0 x10 <sup>-3</sup>	74.6343	71.9669	-190.0770
	4.0 x10 <sup>-3</sup>	74.9943	72.3940	-190.0246
	5.0 x10 <sup>-3</sup>	77.3131	74.2839	-189.7438

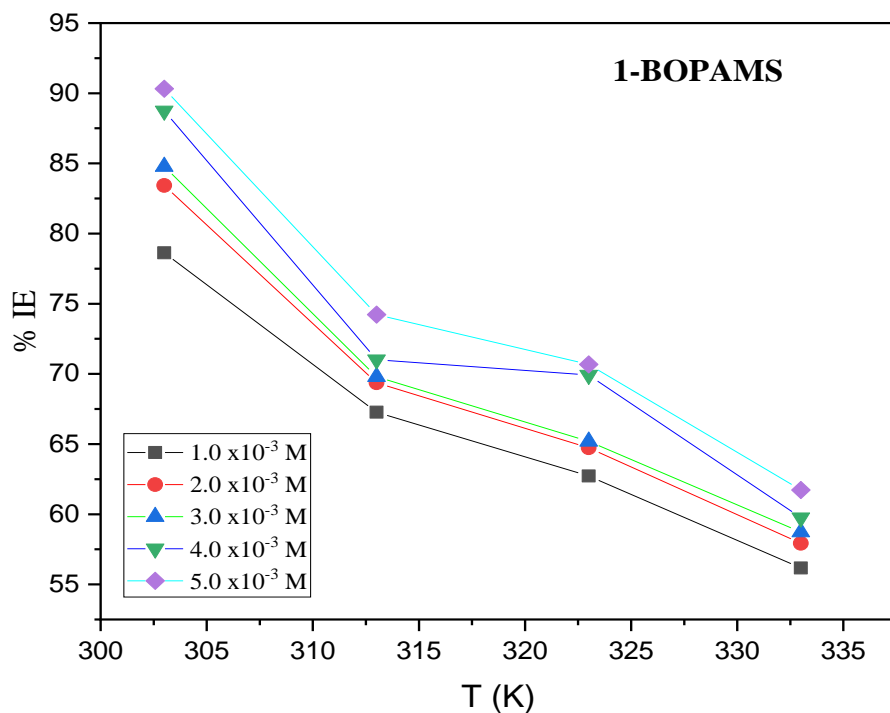


**Figure 4.26:** The variation of %IE with temperature for MS corrosion in 1.0 M HCl in the presence of a various concentrations of 1-BOPAMS.

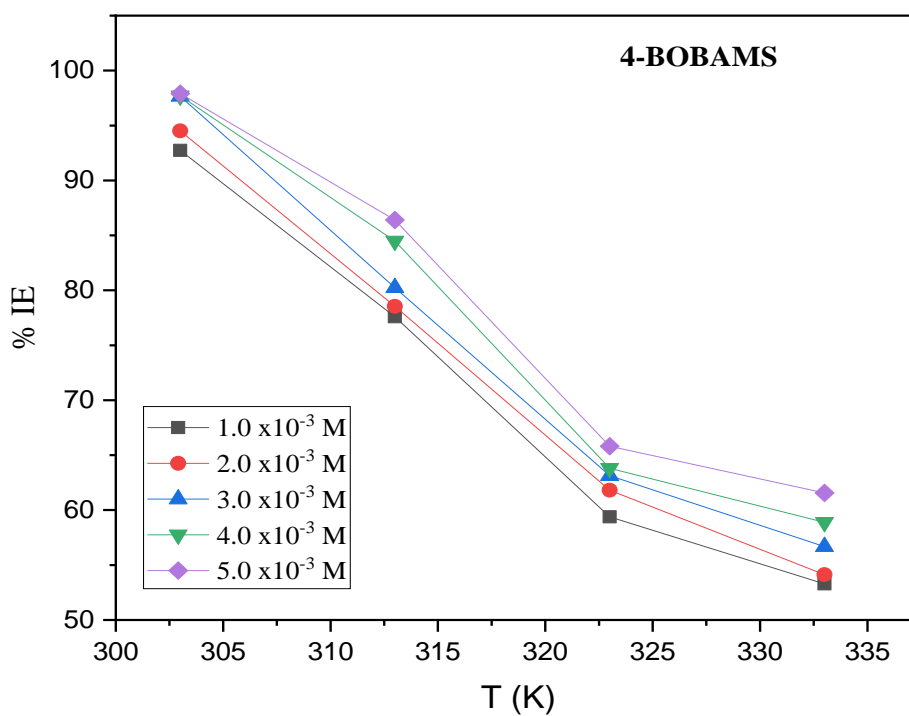


**Figure 4.27:** The variation of %IE with temperature for MS corrosion in 1.0 M HCl in the presence of a various concentrations of 4-BOBAMS.

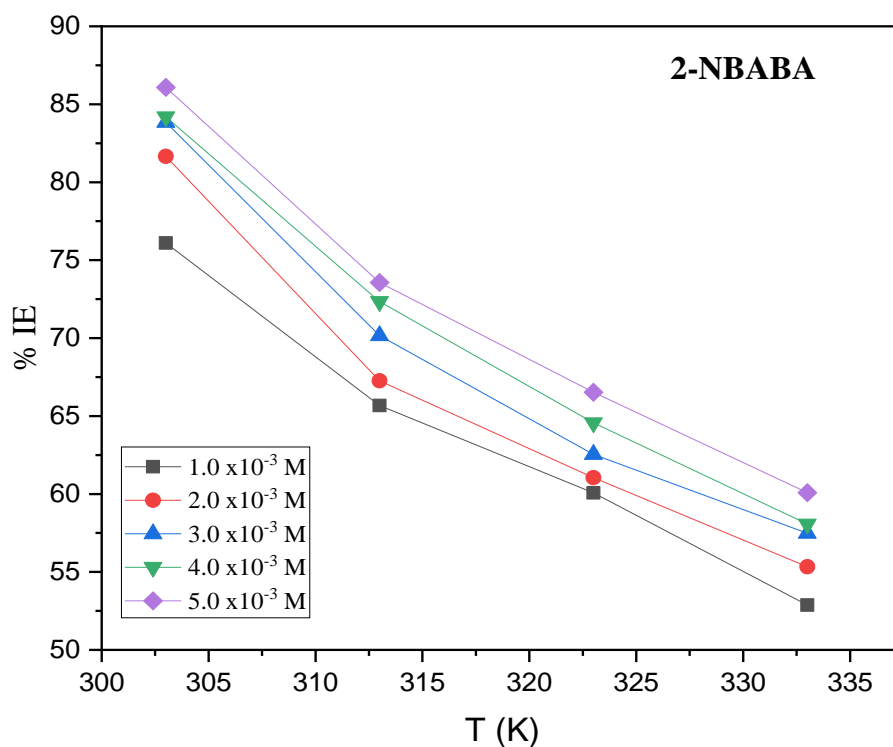


**Figure 4.28:** The variation of %IE with temperature for MS corrosion in 1.0 M HCl in the presence of a various concentrations of 2-NBABA.

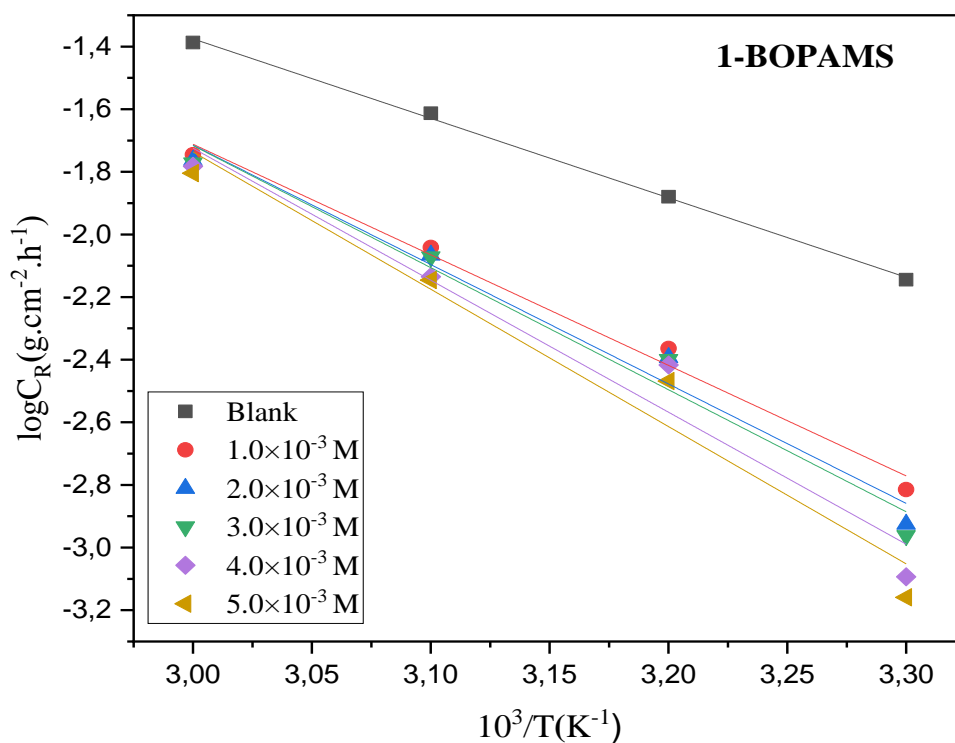


**Figure 4.29:** Arrhenius plots for the corrosion of MS in 1.0 M HCl in the absence and presence of different concentrations of 1-BOPAMS.

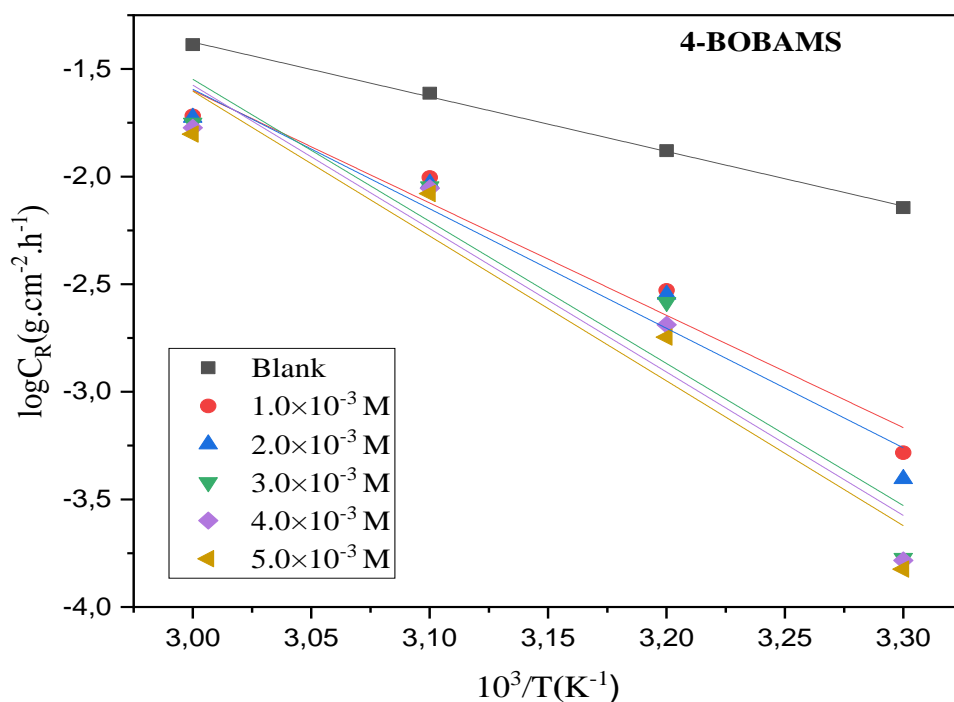


**Figure 4.30:** Arrhenius plots for the corrosion of MS in 1.0 M HCl in the absence and presence of different concentrations of 4-BOBAMS.

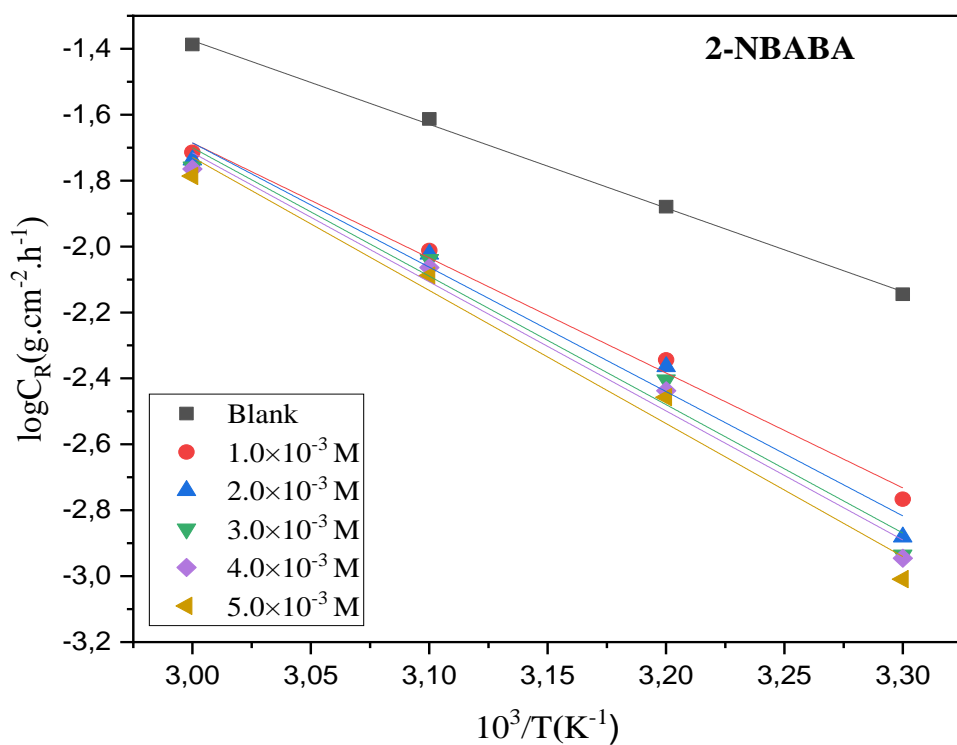


**Figure 4.31:** Arrhenius plots for the corrosion of MS in 1.0 M HCl in the absence and presence of different concentrations of 2-NBABA.



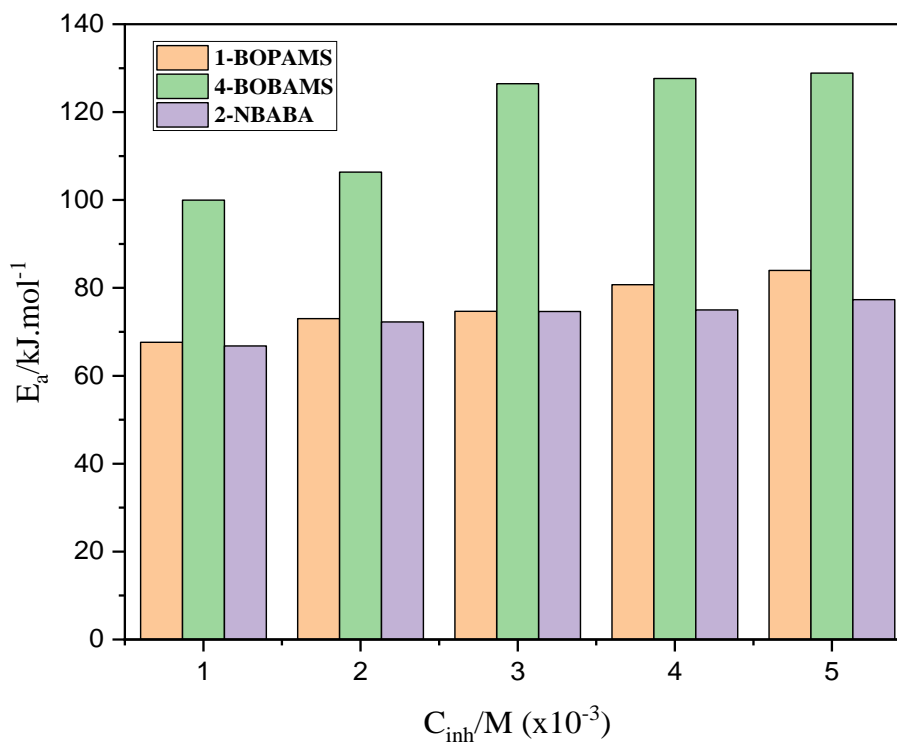


**Figure 4.32:** The variation of the  $E_a$  with various concentration of 2-NBABA, 1-BOPAMS and 4-BOBAMS corrosion inhibitors for MS.

Positive values of the enthalpy of activation reflect the endothermic nature of the steel dissolution process, which implies that the dissolution of MS is challenging [312]. The  $\Delta H_a^*$  value for the blank is less compared to those of the three studied corrosion inhibitors. This indicates that an adsorption process took place between the inhibitor molecules and the surface of MS. Also, a considerable amount of energy was required to move from the reactants and form the corrosion products, confirming the adsorption of the inhibitors and the lowering of the MS corrosion. It has been shown in the literature that values of enthalpy of activation  $\leq 41.86 \text{ kJ.mol}^{-1}$  are associated with physisorption type of adsorption while those around  $100 \text{ kJ.mol}^{-1}$  or higher are associated with chemisorption [313]. The results indicated in Table 4.2 show that enthalpy of activation values are slightly less than those of their respective activation energies and are above  $41.86 \text{ kJ.mol}^{-1}$  yet somewhat less than  $100 \text{ kJ.mol}^{-1}$ . This kind of behaviour may be as a result of a mixed-type of adsorption on the MS surface.

High negative values of  $\Delta S_a^*$  implies the activated complex in the rate-determining step represents association rather than dissociation of inhibitors. This indicates that a decrease in the system disorder takes place going from reactants to the activated complex due to the adsorption of inhibitor molecules on the MS surface [314, 315]. The increase in the entropy of

activation values due to the adsorption of inhibitor molecules on the MS surface from the acid solution could be regarded as a quasi-substitution process between organic molecules in the aqueous phase and water molecules on the electrode surface. In such a process, the adsorptions of inhibitor molecules are said to follow desorption of water molecules from the electrode surface, and this results in the decrease of the electrical capacity of MS [316].

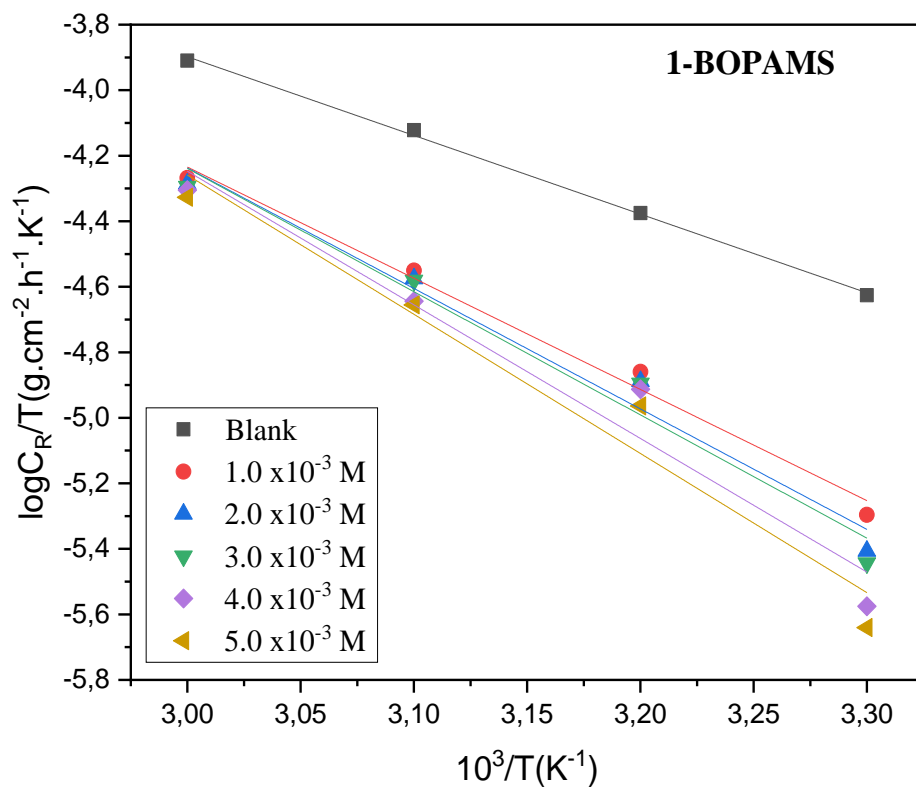


**Figure 4.33:** Transition state plots for the corrosion of MS in 1.0 M HCl in the absence and presence of different concentrations of 1-BOPAMS.

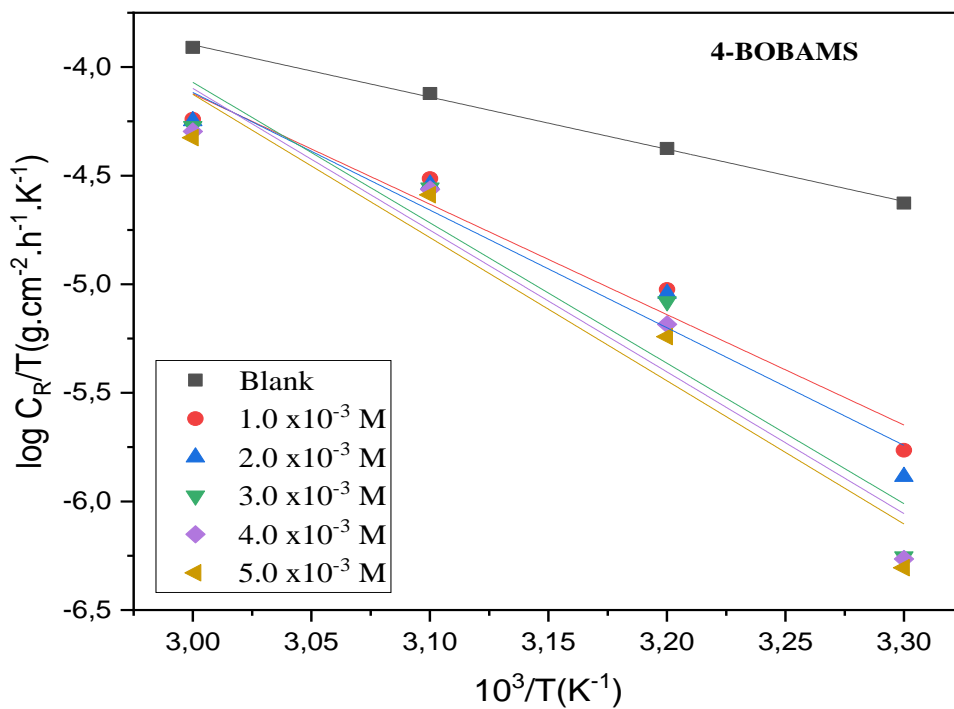


**Figure 4.34:** Transition state plots for the corrosion of MS in 1.0 M HCl in the absence and presence of different concentrations of 4-BOBAMS.

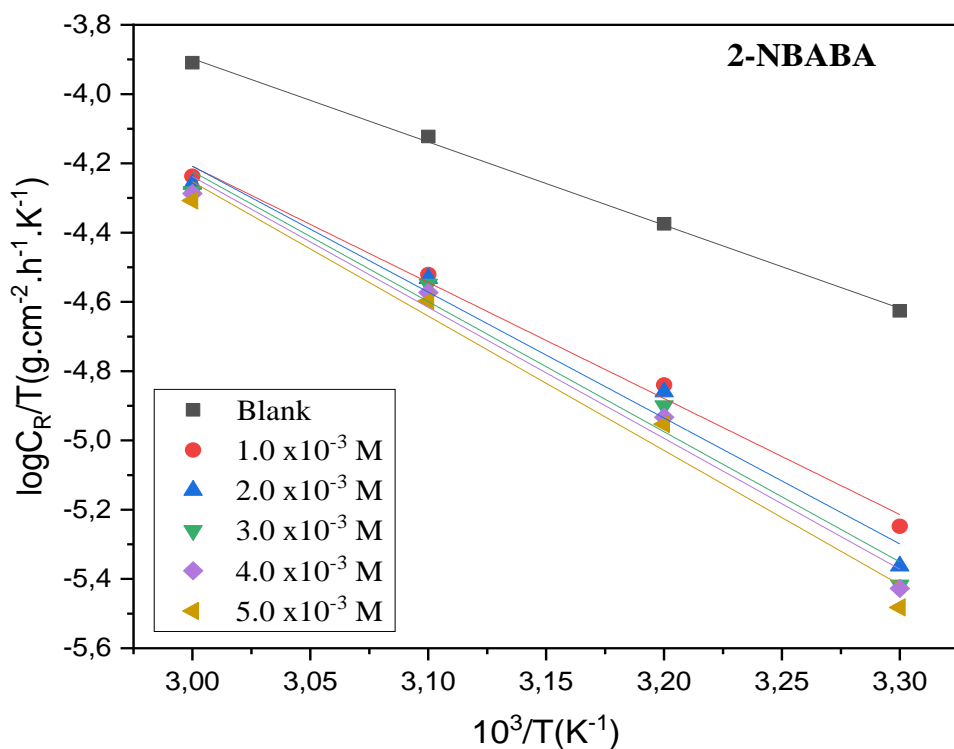
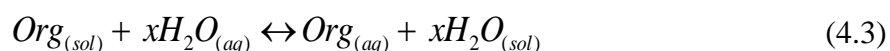


**Figure 4.35:** Transition state plots for the corrosion of MS in 1.0 M HCl in the absence and presence of different concentrations of 2-NBABA.

### 4.2.3 ADSORPTION ISOTHERMS AND THERMODYNAMIC PARAMETERS

Corrosion inhibitor efficiency is mainly dependent on the extent of the adsorption of inhibitor molecules on the metal surface. This process may adopt physisorption, chemisorption or mixed-type of adsorption mode. The adsorption phenomenon of the inhibitor molecules from the aqueous solution on the metal surface is regarded as a quasi-substitution process that occurs between the organic compound in the aqueous phase and water molecules at the surface of the electrode. This postulation is deemed passable since the adsorption phenomenon on the corroding MS surface never attains a complete equilibrium but instead achieves an adsorption steady-state. The adsorption process involves the replacement of water molecules at the corroding interface according to the pattern represented in equation (4.3) [317, 318]:



where Org is the inhibitors in solution, x (size ratio) is the number of water molecules replaced by the adsorbed molecules.

The degree of surface coverage ( $\theta$ ) as a function of the concentration of inhibitor ( $C_{inh}$ ) was graphically studied by fitting it to various adsorption isotherms like Langmuir isotherm, Temkin isotherm, Freundlich isotherm, and El-Awady adsorption isotherm (Modified Langmuir adsorption isotherm) to find the best fit adsorption isotherm. Langmuir adsorption isotherm provides information on the type of adsorption that results between the metal surface and the inhibitors such as physisorption or chemisorption phenomenon. Temkin adsorption isotherm explains the heterogeneity created on the metal surface. Temkin adsorption isotherm is also a feature of chemical adsorption [319]. Freundlich isotherm describes the isothermal deviation of adsorption of some inhibitor molecules adsorbed by a unit mass of solid adsorbent pressure. El-Awady adsorption isotherm provides information on the multilayer adsorption film formed by the inhibitor molecules on the surface of the metal [320, 321]. All these adsorption isotherms can be described by a generalized equation (4.4) [322]:

$$f(\theta, x) \exp(-2a\theta) = KC_{inh} \quad (4.4)$$

where,  $f(\theta, x)$  is the configurational term, which depends on the assumptions made to derive the isotherms,  $C_{inh}$  is the inhibitor concentration in the corroding medium,  $\theta$  is the degree of surface coverage,  $a$  is the molecular interaction parameter,  $x$  is the size ratio factor, and  $K$  is the equilibrium constant for the adsorption. According to Kern and Landolt [322], the size ratio

factor indicates the number of water molecules displaced by one molecule of organic inhibitor and the molecular interaction parameter accounts for the lateral interactions between adsorbed species. In other words, adsorption isotherms contain either a or x or both parameters at times. The two isotherms parameters (a and x) can be analyzed by fitting double logarithmic curves [322, 323].

El-Awady adsorption isotherm equation can be written as follows [324];

$$\log \left( \frac{\theta}{1-\theta} \right) = \log K + y \log C \quad (4.5)$$

where  $y$  is the number of inhibitor molecules occupying one active site,  $\theta$  is the surface coverage,  $C$  is the concentration of the inhibitors,  $K$  is a constant related to the equilibrium constant of adsorption process,  $K_{\text{ads}} = K^{1/y}$  and  $y$  represents the number of active sites of the surface occupied by one molecule of the inhibitor. The El-Awady adsorption isotherms are represented by figure 4.45-4.47.

Temkin adsorption isotherm was tested by using the following equation below [325]:

$$KC = \exp(2a\theta) \quad (4.6)$$

where  $\theta$  is the degree of surface coverage of the inhibitor,  $K$  is the equilibrium constant of adsorption,  $a$  is the molecules interaction parameter and  $C$  is the inhibitor concentration. The plot of  $\theta$  against  $\log C$  was linear and are shown in figure 4.39-4.41.

Freundlich isotherm model is expressed by the equation [326]:

$$\theta = KC^{1/n} \quad (4.7)$$

where  $n$  is an empirical constant,  $K$  is the equilibrium constant of adsorption, and  $C$  is the inhibitor concentration. The linearized form of the model (equation 4.8) is preferred for plotting isotherms. A linear plot of  $\log \theta$  against  $\log C$  was obtained are shown in figure 4.42-4.44.

$$\log \theta = \log K + \frac{1}{n} \log C \quad (4.8)$$

Amongst all the plotted isotherm, Langmuir adsorption isotherm was found to give the best description for all three synthesized compounds on MS in 1.0 M HCl solution. Langmuir adsorption isotherm is provided by the following equation below:

$$\frac{C_{inh}}{\theta} = \frac{1}{K_{ads}} + C_{inh} \quad (4.9)$$

Using equation (4.9), the plots of  $C_{inh}/\theta$  versus  $C_{inh}$  gave a straight line (figure 4.36-4.38) with a regression coefficient ( $R^2$ ) around unity confirming that the adsorption of 4-BOBAMS, 1-BOPAMS and 2-NBABA on MS surface in 1.0 M HCl obeys the Langmuir adsorption isotherm. From these figures, the equilibrium constant of adsorption was obtained from the slopes and enabled the calculation of the free Gibb's energy for the adsorption of 4-3BOBAMS, 1-BOPAMS and 2-NBABA on the surface of MS. Even though the linearity of these plots suggests the adsorption of these three inhibitors on MS surface obeys the Langmuir isotherm, there was considerable deviation of the gradients (slope) from unity. The variance of the gradients is contrary to what is expected for ideal Langmuir adsorption isotherm equation. The departure of Langmuir adsorption isotherm postulates that the adsorbed inhibitor molecules do not interact with one another, but this was found to be not true for large polymer molecules having polar atoms of groups which could be adsorbed on the metal surface. Such adsorbed molecules are said to interact with one another by mutual attraction or repulsion, and this can be explained as the reason for the departure of the slope from unity. The nonconformity of the slope could also be due to the changes in the heat of adsorption with increasing surface coverage which is ignored by the derivation of Langmuir isotherm [327]. The modified Langmuir isotherm (El-Awady isotherm) was fitted to account for the deviation of the slope from unity. The El-Awady isotherm was fitted by plotting  $\log(\theta/1-\theta)$  against  $\log C_{inh}$ . The plots  $\log(\theta/1-\theta)$  versus  $\log C_{inh}$  gave a straight line which shows that the adsorption process also conforms to El-Awady isotherm. Nevertheless, the values of the regression coefficients ( $R^2$ ) obtained from El-Awady are far from unity (Table 4.4), which shows that even though the slopes deviates from unity, Langmuir adsorption isotherm is the most appropriate isotherm for the compounds used in the present study. From the Langmuir equation,  $K_{ads}$  can be calculated from the intercept. The standard Gibb's free energy of adsorption values can be calculated from  $K_{ads}$  using equation (4.10).

$$\Delta G_{ads}^{\circ} = -RT \ln(55.5K_{ads}) \quad (4.10)$$

where the value 55.5 represents the molar concentration of water in the solution,  $\Delta G_{ads}^{\circ}$  is the standard Gibb's free energy of adsorption, R is the universal gas constant and T is the absolute temperature. The standard adsorption free energy ( $\Delta G_{ads}^{\circ}$ ) provides information on the type of adsorption occurring on the metal surface.

Studies show that values of  $\Delta G^{\circ}_{\text{ads}}$  around  $-20 \text{ kJ.mol}^{-1}$  and lower are consistent with the electrostatic interaction between charged molecules and the charged surface of the substrate (physisorption) which is a process that possesses weak Van Der Waals interaction rather than chemical bonding. While those that are around  $-40 \text{ kJ.mol}^{-1}$  and above correspond to chemical adsorption (chemisorption), that occurs through the sharing or transfer of an electron from the adsorbate molecules on the surface of MS resulting in a coordinate type of bond [178]. The  $\Delta G^{\circ}_{\text{ads}}$  values listed in Tables 4.3 are negative, which indicates the spontaneity of the adsorption process and the strong interaction that occurred between the inhibitors molecules and MS surface [321]. The trend of the values of  $\Delta G^{\circ}_{\text{ads}}$  can be analysed to thoroughly explain the adsorption of the inhibitors on the surface of MS. For 2-NBABA 4-BOBAMS and 1-BOPAMS  $\Delta G^{\circ}_{\text{ads}}$  values are above  $-20 \text{ kJ.mol}^{-1}$  and below  $-40 \text{ kJ.mol}^{-1}$ , which implies that mixed-type adsorption is taking place, i.e., a mixture of both physisorption and chemisorption. The pattern or trends of these values can be utilized to elaborate on the nature of the adsorption that occurs between the MS surface and the corrosion inhibitors. Literature studies indicate that an increase in  $\Delta G^{\circ}_{\text{ads}}$  values with increase in temperature is indicative of exothermic adsorption [328], whereas a decrease in  $\Delta G^{\circ}_{\text{ads}}$  values with increase in temperature are indicative of endothermic adsorption. In the present study, the  $\Delta G^{\circ}_{\text{ads}}$  values are seen to be increasing with the rise in temperature, indicating that the adsorption mechanism between MS surface and the three inhibitors is of an exothermic nature which signifies either chemisorption or physisorption mechanism.

The  $\Delta H^{\circ}_{\text{ads}}$  were deduced from both the Van't Hoff equation (2.15) and the Gibbs-Helmholtz equation (2.17). The Van't Hoff plot of  $\ln K_{\text{ads}}$  Vs  $1/T$  gave a straight line with slope ( $-\Delta H^{\circ}_{\text{ads}}/R$ ) and the Gibbs-Helmholtz plot of  $\Delta G^{\circ}_{\text{ads}}/T$  with  $1/T$  gave a straight line with a slope equal to  $\Delta H^{\circ}_{\text{ads}}$ . The  $\Delta S^{\circ}_{\text{ads}}$  were calculated from equation (2.18). All the obtained standard thermodynamic parameters ( $\Delta H^{\circ}_{\text{ads}}$  and  $\Delta S^{\circ}_{\text{ads}}$ ) are listed in Table 4.3.

**Table 4.3:** Thermodynamic and adsorption parameters (Langmuir adsorption isotherms) for Al in 1.0 M HCl at various temperatures for 2-NBABA, 1-BOPAMS and 4-BOBAMS

Inhibitor	T (K)	R <sup>2</sup>	Slope	K <sub>ads</sub> (L.mol <sup>-1</sup> )	ΔG° <sub>ads</sub> (kJ.mol <sup>-1</sup> )	ΔH° <sub>ads</sub> (kJ. mol <sup>-1</sup> )	ΔS° <sub>ads</sub> (J.mol <sup>-1</sup> .K <sup>-1</sup> )
1-BOPAMS	303	0.9985	1.0638	3864.2863	-30.9266	-4* -4#	88.8667
	313	0.9971	1.3249	4296.8246	-32.2234		90.1706
	323	0.9962	1.3590	2949.1565	-32.2422		87.4372
	333	0.9985	1.5881	3806.9134	-33.9473		89.9318
4-BOBAMS	303	0.9999	1.0035	12025.0120	-33.7866	-43* -43#	-30.4073
	313	0.9976	1.1184	3790.4632	-31.8971		-35.4725
	323	0.9992	1.4861	4009.7839	-33.0673		-30.7514
	333	0.9966	1.5589	2086.5066	-32.2823		-32.1853
2-NBABA	303	0.9997	1.1291	5182.4212	-31.6660	-15* -15#	55.0033
	313	0.9988	1.3103	3466.0844	-31.6643		53.2406
	323	0.9978	1.4622	3299.6766	-32.5438		54.3152
	333	0.9988	1.6136	2887.0861	-33.1815		54.5991

\* Parameters derived from the Van't Hoff equation.

# Parameters derived from the Gibbs-Helmholtz equation.

The value of the enthalpy of adsorption found by the Van't Hoff and Gibbs-Helmholtz relations are in good agreement. The  $\Delta H^\circ_{\text{ads}}$  values obtained are negative and indicates an exothermic adsorption process which can either be chemisorption or physisorption or mixed-type adsorption [216], whereas the endothermic process is attributed to chemisorption [329]. The adsorption process being exothermic means the inhibition efficiency at higher temperatures is lower, and this supported by the decrease in %IE with an increase in temperature. This indicates that the inhibitor molecules gradually desorbs from the MS surface [330]. In the exothermic adsorption process, physisorption can be distinguished from the chemisorption based on  $\Delta H^\circ_{\text{ads}}$  values. For the physisorption process, the magnitude of  $\Delta H^\circ_{\text{ads}}$  is about - 40 kJ mol<sup>-1</sup> or less negative while the value of -100 kJ mol<sup>-1</sup> or more negative is for chemisorption [331]. It is reported that if  $\Delta H^\circ_{\text{ads}} > 0$ , the adsorption is chemisorption and if  $\Delta H^\circ_{\text{ads}} < 0$ , then the adsorption can either be chemisorption or physisorption [332]. It is evident from Table 4.3 that the  $\Delta H^\circ_{\text{ads}}$  values for all the investigated inhibitors are  $\Delta H^\circ_{\text{ads}} < 0$  and negative, indicating that the adsorption of the inhibitors on MS is physisorption. Inspection of Table 4.3 shows positive values of  $\Delta S^\circ_{\text{ads}}$  in the inhibited system for 1-BOPAMS and 2-NBABA, which indicates that solvent entropy predominates over solute entropy [333]. The  $\Delta S^\circ_{\text{ads}}$  values for 4-BOBAMS are all negative and suggest that the adsorption of inhibitor on MS surface is of an exothermic nature. This behaviour can be explained as follows: the inhibitors molecules move freely in the



bulk solution (inhibitor molecule were chaotic) before they are adsorbed on the MS surface, but during the adsorption process, the inhibitors molecules adsorb in an orderly fashion onto MS surface, resulting in a decrease in entropy [334, 335].

Furthermore, because the adsorption process was exothermic, thermodynamics principle implies that it must be accompanied by a decrease in entropy [336]. The  $\Delta S^{\circ}_{\text{ads}}$  values for 1-BOPAMS and 2-NBABA are all positive, and this can be regarded as an indication of a quasi-substitution process between the inhibitor molecules and water molecules on the electrode surface. This process means that the adsorption of the inhibitors is accompanied by the desorption of the water molecules on the MS surface. The process of adsorption occurs as a result of the substitution process that happens between the inhibitor molecules present in solution and the water molecule previously adsorbed on the metallic surface [337]. The  $\Delta S^{\circ}_{\text{ads}}$  values being positive is the opposite to what is expected, and this suggests an exothermic adsorption process supplemented by a decrease in entropy which results in the adsorption of the inhibitors on the surface of MS [338].

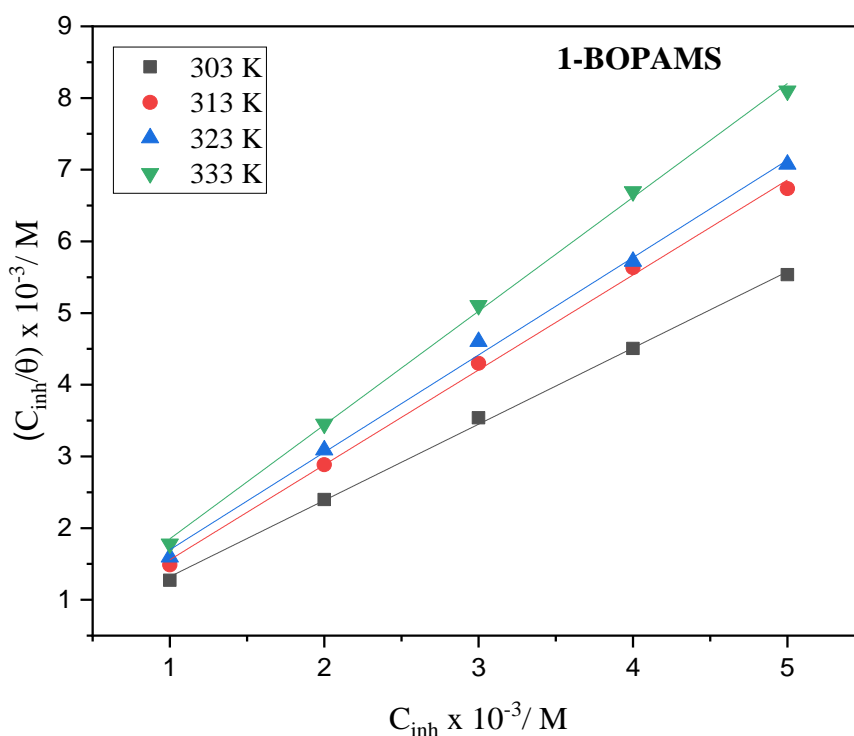


**Figure 4.36:** Langmuir adsorption isotherm plot for the adsorption of different concentrations of 1-BOPAMS on the surface of MS in 1.0 M HCl at different temperatures.

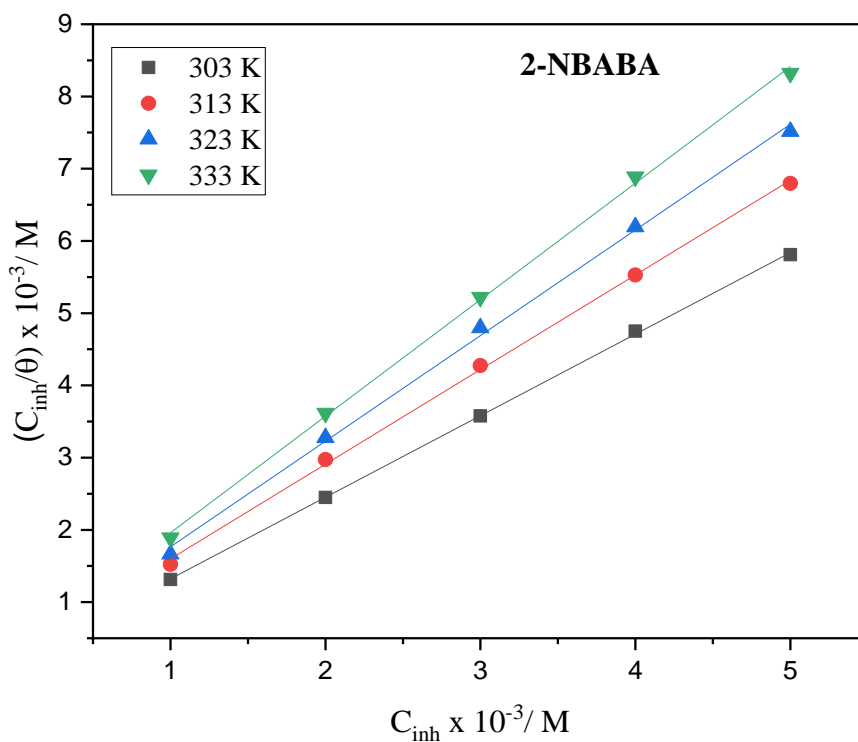


**Figure 4.37:** Langmuir adsorption isotherm plot for the adsorption of different concentrations of 2-NBABA on the surface of MS in 1.0 M HCl at different temperatures.

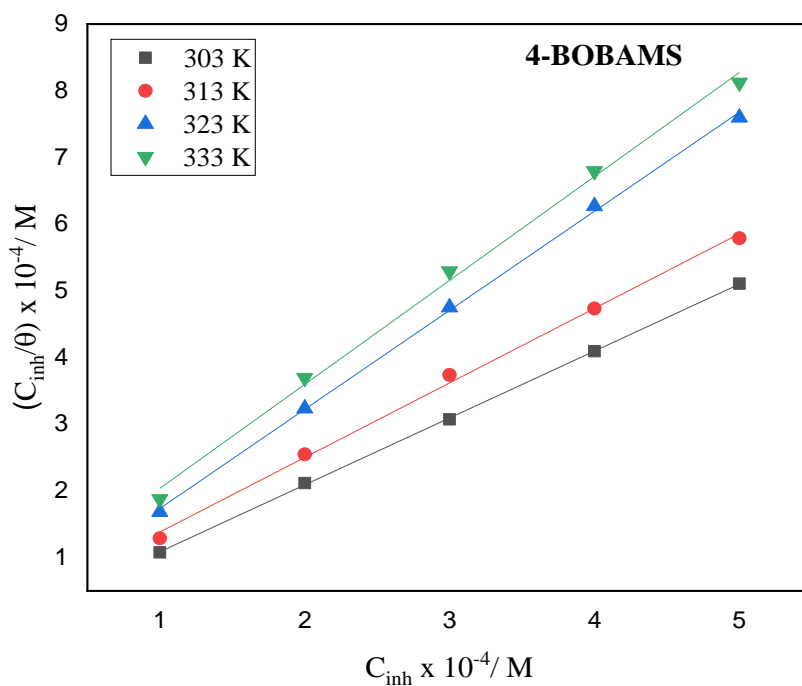


**Figure 4.38:** Langmuir adsorption isotherm plot for the adsorption of different concentrations of 4-BOBAMS on the surface of MS in 1.0 M HCl at different temperatures.

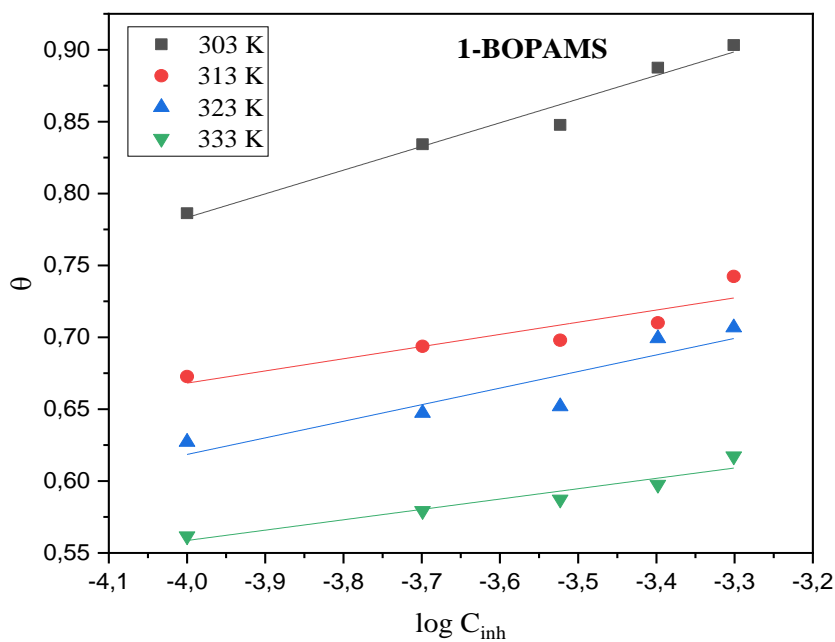


**Figure 4.39:** Temkin adsorption isotherm plot for the adsorption of different concentrations of 1-BOPAMS on the surface of MS in 1.0 M HCl at different temperatures.

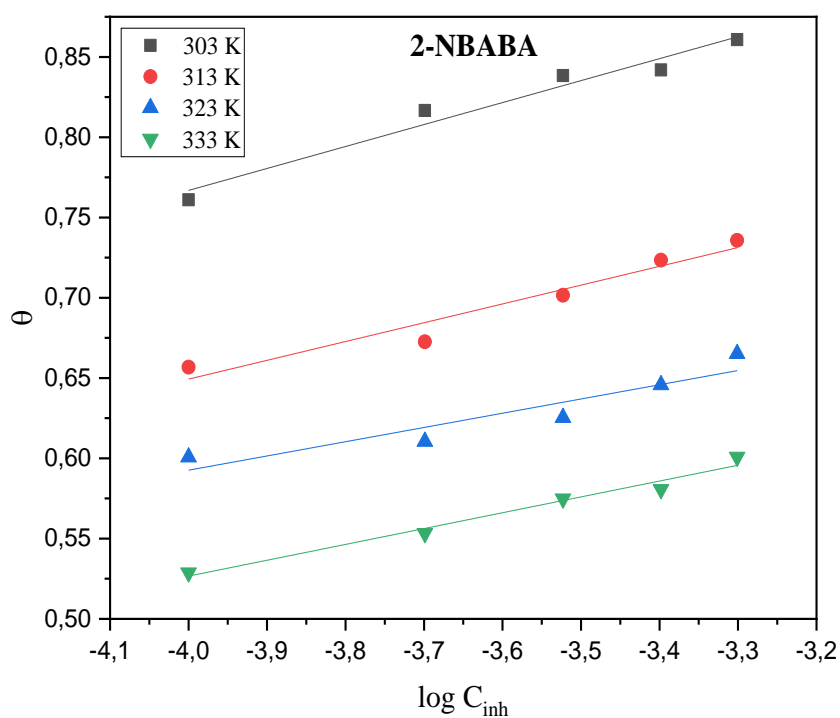


**Figure 4.40:** Temkin adsorption isotherm plot for the adsorption of different concentrations of 2-NBABA on the surface of MS in 1.0 M HCl at different temperatures.

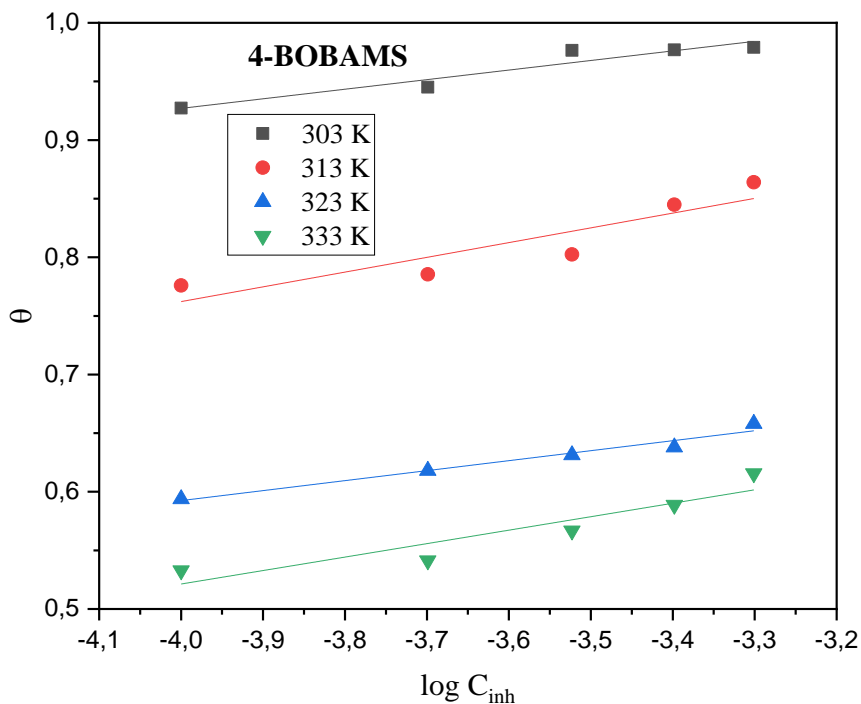


**Figure 4.41:** Temkin adsorption isotherm plot for the adsorption of different concentrations of 4-BOBAMS on the surface of MS in 1.0 M HCl at different temperatures.

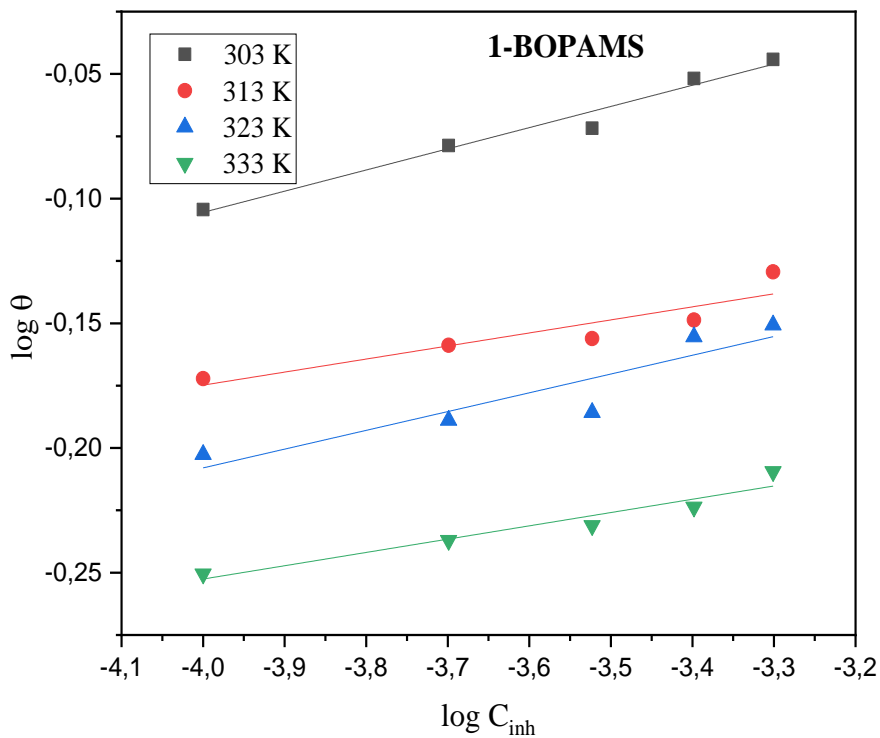


**Figure 4.42:** Freundlich adsorption isotherm plot for the adsorption of different concentrations of 1-BOPAMS on the surface of MS in 1.0 M HCl at different temperatures.

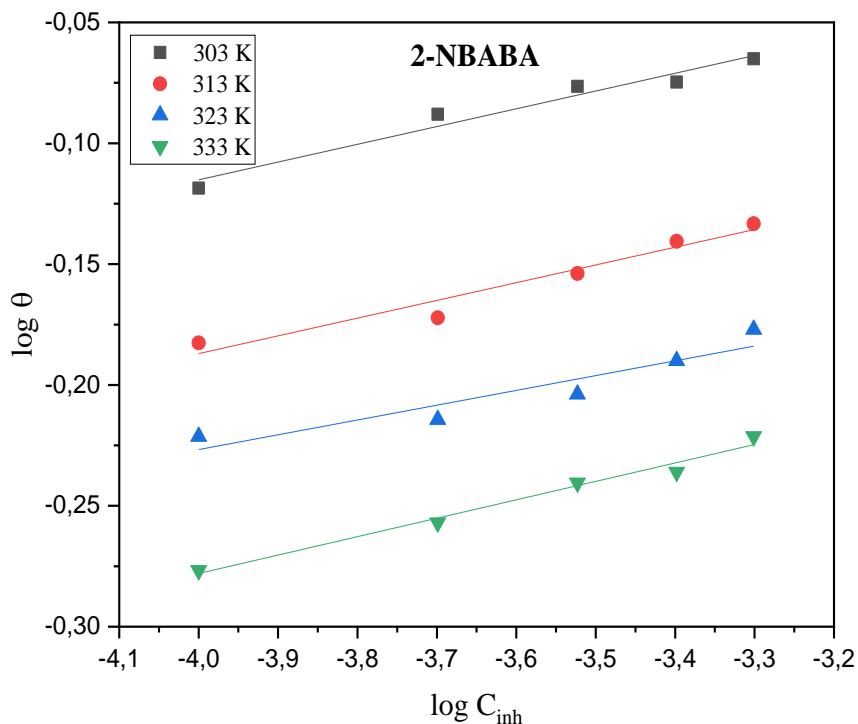


**Figure 4.43:** Freundlich adsorption isotherm plot for the adsorption of different concentrations of 2-NBABA on the surface of MS in 1.0 M HCl at different temperatures.

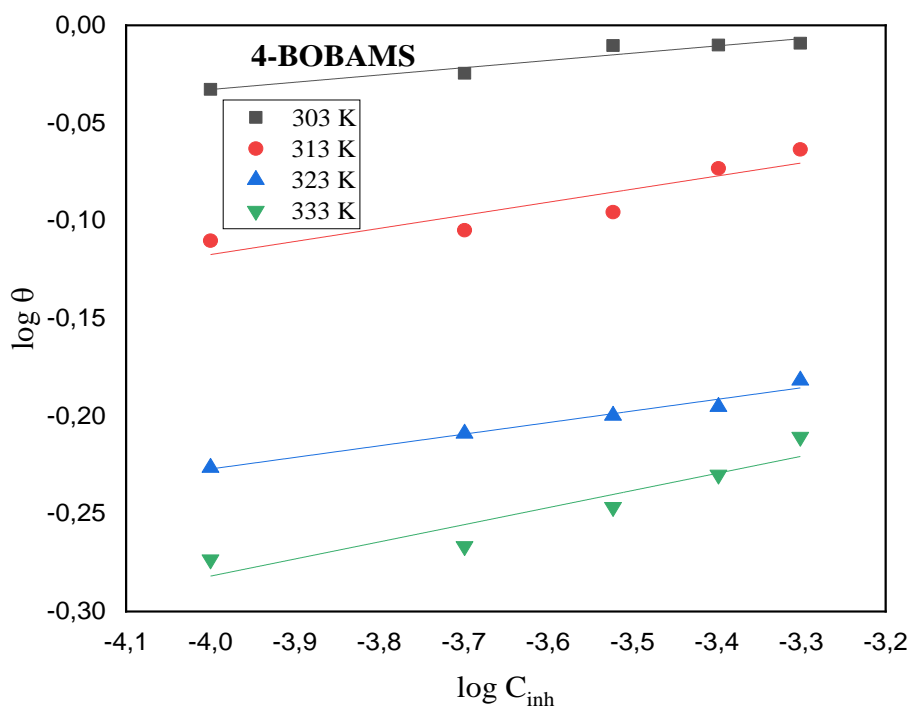


**Figure 4.44:** Freundlich adsorption isotherm plot for the adsorption of different concentrations of 4-BOBAMS on the surface of MS in 1.0 M HCl at different temperatures.

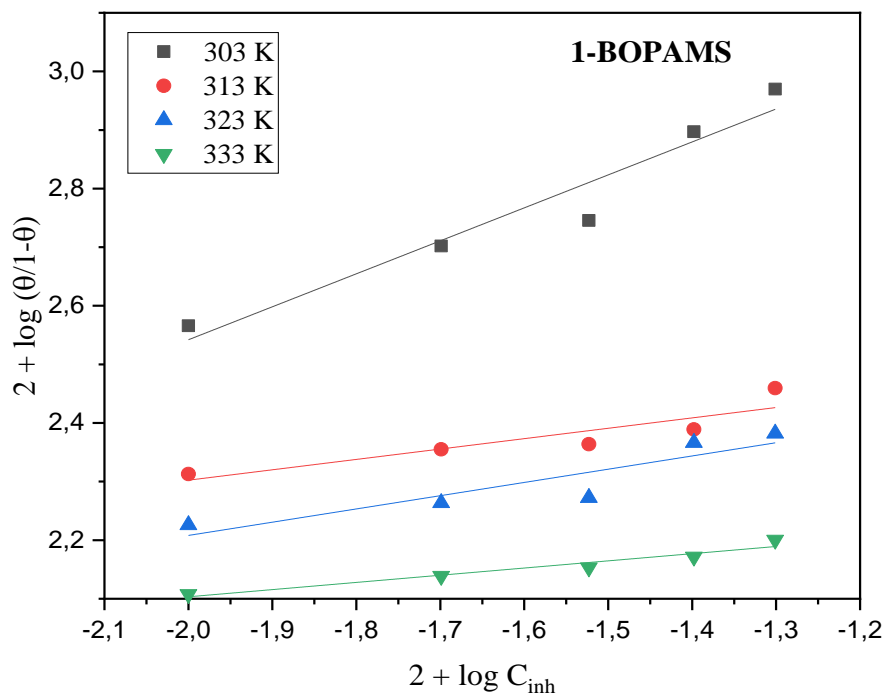


**Figure 4.45:** EL-Awady adsorption isotherm plot for the adsorption of different concentrations of 1-BOPAMS on the surface of MS in 1.0 M HCl at different temperatures.

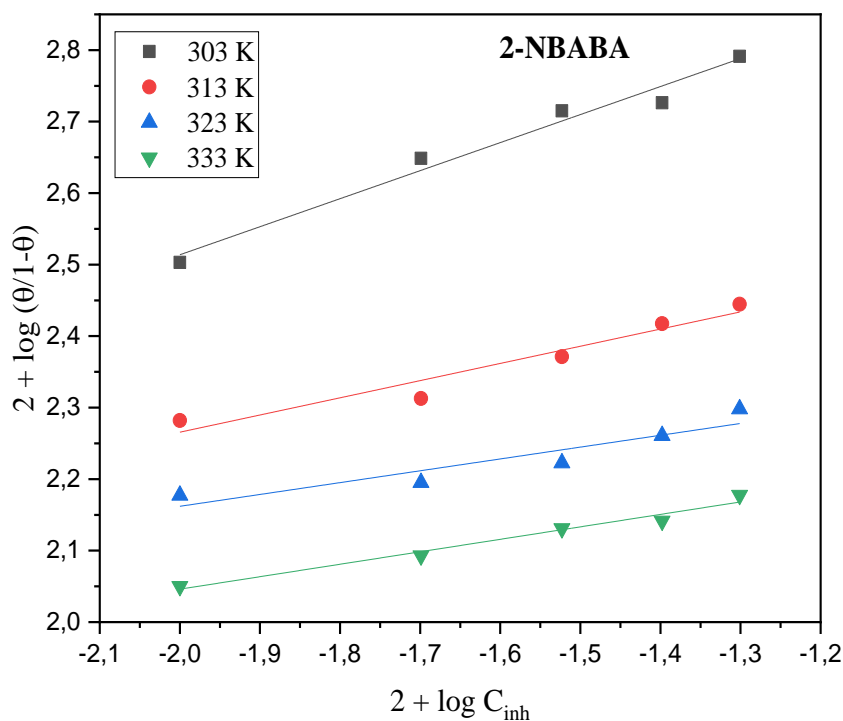


**Figure 4.46:** EL-Awady adsorption isotherm plot for the adsorption of different concentrations of 2-NBABA on the surface of MS in 1.0 M HCl at different temperatures.

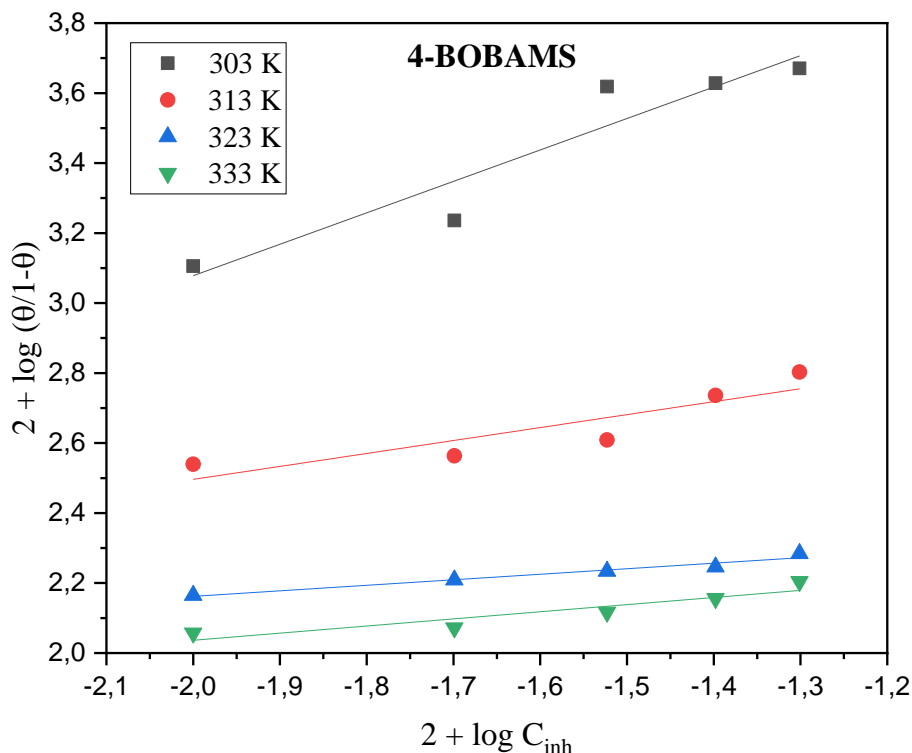


**Figure 4.47:** EL-Awady adsorption isotherm plot for the adsorption of different concentrations of 4-BOBAMS on the surface of MS in 1.0 M HCl at different temperatures.

**Table 4.4:** Thermodynamic and adsorption parameters obtained from various isotherms for MS in 1.0 M HCl at various temperatures for the utilized corrosion inhibitors

Inhibitor	Temperature (K)	Correlation coefficient (R <sup>2</sup> )			
		Langmuir	Temkin	Freundlich	El-Awady
1-BOPAMS	303	0.9985	0.9593	0.9648	0.9179
	313	0.9971	0.7778	0.7933	0.7552
	323	0.9962	0.7886	0.7999	0.7785
	333	0.9985	0.8971	0.9077	0.9291
4-BOBAMS	303	0.9999	0.9192	0.9202	0.9001
	313	0.9976	0.8231	0.8305	0.7984
	323	0.9992	0.9673	0.9716	0.9636
	333	0.9966	0.8644	0.8741	0.8605
2-NBABA	303	0.9997	0.9541	0.9484	0.9676
	313	0.9988	0.9260	0.9329	0.9179
	323	0.9978	0.8319	0.8424	0.8237
	333	0.9988	0.9690	0.9752	0.9669

#### 4.2.4 ADSORPTION FILM ANALYSIS

The FT-IR spectral studies were performed to gain more insight into the functional groups responsible for the adsorption of inhibitors on the MS surface. The FT-IR spectra obtained from the pure amino ester and carboxylic acid are compared to the spectra obtained from the scratched metal surfaces after running the corrosion experiments. Figures 4.48-4.50 show the comparison of the FT-IR spectra of the synthesized compounds to the adsorption film formed in the presence of the amino ester and carboxylic acid after corrosion. These figures reveal that some of the functional groups that were observed in the pure compounds disappeared and these functional groups can be said to be responsible for the complex formation with the MS surface, preventing the dissolution process. The scratched FT-IR spectra (adsorption film formed) shows the intensity of the peaks decreased which indicated that a coordinate bond was created through the functional groups of these peaks with the  $\text{Fe}^{2+}$ , forming the  $\text{Fe}^{2+}$ -inhibitor complex on the surface of MS, preventing the dissolution process. The FT-IR spectra for the two pure amino ester, namely 4-BOBAMS and 1-BOPAMS are similar and showed an ammonium salt ( $^+\text{NH}_3$ ) which gave a strong, broad absorption band at around  $3066\text{-}3095\text{ cm}^{-1}$ . These peaks intensity decreased and shifted to about  $3326\text{ cm}^{-1}$ . The other peaks that were observed in the pure compound disappeared ( $\text{O}=\text{S}=\text{O}$ ,  $\text{C}=\text{O}$ ,  $\text{S}-\text{O}^-$ ,  $\text{C}-\text{O}$ ,  $\text{C}=\text{C}$ ,  $\text{C}-\text{N}$ , and  $\text{O}-\text{H}$ ) in the spectra of the adsorption film for both amino ester and carboxylic acids, and new peaks resulted. For 2-NBABA, the N-H stretching absorption band observed at the frequency around  $3032\text{-}3281\text{ cm}^{-1}$  for the pure compound decreased in intensity and shifted to around  $3500\text{ cm}^{-1}$  in the adsorption film spectrum. Just like the two amino esters, the other peaks that were observed in the pure compound of 2-NBABA disappeared on the scratched spectrum, and new ones were formed. The adsorption film spectra show the appearance of new peaks for all the inhibitors studied. For 2-NBABA, the peaks appeared roughly at around  $811.50$  and  $638.81\text{ cm}^{-1}$ . For 1-BOPAMS the new peaks appeared about  $821.42$  and  $655.72\text{ cm}^{-1}$  and those for 4-BOBAMS were located around  $818.59$  and  $644.39\text{ cm}^{-1}$ . The peaks around  $810\text{-}825\text{ cm}^{-1}$  wavenumber could be attributed to the Fe-C stretching bond due to the formation of a strong bond between the MS surface due to synergistic effect, resulting in less accumulation of rust (iron oxide). The peaks located around  $630\text{-}660\text{ cm}^{-1}$  represents the Fe-O stretching bond frequency, indicating the modification of the MS surface by the formation of a Fe-inhibitor complex through the oxygen atoms present in the structures of the compounds. The peak around  $3326.22\text{ cm}^{-1}$  and  $1614.52\text{ cm}^{-1}$  for MS immersed in  $1.0\text{ M HCl}$  in the absence of the inhibitor represents the hydrated iron



oxide molecule of ( $\text{Fe}_2\text{O}_3 \cdot x\text{H}_2\text{O}$ ) and the presence of CO group in the form of  $\text{HCO}_3^-$  ion participating during corrosion [339].

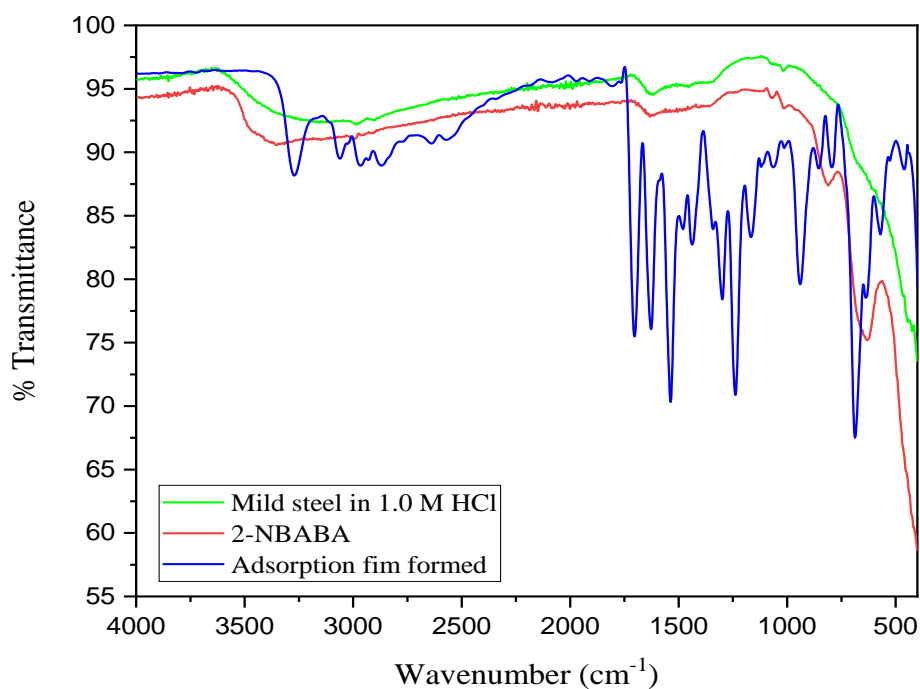


**Figure 4.48:** FT-IR spectra comparison of the frequencies for the pure compound and adsorption films formed on the MS in 1.0 M HCl by 2-NBABA corrosion inhibitor.

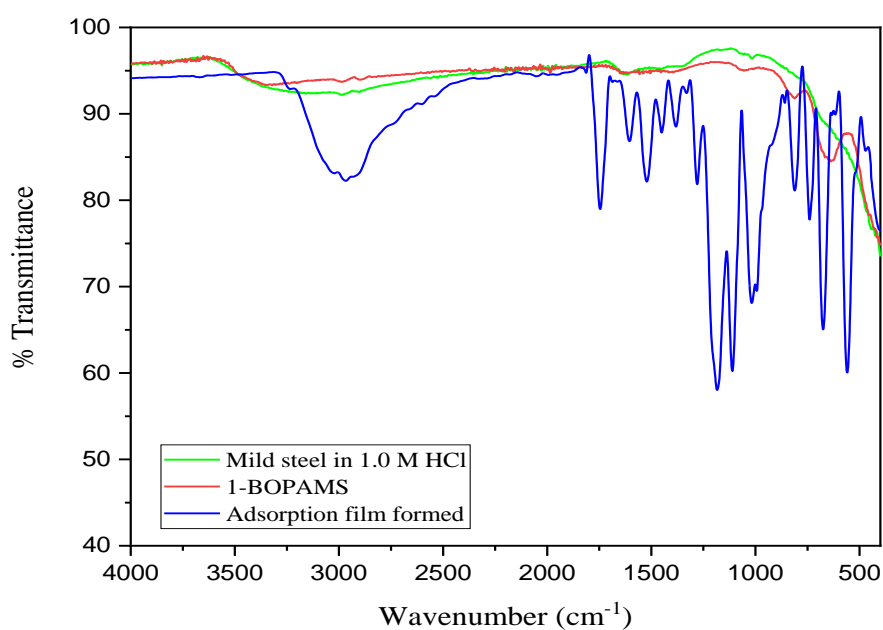


**Figure 4.49:** FT-IR spectra comparison of the frequencies for the pure compound and adsorption films formed on the MS in 1.0 M HCl by 1-BOPAMS corrosion inhibitor.

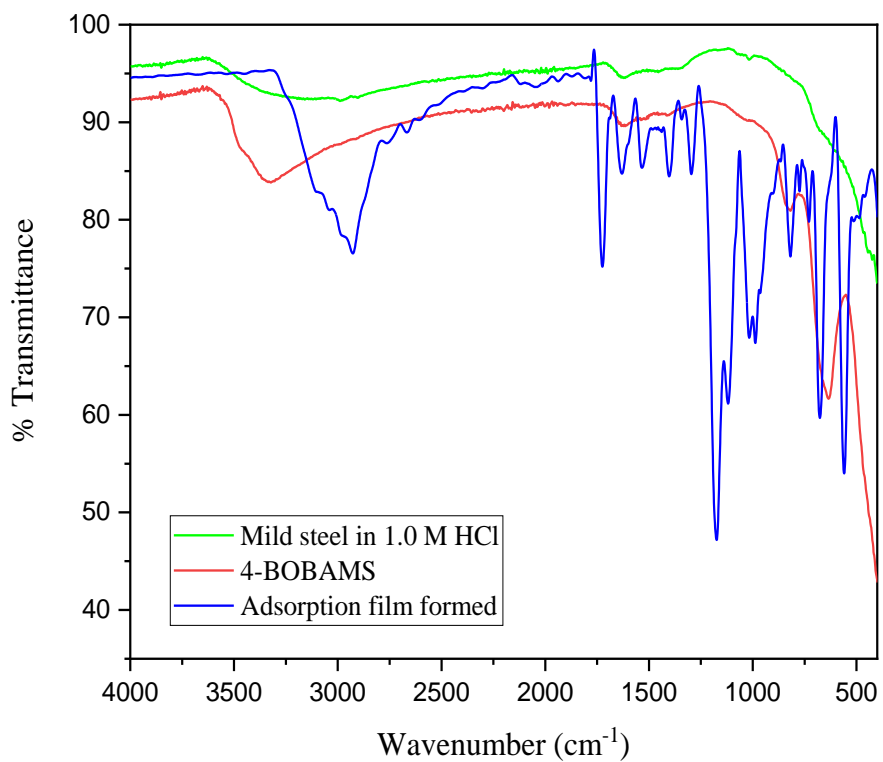


**Figure 4.50:** FT-IR spectra comparison of the frequencies for the pure compound and adsorption films formed on the MS in 1.0 M HCl by 4-BOBAMS corrosion inhibitor.

#### 4.2.5 POTENTIODYNAMIC POLARIZATION (PDP)

PDP measurements were carried out to fully understand the role of inhibitors in biasing anodic and cathodic reactions of MS. This is because the MS comprises of simultaneous anodic dissolution of MS and cathodic reduction of hydrogen ions [340]. Anodic and cathodic Tafel curves for MS corrosion in 1.0 M HCl solution were obtained in the absence and presence of various concentrations of 2-NBABA, 4-BOBAMS and 1-BOPAMS at 303 K, as shown in figures 4.51-4.53. Potentiodynamic parameters such as corrosion potential ( $E_{\text{corr}}$ ), corrosion current density ( $i_{\text{corr}}$ ), anodic ( $\beta_a$ ) and cathodic ( $\beta_c$ ) Tafel slopes and linear polarization resistance were extrapolated from these curves and are listed in Table 4.5. %IE<sub>PDP</sub> was then calculated from the equation (3.2). It can be noted from the Tafel curves and Table 4.5 that, the corrosion current densities markedly decreased upon the introduction of the three inhibitors both in the anodic and cathodic regions, indicating that the inhibitors are adsorbed on the surface of MS and inhibit its corrosion process. The maximum inhibition efficiency for all inhibitors was observed with the addition of an optimum concentration ( $5.0 \times 10^{-3}$  M). This implies that there was inhibition of both the anodic dissolution of MS and cathodic reduction of the hydrogen ions. The magnitude of the displacement in the  $E_{\text{corr}}$  values between the inhibited and uninhibited systems can be used to classify the mode of inhibition as either anodic, cathodic or mixed-type. An inhibitor can be classified as anodic or cathodic type if the change in the  $E_{\text{corr}}$  values is greater than  $\pm 85$  mV [341]. In the present study, the magnitude of the shift  $E_{\text{corr}}$  values in the presence of carboxylic acids and amino ester compounds is towards more negative values and the shift is less than 85 mV at all inhibitor concentrations with respect to the blank solution which implies that these are mixed-type inhibitors thereby controlling both the cathodic and anodic reactions of MS. On the other hand, the addition of different concentrations of these inhibitors in 1.0 M HCl solution altered the Tafel slopes ( $\beta_a$  and  $\beta_c$ ) approximately to the same extent, supporting the fact that both the retardation of the anodic metal dissolution and cathodic hydrogen reduction were affected [173, 321]. The variation of  $\beta_a$  and  $\beta_c$  in the presence of the inhibitors compared to the blank can be attributed to the alteration of the kinetics of hydrogen evolution as result of the diffusion or barrier effect [342, 343]. The cathodic polarization curves are almost parallel to each other, indicating that the hydrogen evolution reaction is under activation control [344, 345]. The changing of the  $\beta_a$  values with the addition of the inhibitors suggests that the inhibition process could be attributed to the formation of adsorption film on metals surface and impeding the corrosion of MS by blocking the active sites of the metal without affecting the anodic reaction mechanism [346].

The addition of the amino ester and carboxylic acids surfactants to the corrosive solution resulted in the increase in the  $R_p$  values, which increased to maximum at the highest concentration of the surfactants, indicating an effective inhibition by the compounds. The increase in the  $R_p$  values with the increase in the inhibitor concentration implies that further polarization of MS was opposed by the formation of an adsorption film formed by the inhibitor molecules present in the solution at the metal/solution interface.  $\%IE_{PDP}$  values obtained were found to increase with the increase in the concentration of all the inhibitors utilized in the present study. The  $\%IE_{PDP}$  values are in agreement with those of  $\%IE_{WL}$  values.

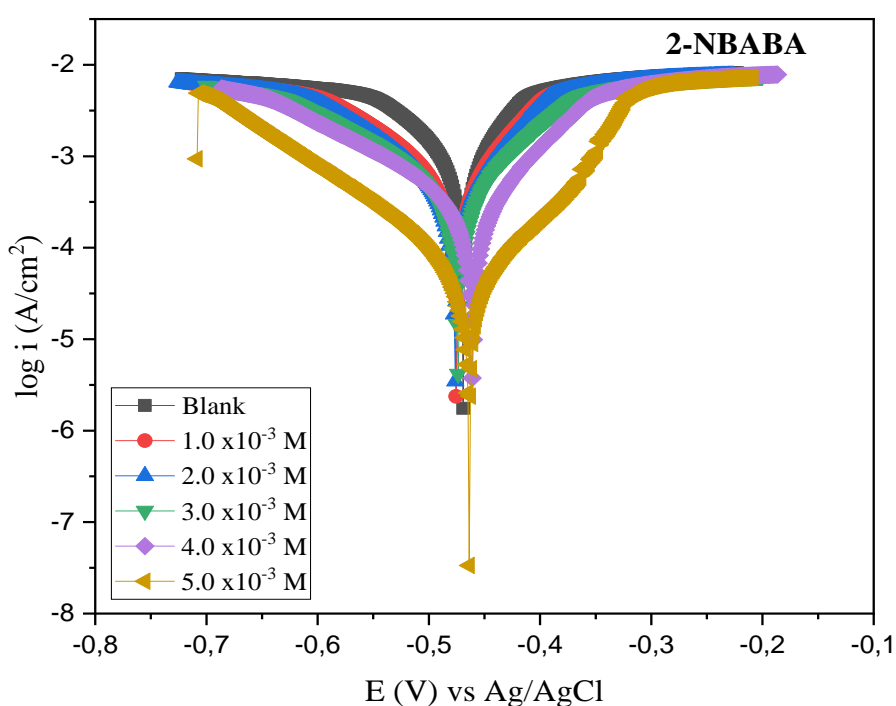


**Figure 4.51:** Tafel plots for MS in 1.0 M HCl in the absence and presence of different concentrations of 2-NBABA inhibitor compound.

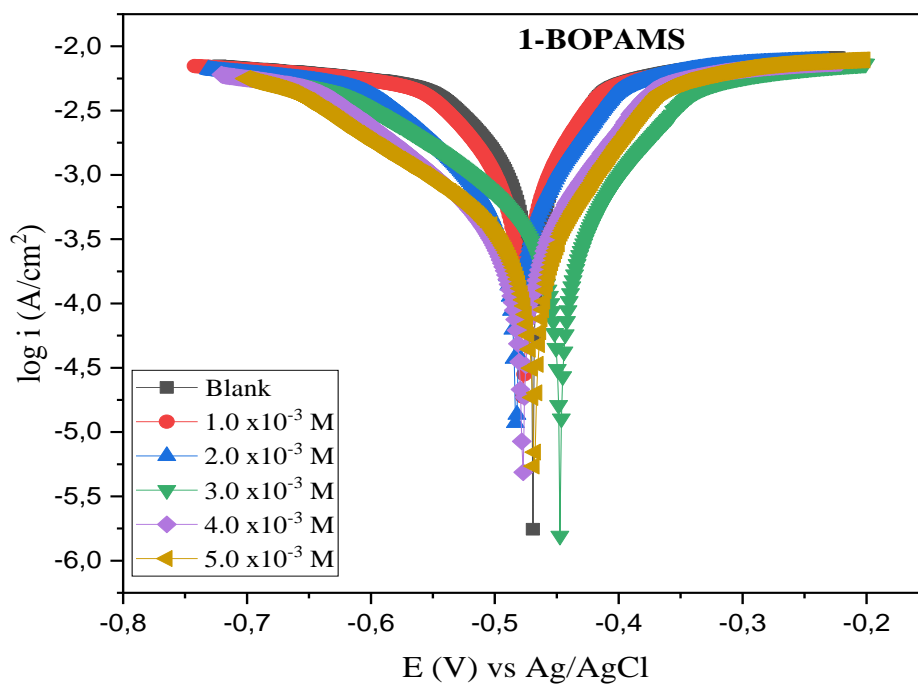


**Figure 4.52:** Tafel plots for MS in 1.0 M HCl in the absence and presence of different concentrations of 1-BOPAMS inhibitor compound.

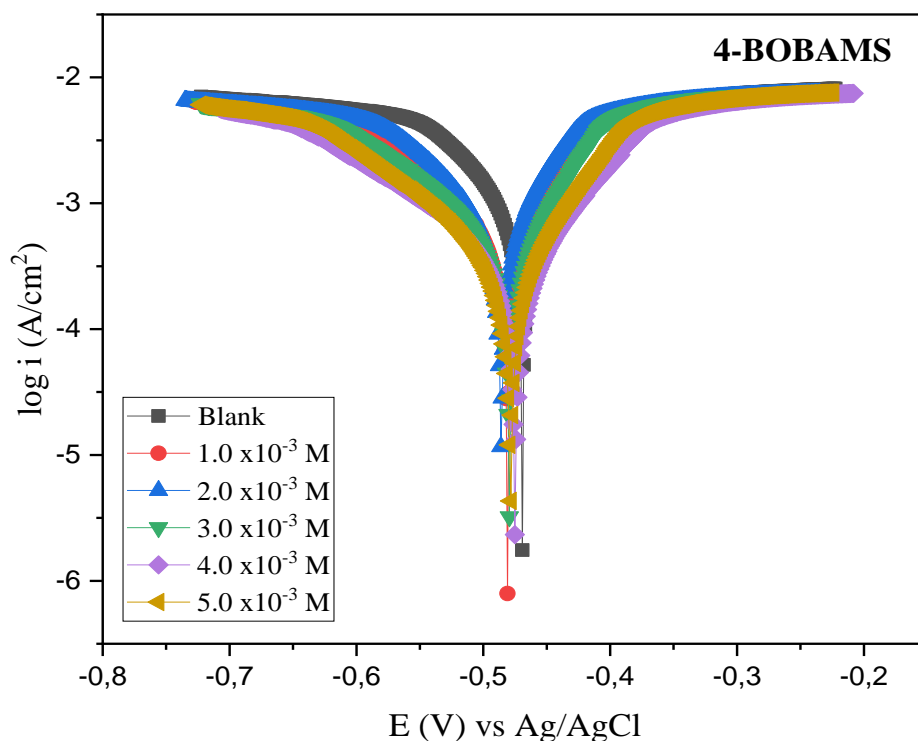


**Figure 4.53:** Tafel plots for MS in 1.0 M HCl in the absence and presence of different concentrations of 4-BOBAMS inhibitor compound.

**Table 4.5:** Potentiodynamic polarization (PDP) parameters such as corrosion potential ( $E_{\text{corr}}$ ), corrosion current density ( $i_{\text{corr}}$ ) and anodic and cathodic Tafel slopes ( $\beta_a$  and  $\beta_c$ ) for MS corrosion in 1.0 M HCl in with and without different concentrations of 2-NBABA, 1-BOPAMS and 4-BOBAMS at 303 K.

Inhibitor	$C_{\text{inh}}$ (M)	$E_{\text{corr}}$ (mV)	$i_{\text{corr}}$ (mAcm <sup>-2</sup> )	$\beta_a$ (mVdec <sup>-1</sup> )	$\beta_c$ (mVdec <sup>-1</sup> )	$R_p$ (10 <sup>-1</sup> ) ( $\Omega$ cm <sup>2</sup> )	$IE_{\text{PDP}}$ (%)	$IE_{\text{WL}}$ (%)
Blank	-	-469	0.0021248	20	26	22.97	-	-
1-BOPAMS	1.0 x10 <sup>-3</sup>	-477	0.0006682	8	10	28.33	68.55	78.63
	2.0 x10 <sup>-3</sup>	-483	0.0002253	5	6	54.60	89.40	83.43
	3.0 x10 <sup>-3</sup>	-447	0.0002905	9	13	79.69	86.33	84.77
	4.0 x10 <sup>-3</sup>	-478	0.0002314	8	11	87.46	89.11	88.75
	5.0 x10 <sup>-3</sup>	-468	0.0001716	7	10	100.34	91.92	90.32
4-BOBAMS	1.0 x10 <sup>-3</sup>	-481	0.0004532	7	11	41.04	78.67	92.73
	2.0 x10 <sup>-3</sup>	-486	0.0004524	6	8	33.40	78.71	94.51
	3.0 x10 <sup>-3</sup>	-480	0.000334	7	10	52.38	84.28	97.65
	4.0 x10 <sup>-3</sup>	-475	0.0002601	8	12	82.16	87.75	97.70
	5.0 x10 <sup>-3</sup>	-478	0.0002407	7	10	76.82	88.67	97.91
2-NBABA	1.0 x10 <sup>-3</sup>	-475	0.0003741	7	9	46.90	82.39	76.10
	2.0 x10 <sup>-3</sup>	-476	0.0003295	7	10	55.82	84.49	81.66
	3.0 x10 <sup>-3</sup>	-474	0.0003121	9	11	68.60	85.31	83.84
	4.0 x10 <sup>-3</sup>	-461	0.0002412	9	13	91.76	88.65	84.19
	5.0 x10 <sup>-3</sup>	-464	3.7549E-5	9	9	501.26	98.23	86.08

#### 4.2.6 ELECTROCHEMICAL IMPEDANCE SPECTROSCOPY (EIS)

Electrochemical impedance spectroscopy is a powerful tool in the investigation of the corrosion and adsorption phenomena. Further information regarding the corrosion behaviour of Al and MS in an acidic solution and the inhibition by different concentrations of carboxylic acids and amino esters in 1.0 M HCl was obtained using the electrochemical impedance spectroscopy. An equivalent circuit can be fitted to interpret experimental data collected from EIS where the individual elements of the circuit correspond to the electrochemical properties of the tested system [347], in this case, 1.0 M HCl in the absence and presence of the corrosion inhibitors. The Nyquist plots consisting of capacitive loops for MS in 1.0 M HCl solution in the absence and presence of different concentrations of 2-NBABA 4-BOBAMS and 1-BOPAMS utilized at 303 K are shown in figures 4.55-4.57, respectively. Keen observation of these plots shows that incomplete semicircles capacitive loops represent them. This imperfection indicates that the charge transfer process governs the corrosion of MS in acidic solutions [348] and is possibly due to the frequency dispersion, distribution of surface active sites, inhomogeneity of the metal surface, grain boundaries, roughness and impurities. Hence, CPE is introduced in the circuit to get a more accurate fit [349, 350]. From the plots, it is evident that the impedance response of MS after the addition of the corrosion inhibitors to the acidic solution has significantly changed. This change can be attributed to the increases in the incomplete semicircles capacitive loops diameter with the increase in inhibitor concentration which specify the increasing coverage of the MS surface. The electrochemical impedance parameters derived from the Nyquist plots and the %IE<sub>EIS</sub> are listed in Table 4.6. The %IE<sub>EIS</sub> was calculated using the charge transfer resistance equation (3.1). Nyquist impedance plots were analysed by fitting experimental data to a simple electrical equivalent circuit (figure 4.54) that included the solution resistance ( $R_s$ ) which is represented by ( $R_1$ ), charge transfer resistance ( $R_{ct}$ ), represented by ( $R_2$ ) and constant phase element ( $Q_1$ )

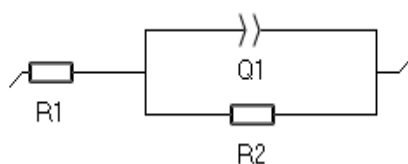


**Figure 4.54:** Equivalent circuit used to fit the impedance spectra obtained for MS corrosion in 1.0 M HCl in the absence and presence of 2-NBABA, 4-BOBAMS and 1-BOPAMS.

The expression below defines the impedance of the CPE with a fixed phase shift angle:

$$Z_{CPE} = \frac{1}{Y_o(j\omega)^n} \quad (4.11)$$

where  $Y_o$  is the CPE constant,  $\omega$  is the angular frequency ( $\omega = 2\pi f$ , where  $f$  is the AC frequency),  $j$  is the imaginary unit, and  $n$  is the CPE exponent (phase shift) related to the degree of surface inhomogeneity [351]. Depending on the value of  $n$ , CPE can represent resistance ( $n=0$ ,  $Y_o = R$ ), capacitance ( $n=1$ ,  $Y_o = C$ ), inductance ( $n=-1$ ,  $Y_o = L$ ) or Warburg impedance ( $n = 0.5$ ,  $Y_o = W$ ). The value of  $n$  (varying between 0.7 and 0.95) represents a deviation from ideal behaviour (where  $n=1$ ) which is also the measure of inhomogeneity of the surface.

The  $R_{ct}$  values are directly proportional to the corrosion inhibition efficiency and provide details on the magnitude of the electron transfer over the surface of MS [348]. It is conspicuous from Table 4.6 that by raising the concentration inhibitor, the  $R_{ct}$  values also increases while the CPE decreases. This is because the addition of the inhibitor increases the surface coverage on the MS surface by the inhibitor molecules, due to the formation of a protective film which results in the decrease of the electron transfer between the metal surface and the corrosive medium [301]. The CPE constant for the studied inhibitors at all studied concentration decreased when compared to the blank. The decrease in  $Y_o$  after the addition of inhibitors may be either due to the increase in the thickness of the double layer or the desorption of water molecules from MS followed by the adsorption of the inhibitor on the metal surface. CPE indicates the reduction in local dielectric constant or an enhancement in the thickness of the electric double layer. This is as a result of the adsorption of carboxylic acid compounds on the MS surface which creates a barrier between the metal surface the corrosive medium [352, 353]. The values of CPE exponent ( $n$ ) are between 0.0947 and 0.8989 which represents the inhomogeneity of the MS surface. The values of  $n$  are approaching unity which signifies the capacitive nature of the MS/HCl interface.



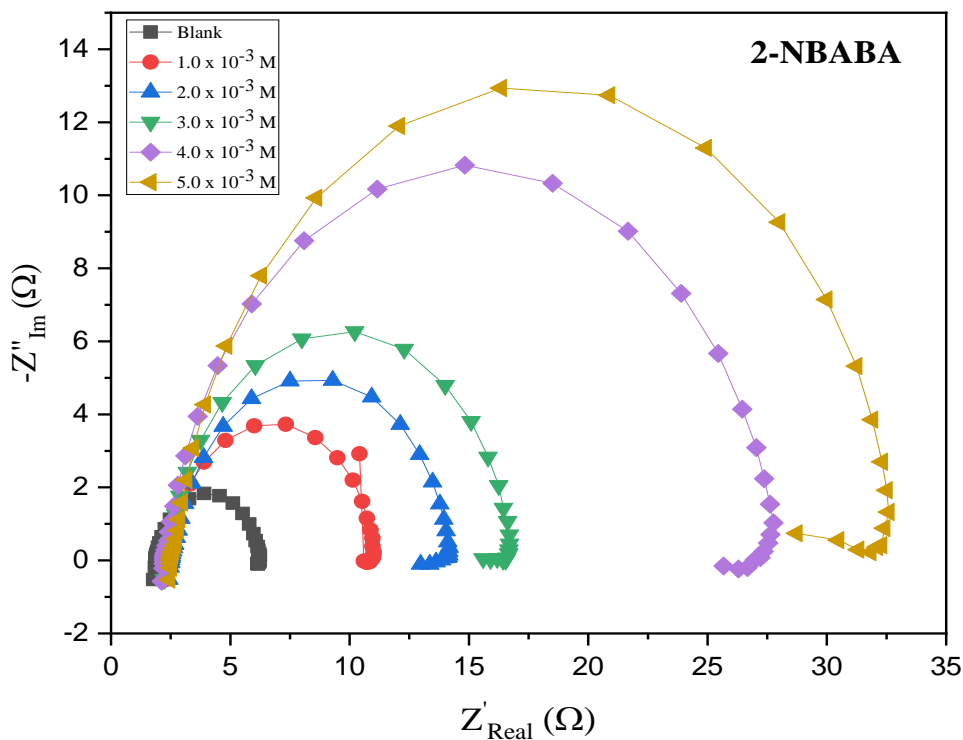


**Figure 4.55:** Nyquist plots for MS in 1.0 M HCl in the absence and presence of different concentrations of 2-NBABA.

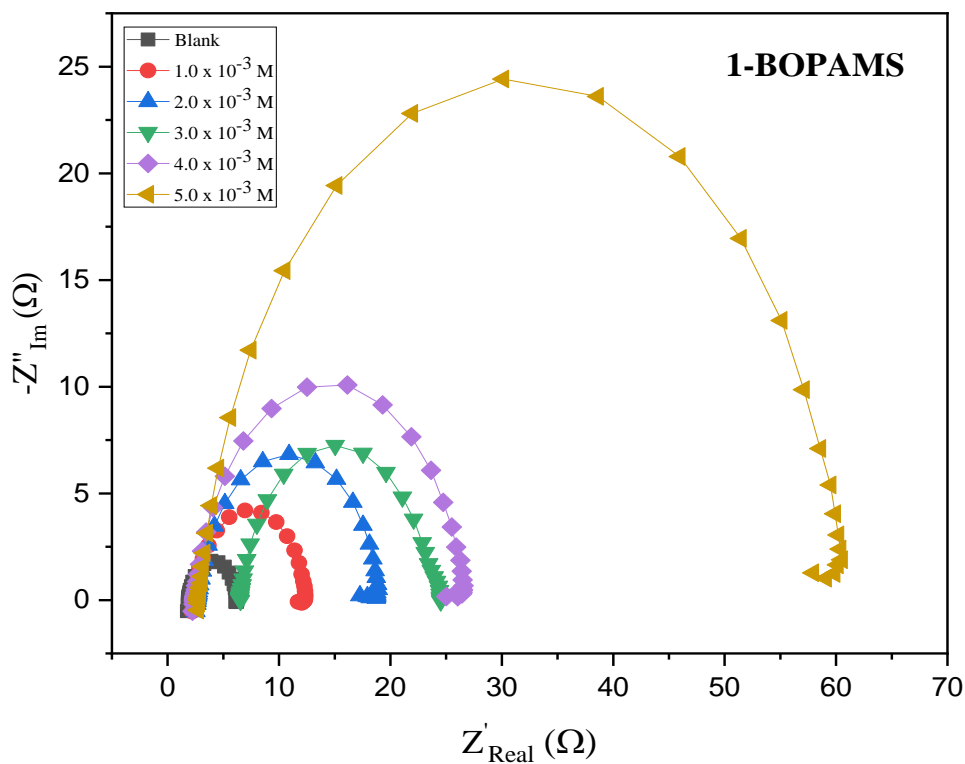


**Figure 4.56:** Nyquist plots for MS in 1.0 M HCl in the absence and presence of different concentrations of 1-BOPAMS.

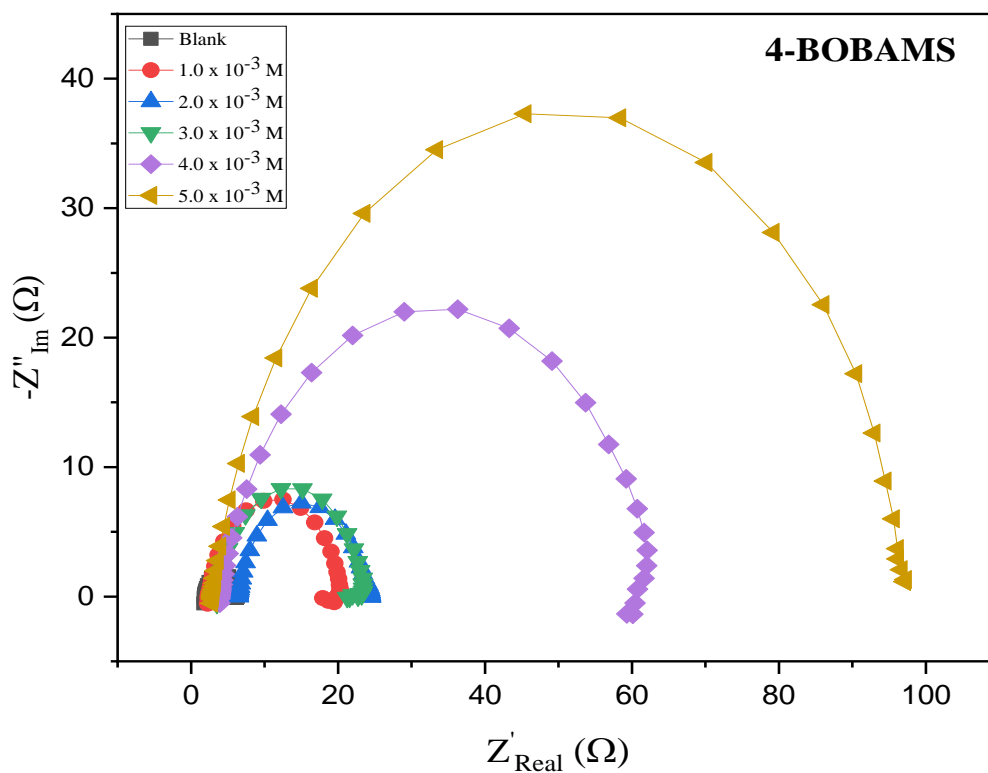


**Figure 4.57:** Nyquist plots for MS in 1.0 M HCl in the absence and presence of different concentrations of 4-BOBAMS.

**Table 4.6:** Electrochemical impedance spectroscopy (EIS) parameters such as the resistance of charge transfer ( $R_{ct}$ ), constant phase element ( $Y_0$ ), solution resistance ( $R_s$ ) and the CPE exponent ( $n$ ) for MS corrosion in 1.0 M HCl in absence and presence of different concentrations of 2NBABA, 1-BOPAMS and 4-BOBAMS at 303 K.

Inhibitor	$C_{inh}$ (M)	$R_{ct}$ ( $\Omega$ )	$Q_1$ ( $F.s^{(a-1)}$ )	$R_s$ ( $\Omega$ )	$n$	$\theta$	$IE_{EIS}$ (%)	$IE_{WL}$ (%)
Blank	-	4.365	0.26e-3	1.867	0.8827	-	-	-
1-BOPAMS	$1.0 \times 10^{-3}$	9.981	0.2349e-3	2.314	0.8787	0.5627	56.27	78.63
	$2.0 \times 10^{-3}$	16.06	0.1771e-3	2.665	0.8551	0.7282	72.82	83.43
	$3.0 \times 10^{-3}$	17.75	0.2568e-3	6.478	0.8729	0.7541	75.41	84.77
	$4.0 \times 10^{-3}$	24.11	0.1523e-3	2.36	0.8795	0.8190	81.90	88.75
	$5.0 \times 10^{-3}$	57.5	0.144e-3	2.827	0.8958	0.9241	92.41	90.32
4-BOBAMS	$1.0 \times 10^{-3}$	17.57	0.1996e-3	2.391	0.8833	0.7541	75.41	92.73
	$2.0 \times 10^{-3}$	17.75	0.2568e-3	6.478	0.8729	0.7541	75.41	94.51
	$3.0 \times 10^{-3}$	19.46	0.1602e-3	3.578	0.8938	0.7757	77.57	97.65
	$4.0 \times 10^{-3}$	58.05	0.2223e-3	3.95	0.8352	0.9248	92.48	97.70
	$5.0 \times 10^{-3}$	94.62	0.2245e-3	2.885	0.8571	0.9539	95.39	97.91
2-NBABA	$1.0 \times 10^{-3}$	8.657	0.2691e-3	2.309	0.8918	0.4958	49.58	76.10
	$2.0 \times 10^{-3}$	11.51	0.1989e-3	2.53	0.8917	0.6208	62.08	81.66
	$3.0 \times 10^{-3}$	14.25	0.2283e-3	2.34	0.0947	0.6937	69.37	83.84
	$4.0 \times 10^{-3}$	25.21	0.1592e-3	2.221	0.8899	0.8269	82.69	84.19
	$5.0 \times 10^{-3}$	29.62	0.1969e-3	2.559	0.8989	0.8526	85.26	86.08

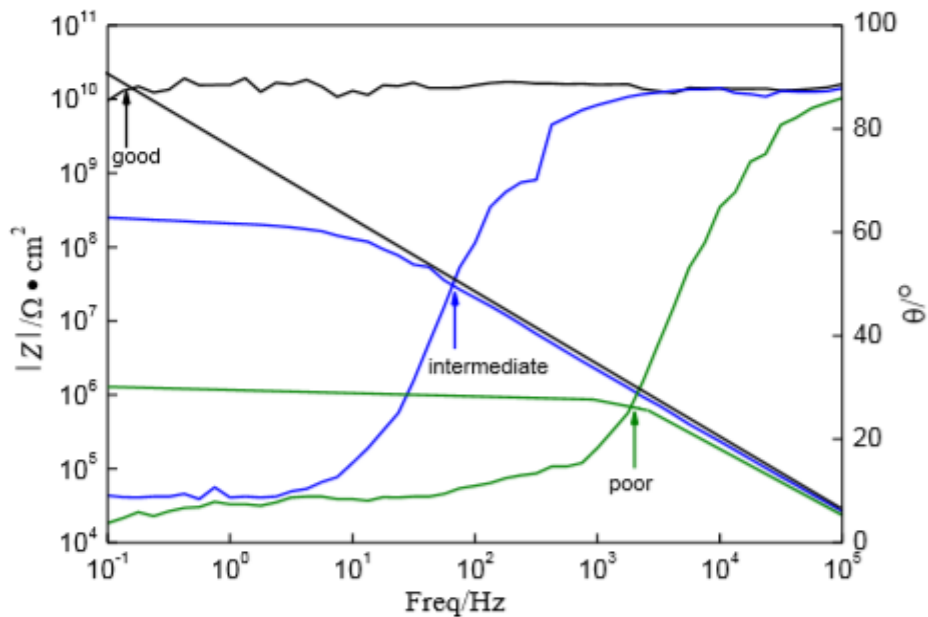


**Figure 4.58:** Theoretical Bode plots of good, intermediate, poor quality coating [354].

The performance of coatings is usually represented by the three phases (good, intermediate and poor) as shown by the typical Bode plots in figure 4.58. It can be seen from this figure that the first phase of intermediate Bode plots (IBP) is in the upper left of the Bode plots when the performance of the coatings is good, and when the performance of the coating is poor, the IBP is in the lower right of the Bode plots. In general, the IBP has been moved from a good performance phase gradually to a poor performance phase with time. Furthermore, as the performance of the coating is decreasing, both the corresponding phase angle, as well as the impedance of the IBP, show a similar decreasing pattern, while the corresponding frequency shows a gradually increasing trend. Thus, the IBP can be used as a valuable reference to evaluate the performance of the protection provided by the coatings [354].

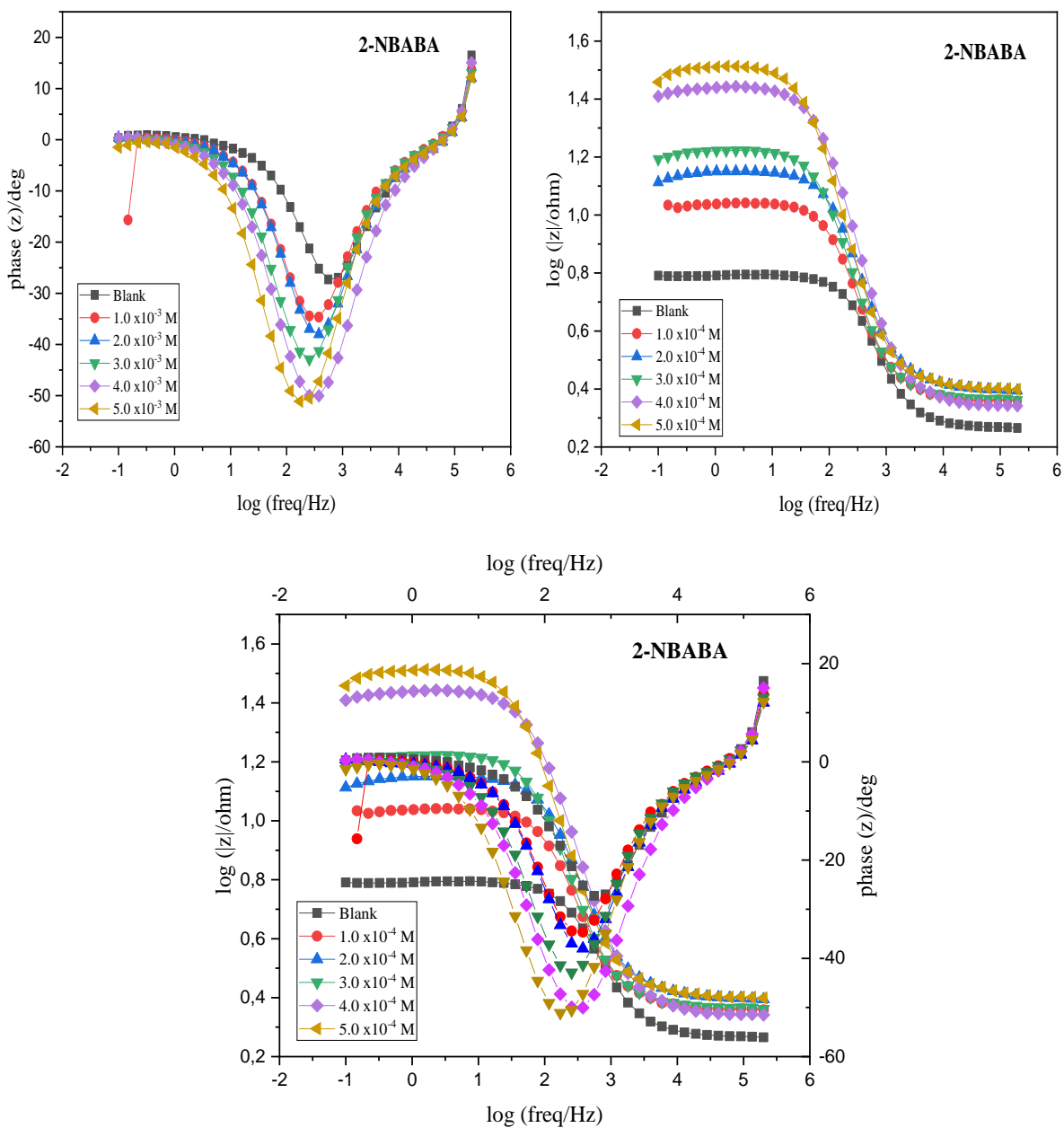


**Figure 4.59:** Bode diagrams of the impedance for MS in 1.0 M HCl without and with different concentrations of 2-NBABA at 303 K.

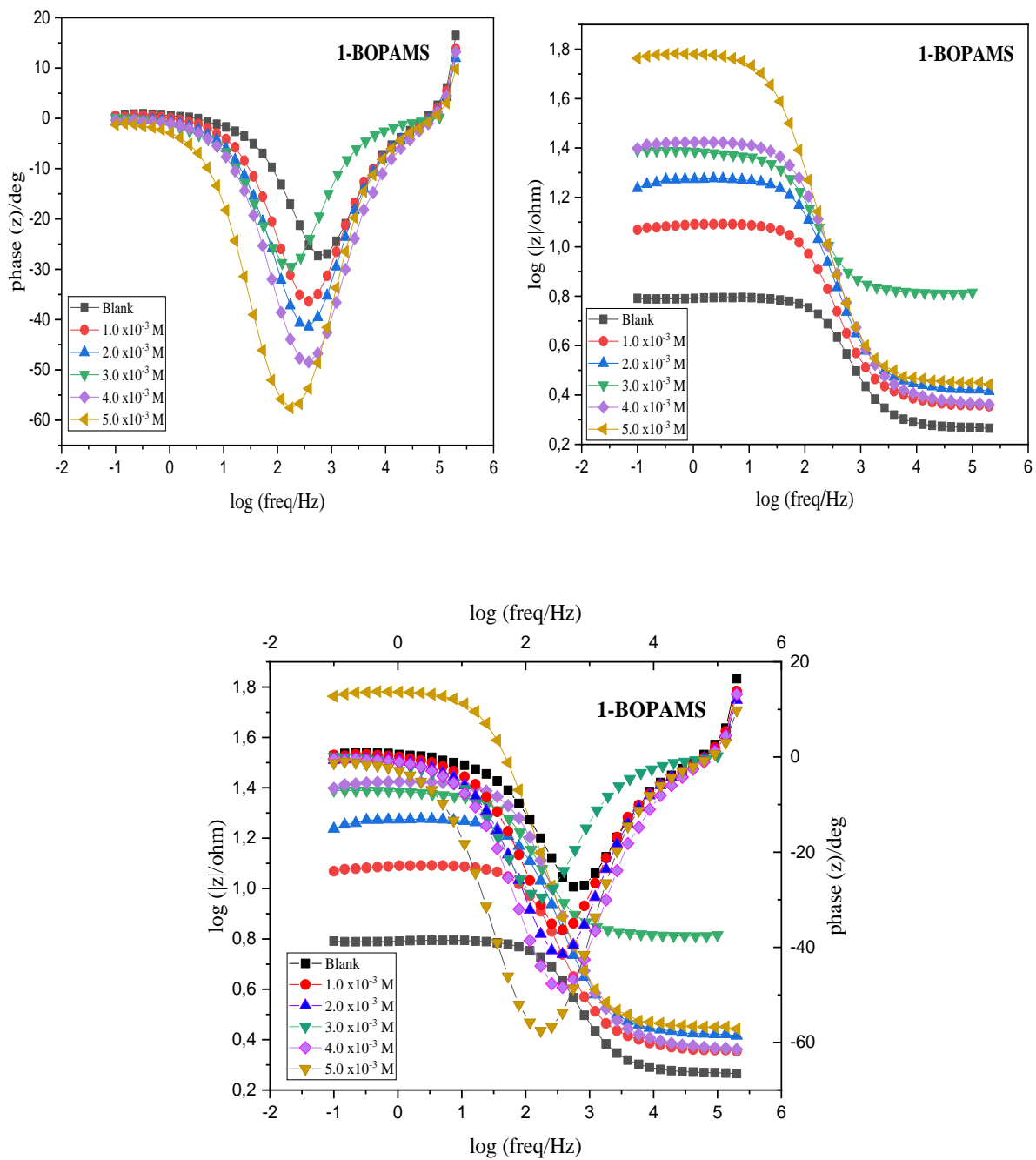


**Figure 4.60:** Bode diagrams of the impedance for MS in 1.0 M HCl without and with different concentrations of 1-BOPAMS at 303 K.

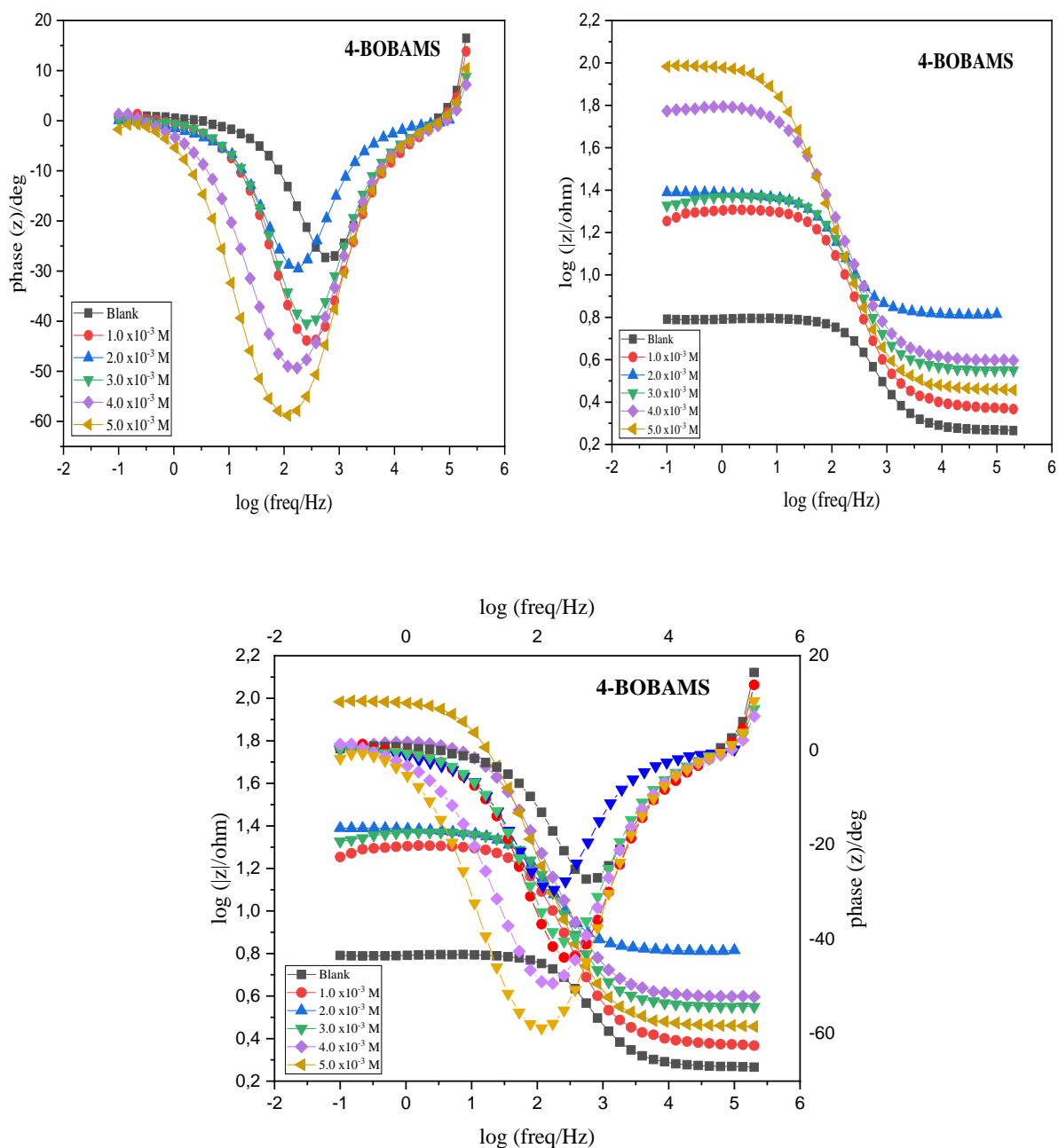


**Figure 4.61:** Bode diagrams of the impedance for MS in 1.0 M HCl without and with different concentrations of 4-BOBAMS at 303 K.

#### 4.2.7 PROPOSED INHIBITION MECHANISM ON MS SURFACE

Experimental results obtained from several techniques established that the %IE values are high and increase as the concentration of the inhibitors increases. This proves that the inhibitors get adsorbed on the MS surface and inhibits the dissolution of MS. The inhibition mechanism of 2-NBABA, 1-BOPAMS and 4-BOBAMS against MS corrosion can be suggested based on adsorption phenomenon of these inhibitors on the MS surface. The high inhibition efficiency afforded by these inhibitors can be attributed to the electronegative nitrogen atoms, the presence of the  $\pi$ -electrons on the phenyl group, the positively charged ammonium group ( $^+\text{NH}_3$ ), the carboxylate group ( $-\text{COOH}$ ), the carbonyl group ( $\text{C}=\text{O}$ ) and the secondary amine group ( $-\text{NH}$ ). Through these functional groups and electrons, these inhibitors physisorbed and chemisorbed on the MS surface by forming coordinate bonds. PDP results indicated that the inhibitors 2-NBABA, 1-BOPAMS and 4-BOBAMS are mixed-type corrosion inhibitors. The mixed-type inhibition mechanism of the 1-BOPAMS and 4-BOBAMS is as a result of the cationic groups which adsorb at the cathodic region of the metal surface and in turn, prevents hydrogen evolution reaction from taking place. In acidic conditions, the surface of MS is positively charged at the electrode potential. The excess positive charge at the electrode/solution interface enables the adsorption of the chlorine ions by coulombic attraction. The adsorbed chlorine ion molecules make the electrode surface to become negatively charged. The electrode being negatively charged allows the adsorption of protonated species of the inhibitors on the surface of MS via electronic attraction (physisorption) [205, 355, 356]. The inhibitor 2-NBABA contains a secondary amine group ( $-\text{NH}$ ) in its structure, and non-substituted secondary amine compounds have shown to be less effective as corrosion inhibitors. However, the introduction of other substituents ( $-\text{Cl}$ ,  $-\text{Br}$ ,  $-\text{NO}_2$ ,  $-\text{CH}_3$ ) into the structure of the inhibitors increases their inhibition capabilities [357]. The adsorption of 2-NBABA on MS surface could be as a result of the electron-rich carboxylate functional group ( $-\text{COOH}$ ) and the secondary amine group ( $-\text{NH}$ ). This is because in acidic environments the carboxylate group ( $-\text{COOH}$ ) of 2-NBABA gets deprotonated and loses a proton to become negatively charged ( $-\text{COO}^-$ ) and the lone pairs present in the oxygen and nitrogen atom are capable of coordinating with the MS surface and forming a layer. The movement of electrons from these atoms to the electron-deficient surface of MS is what prevents the dissolution of MS [358, 359]. The nitrogen atom in the 2-NBABA gets protonated and becomes positively charged ( $^+\text{NH}_2$ ). The protonated nitrogen atom is capable of bonding physically to the positively charged metal surface [360]. Chemisorption inhibition mechanism can occur through the formation of



coordinate bonds that forms between the vacant d-orbitals of iron and lone pairs electrons of the heteroatoms (N, O and S) and the phenyl  $\pi$ -electrons. The electron-donating group (-OCH<sub>2</sub>) of 1-BOPAMS and 4-BOBAMS helps in the chemisorption adsorption on the metal surface, and this functional group is one of the reasons this two compounds had the best inhibition performance. All the three corrosion inhibitors have a cationic form in acidic solution and when adsorbed, only a monolayer adsorption film can be formed due to the positively charged groups that repel each other. This therefore, advocates for the compounds obeying the Langmuir adsorption mechanism.

## 4.3 ALUMINIUM

### 4.3.1 EFFECT OF INHIBITOR CONCENTRATION

The inhibiting effect of the inhibitors (1-BOPAMS, 4-BOBAMS and 2-NBABA) in retarding the corrosion of Al was determined by weight loss measurement in the inhibitors concentrations range of  $1 \times 10^{-4}$  -  $5 \times 10^{-4}$  M after 8h of the immersion in 1.0 M HCl at 30-60 °C. The corrosion rate ( $C_R$ ) and percentage inhibition efficiency (%IE) were calculated (Table 4.7). The figures 4.62-4.65 shows the variations of the %IE with the concentrations of the inhibitors at various temperatures. Scrutiny of the plots revealed that the %IE increases with an increase in the concentration of all the three inhibitors studied. For instance, at 30 °C when the concentration of 1-BOPAMS was  $1.0 \times 10^{-4}$  M the inhibition efficiency was found to be 87.16 % and increased to a maximum of 93.52 % at  $5.0 \times 10^{-4}$  M. The same trend was observed in the case of 4-BOBAMS wherein the obtained inhibition efficiency at  $1.0 \times 10^{-5}$  M was 89.74% and at  $5.0 \times 10^{-5}$  M was 91.94%. This trend is observed in all the inhibitors investigated. These figures also show that inhibition efficiency increases with an increase in the inhibitor concentration in the corrosive environment. For all inhibitors, the maximum %IE of 93.52 %, 91.94 % and 91.73% was obtained at an optimum concentration of  $5 \times 10^{-4}$  M for 1-BOPAMS, 4-BOBAMS, and 2-NBABA respectively. The increase in %IE with an increase in the concentrations of the inhibitors is due to the accumulation of a greater number of molecules on the surface of Al as the inhibitors concentrations is increased, which lead to the separation of the Al surface from the acidic solution and retarding the dissolution of Al [361]. The inhibition efficiency of the inhibitors follow the order: 2-NBABA > 1-BOPAMS > 4-BOBAMS. The two amino esters derivatives, namely 1-BOPAMS and 4-BOBAMS, showed the highest inhibition efficiency compared to the carboxylic acids, 2-NBABA. The inhibitive action of all the three inhibitors may probably be due to the presence of the heteroatoms such as nitrogen, sulphur, oxygen and  $\pi$ -electrons in their structures which interacted with the positively charged Al surface [301, 362]. This difference in the inhibition efficiency between the carboxylic acids and the amino esters may be attributed to the presence of an extra benzene ring, presence of sulphur, and two additional oxygen group in the amino esters.

The degree of surface coverage typifies the part of the metal surface that is covered by the inhibitors and from the results, the surface coverage increases as the inhibitor concentration are increased. This shows that the three inhibitors studied successfully covered the Al surface, creating a barrier layer between the acidic medium and the Al surface. The relationship between the corrosion rate and the temperature at various concentrations of inhibitors are shown by the

figures 4.66-4.68. Inspection of the results indicates that as the temperature of the system is increased the corrosion rate increases, and the inhibition efficiency is lowered. The reduction in %IE with an increase in temperature is due to the desorption effect of the inhibitor molecules with time on the surface of Al [363], leaving the Al surface exposed to attack by the acidic medium. The decrease in the strength of the adsorption on the Al surface at higher temperature causes the %IE to decrease. This type of behaviour can be explained to be as results of physical type of adsorption mechanism and can be attributed to the increase in the solubility of the protective films, and any reaction products precipitated on the Al surface that may inhibit the corrosion process [325, 364, 365]. For 1-BOPAMS at 303 K, a corrosion rate of  $0.00083 \text{ g.cm}^2.\text{h}^{-1}$  and a 93.52% inhibition efficiency was attained while at 313, 323 and 333 K, the corrosion rate was 0.00225, 0.00383 and  $0.00673 \text{ g.cm}^2.\text{h}^{-1}$  and inhibition efficiency was 84.93%, 75.94% and 63.86% respectively, at the highest inhibitor concentration ( $5 \times 10^{-4} \text{ M}$ ). This shows that increasing temperature increases the corrosion rate and as a consequence reduces the inhibition efficiency. However, there were instances where the corrosion rate was approximately constant. This observation is more evident at 333 K for 4-BOBAMS and 1-BOPAMS, even though the same trend is seen for 4-BOBAMS at 303 K. This observation can be explained to be a result of the increase of the adsorption of the inhibitors molecules on the Al surface, which shows the excellent inhibitive capabilities of these inhibitors. The same trend of the increase in the corrosion rate and reduction of the inhibition efficiency due to the effect of temperature is observed in all three investigated inhibitors. Several studies have shown that the dissolution of metals can be reduced by increasing the concentration of the inhibitor [366, 367]. In this present study, similar behaviour or outcome was observed wherein the dissolution rate of Al decreased as the concentration of the inhibitor was increased. The corrosion rate in the absence of the inhibitors was significantly high at all temperatures studied. But the moment when the inhibitor/s was introduced in the solution, the rate of corrosion was decreased. For example, in the absence of the inhibitors at 303, 313, 323 and 333 K, the corrosion rate of Al obtained were 0.0128, 0.0150, 0.0190 and  $0.0186 \text{ g.cm}^2.\text{h}^{-1}$  respectively. From the results, it is evident that introducing an inhibitor into the solution the rate of corrosion is lowered and this is observed at all temperatures for all the inhibitors studied. Such type of results have been observed and reported by several authors [368, 369].

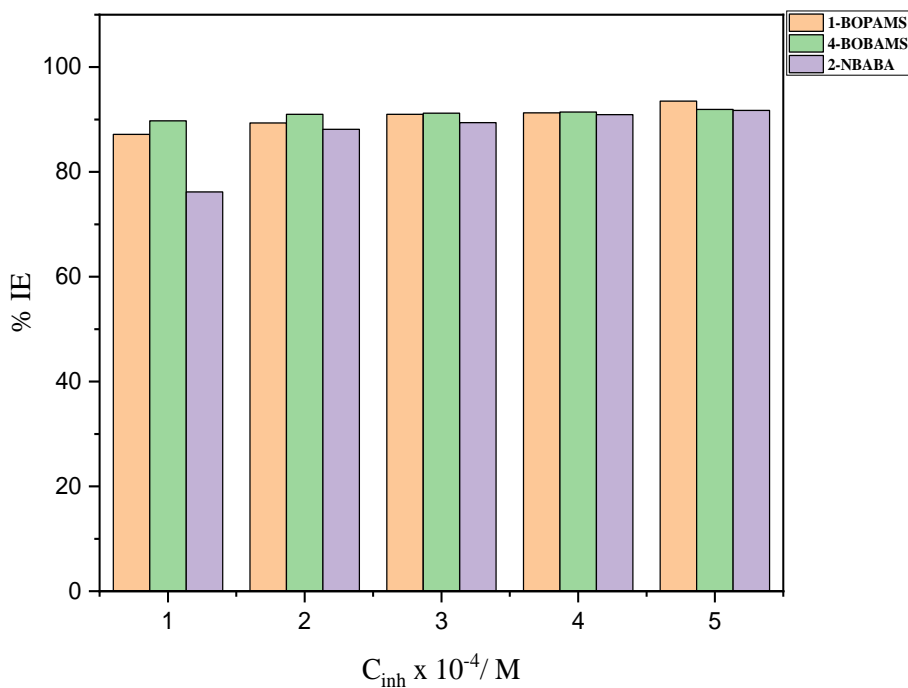


**Figure 4.62:** The variations of the %IE with various concentrations of 2-NBABA, 1-BOPAMS and 4-BOBAMS corrosion inhibitors at 303 K.

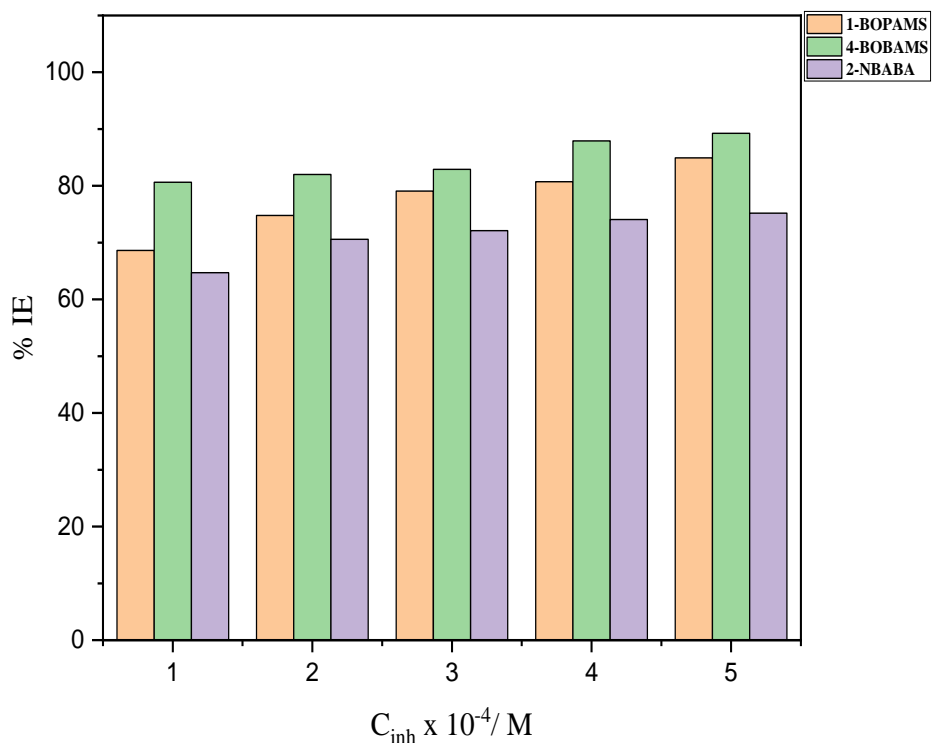


**Figure 4.63:** The variations of the %IE with various concentrations of 2-NBABA, 1-BOPAMS and 4-BOBAMS corrosion inhibitors at 313 K.

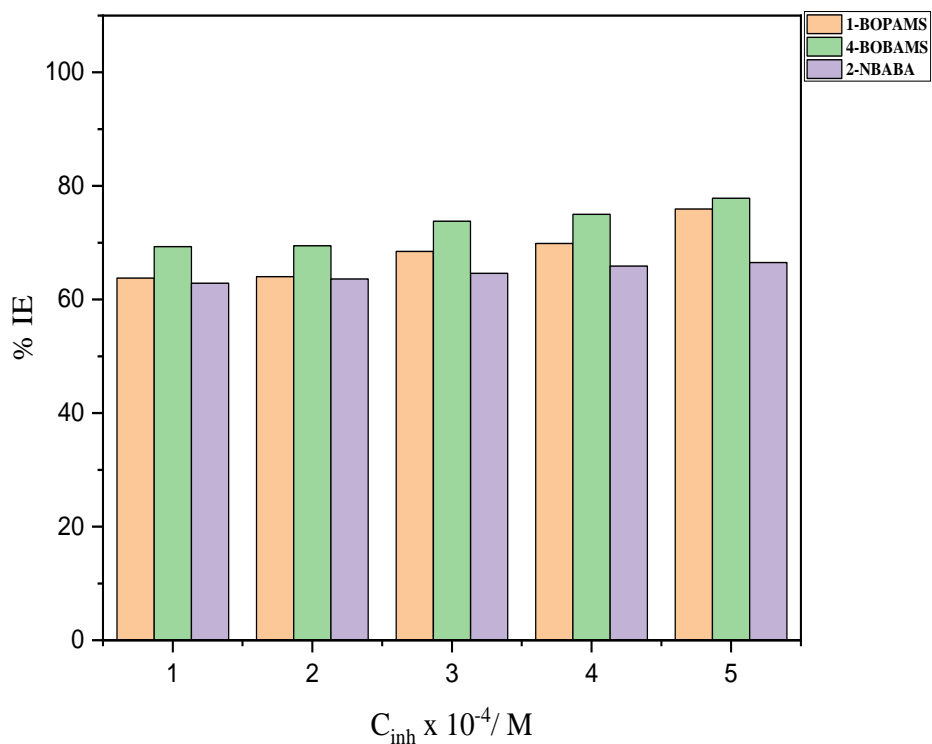


**Figure 4.64:** The variations of the %IE with various concentrations of 2-NBABA, 1-BOPAMS and 4-BOBAMS corrosion inhibitors at 323 K.

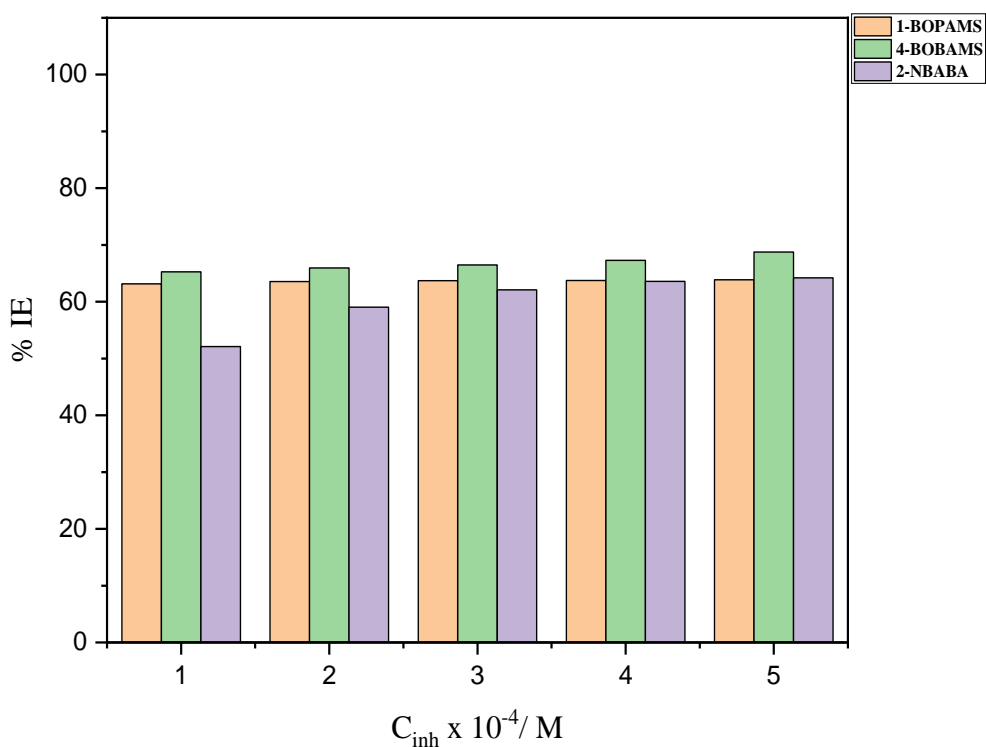


**Figure 4.65:** The variations of the %IE with various concentrations of 2-NBABA, 1-BOPAMS and 4-BOBAMS corrosion inhibitors at 333 K.

**Table 4.7:** Weight loss measurements of Al in 1.0 M HCl containing various concentrations of 1-BOPAMS, 4-BOBAMS and 2-NBABA at different temperatures.

Inhibitor	$C_{inh}$ (M)	303 K		313 K		323 K		333 K	
		$C_R$ ( $g \cdot cm^{-2} \cdot h^{-1}$ )	IE (%)	$C_R$ ( $g \cdot cm^{-2} \cdot h^{-1}$ )	IE (%)	$C_R$ ( $g \cdot cm^{-2} \cdot h^{-1}$ )	IE (%)	$C_R$ ( $g \cdot cm^{-2} \cdot h^{-1}$ )	IE (%)
Blank	-	0.0128	-	0.0150	-	0.0190	-	0.0186	-
1-BOPAMS	$1.0 \times 10^{-4}$	0.00164	87.16	0.00470	68.62	0.00576	63.78	0.00821	63.16
	$2.0 \times 10^{-4}$	0.00136	89.33	0.00377	74.79	0.00572	64.02	0.00679	63.56
	$3.0 \times 10^{-4}$	0.00152	90.98	0.00313	79.09	0.00501	68.47	0.00676	63.70
	$4.0 \times 10^{-4}$	0.00112	91.26	0.00306	80.72	0.00479	69.86	0.00675	63.75
	$5.0 \times 10^{-4}$	0.00083	93.52	0.00225	84.93	0.00383	75.94	0.00673	63.86
4-BOBAMS	$1.0 \times 10^{-4}$	0.00131	89.74	0.00290	80.64	0.00460	69.30	0.00647	65.26
	$2.0 \times 10^{-4}$	0.00115	91.00	0.00270	82.00	0.00457	69.47	0.00634	65.96
	$3.0 \times 10^{-4}$	0.00112	91.21	0.00256	82.89	0.00393	73.78	0.00625	66.47
	$4.0 \times 10^{-4}$	0.00109	91.44	0.00181	87.91	0.00374	75.00	0.00610	67.28
	$5.0 \times 10^{-4}$	0.00103	91.94	0.00161	89.25	0.00352	77.84	0.00582	68.75
2-NBABA	$1.0 \times 10^{-4}$	0.00304	76.20	0.00528	64.71	0.00590	62.86	0.00892	52.11
	$2.0 \times 10^{-4}$	0.00151	88.14	0.00440	70.59	0.00578	63.62	0.00763	59.04
	$3.0 \times 10^{-4}$	0.00135	89.41	0.00418	72.10	0.00563	64.60	0.00706	62.10
	$4.0 \times 10^{-4}$	0.00116	90.92	0.00388	74.08	0.00542	65.89	0.00678	63.59
	$5.0 \times 10^{-4}$	0.00106	91.73	0.00371	75.18	0.00532	66.52	0.00667	64.20

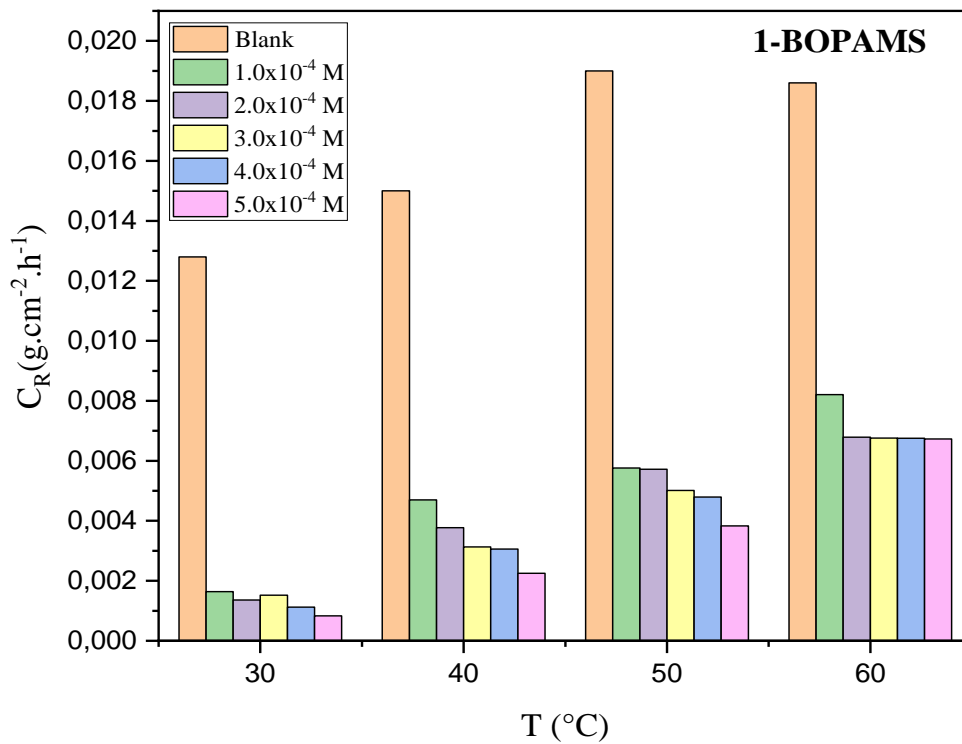


**Figure 4.66:** Variation of  $C_R$  of Al as a function of temperature for 1-BOPAMS.

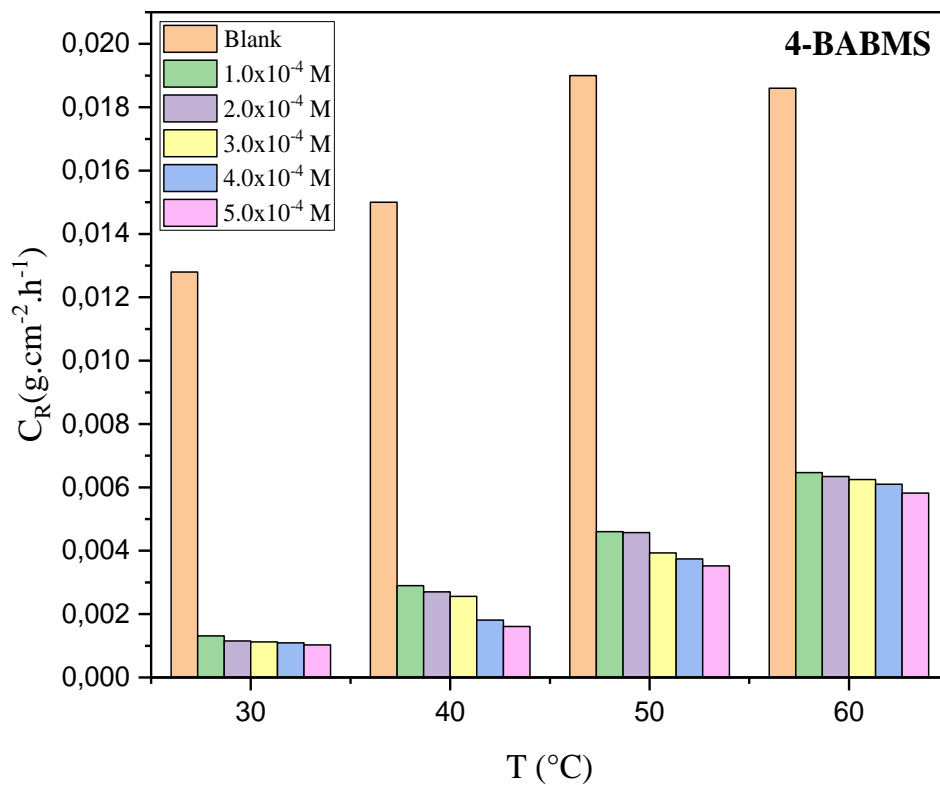


**Figure 4.67:** Variation of CR of Al as a function of temperature for 4-BOBAMS.

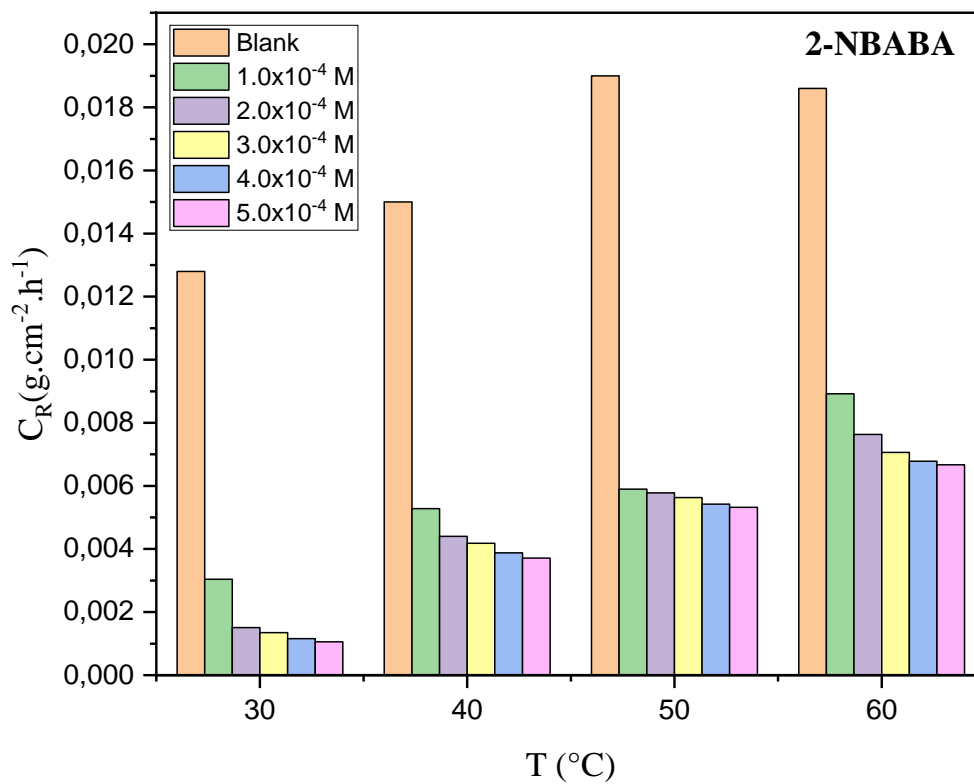


**Figure 4.68:** Variation of  $C_R$  of Al as a function of temperature for 2-NBABA.



### 4.3.2 EFFECT OF TEMPERATURE

The temperature has an important effect on the rate of corrosion. The interaction between the Al electrode and the corrosive acidic medium can be altered significantly due to the increase in temperature and the absence or presence of corrosion inhibitors. The effect of temperature on the adsorption of the inhibitor on the metal surface is highly complex because many changes may occur on the metal surface, such as rapid etching, desorption of inhibitor, the inhibitor may undergo decomposition and/or rearrangement [370]. To understand the mode of the inhibitor adsorption on Al surface and assess the impact of temperature on the corrosion process, weight loss measurements were studied at different temperature ranges (303-333 K) for 8 h immersion in the absence and presence of inhibitors at various concentration ranges ( $1.0 \times 10^{-4}$ - $5.0 \times 10^{-4}$  M) in 1.0 M HCl solution. The Arrhenius and transition-state equations can express the relationship between the corrosion rate of Al and temperature in the acidic medium. The Arrhenius equation (4.1) and the alternate form of Arrhenius equation (4.2) were used to produce the Arrhenius and transition states plots. From the plots of the  $\log C_R$  versus  $1/T$  (figures 4.72-4.74), the values of  $E_a$  and  $K$  at various concentrations of carboxylic acids and amino esters were calculated from the slopes and intercepts, respectively, and can be used to explain the inhibitive mechanism further. The results obtained from these plots are shown in Table 4.8. The adsorption process of inhibitor molecules on the metal surface can either be an exothermic process or an endothermic process. The value of  $E_a$  attained in the absence of an inhibitor was  $9.9215 \text{ kJ}\cdot\text{mol}^{-1}$ . However, it is evident that the  $E_a$  value when the inhibitor concentration of  $1.0 \times 10^{-5}$  M for 1-BOPAMS was added, increased instantly to  $41.8773 \text{ kJ}\cdot\text{mol}^{-1}$ . This signifies that the presence of inhibitor induces an energy barrier for the corrosion reaction and the extent of the increase of the barrier is proportional to the concentration of the inhibitor. This shows that the energy barrier for the dissolution of Al increases with the increase in the inhibitors concentrations. Thus, the reaction between the chlorine ions and the surface of the metal was lowered. At  $2.0 \times 10^{-5}$  M,  $3.0 \times 10^{-5}$  M,  $4.0 \times 10^{-5}$  M, and  $5.0 \times 10^{-5}$  M for 1-BOPAMS, the activation energy values increased to  $43.5356 \text{ kJ}\cdot\text{mol}^{-1}$ ,  $48.0641 \text{ kJ}\cdot\text{mol}^{-1}$ ,  $48.6194 \text{ kJ}\cdot\text{mol}^{-1}$  and  $56.7115 \text{ kJ}\cdot\text{mol}^{-1}$ , respectively. The increase in the values of  $E_a$  after the addition of the inhibitor suggests that the corrosion reaction of Al has been lowered. It was observed that increasing the temperature decreases the adsorption of the inhibitors on the metal surface and a corresponding rise in the corrosion rate occurred. This is more evident at 333 K, where the  $C_R$  increased drastically, and the %IE was low compared to the other temperatures. The other two inhibitors, 4-BOBAMS and 2-NBABA, also reveal a similar trend of the increase

in activation energy which rises immediately as the smallest concentration of the inhibitor is introduced into the system. The variations of the activation energy with respect to various inhibitor concentrations are represented by figure 4.75. Amongst all the investigated corrosion inhibitors, the amino esters have the highest activation energy values, which increased as the inhibitor concentration was raised. For instance, an  $E_a$  value of  $43.6773 \text{ kJ.mol}^{-1}$  for 4-BOBAMS at  $1.0 \times 10^{-4} \text{ M}$  was obtained. When the amino esters, 4-BOBAMS concentration was increased the activation energy increased as a result and increased to a maximum of  $49.7281 \text{ kJ.mol}^{-1}$  at  $5.0 \times 10^{-4} \text{ M}$ . For all the three inhibitors the  $E_a$  values are high compared to the blank, which is indicative of good inhibitive properties of the inhibitors for Al surface. It has been reported that higher values of  $E_a$  in the inhibited system compared to the blank are indicative of a physical type of adsorption mechanism [312], whereas lower values of  $E_a$  are in accordance with the sharing or transfer of an electron from the adsorbate molecules to the substrate substances resulting into a coordinate type of bond (chemisorption) [371]. The results obtained in this study show that the activation energy values for Al corrosion in the presence of the inhibitors are much higher than in the absence of the inhibitors. This trend is observed for all the three inhibitors and strongly supports that the type of adsorption taking place on the Al surface in the present study is physisorption.

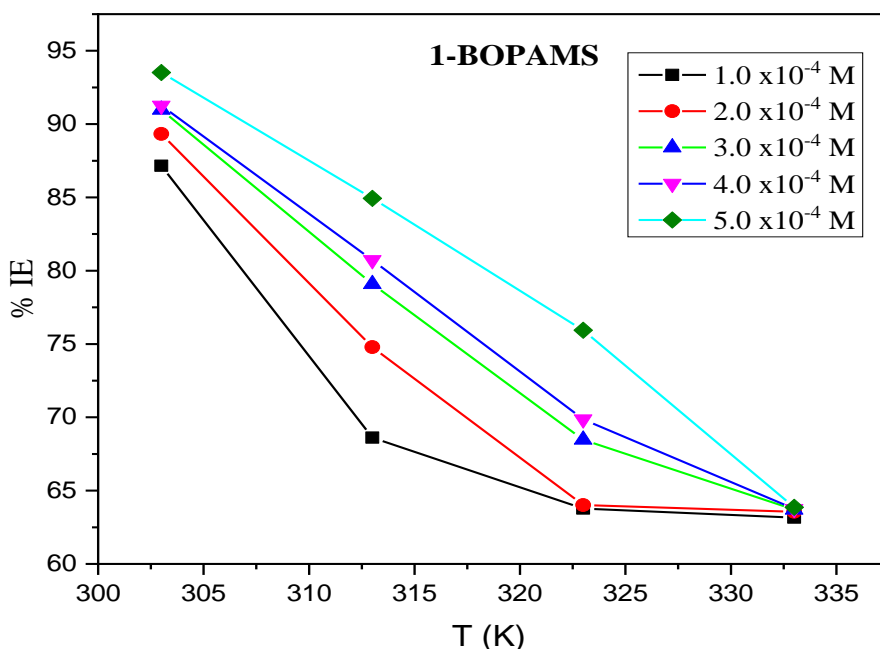


**Figure 4.69:** The variation of %IE with temperature for Al corrosion in 1.0 M HCl in the presence of a various concentrations of 1-BOPAMS.

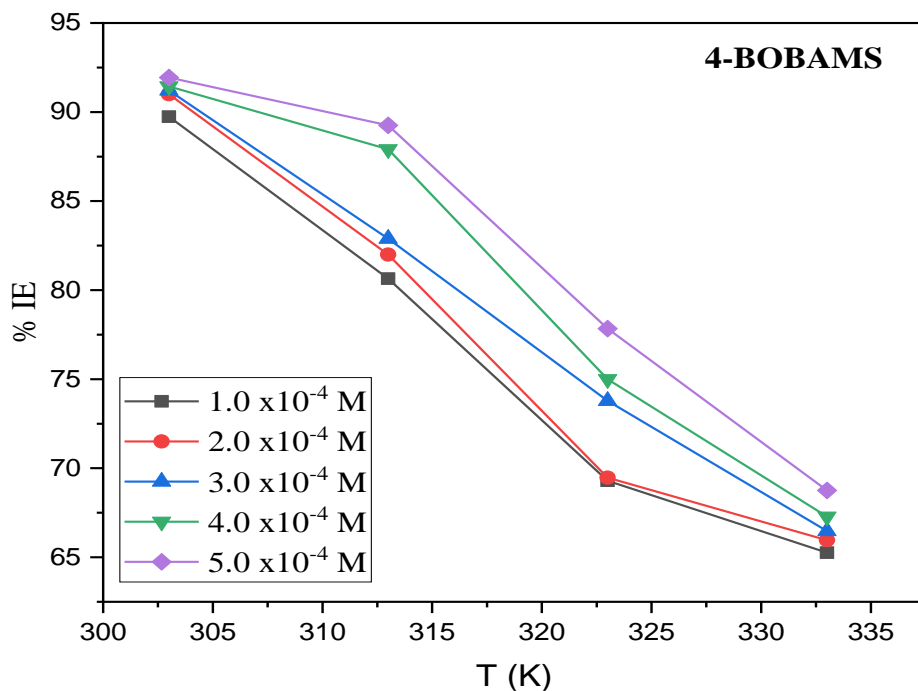


**Figure 4.70:** The variation of %IE with temperature for Al corrosion in 1.0 M HCl in the presence of a various concentrations of 4-BOBAMS.

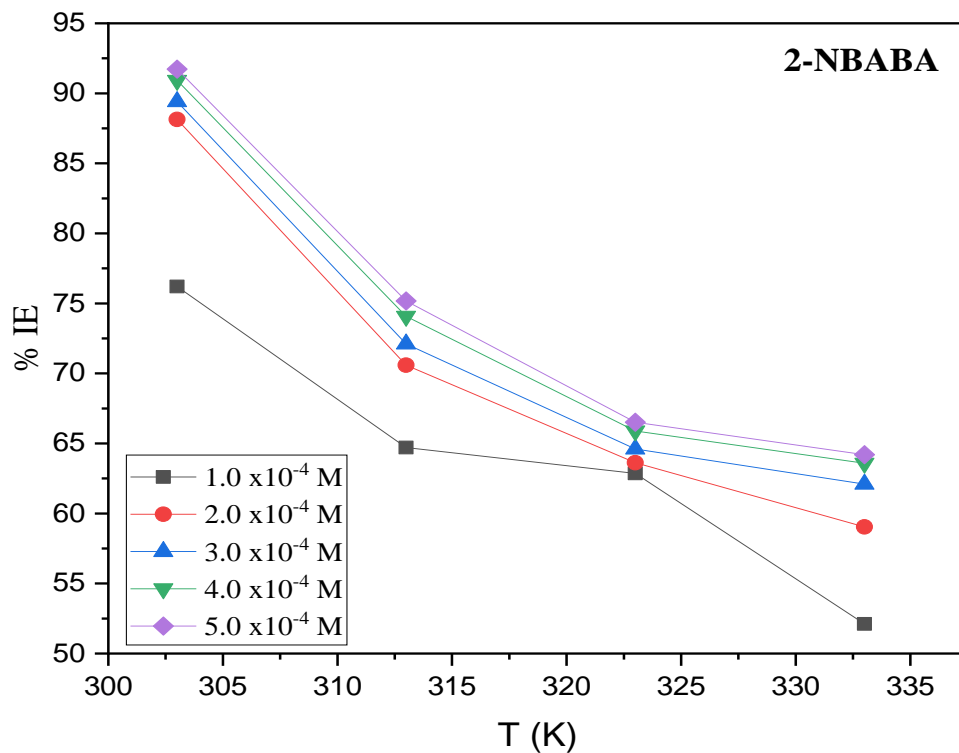


**Figure 4.71:** The variation of %IE with temperature for Al corrosion in 1.0 M HCl in the presence of a various concentrations of 2-NBABA.

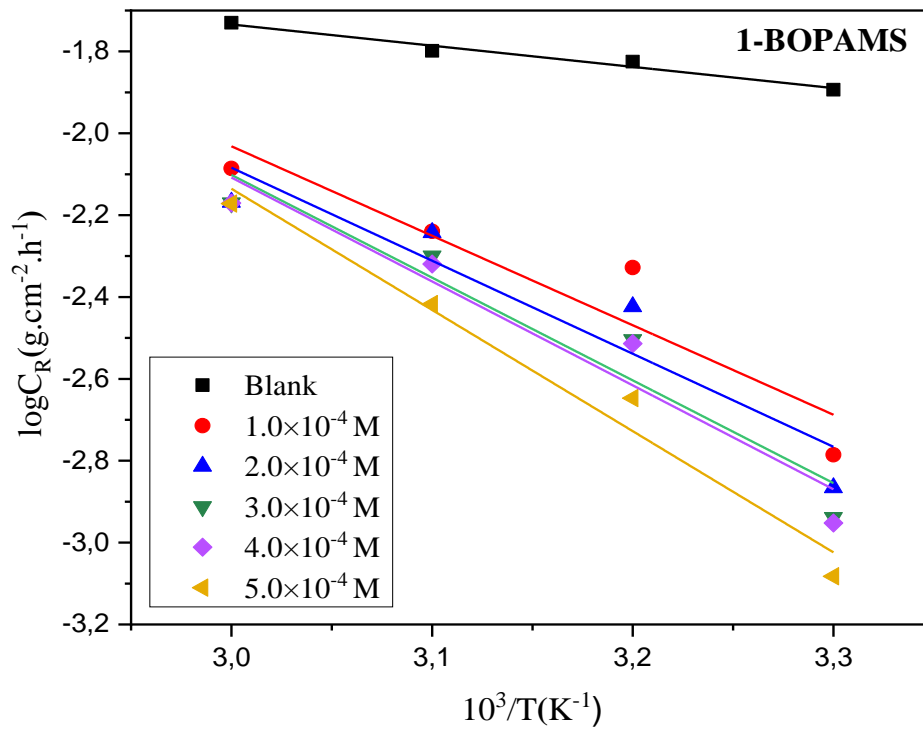


**Figure 4.72:** Arrhenius plots for the corrosion of Al in 1.0 M HCl in the absence and presence of different concentrations of 1-BOPAMS.

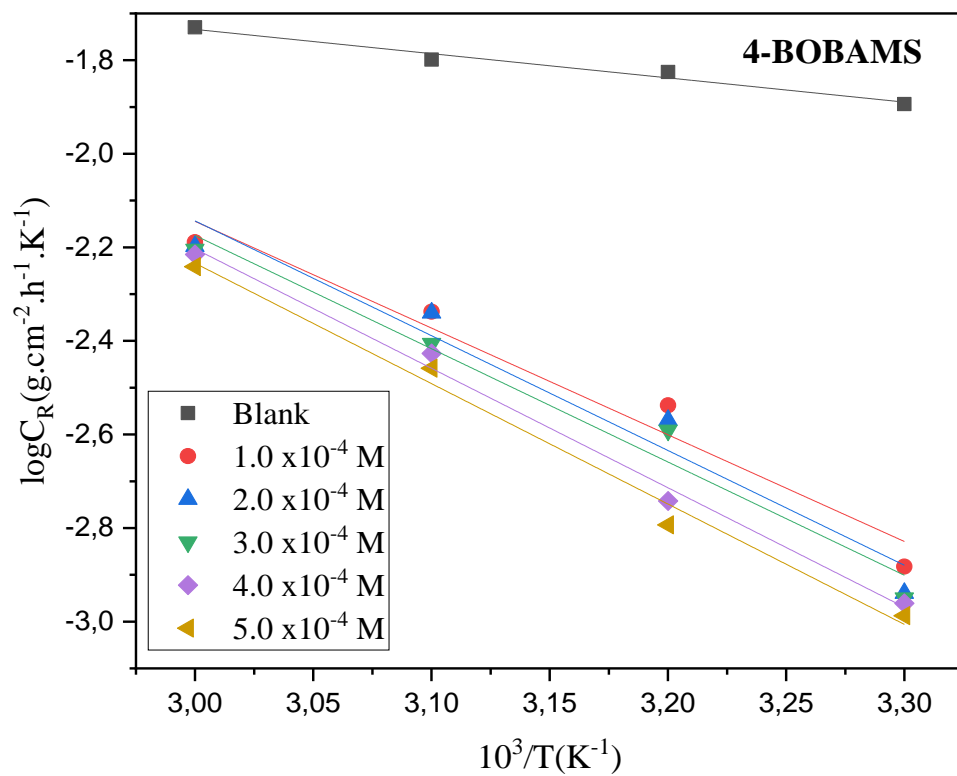


**Figure 4.73:** Arrhenius plots for the corrosion of Al in 1.0 M HCl in the absence and presence of different concentrations of 4-BOBAMS.

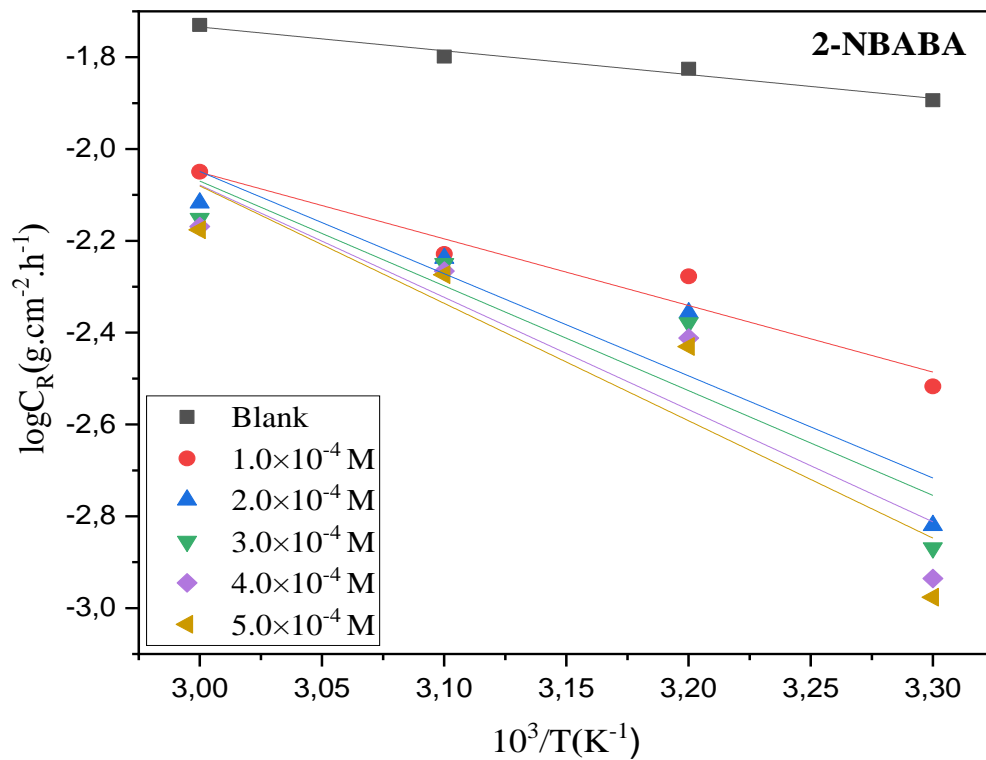


**Figure 4.74:** Arrhenius plots for the corrosion of Al in 1.0 M HCl in the absence and presence of different concentrations of 2-NBABA.

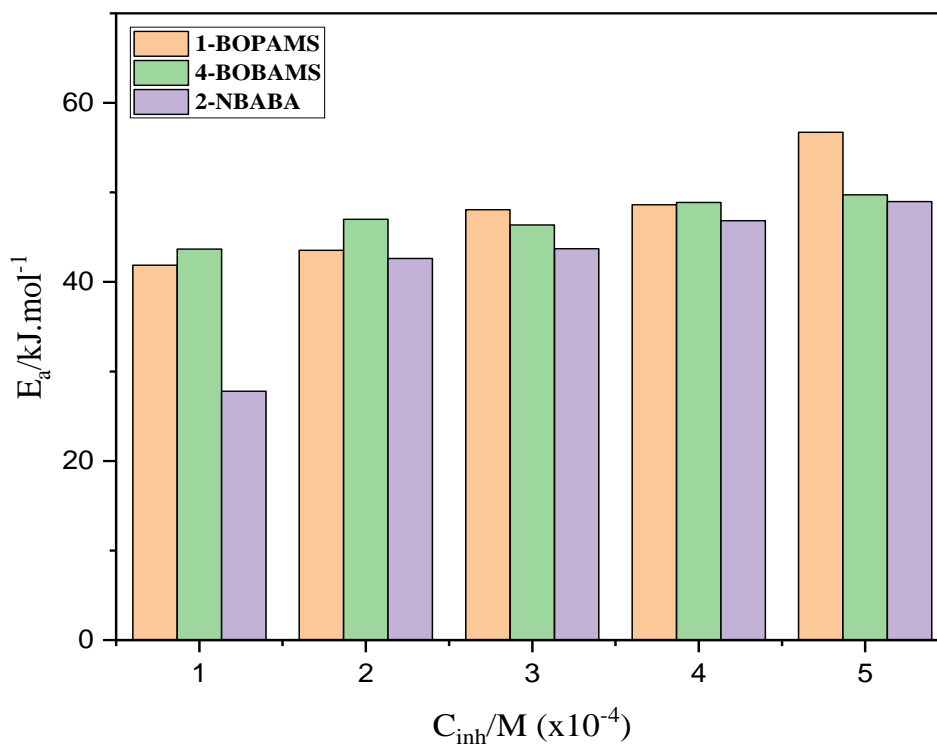


**Figure 4.75:** The variation of the  $E_a$  with various concentration of 2-NBABA, 1-BOPAMS and 4-BOBAMS corrosion inhibitors for Al.

**Table 4.8:** Kinetic and activation parameters (derived from the Arrhenius and transition-states plots) for Al in 1.0 M HCl in the absence and presence of various concentrations of 2-NBABA 4-BOBAMS and 1-BOPAMS.

Inhibitor	$C_{inh}$ (M)	$E_a$ (kJ.mol <sup>-1</sup> )	$\Delta H_a^*$ (kJ.mol <sup>-1</sup> )	$\Delta S_a^*$ (J.mol <sup>-1</sup> .K <sup>-1</sup> )
Blank	-	9.9215	7.3147	-200.2395
1-BOPAMS	1.0 x10 <sup>-4</sup>	41.8773	39.2549	-195.5330
	2.0 x10 <sup>-4</sup>	43.5356	40.8088	-195.3432
	3.0 x10 <sup>-4</sup>	48.0641	45.4519	-194.6320
	4.0 x10 <sup>-4</sup>	48.6194	45.9999	-194.5527
	5.0 x10 <sup>-4</sup>	56.7115	54.6709	-193.2145
4-BOBAMS	1.0 x10 <sup>-4</sup>	43.6773	41.6667	-195.2710
	2.0 x10 <sup>-4</sup>	46.9899	44.7879	-194.7799
	3.0 x10 <sup>-4</sup>	46.3580	46.6452	-194.5330
	4.0 x10 <sup>-4</sup>	48.8856	50.3792	-193.9810
	5.0 x10 <sup>-4</sup>	49.7281	51.2025	-193.8779
2-NBABA	1.0 x10 <sup>-4</sup>	27.7976	25.2509	-197.7456
	2.0 x10 <sup>-4</sup>	42.6164	40.0008	-195.4335
	3.0 x10 <sup>-4</sup>	43.7079	41.0922	-195.2833
	4.0 x10 <sup>-4</sup>	46.8386	44.8913	-194.7002
	5.0 x10 <sup>-4</sup>	48.9737	46.3638	-194.4680

Thermodynamic parameters, such as enthalpy ( $\Delta H_a^*$ ) and entropy ( $\Delta S_a^*$ ) of activation can be used to provide further details on the effect of temperature on the inhibition efficiency of the inhibitors. These parameters were determined using the transition state equation (4.2). The plots of  $\log(C_R/T)$  versus  $1/T$  gave straight lines (figures 161-162) with a slope of  $(-\Delta H_a^*/2.303R)$  and an intercept of  $[\log(R/Nh) + \Delta S_a^*/2.303R]$ , from which the activation thermodynamic parameters ( $\Delta H_a^*$  and  $\Delta S_a^*$ ) was calculated, and the results are listed in Table

4.8. Some insight into the possible type of adsorption mechanism of the inhibitor can be gained by comparing the corrosion activation parameters in the absence and presence of the synthesized three compounds. Negative values of  $\Delta S_a^*$  indicate that the destruction on the metal surface has decreased and the positive values indicate that the disordering of the system has increased. The results obtained in the present study show that large negative values of  $\Delta S_a^*$  were obtained for all three inhibitors investigated and are indicative of association of the activated complex in the rate-determining step rather than dissociation. This means that the destruction on the Al surface has been lessened during the transition from reactants to the activated complex due to the adsorption of inhibitor molecules on the Al surface [183, 372, 373]. The  $\Delta S_a^*$  values in the presence of inhibitors in solution are higher than those for the uninhibited solution indicating an increase in the randomness moving from reactants to the activated complex. The increase in values of  $\Delta S_a^*$  is due to the adsorption of the inhibitor molecules on the surface of Al and could be regarded as quasi-substitution that occurs between the water molecules on the electrode surface and inhibitor molecules in the aqueous phase. When this happens, it is said that the adsorptions of inhibitor molecules follows the desorption of water molecules from the electrode surface and results in the decrease of the electrical capacity of the metal [316]. Whether the reaction is exothermic or endothermic is contingent on the sign of the enthalpy values. The positive sign of  $\Delta H_a^*$  values of the results reflects that the adsorption of all three inhibitor molecules is of the endothermic nature of the Al dissolution process.

The  $\Delta H_a^*$  value for the uninhibited solution was  $7.3147 \text{ kJ.mol}^{-1}$  and increased to 39.2549, 41.6667 and  $25.2509 \text{ kJ.mol}^{-1}$  after the addition of the lowest concentration of  $1.0 \times 10^{-4} \text{ M}$  for 1-BOPAMS, 4-BOBAMS and 2-NBABA, respectively. Since the  $\Delta H_a^*$  values are above  $7.3147 \text{ kJ.mol}^{-1}$  for all three inhibitors, this indicates that significant amount of energy was required to form corrosion product, signifying that the presence of the inhibitors resulted in the difficulty for the dissolution of the Al surface which increased as the inhibitor concentration was increased. The enthalpy values of activation that are close to  $41.86 \text{ kJ.mol}^{-1}$  have been reported to be associated with physisorption type of adsorption, and those ranging around  $100 \text{ kJ.mol}^{-1}$  or higher are linked with chemisorption [313]. The results in Table 4.8 shows that for the inhibitors in this study the values of  $\Delta H_a^*$  are around  $41.86 \text{ kJ.mol}^{-1}$ , especially for the carboxylic acid (2-NBABA) at lower concentrations but rises as the concentration is increased. For the amino esters,  $\Delta H_a^*$  values are above  $41.86 \text{ kJ.mol}^{-1}$  but less than  $100 \text{ kJ.mol}^{-1}$ . Even though at  $1.0 \times 10^{-4} \text{ M}$  for 1-BOPAMS a  $\Delta H_a^*$  value of  $41.8773 \text{ kJ.mol}^{-1}$  was obtained. This

kind of behaviour for the amino esters may be attributed to mixed-type adsorption taking place on Al surface.

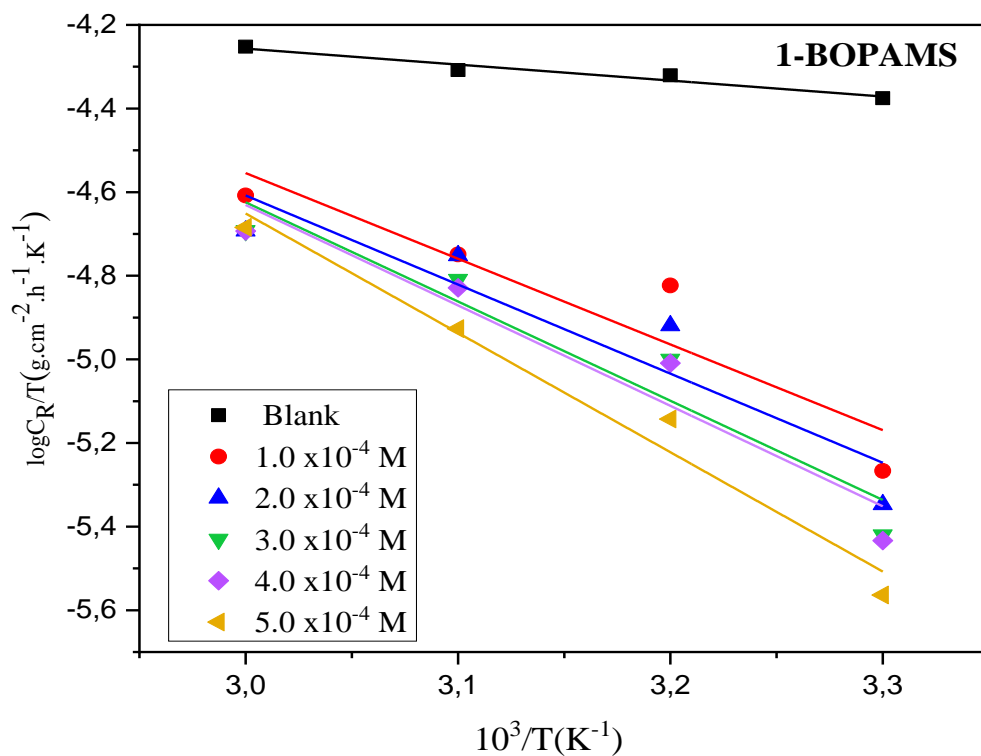


**Figure 4.76:** Transition state plots for the corrosion of Al in 1.0 M HCl in the absence and presence of different concentrations of 1-BOPAMS.



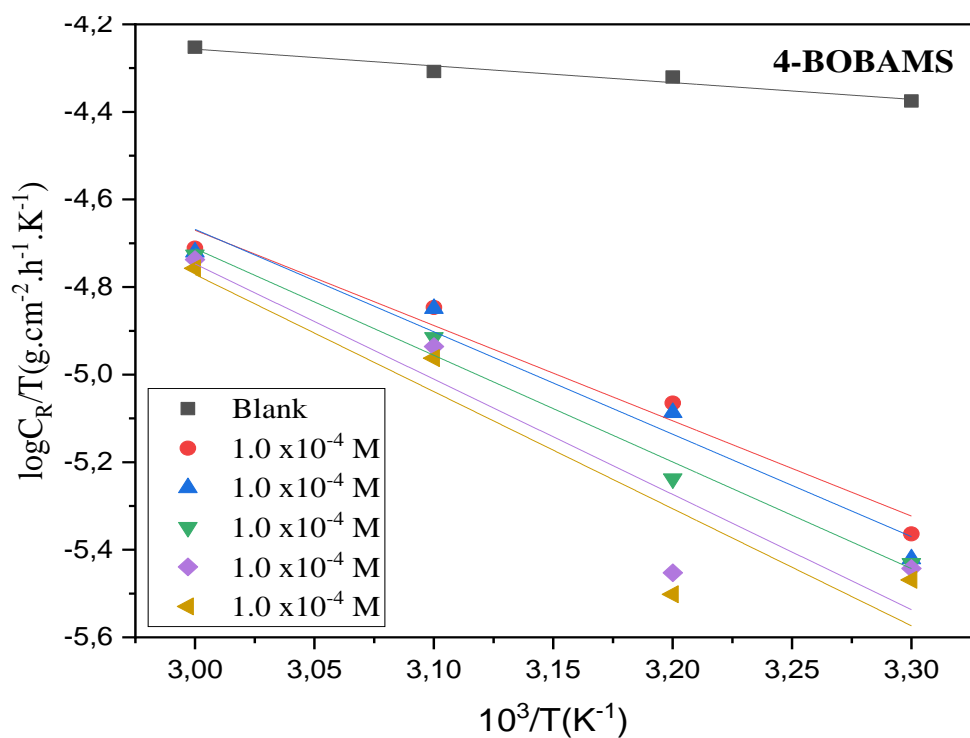


**Figure 4.77:** Transition state plots for the corrosion of Al in 1.0 M HCl in the absence and presence of different concentrations of 4-BOBAMS.

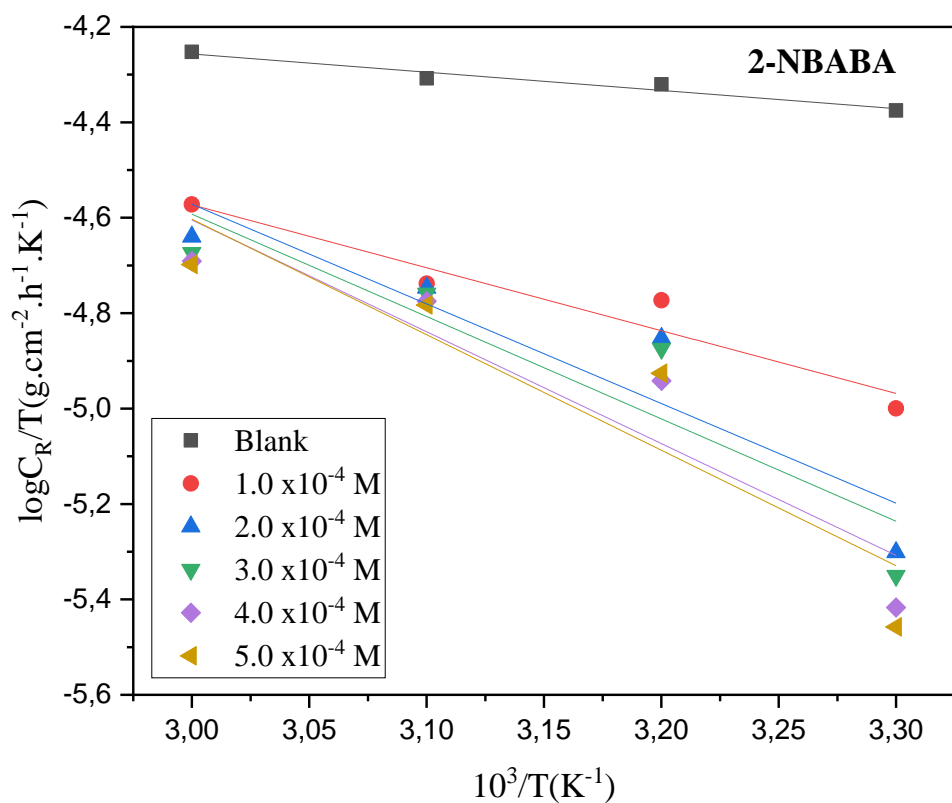


**Figure 4.78:** Transition state plots for the corrosion of Al in 1.0 M HCl in the absence and presence of different concentrations of 2-NBABA.

### 4.3.3 ADSORPTION ISOTHERMS AND THERMODYNAMIC PARAMETERS

The adsorption of the inhibitors on the metal surface is a critical step in the corrosion inhibition mechanism, which can be explained by adsorption isotherms [374]. The adsorption process of inhibitor is described as a displacement reaction in which the adsorbed water molecules on the metal surface are being replaced by inhibitor molecules [375]. For the inhibitor molecules to adsorb effectively on the metal surface, the interaction force between the metal and the inhibitor must be greater than the interaction force of the metal and water molecules [376]. Therefore, to ascertain the mode of adsorption corresponding to the studied organic compounds, a linear relationship between the degree of surface coverage and concentration of the inhibitors is required. Several well-known adsorption isotherms were adopted, and these included the Langmuir, Temkin, Freundlich, and El-Awady adsorption isotherms. The correlation coefficient ( $R^2$ ) obtained from the Langmuir, Temkin, Freundlich and El-Awady adsorption isotherm models are listed in Table 4.10. The best linear relationship was obtained by the Langmuir adsorption isotherm, which was attained by plotting the concentration of the inhibitor/surface coverage against the concentration of the inhibitors. According to this isotherm, the surface coverage ( $\theta$ ) of the inhibitor on the Al surface is related to the inhibitor concentration ( $C_{inh}$ ) in the bulk of the solution and the  $K_{ads}$ , according to equation (4.9).

The relation between  $C_{inh}/\theta$  versus  $C_{inh}$  gave straight lines (figures 4.79-4.81) for the three inhibitors with a slope approximately equal to unity and non-zero intercepts at all temperatures investigated. For example, the linear correlation coefficient ( $R^2$ ) for 1-BOPAMS are 0.9966, 0.9974, 0.9957 and 1 at 303K, 313K, 323K and 333K, respectively. This confirms that the adsorption layer formed by the three inhibitors on the Al surface in 1.0 M HCl obeys the Langmuir adsorption isotherm. The closeness of the slope to unity also indicates that the type of the adsorption layer formed on the Al surface is monolayer [173, 377]. According to Langmuir adsorption isotherm, the adsorbed molecules remain at the site of adsorption until they are desorbed (i.e., adsorption is localized) and no interaction occurs between them, and the energy of adsorption is independent of the degree of surface coverage [378]. As such, the monolayer type of adsorption means that molecules of adsorbate must have adsorbed to Al surface without been deposited or interacting with the already adsorbed inhibitor molecules but only interacted with the free adsorbent Al surface [379]. It should be noted that some of the slopes obtained from the Langmuir plots were slightly above unity. This is more evident with the slopes for 1-BOPAMS which were 1.5621 at 333 K and 2-NBABA, which were 1.4778 and 1.4641 at 323 K and 333 K respectively. The slopes obtained from the Langmuir pots that

are greater than unity could signify that they were interactions between the absorbed species on the Al surface, one or more molecules of each inhibitor occupies more than one adsorption site or the enthalpy values changes with increasing surface coverage [380]. When this deviation of the slope from unity is encountered, the Langmuir adsorption model cannot be applied with accuracy, and a hybrid isotherm called the modified Langmuir (El-Awady) [381] isotherm may be used. However, even with the plot of El-Awady, Langmuir isotherm was chosen as the best-fit isotherm for the investigated inhibitors. This is because the correlation coefficient ( $R^2$ ) values at all temperatures were found to be more near unity for the Langmuir adsorption plot than for El-Awady. As a result, the Langmuir adsorption plots were used to obtain the values of  $K_{ads}$  (Table 4.9), which were obtained from the reciprocal of the intercepts of the plots.  $K_{ads}$  is an important parameter as it helps in determining the inhibitor binding potential efficiency on the metal surface. Higher values of  $K_{ads}$  for the carboxylic acids and amino esters implies that the studied inhibitors adsorb strongly on the surface of Al [382-385]. Table 4.9 shows that there is no regular pattern in the values of  $K_{ads}$  obtained at all temperatures. The adsorption process of the inhibitors is marked with a higher magnitude of  $K_{ads}$  for all three studied inhibitors. This implies that the adsorption of the compounds is strong and can be interpreted as an indication of mixed-type adsorption. Of all the studied compounds,  $K_{ads}$  values for 1-BOPAMS are of particular interest as they seem to increase as the temperature rises from 303-333K. This implies that as the temperature is increased, the inhibitors bind firmly onto the Al surface and becomes almost irreversible. This type of behaviour by 1-BOPAMS suggests that its adsorption on Al surface shifts from dominating physisorption at lower temperatures to a chemisorption type of adsorption at higher temperatures, which is an indication of a mixed-type adsorption inhibitor. The slopes of these lines were near unity, indicating that the inhibitor molecules occupied only one active site on the surface of Al. This further shows that plotting the modified Langmuir adsorption is not necessary for this study. A comparison of the correlation coefficient ( $R^2$ ) obtained from different adsorption isotherm is tabulated (Table 4.9) to highlight that Langmuir adsorption was the best-fit isotherm. Thermodynamic parameters provide information relating to the strength and inhibitive mechanism of corrosion by the inhibitors. The  $\Delta G^{\circ}_{ads}$  values were obtained from  $K_{ads}$  using equation 4.10. The values of  $\Delta G^{\circ}_{ads}$  up to  $-20 \text{ kJ mol}^{-1}$  are generally associated with an interaction between the charged molecules and charged metal (physical adsorption) while those that are  $-40 \text{ kJ mol}^{-1}$  above are associated with the sharing or transfer of an electron from the inhibitors to the surface of the metal to form a coordinate type of bond (chemical adsorption) [173, 377]. In the present study, the  $\Delta G^{\circ}_{ads}$  values for 4-BOBAMS, 2-NBABA and 1BOPAMS were all above  $-20 \text{ kJ.mol}^{-1}$  but slightly

below  $-40 \text{ kJ mol}^{-1}$ , indicating that the adsorption mechanism of the surface of Al by the synthesized amino ester and carboxylic acid in 1.0 M HCl are all mixed-type adsorption inhibitors, with a dominating chemisorption mechanism as the values are nearing the  $-40 \text{ kJ mol}^{-1}$  value. This means that both a chemical and physical adsorption bond was formed between the adsorbate and the substrate surface. However, the values of  $\Delta G^{\circ}_{\text{ads}}$  for 1-BOPAMS shows similar behaviour to those for  $K_{\text{ads}}$  as they seem to increase with an increase in temperature. This again implies a shift in the adsorption mechanism from a physical to a chemical type of adsorption, with a dominating chemisorption process. The inhibitor 1-BOPAMS can be classified as a chemical inhibitor as the concentration of the inhibitors is increased,  $\Delta G^{\circ}_{\text{ads}}$  also increase up to  $-40 \text{ kJ mol}^{-1}$ . The negative values of  $\Delta G^{\circ}_{\text{ads}}$  were obtained for all the three inhibitors indicating that the adsorbed layer formed by the inhibitors was stable and the adsorption process on Al was a spontaneous process.

Adsorption thermodynamic parameters such as the  $\Delta H^{\circ}_{\text{ads}}$  were calculated from both the Van't Hoff equation (2.15) and Gibbs-Helmholtz equation (2.17). The  $\Delta S^{\circ}_{\text{ads}}$  was calculated from equation (2.18). Table 4.9 shows the calculated values of  $\Delta H^{\circ}_{\text{ads}}$  and  $\Delta S^{\circ}_{\text{ads}}$  over the temperature range 303-313 K. Literature studies report that if  $\Delta H^{\circ}_{\text{ads}} > 0$  (endothermic), then the inhibitors adsorbs chemically on the metal surface and if  $\Delta H^{\circ}_{\text{ads}} < 0$  (exothermic), then the adsorption process can either be taking place through chemisorption or physisorption process. In cases where the  $\Delta H^{\circ}_{\text{ads}} < 0$ , physisorption process can be differentiated from chemisorption based on the magnitude of  $\Delta H^{\circ}_{\text{ads}}$  [359]. To classify the adsorption as physisorption, the  $\Delta H^{\circ}_{\text{ads}}$  is usually is less than  $40 \text{ kJ mol}^{-1}$  and greater than  $100 \text{ kJ mol}^{-1}$  for chemisorption [314]. For 1-BOPAMS, the  $\Delta H^{\circ}_{\text{ads}}$  values are higher than  $40 \text{ kJ mol}^{-1}$  but less than  $100 \text{ kJ mol}^{-1}$  indicating that the adsorption process is both of physisorption and chemisorption nature. For 4-BOBAMS and 2-NBABA, the  $\Delta H^{\circ}_{\text{ads}}$  values are  $-36$  and  $-11 \text{ kJ mol}^{-1}$  respectively, which is indicative of dominating physisorption adsorption process. Moreover, the positive value of  $\Delta S^{\circ}_{\text{ads}}$  in the presence of 1-BOPAMS and 2-NBABA is an indication of an increase in the solvent entropy. This means that there is a disorder occurring on the metal surface due to the water molecules which gets desorbed from the Al surface by one molecule of 1-BOPAMS and 2-NBABA inhibitors. In this case, where the  $\Delta S^{\circ}_{\text{ads}}$  values are positive, it is stated that the decrease in enthalpy is the chief motive for the adsorption of the inhibitor molecules on the metal surface [333]. The negative  $\Delta S^{\circ}_{\text{ads}}$  values for 4-BOBAMS suggest that the adsorption of inhibitor on MS surface is of an exothermic nature. In this instance, the inhibitor molecules are said to firstly move in the solution before getting adsorbed on the Al surface, and when they get

adsorbed, they do so in an orderly fashion onto MS surface, resulting in a decrease in entropy [334, 335]. The adsorption process being exothermic, thermodynamics principle indicates that it must be accompanied by a reduction in entropy [336].

**Table 4.9:** Thermodynamic and adsorption parameters (Langmuir adsorption isotherms) for Al in 1.0 M HCl at various temperatures for 2-NBABA, 1-BOPAMS and 4-BOBAMS.

Inhibitor	T (K)	R <sup>2</sup>	Slope	K <sub>ads</sub> (L.mol <sup>-1</sup> )	ΔG <sup>o</sup> <sub>ads</sub> (kJ.mol <sup>-1</sup> )	ΔH <sup>o</sup> <sub>ads</sub> (kJ. mol <sup>-1</sup> )	ΔS <sup>o</sup> <sub>ads</sub> (J.mol <sup>-1</sup> .K <sup>-1</sup> )
1-BOPAMS	303	0.9966	0.9942	2779.2	-30.0962	68* 68#	324
	313	0.9974	1.1141	2432.1	-30.7423		315
	323	0.9957	1.2634	2055.9	-31.2732		307
	333	1	1.5621	44306.6	-40.7426		327
4-BOBAMS	303	0.9999	1.0825	28264.6	-35.9396	-36* -36#	-0.2
	313	0.9968	1.0835	4174.5	-32.1483		-12
	323	0.9962	1.2487	3365.1	-32.5965		-11
	333	0.9992	1.4394	7095.2	-35.6711		-0.99
2-NBABA	303	0.9995	1.0407	4252.1	-31.1676	-11* -11#	67
	313	0.9998	1.2777	3509.9	-31.6970		66
	323	0.9996	1.4778	6264.9	-34.2656		72
	333	0.9999	1.4641	2218.2	-32.4518		64

\* Parameters calculated from Van't Hoff equation.

# Parameters derived from the Gibbs-Helmholtz equation.

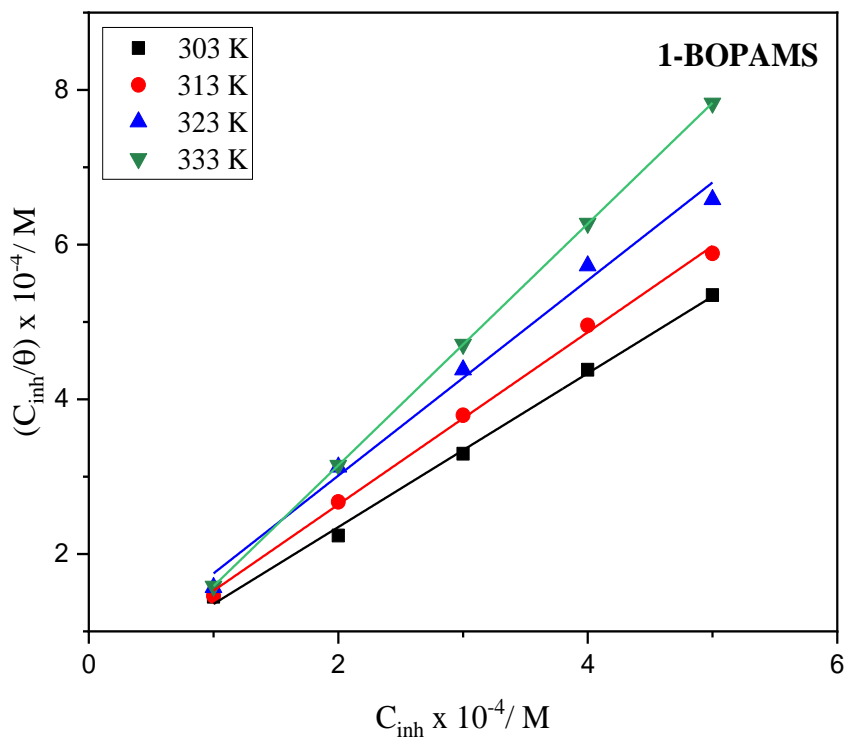


**Figure 4.79:** Langmuir adsorption isotherm plot for the adsorption of different concentrations of 1-BOPAMS on the surface of Al in 1.0 M HCl at different temperatures.

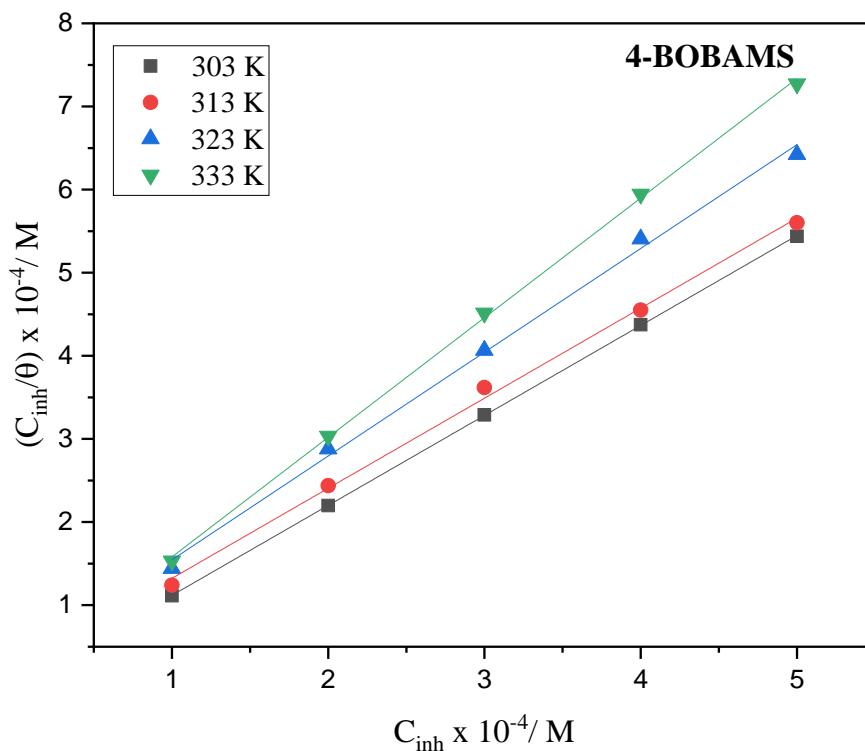


**Figure 4.80:** Langmuir adsorption isotherm plot for the adsorption of different concentrations of 4-BOBAMS on the surface of Al in 1.0 M HCl at different temperatures.

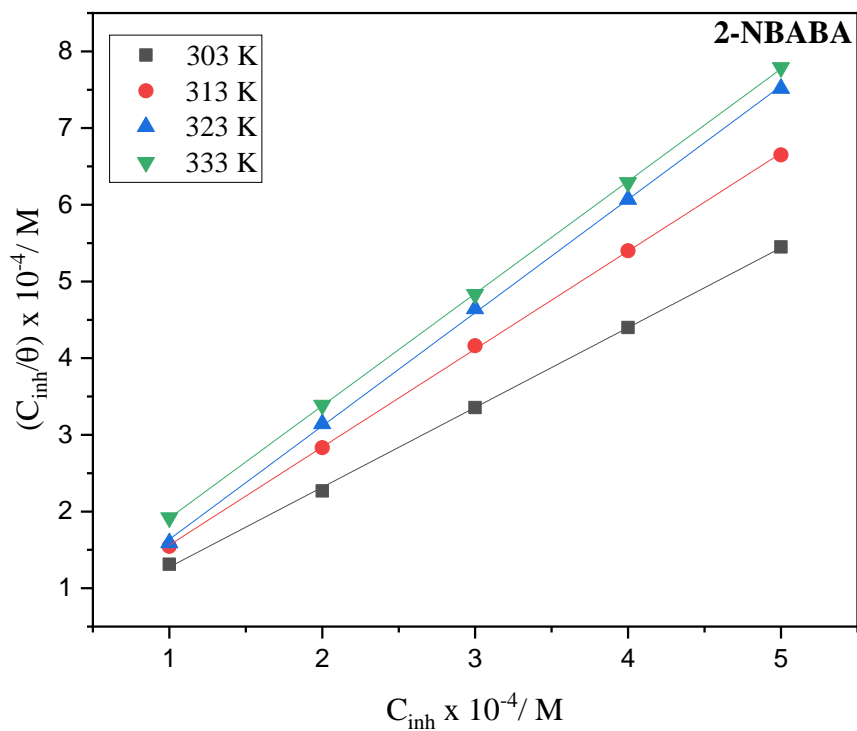


**Figure 4.81:** Langmuir adsorption isotherm plot for the adsorption of different concentrations of 2-NBABA on the surface of Al in 1.0 M HCl at different temperatures.

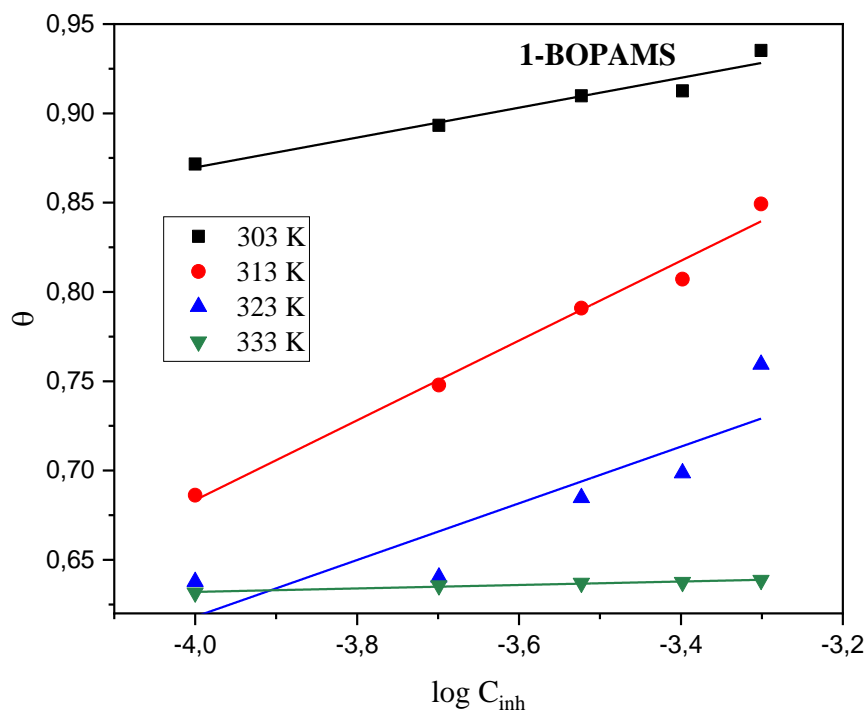


**Figure 4.82:** Temkin adsorption isotherm plot for the adsorption of different concentrations of 1-BOPAMS on the surface of Al in 1.0 M HCl at different temperatures.

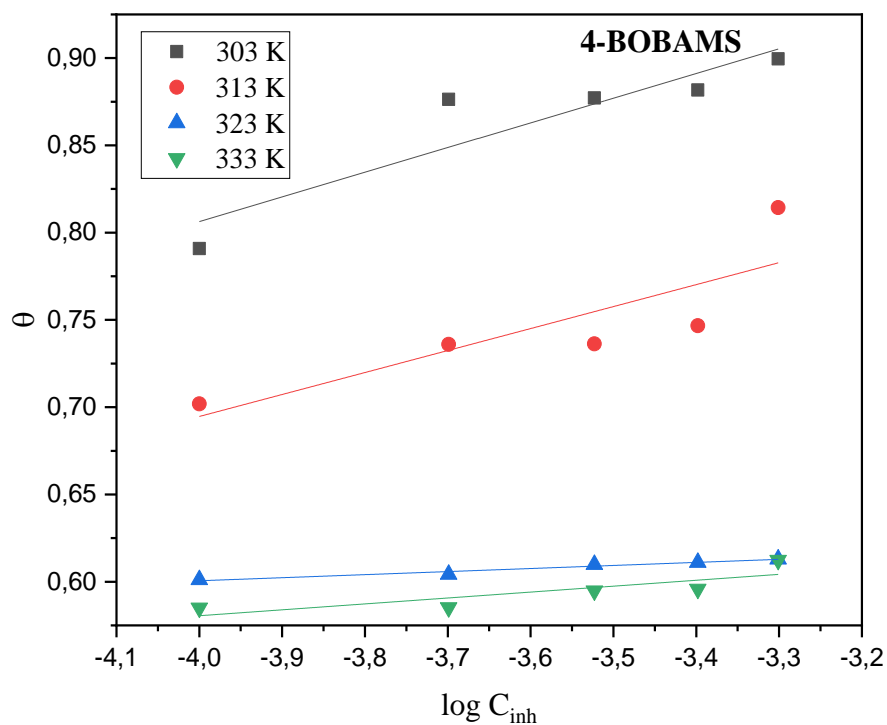


**Figure 4.83:** Temkin adsorption isotherm plot for the adsorption of different concentrations of 4-BOBAMS on the surface of Al in 1.0 M HCl at different temperatures.

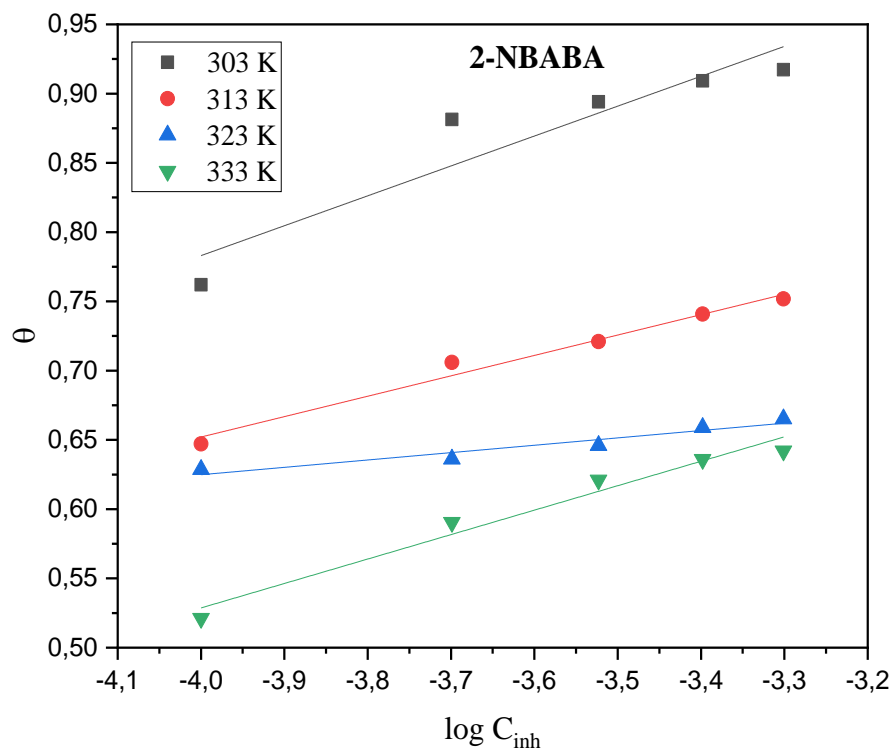


**Figure 4.84:** Temkin adsorption isotherm plot for the adsorption of different concentrations of 2-NBABA on the surface of Al in 1.0 M HCl at different temperatures.



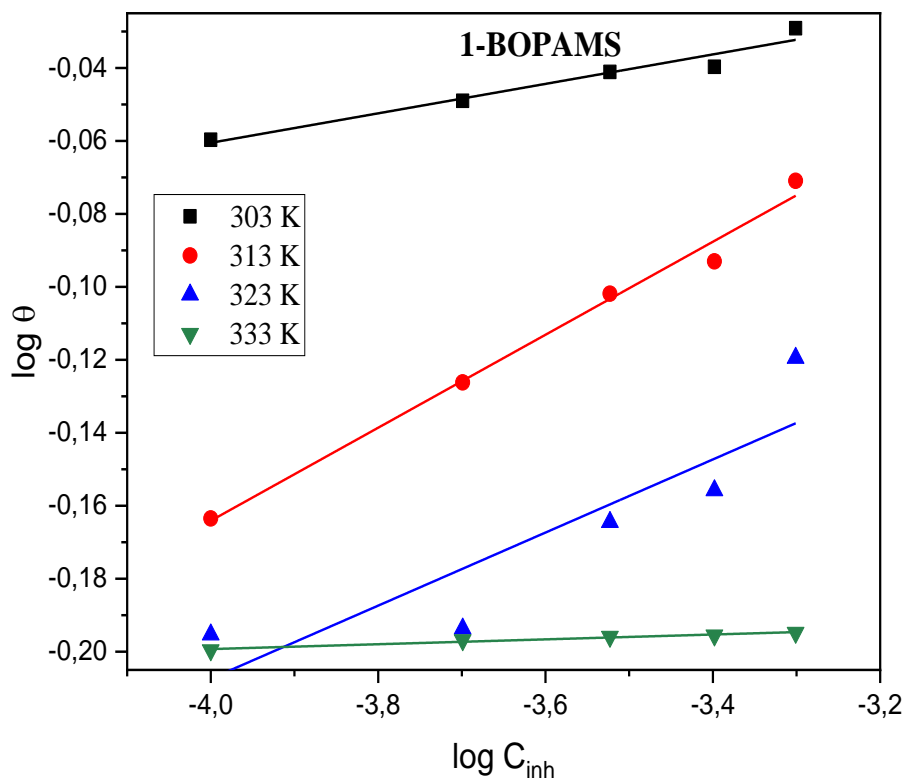


**Figure 4.85:** Freundlich adsorption isotherm plot for the adsorption of different concentrations of 1-BOPAMS on the surface of Al in 1.0 M HCl at different temperatures.

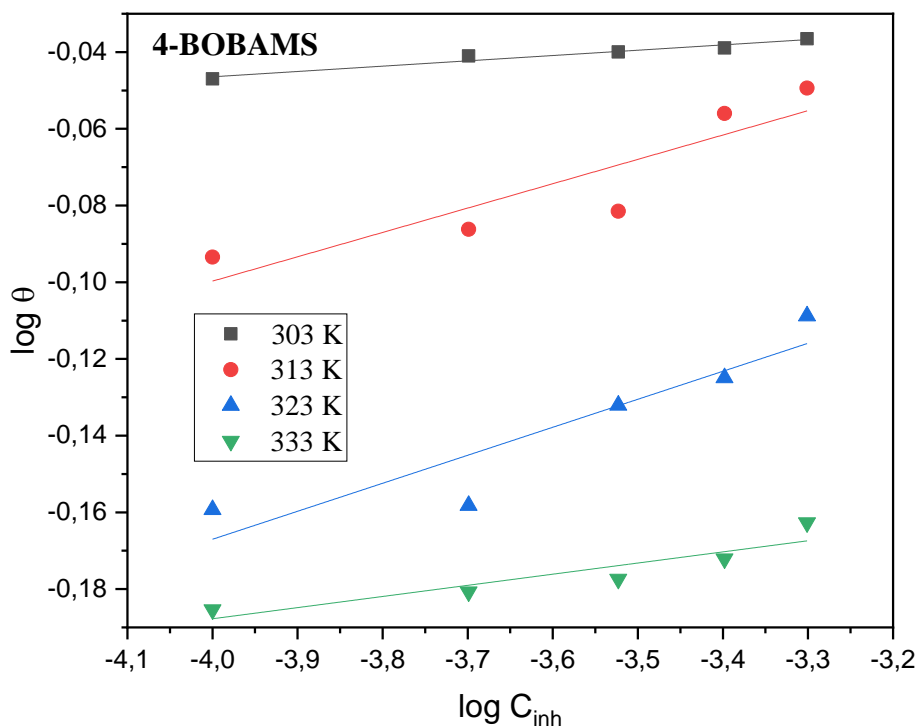


**Figure 4.86:** Freundlich adsorption isotherm plot for the adsorption of different concentrations of 4-BOBAMS on the surface of Al in 1.0 M HCl at different temperatures.

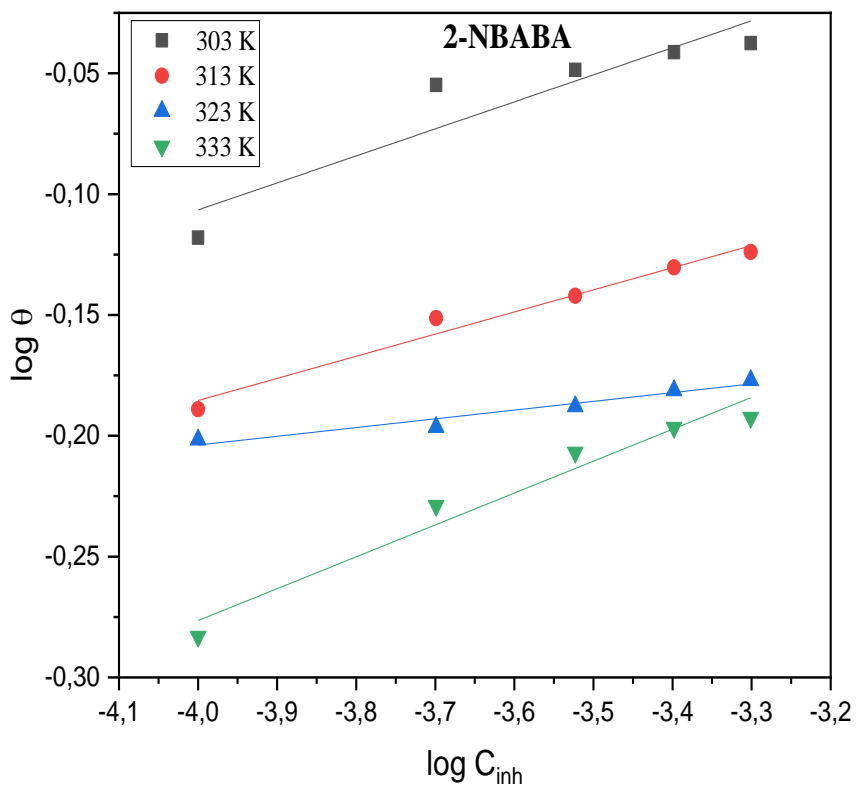


**Figure 4.87:** Freundlich adsorption isotherm plot for the adsorption of different concentrations of 2-NBABA on the surface of Al in 1.0 M HCl at different temperatures.

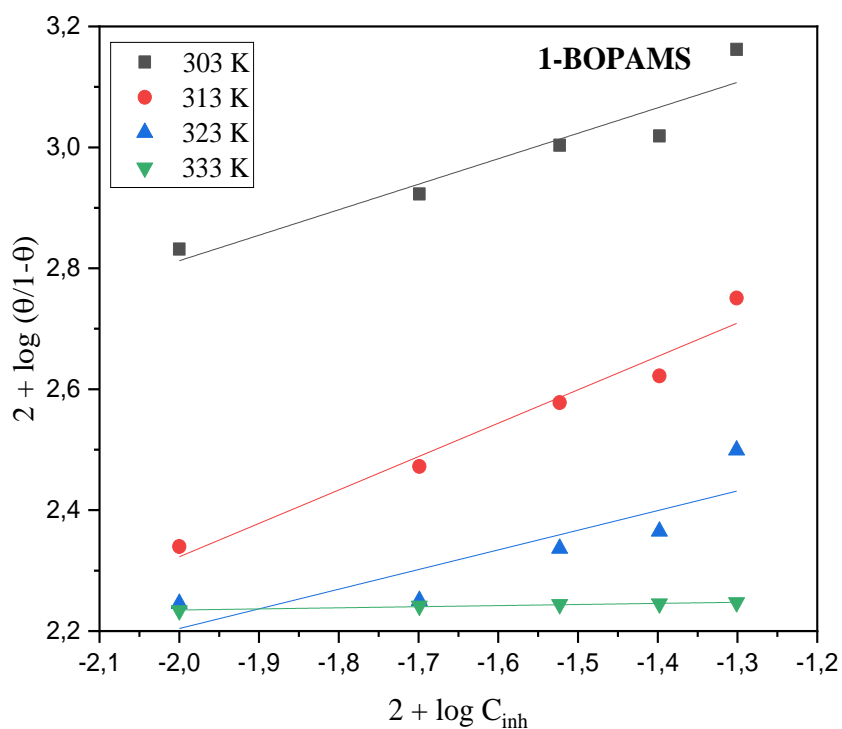


**Figure 4.88:** EL-Awady adsorption isotherm plot for the adsorption of different concentrations of 1-BOPAMS on the surface of Al in 1.0 M HCl at different temperatures.

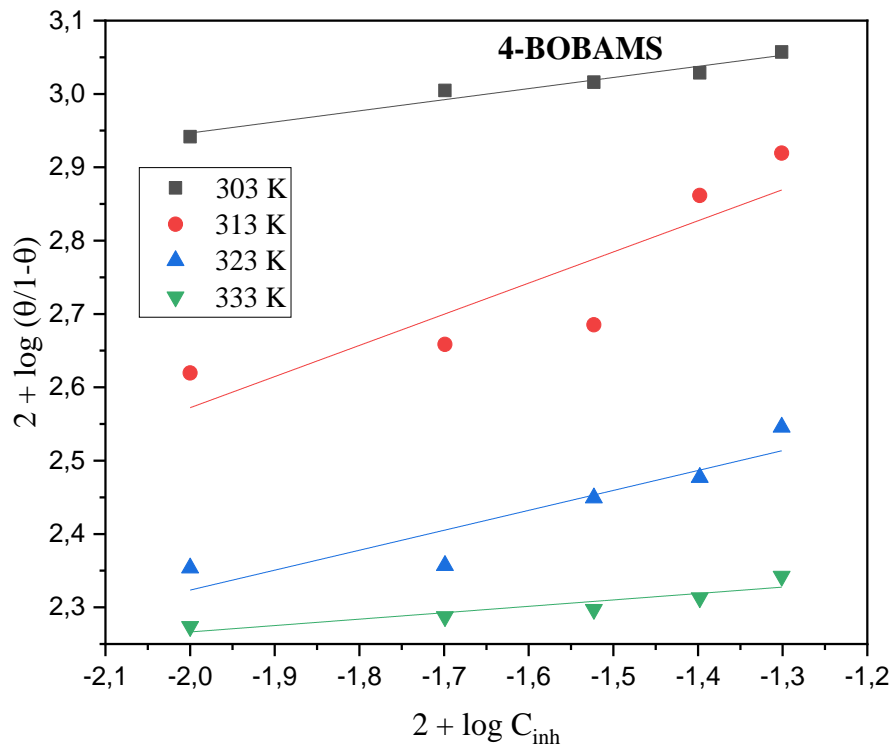


**Figure 4.89:** EL-Awady adsorption isotherm plot for the adsorption of different concentrations of 4-BOBAMS on the surface of Al in 1.0 M HCl at different temperatures.

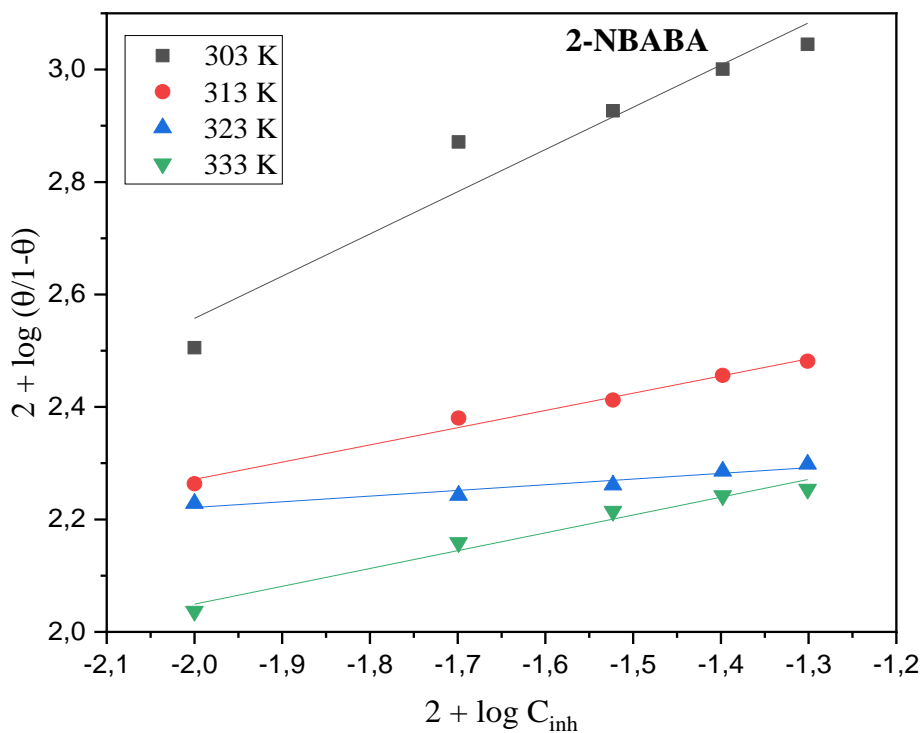


**Figure 4.90:** EL-Awady adsorption isotherm plot for the adsorption of different concentrations of 2-NBABA on the surface of Al in 1.0 M HCl at different temperatures.

**Table 4.10:** Thermodynamic and adsorption parameters obtained from various isotherms for Al in 1.0 M HCl at various temperatures for the utilized corrosion inhibitors.

Inhibitor	Temperature (K)	Correlation coefficient (R <sup>2</sup> )			
		Langmuir	Temkin	Freundlich	El-Awady
1-BOPAMS	303	0.9966	0.9340	0.9398	0.8664
	313	0.9974	0.9805	0.9865	0.9513
	323	0.9957	0.6947	0.7136	0.6672
	333	1	0.9591	0.9568	0.9584
4-BOBAMS	303	0.9999	0.7912	0.9423	0.9461
	313	0.9968	0.6139	0.7512	0.7049
	323	0.9962	0.9448	0.7994	0.7830
	333	0.9992	0.6075	0.7956	0.7799
2-NBABA	303	0.9995	0.8416	0.8273	0.9131
	313	0.9998	0.9748	0.9684	0.9822
	323	0.9996	0.9027	0.9315	0.8988
	333	0.9999	0.9523	0.9474	0.9639

#### 4.3.4 ADSORPTION FILM ANALYSIS

FT-IR technique was used to analyze the nature of the protective film formed on the surface of Al. The FT-IR spectra of Al immersed in 1.0 M HCl in the absence and presence of inhibitors (adsorption film formed) are compared to the spectra of the three pure synthesized compounds (2-NBABA, 1-BOPAMS and 4-BOBAMS) as shown in figures 4.91-4.93. The inspection of the spectra of Al in 1.0 M HCl without the inhibitor shows a broad peak around  $3261.62\text{ cm}^{-1}$  and a weak peak around  $1624.44\text{ cm}^{-1}$  which is indicative of the presence of hydrated aluminium oxide molecule ( $\text{Al}_2\text{O}_3 \cdot x\text{H}_2\text{O}$ ) and the presence of water. The stretching frequency of around  $849.75$  and  $502\text{ cm}^{-1}$  represents the  $\gamma\text{-AlO}_4$  and  $\gamma\text{-AlO}_6$ , respectively. Thus, the  $\gamma\text{-Al}_2\text{O}_3$  phase contained both octahedral and tetrahedral coordination [386]. For 2-NBABA, the FT-IR spectra for the adsorption film formed show that the formation of the hydrated Al oxide has been lowered since the intensity of the peak decrease and the Al-O stretch has shifted upwards, indicating the weakening of the bond created by the reaction between Al and oxygen in the presence of the inhibitor, consequently preventing the dissolution of Al. The expanded adsorption film formed spectra for 4-BOBAMS and 1-BOPAMS are drawn to highlight the fact that the intensity of the peaks decreased to the point that they look as if they have disappeared due to the smaller scale. This indicates a strong interaction between the functional groups of the two compound with the Al surface. This includes the ammonium salt ( $^+\text{NH}_3$ ),  $\text{O}=\text{S}=\text{O}$ ,  $\text{S}-\text{O}^-$ ,  $\text{C}-\text{N}$  and  $\text{C}-\text{O}$ , which are one of the possible electron donors. The disappearance of the peaks can be attributed to the formation of strong Fe-inhibitor complex and the reason for the high inhibition efficiency afforded by the two inhibitors.

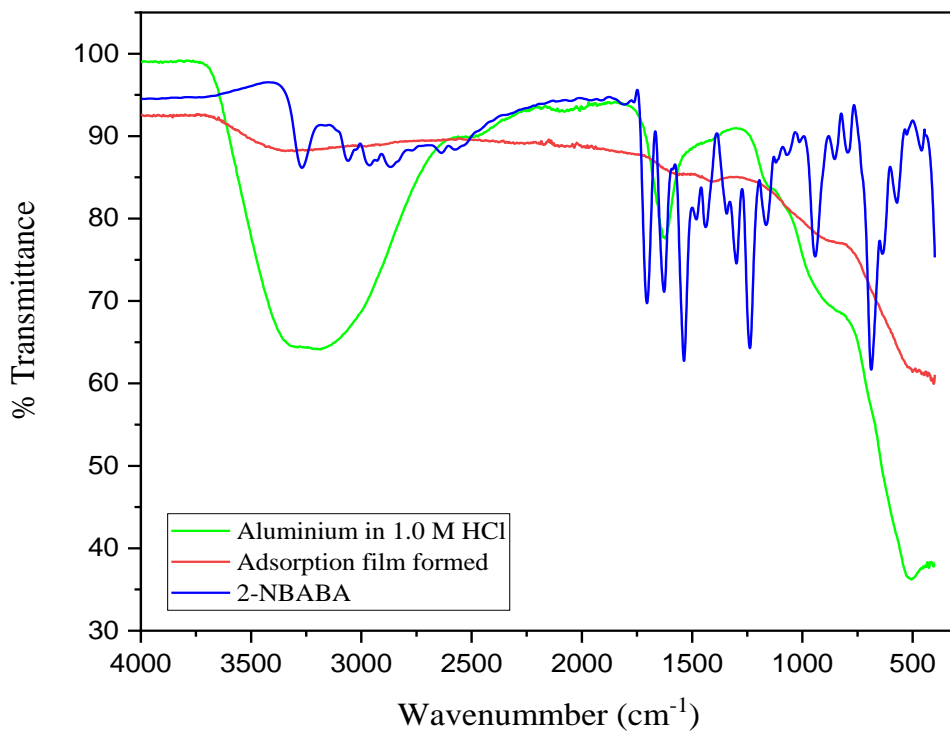


**Figure 4.91:** FT-IR spectra comparison of the frequencies for the pure compound and adsorption films formed on the Al in 1.0 M HCl by 2-NBABA corrosion inhibitor.

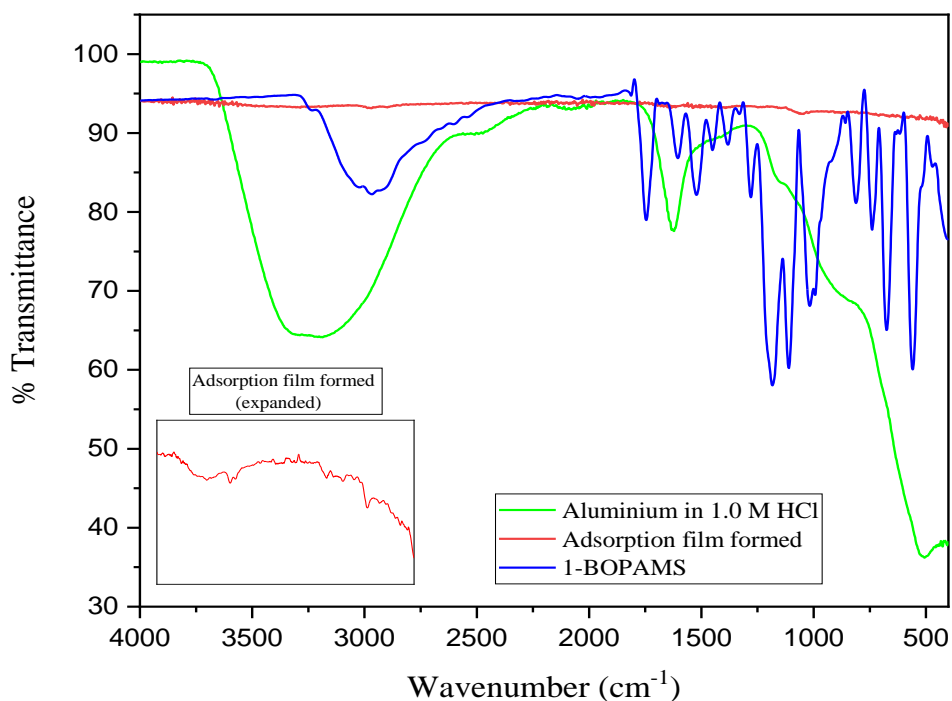


**Figure 4.92:** FT-IR spectra comparison of the frequencies for the pure compound and adsorption films formed on the Al in 1.0 M HCl by 1-BOPAMS corrosion inhibitor.

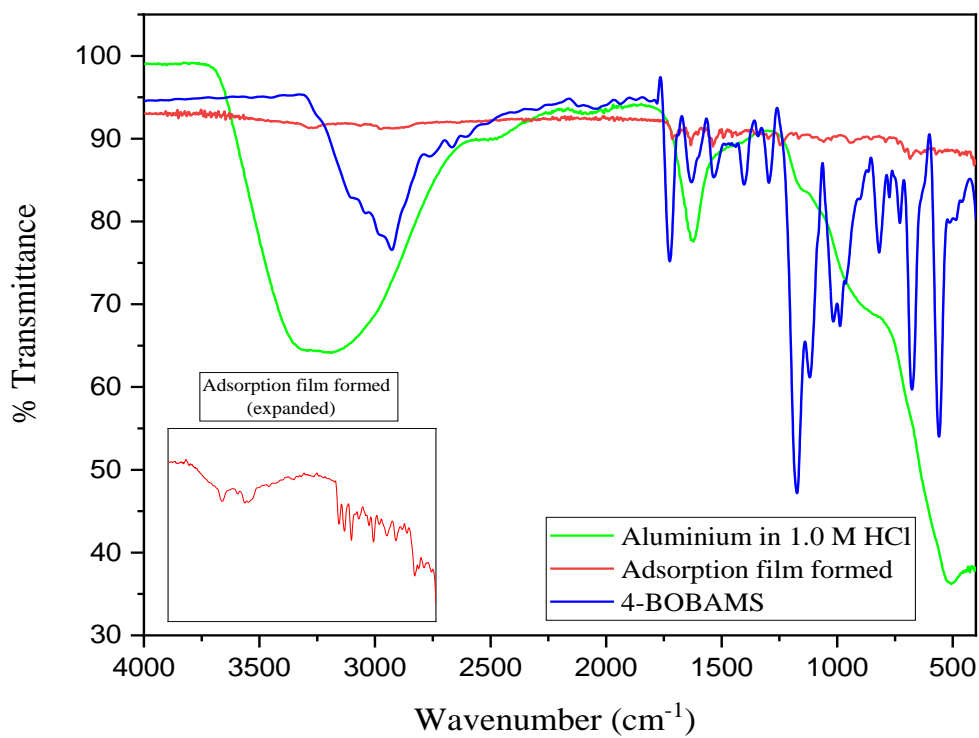


**Figure 4.93:** FT-IR spectra comparison of the frequencies for the pure compound and adsorption films formed on the Al in 1.0 M HCl by 4-BOBAMS corrosion inhibitor.

#### 4.3.5 POTENTIODYNAMIC POLARIZATION (PDP)

Potentiodynamic polarization curves obtained from the corrosion behaviour of Al in 1.0 M HCl in the absence and presence of different concentrations of 2-NBABA, 1-BOPAMS and 4-BOBAMS at 303 K are shown in figures 4.94-4.96. The values of different electrochemical parameters like  $I_{\text{corr}}$ ,  $E_{\text{corr}}$ ,  $\beta_a$  and  $\beta_c$  and  $\%IE_{\text{PDP}}$  are listed in Table 4.11. The  $\%IE_{\text{PDP}}$  was calculated from polarization measurements through equation (3.2). The Tafel extrapolation plots show that the addition of the inhibitors affected both the anodic and cathodic branches and caused a decrease in the current densities compared those recorded in the blank; the decrease is slightly pronounced with increases of the 2-NBABA, 1-BOPAM and 4-BOBAMS concentrations. The cathodic effect, however, is slightly marked for all the three inhibitors studied, indicating their predominant cathodic nature. This kind of behaviour of the inhibitors suggests that they hinder the acidic attack on the Al surface. In the cathodic region, there is a rise to the parallel effect of the Tafel lines, signifying the activation control of the hydrogen evolution process. This indicates that the discharge of hydrogen occurs via the charge transfer process at the metal interface [387, 388]. Literature studies show that if the displacement in  $E_{\text{corr}}$  is higher than  $\pm 85$  mV relating to the corrosion potential of the blank, then the inhibitor is said to be either anodic or cathodic inhibitor [107]. The maximum shift in the  $E_{\text{corr}}$  values in the present study is less than 85 mV in the presence of 2-NBABA, 1-BOPAMS and 4-BOBAMS. This confirms that none of these inhibitors is wholly anodic or cathodic but are mixed-type inhibitors. The results presented in Table 4.11 show that there is variation in the shift of both  $\beta_a$  and  $\beta_c$  compared to blank.

Furthermore, the inhibitors caused a small positive change in the corrosion potential when the three inhibitors were introduced into the 1.0 M HCl solution. The change in both the  $\beta_a$  and  $\beta_c$  values indicates that both the anodic and cathodic reactions are affected by the inhibitors and as observed with the plots, the shift in  $\beta_c$  is more pronounced, which reveals that the hydrogen evolution is more influence than the dissolution of Al [389, 390]. The electrochemical parameters obtained (Table 4.11) shows that  $i_{\text{corr}}$  values lower markedly with the increase in the concentration of the inhibitors and the  $\%IE_{\text{PDP}}$  congruently increase and increases to a maximum at the highest concentration of the three inhibitors. This type of behaviour by the inhibitors suggest that they get adsorb on the Al surface and the adsorption effect increases and become stable as their concentration increases due to the availability of more inhibitors molecules at higher concentration.



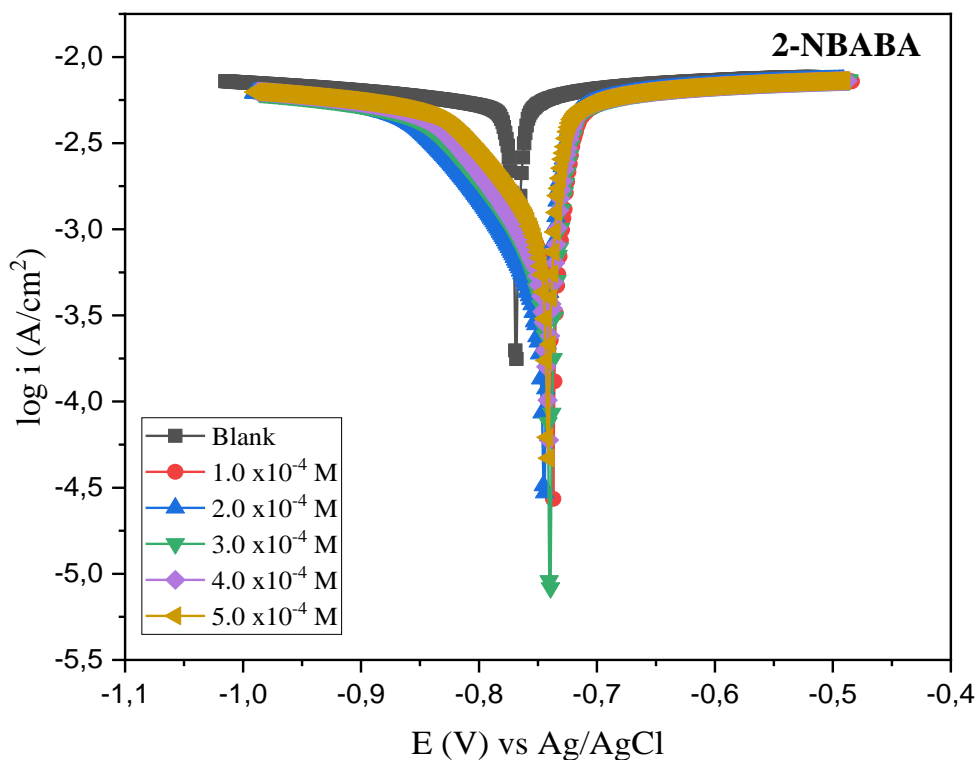


**Figure 4.94:** Tafel plots for Al in 1.0 M HCl in the absence and presence of different concentrations of 2-NBABA inhibitor compound.

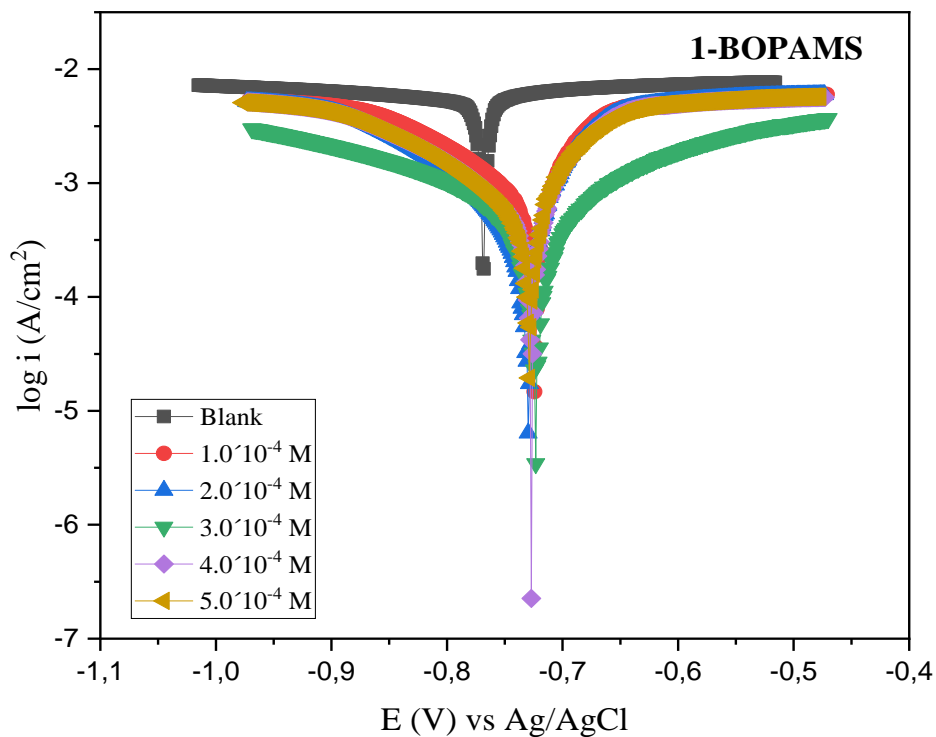


**Figure 4.95:** Tafel plots for Al in 1.0 M HCl in the absence and presence of different concentrations of 1-BOPAMS inhibitor compound.

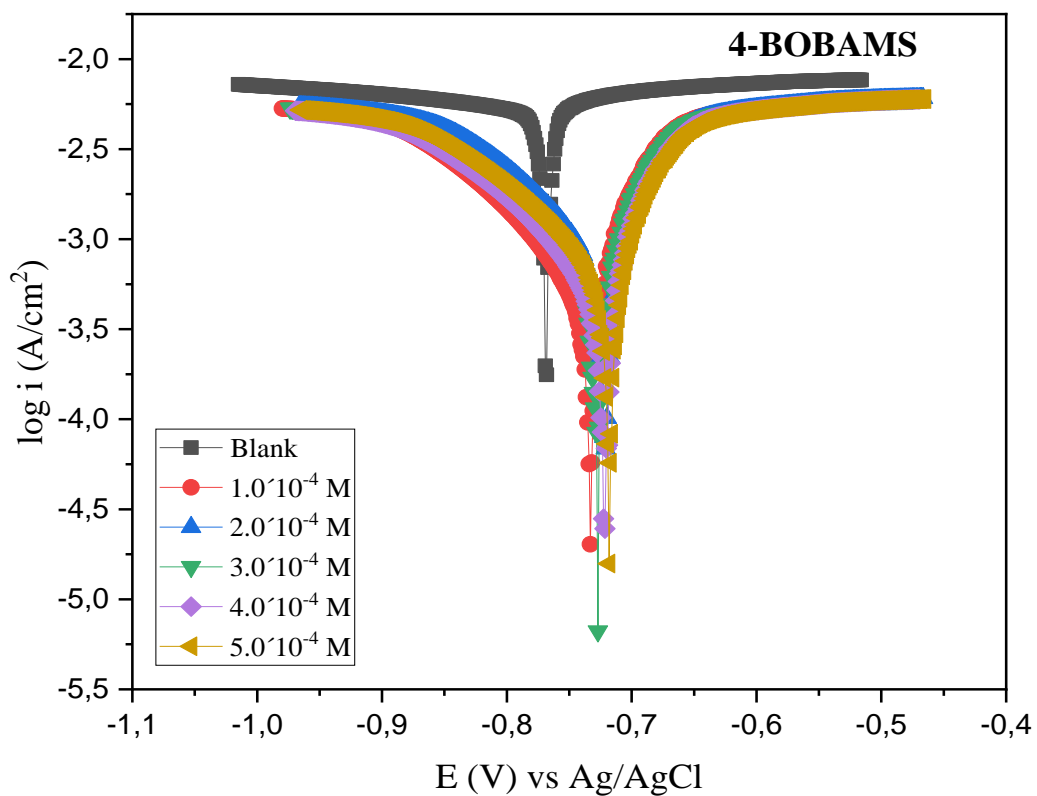


**Figure 4.96:** Tafel plots for Al in 1.0 M HCl in the absence and presence of different concentrations of 4-BOBAMS inhibitor compound.

**Table 4.11:** Potentiodynamic polarization (PDP) parameters such as corrosion potential ( $E_{\text{corr}}$ ), corrosion current density ( $i_{\text{corr}}$ ) and anodic and cathodic Tafel slopes ( $\beta_a$  and  $\beta_c$ ) for Al corrosion in 1.0 M HCl in with and without different concentrations of 2-NBABA, 1-BOPAMS and 4-BOBAMS at 303 K.

Inhibitor	$C_{\text{inh}}$ (M)	$E_{\text{cor}}$ (mV)	$i_{\text{corr}}$ (mAcm <sup>-2</sup> )	$\beta_a$ (mVdec <sup>-1</sup> )	$\beta_c$ (mVdec <sup>-1</sup> )	$R_p$ ( $10^{-1}$ ) ( $\Omega$ cm <sup>2</sup> )	$IE_{\text{PDP}}$ (%)	$IE_{\text{WL}}$ (%)
Blank	-	-769	0.00491	51	101	30.10	-	-
1-BOPAMS	$1.0 \times 10^{-4}$	-724	0.00070	7	16	30.50	85.74	87.16
	$2.0 \times 10^{-4}$	-730	0.00043	6	15	43.76	91.24	89.33
	$3.0 \times 10^{-4}$	-723	0.00027	11	12	98.28	94.50	90.98
	$4.0 \times 10^{-4}$	-727	0.00019	3	4	38.94	96.13	91.26
	$5.0 \times 10^{-4}$	-729	0.00012	2	2	36.44	97.59	93.52
4-BOBAMS	$1.0 \times 10^{-4}$	-723	0.00083	10	24	36.62	83.10	89.74
	$2.0 \times 10^{-4}$	-721	0.00072	8	1	29.63	85.34	91.00
	$3.0 \times 10^{-4}$	-727	0.00048	6	12	34.15	90.22	91.21
	$4.0 \times 10^{-4}$	-722	0.00034	4	10	38.44	93.08	91.44
	$5.0 \times 10^{-4}$	-718	0.00015	2	2	28.08	96.95	91.94
2-NBABA	$1.0 \times 10^{-4}$	-737	0.00061	3	10	15.75	87.57	76.20
	$2.0 \times 10^{-4}$	-745	0.00051	3	13	20.48	89.61	88.14
	$3.0 \times 10^{-4}$	-740	0.00049	3	11	18.33	90.02	89.41
	$4.0 \times 10^{-4}$	-741	0.00026	1	3	15.22	94.70	90.92
	$5.0 \times 10^{-4}$	-792	0.00018	1	2	14.28	96.17	91.73

#### 4.3.6 ELECTROCHEMICAL IMPEDANCE SPECTROSCOPY (EIS)

Electrochemical impedance spectroscopy is a well-documented quantitative technique for the investigation of corrosion and adsorption phenomenon. In the present study, EIS was made use of the examination the corrosion behaviour of Al in 1.0 M HCl in the absence and presence of inhibitors after 30 minutes of immersion at 303 K. The impedance spectra obtained are presented as Nyquist (figure 4.98-4.100) and Bode plots (figures 4.101-4.103). The EIS parameters derived from these data are presented in Table 4.12. The shape of the curves is the same in the absence or presence of the inhibitors, indicating that the presence of inhibitors does not alter the anodic and cathodic process of the dissolution of Al. The diameter of the blank is significantly smaller than those of the inhibited process. From these Nyquist plots, it is also observed that increasing the concentration of the three inhibitors did not necessarily increase the size of the diameter of the semi-circle.

In some cases, there was a shift in Nyquist plots origin as the concentration of the inhibitors were increased. This behaviour was due to the formation of the adsorption film layer on the Al surface and as the concentration of the inhibitors was amplified more inhibitors molecules were able to provide higher coverage of the Al surface. The shift in the semicircle loops with an increase in inhibitors concentration might be a result of the stabilization of the adsorption process and reduction of the passivation of Al. The semicircles obtained are not perfect, and a smaller arch for the blank indicates that the corrosion of Al is controlled mainly by charge transfer process and that the Faradaic processes that occur on bare Al surface lower with the introduction of inhibitors and as their concentration is increased. As such, the inhibitors do not change the electrochemical process of corrosion but prevent it by adsorbing on the metal surface [391]. The Nyquist diagrams presented consists of a capacitive loop in the high-frequency regions followed by an inductive loop in the low-frequency regions. The high-frequency capacitive loop is said to be representative of the charge transfer resistance of the corrosion process and the double layer behaviour.

On the other hand, the behaviour of the inductive loop may be attributed to several phenomena. For instance, Brustein et al., [392] referred to it as the surface or bulk relaxation of the species present in the oxide layer covering the electrode surface, while through the Cinderey and Brustein's measurements [393, 394], the inductive loop has been confirmed to be closely related to the existence/presence of the passive film on Al. Also, another cause for the induction loop could be as a result of the stabilization of the adsorbed intermediate complex on the electrode surface which might involve the reactive products as well as the molecules of the

inhibitors [395]. Moreover, Ashassi-Sorkhabi and Asghari [396] have attributed the presence of the induction loop to the adsorption or desorption equilibrium of surface-active species on the surface of the metal using EIS.

The equivalent circuit model used to fit the impedance spectra has been reported previously [395, 397] and is shown in figure 4.97. In the equivalent circuit below (figure 4.97),  $R_1$  represents the electrolyte resistance ( $R_s$ ),  $Q_1$  is the constant phase element (CPE),  $R_2$  is the charge transfer resistance ( $R_{ct}$ ), and  $R_3$  and  $L_3$  represent the inductive elements. Constant phase element was used in place of double-layer capacitance ( $C_{dl}$ ) to reflect an ideal capacitor to describe the inhomogeneities in the system. The imperfect semicircle loop at higher frequency region indicates the inhomogeneity of the Al surface due to structural or interfacial origin similar to those found during the adsorption processes [398]. Using equation (3.1), the %IE<sub>EIS</sub> at different concentration of the inhibitors was calculated. As shown in Table 4.12, it can be noticed that the %IE<sub>EIS</sub> increases as the charge transfer resistance increases and this increase is proportional to the rise of the concentration of the inhibitors. The decrease in the capacity as the inhibitors concentration is raised may be attributed to the formation of the adsorption film layer by the inhibitor molecules on Al surface [399]. This can also be due to the increase in the thickness of the electrical double layer or the decrease in the local dielectric constant. Which indicates that the molecules of the inhibitors work by adsorbing at the metal/solution interface through the displacement of the water molecules on the metal surface by the molecules of the inhibitors [400].

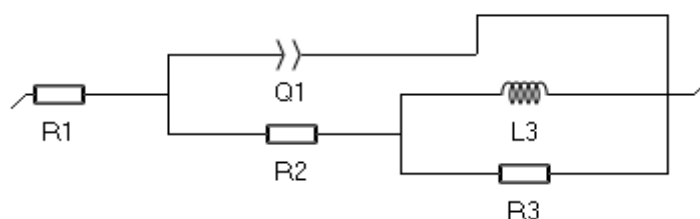


**Figure 4.97:** Equivalent circuit used to fit the impedance spectra obtained for Al corrosion in 1.0 M HCl in the absence and presence of 2-NBABA, 4-BOBAMS and 1-BOPAMS.

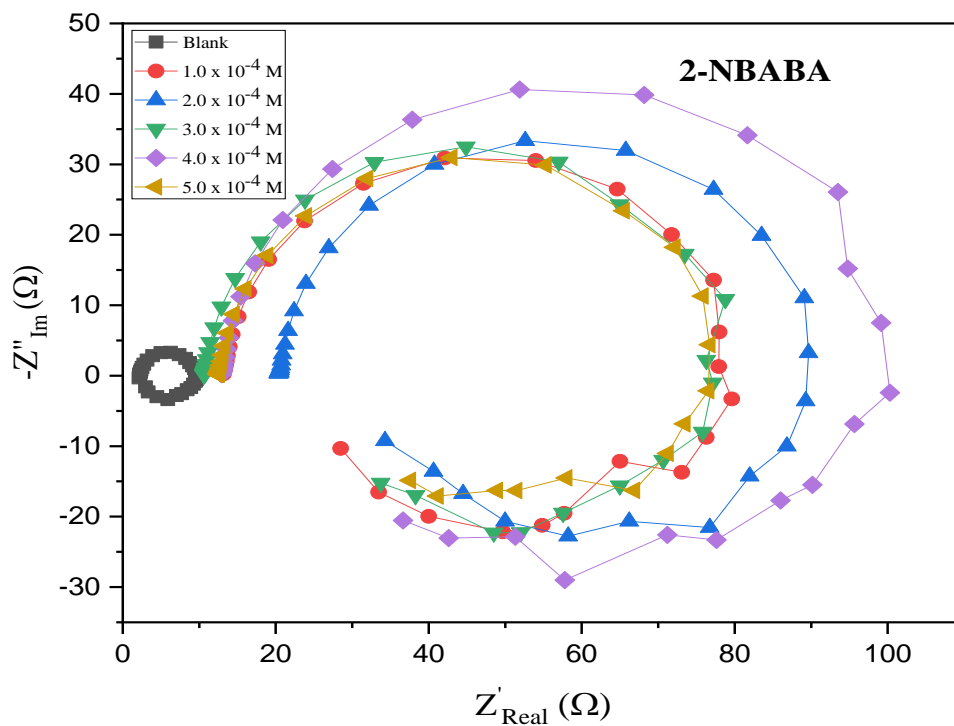


**Figure 4.98:** Nyquist plots for Al in 1.0 M HCl in the absence and presence of different concentrations of 2-NBABA.

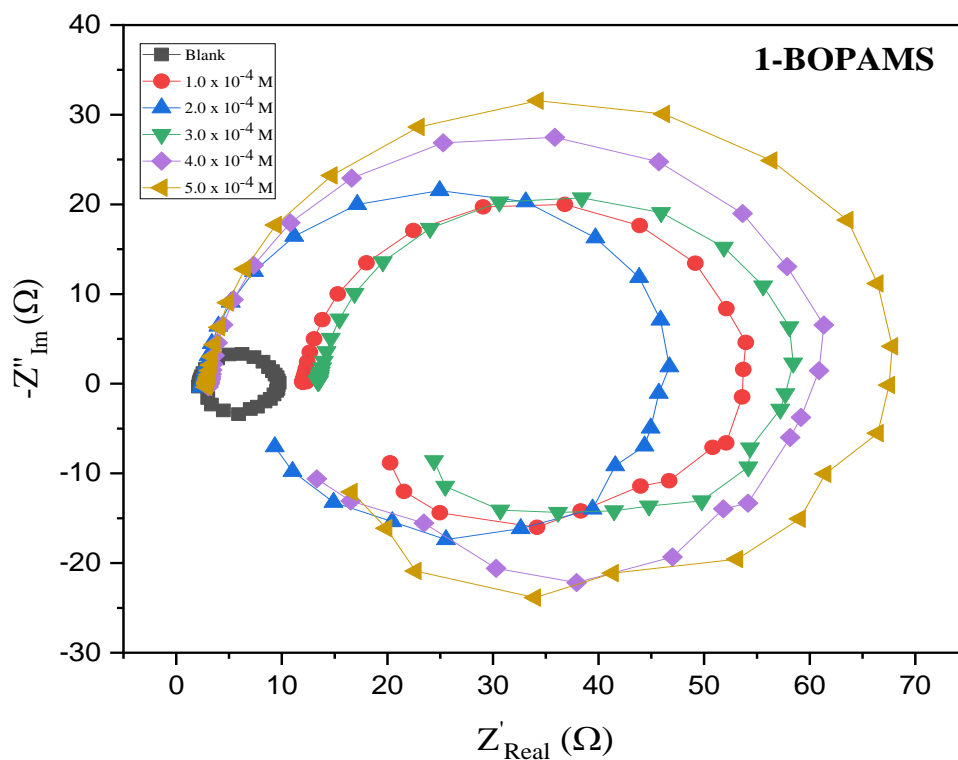


**Figure 4.99:** Nyquist plots for Al in 1.0 M HCl in the absence and presence of different concentrations of 1-BOPAMS.

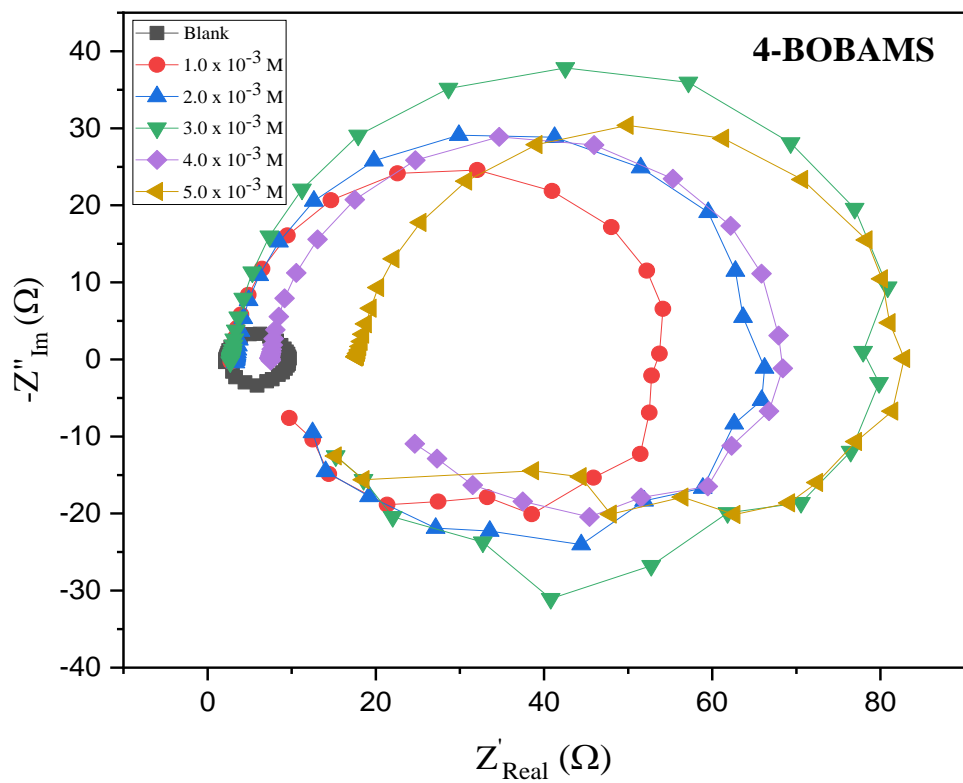


**Figure 4.100:** Nyquist plots for Al in 1.0 M HCl in the absence and presence of different concentrations of 4-BOBAMS.

**Table 4.12:** Electrochemical impedance (EIS) parameters such as the resistance of charge transfer ( $R_{ct}$ ), constant phase element ( $Q_1$ ), solution resistance ( $R_s$ ) and the CPE exponent ( $n$ ) for Al corrosion in 1.0 M HCl in absence and presence of different concentrations of 2NBABA, 1-BOPAMS and 4-BOBAMS at 303 K.

Inhibitor	$C_{inh}$ (M)	$R_{ct}$ ( $\Omega$ )	$Q_1$ ( $F.s^{(a-1)}$ )	$R_s$ ( $\Omega$ )	$R_3$ ( $\Omega$ )	N	$L_3$ (H)	$\theta$	$IE_{EIS}$ (%)	$IE_{WL}$ (%)
Blank	-	0.4036	0.1146e-3	2.2	6.873	0.9463	2.902	-	-	-
1-BOPAMS	$1.0 \times 10^{-4}$	5.864	96.49e-6	12.09	34.85	0.9807	14.01	0.9312	93.12	87.16
	$2.0 \times 10^{-4}$	6.019	83.83e-6	2.537	37.68	0.9611	11.39	0.9329	93.29	89.33
	$3.0 \times 10^{-4}$	9.217	68.51e-6	13.57	34.33	0.9662	12.24	0.9562	95.62	90.98
	$4.0 \times 10^{-4}$	9.41	82.29e-6	3.167	47.3	0.9629	16.29	0.9571	95.71	91.26
	$5.0 \times 10^{-4}$	11.3	88.66e-6	2.961	52.81	0.9599	52.81	0.9643	96.43	93.52
4-BOBAMS	$1.0 \times 10^{-4}$	6.342	61.16e-6	2.889	44.21	0.9678	11.61	0.9364	93.64	89.74
	$2.0 \times 10^{-4}$	7.769	69.66e-6	3.38	53.32	0.9641	15.44	0.9480	94.80	91.00
	$3.0 \times 10^{-4}$	11.52	68.73e-6	2.823	64.62	0.9629	17.80	0.9650	96.50	91.21
	$4.0 \times 10^{-4}$	15.80	99.5e-6	7.467	44.38	0.9623	14.41	0.9745	97.45	91.44
	$5.0 \times 10^{-4}$	18.71	83.55e-6	17.92	44.97	0.9559	18.11	0.9784	97.84	91.94
2-NBABA	$1.0 \times 10^{-4}$	14.54	58.97e-6	13.26	49.07	0.9691	17.98	0.9722	97.22	76.20
	$2.0 \times 10^{-4}$	15.51	75.89e-6	20.53	52.71	0.9749	14.22	0.9740	97.40	88.14
	$3.0 \times 10^{-4}$	19.41	0.1084e-6	10.71	46.80	0.9679	22.02	0.9792	97.92	89.41
	$4.0 \times 10^{-4}$	20.49	62.98e-6	13.05	62.74	0.972	25.91	0.9803	98.03	90.92
	$5.0 \times 10^{-4}$	22.17	0.1203e-6	12.60	41.19	0.9695	18.20	0.9818	98.18	91.73

Bode plots can be used to determine the performance of the inhibitors for the prevention of corrosion. The amplitude data of the Bode plots were characterized by a one-time constant which accounts for the barrier properties of the inhibitors [354]. The measured Bode plots show that the IBP obtained for the inhibitors, 2-NBABA, 1-BOPAMS and 4-BOBAMS is in the upper left corner of the Bode plots in the early stage of immersion, and after a certain period, it moved gradually to the middle of the plots proving that these inhibitors are capable of providing a good protection for Al corrosion. The Bode plots obtained in the absence of the



inhibitors do not interact, which shows that there were no inhibitor molecules present to protect the metal from the corrosive medium.

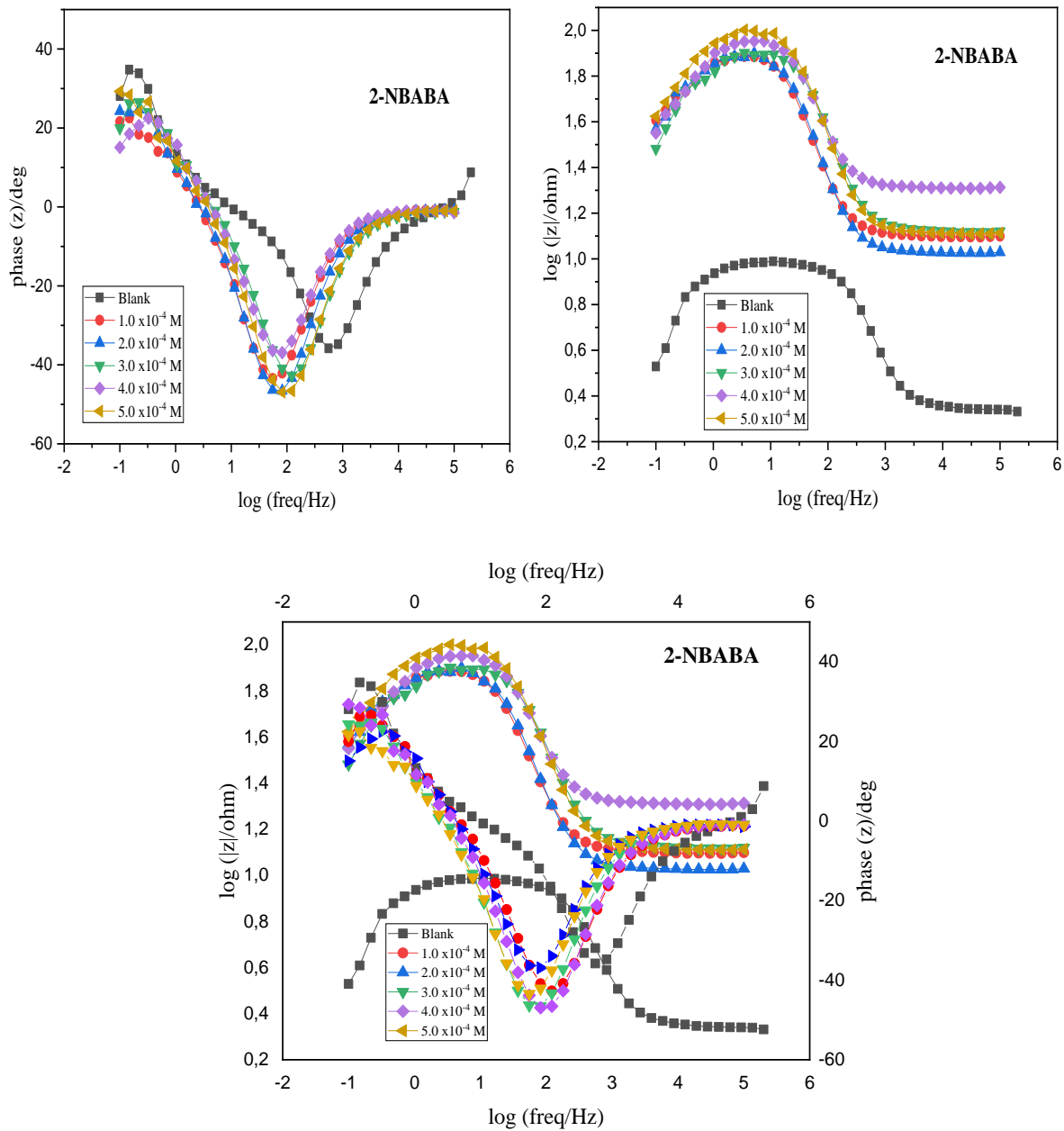


**Figure 4.101:** Bode diagrams of the impedance for Al in 1.0 M HCl without and with different concentrations of 2-NBABA at 303 K.

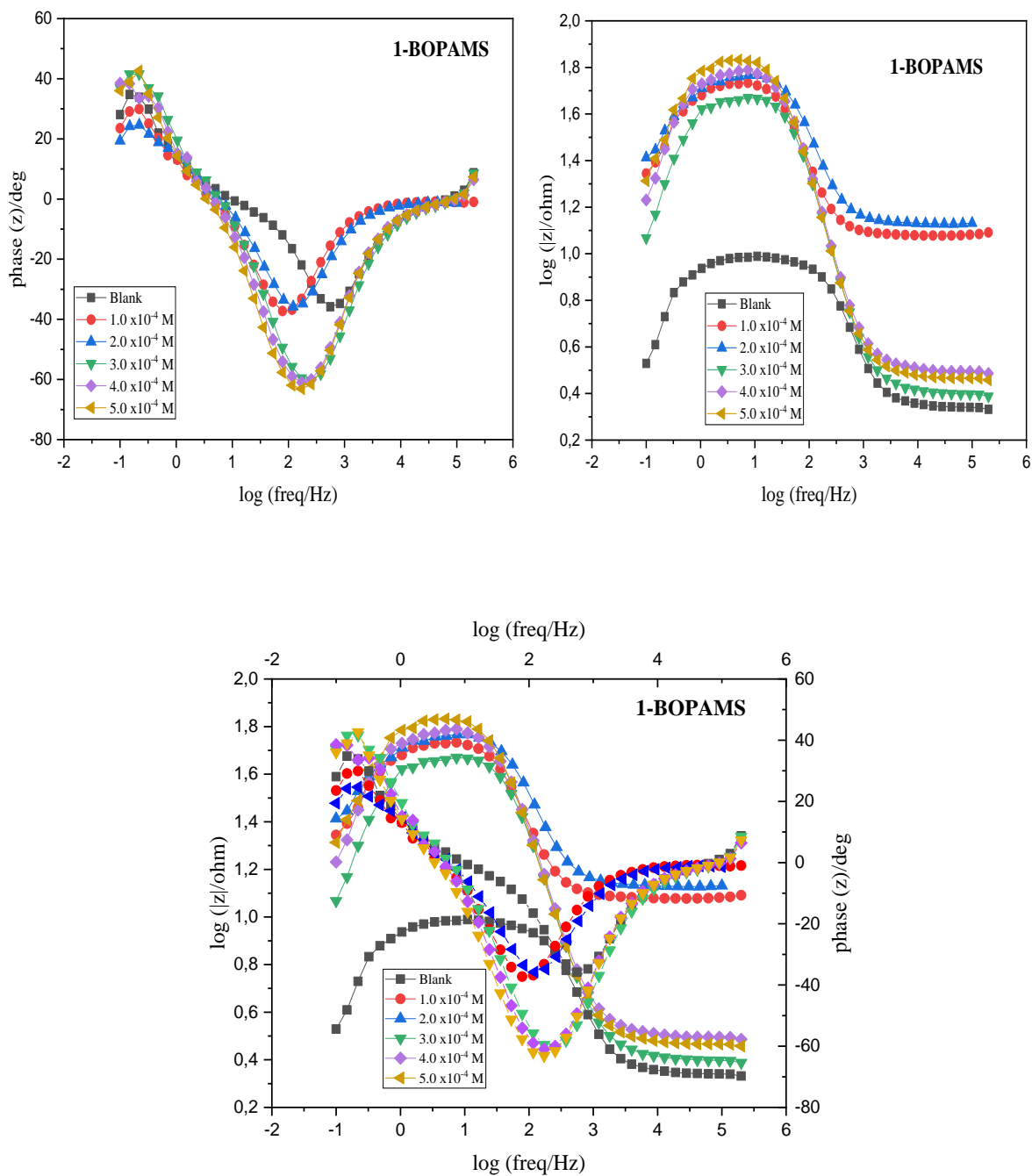


**Figure 4.102:** Bode diagrams of the impedance for Al in 1.0 M HCl without and with different concentrations of 1-BOPAMS at 303 K.

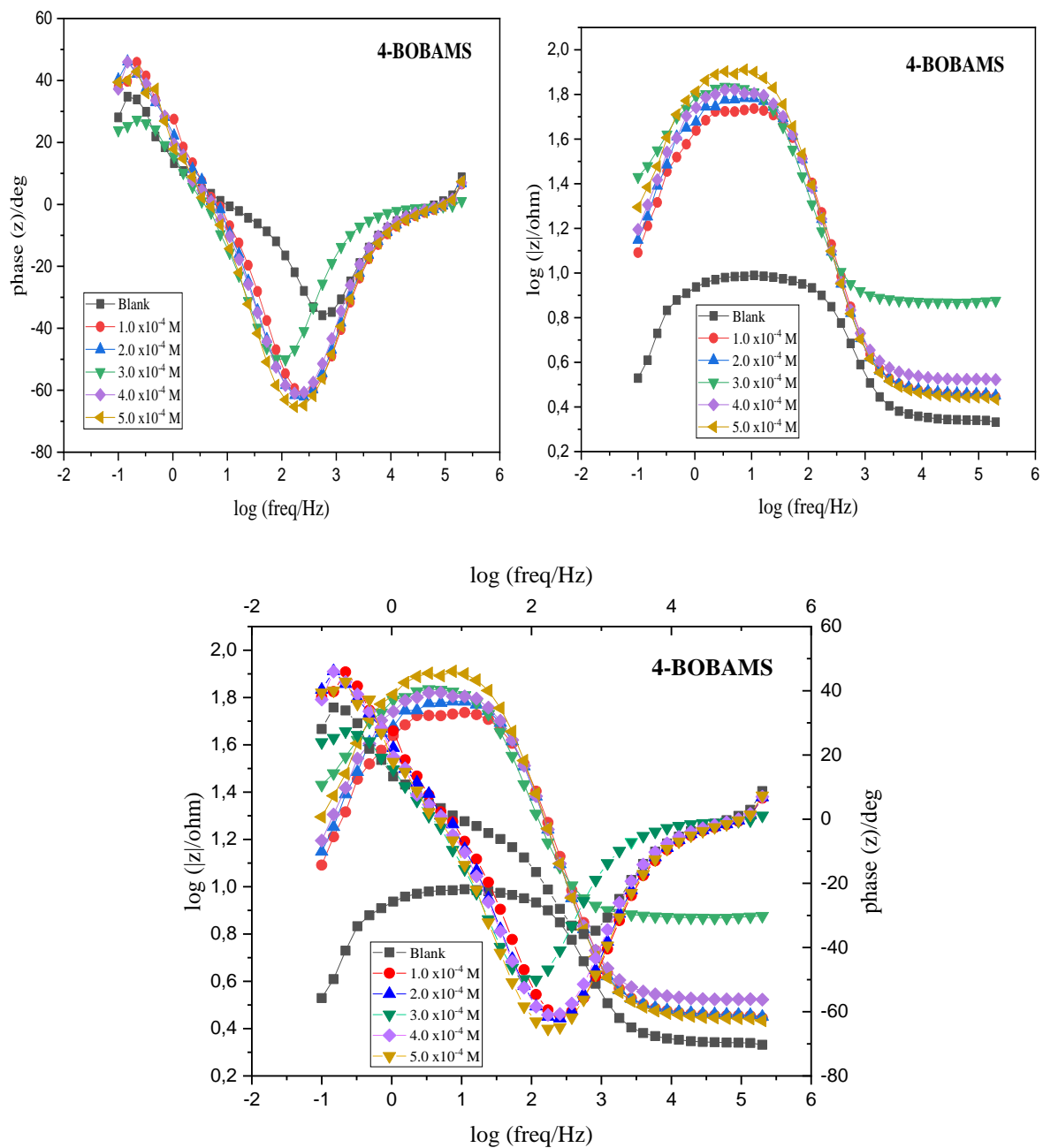


**Figure 4.103:** Bode diagrams of the impedance for Al in 1.0 M HCl without and with different concentrations of 4-BOBAMS at 303 K.

#### 4.3.7 PROPOSED INHIBITION MECHANISM ON AL SURFACE

The inhibition capabilities of inhibitors molecules for Al corrosion are said to be a result of the adsorption of the inhibitor molecules on the Al surface, forming a protective barrier. The degree of adsorption offered by inhibitors depends on several factors like the condition of the metal surface, the nature of the metal and the mode of adsorption of the inhibitor molecules [401]. During the inhibition process in acidic solution, the adsorption of inhibitor molecules at the Al/OH<sup>-</sup> interface is assumed to be the initial step. The adsorption may be because of one of three steps, namely; electrostatic attraction that occurs between charged metal surface and charged inhibitor molecules, the formation of coordination bond by the unshared pair of electrons on the inhibitor molecules and the vacant p-orbitals of the Al atoms and the participation of the  $\pi$ -electrons of the inhibitor molecules in coordination process [202, 402]. As such, the prevention of Al corrosion in HCl is accomplished mainly due to electrostatic interaction; this conclusion is supported by the decrease in the %IE with the rise in temperature. Generally, the amino ester and carboxylic acid can be absorbed on the Al surface either in their neutral or protonated forms. In acidic solution (i.e., HCl), the Al surface is negatively charged and as a result protonated inhibitor molecules find it easier to approach the negatively charged surface due to electrostatic attraction that occurs between them and the Al surface [403]. The process of adsorption of the inhibitor molecules is said to involve the displacement of the water molecules from the surface of Al and the sharing of electrons that occurs between the Al surface and heteroatoms of the inhibitors.

#### 4.4 COMPARISON OF THE CORROSION INHIBITION PERFORMANCE OF THE SYNTHESIZED CARBOXYLIC ACID AND AMINO ESTERS ON Al AND MS

In the present study, one carboxylic acid (2-NBABA) and two amino esters (1-BOPAMS and 4-BOBAMS), were evaluated for their anti-corrosive properties for Al and MS in 1.0 M HCl solution at 303-333 K. Hence, in this section, an attempt has been made to compare the inhibition performance of these inhibitors using the result obtained from the gravimetric analysis, FT-IR, PDP and EIS. The comparison of the %IE from all these techniques show that Al showed the highest %IE for all the three inhibitors investigated. The optimum protection for Al may be attributed to the production of a protective Al film that forms during the corrosion process. Table 4.13 provides a detailed comparison of the effects of 2-NBABA, 1-BOPAMS and 4-BOBAMS for Al and MS corrosion.

**Table 4.13:** Comparison of the performance of 2-NBABA, 1-BOPAMS and 4-BOBAMS on the corrosion inhibition of Al and MS in 1.0 HCl solution.

Technique/Study	Metal	
	Al	MS
<b>PDP</b>	<ul style="list-style-type: none"> <li>Mixed-type adsorption with dominating cathodic protection</li> <li>Consistent <math>E_{\text{corr}}</math> values</li> <li><math>\beta_a</math> (1-11 mV.dec<sup>-1</sup>), <math>\beta_c</math> (1-24 mV.dec<sup>-1</sup>)</li> </ul>	<ul style="list-style-type: none"> <li>Mixed-type adsorption</li> <li>Consistent <math>E_{\text{corr}}</math> values</li> <li><math>\beta_a</math> (5-9 mV.dec<sup>-1</sup>), <math>\beta_c</math> (6-13 mV.dec<sup>-1</sup>)</li> </ul>
<b>EIS</b>	<ul style="list-style-type: none"> <li>Circuit for data fitting: <math>R_s+Q/[R_{\text{ct}}+L_3/R_3]</math></li> <li>Imperfect Nyquist plots with a pronounced passive region (inductive loop)</li> <li>More capacitive behaviour than MS (<math>n \cong 0.95</math>)</li> </ul>	<ul style="list-style-type: none"> <li>Circuit for data fitting: <math>R_s+Q/R_{\text{ct}}</math>.</li> <li>Imperfect Nyquist plots</li> <li>Pseudo-capacitive behaviour (<math>n \cong 0.85</math>), <math>n</math>-values are approaching unity</li> </ul>
<b>Gravimetric</b>	<ul style="list-style-type: none"> <li>Obeys Langmuir model</li> <li><math>\Delta G^{\circ}_{\text{ads}}</math> values (-30.096 to -40.743 kJ.mol<sup>-1</sup>) show mixed-type adsorption process with dominating chemisorption</li> <li><math>\Delta H^{\circ}_{\text{ads}}</math> are both positive (1-BOPAMS) representing chemisorption and also negative (2-NBABA and 4-BOBAMS) depicting mixed-type adsorption process</li> <li>Spontaneous adsorption</li> </ul>	<ul style="list-style-type: none"> <li>Obeys Langmuir model</li> <li><math>\Delta G^{\circ}_{\text{ads}}</math> values (-30.927 to -33.947 kJ.mol<sup>-1</sup>) show mixed-type adsorption, towering near chemisorption process</li> <li><math>\Delta H^{\circ}_{\text{ads}}</math> are negative and indicate exothermic adsorption, representing mixed-type adsorption process</li> <li>Spontaneous adsorption</li> </ul>

## CHAPTER 5

---

# CONCLUSIONS

This chapter concludes and highlights on the aim and objectives that this study was set out to achieve. In summary, the three synthesized compounds were found to inhibit both the corrosion of Al and MS in 1.0 M HCl. The adsorption mechanism of the inhibitors on both metals was found to be mixed-type adsorption. Both the anodic and cathodic reaction was inhibited to almost the same extent.

## 5.1 CONCLUSIONS

The aim of this work was achieved. The carboxylic acid, N-benzoyl-2-aminobutyric acid (2-NBABA) and amino esters, 1-(benzyloxy)-1-oxopropan-2-aminium 4-methylbenzenesulfonate (1-BOPAMS) and 4-(benzyloxy)-4-oxobutan-1-aminium 4-methylbenzenesulfonate (4-BOBAMS) were synthesized and characterized. The characterization of the compounds by Fourier Transform Infrared spectrometry (FT-IR) and Nuclear Magnetic Resonance ( $^1\text{H-NMR}$  and  $^{13}\text{C-NMR}$ ) spectroscopy gave the correct number of signals in the appropriate chemical shifts. The synthesized 2-NBABA, 1-BOPAMS and 4-BOBAMS compounds were tested as inhibitors for Al and MS corrosion in 1.0 M HCl solution at different concentration. The evaluation of the inhibition performance of the three inhibitors was carried out using gravimetric, FT-IR, and electrochemical techniques which included: Potentiodynamic polarization (PDP) and electrochemical impedance spectroscopy (EIS).

The synthesized carboxylic acid and amino esters derivatives showed excellent inhibition properties against Al and MS corrosion. Amongst the studied inhibitors, the amino esters 1-BOPAMS and 4-BOBAMS exhibited higher %IE compared to the carboxylic acid 2-NBABA. The higher %IE of the amino esters is because of the presence of two heterocyclic rings, ammonium, oxygen and sulphur groups. The gravimetric analysis revealed that the corrosion rate decreases with the increase in the concentration of the inhibitors and increases with the increase in the temperature of the solution. For all the investigated inhibitors, the maximum %IE was obtained at the lowest temperature (303 K) and maximum concentration of the inhibitors for both Al and MS. The optimum concentrations for the inhibitors that provided good %IE for MS were  $5 \times 10^{-3}$  M and for Al, it was  $5 \times 10^{-4}$  M.

The temperature studies allowed the evaluation of the thermodynamic and kinetics parameters of corrosion and corrosion inhibition of Al and MS. Such studies revealed that the adsorption mechanism of 2-NBABA, 1-BOPAMS and 4-BOBAMS is a combination of both physisorption and chemisorption (i.e., mixed-type adsorption), chemisorption being the dominating adsorption process. Kinetics studies showed that the energy (activation energy) required to form the corrosion products increased as the inhibitors were introduced into the solution; this was said to be due to the formation of protective film on the surface of the two metals.

Surface coverage values obtained from gravimetric analysis were found to follow El-Awady, Temkin, Freundlich, and Langmuir adsorption, isotherm models. Langmuir adsorption isotherm, however, was revealed to best describe the adsorption of the organic compounds of the surface of Al and MS steel; this is because among the fitted isotherm the slope and the regression coefficient for Langmuir were found to be the closest to unity. The adsorption process was found to be spontaneous for both Al and MS since negative values for  $\Delta G^{\circ}_{\text{ads}}$  were obtained.

Polarization study revealed that the inhibitors act in both anodic and cathodic ways for both MS and Al, for Al the cathodic reaction was being polarized more. From the polarization study corrosion parameters  $E_{\text{corr}}$ ,  $I_{\text{corr}}$ ,  $\beta_a$  and  $\beta_c$  were obtained. These parameters indicated that 2-NBABA, 1-BOPAMS and 4-BOBAMS are the mixed type corrosion inhibitors and the inhibition of Al and MS was mainly controlled by charge transfer. The increase of the  $R_p$  values with an increase in the concentration of the inhibitors indicated that the inhibition of corrosion is primarily due to the formation of the protective film.

EIS results showed an imperfect semicircle loop for MS, indicating effective inhibition capabilities for MS corrosion by the inhibitors. Al showed Nyquist plots with a more pronounced passive region, and this is attributed to the higher tendency of Al in forming an oxide film than MS. EIS results showed that the charge transfer resistance increased as the concentration of the inhibitors were increased leading to the decrease of the corrosion rate and higher %IE. The constant phase element exponent ( $n$ ) values were near unity for both Al and MS, which is indicative of a pseudo-capacitive behaviour of the electrode. Mixed-Type adsorption was exhibited for all the three inhibitors studied.

## 5.2 RECOMMENDATIONS FOR FUTURE STUDIES

The present study focused on the evaluation of the inhibition potential of 2-NBABA, 1-BOPAMS and 4-BOBAMS on MS and Al in only one acidic medium (1.0 M HCl). Therefore, future studies should also focus on testing these compounds in different corrosive medium to provide greater scrutiny and also attest to their inhibition capabilities. Quantum chemical studies could also highlight the best molecular geometry that could offer high inhibition efficiencies. Future studies could also be conducted while the testing solution is in motion (stirring) to evaluate the effect of moving solution on the inhibition efficiency.



# REFERENCES

---

1. Uhlig, H.H. and R.W. Revie, *Corrosion and corrosion control: an introduction to corrosion science and engineering*. 2008: John Wiley & Sons.
2. Umoren, S. and M. Solomon, *Recent developments on the use of polymers as corrosion inhibitors-A review*. **Open Materials Science Journal**. 8 (2014) 39-54.
3. Callister Jr, W.D. and D.G. Rethwisch, *Fundamentals of materials science and engineering: an integrated approach*. 2012: John Wiley & Sons.
4. Shalash, L.B.T. and L.S.H. Nasher, *Study the effect of magnetic field on the corrosion of steel in sodium chloride solution (NaCl)*. **Misan Journal of Academic Studies**. 9 (2010) 30-38.
5. Buchweishaija, J., *Phytochemicals as green corrosion inhibitors in various corrosive media: a review*. **Tanzania Journal of Science**. 35 (2009) 77-92.
6. Raja, P.B., M. Ismail, S. Ghoreishiamiri, J. Mirza, M.C. Ismail, S. Kakooei, and A.A. Rahim, *Reviews on corrosion inhibitors: a short view*. **Chemical Engineering Communications**. 203 (2016) 1145-1156.
7. Wang, H., X. Wang, H. Wang, L. Wang, and A. Liu, *DFT study of new bipyrazole derivatives and their potential activity as corrosion inhibitors*. **Journal of Molecular Modeling**. 13 (2007) 147-153.
8. Sastri, V.S., *Green corrosion inhibitors: theory and practice*. 2012: John Wiley & Sons.
9. Candoni, F., *The assessment of nitrogen emissions from manure management and their mitigation adopting short rotation coppice crops*. 2016, University of Udine.
10. Carino, N.J., *Nondestructive techniques to investigate corrosion status in concrete structures*. **Journal of Performance of Constructed Facilities**. 13 (1999) 96-106.
11. Quraishi, M., I. Ahamad, A.K. Singh, S.K. Shukla, B. Lal, and V. Singh, *N-(Piperidinomethyl)-3-[(pyridylidene) amino] isatin: A new and effective acid corrosion inhibitor for mild steel*. **Materials Chemistry and Physics**. 112 (2008) 1035-1039.
12. S Saji, V., *Contemporary developments in corrosion inhibitors-Review of patents*. **Recent Patents on Corrosion Science**. 1 (2011) 63-71.
13. Smith, L., *Control of corrosion in oil and gas production tubing*. **British Corrosion Journal**. 34 (1999) 247-253.
14. Ahmad, Z., *Principles of corrosion engineering and corrosion control*. 2006: Elsevier.
15. Villamizar, W., M. Casales, J. Gonzalez-Rodriguez, and L. Martinez, *CO<sub>2</sub> corrosion inhibition by hydroxyethyl, aminoethyl, and amidoethyl imidazolines in water-oil mixtures*. **Journal of Solid State Electrochemistry**. 11 (2007) 619-629.

16. Yahaya, N., N.M. Noor, M.M. Din, and S.H.M. Nor, *Prediction of CO<sub>2</sub> corrosion growth in submarine pipelines*. **Malaysian Journal of Civil Engineering**. 21 (2009) 69-81.
17. Zardasti, L., N.M. Hanafiah, N.M. Noor, Y. Nordin, and A.S.A. Rashid. *The consequence assessment of gas pipeline failure due to corrosion*. in *Solid State Phenomena*. 2015. Trans Tech Publications.
18. Zakowski, K., K. Darowicki, J. Orlikowski, A. Jazdzewska, S. Krakowiak, M. Gruszka, and J. Banas, *Electrolytic corrosion of water pipeline system in the remote distance from stray currents, Case study*. **Case Studies in Construction Materials**. 4 (2016) 116-124.
19. Putilova, I.N., *Metallic corrosion inhibitors*. 1960: Pergamon Press.
20. Uhlig, H.H. and C. King, *Corrosion and corrosion control*. **Journal of the Electrochemical Society**. 119 (1972) 327-327.
21. Handbook, A., *Surface Engineering*. 1994: ASM International, Materials Park.
22. Anders, B., *100% Stainless-Pickling Handbook, Surface treatment of stainless steels*. 2009: Avesta Finishing Chemicals.
23. Dara, S.S. and S.D. Shete, *S. Chand's applied chemistry (According to the syllabus of 2nd semester University of Mumbai)*. 2010: S. Chand Publications.
24. Koch, G.H., M.P. Brongers, N.G. Thompson, Y.P. Virmani, and J.H. Payer, *Cost of corrosion in the United States, in Handbook of environmental degradation of materials*. 2005, Elsevier.
25. Bai, N., Q. Li, H. Dong, C. Tan, P. Cai, and L. Xu, *A versatile approach for preparing self-recovering superhydrophobic coatings*. **Chemical Engineering Journal**. 293 (2016) 75-81.
26. Banerjee, S., M. Wehbi, A. Manseri, A. Mehdi, A. Alaaeddine, A. Hachem, and B. Ameduri, *Poly (vinylidene fluoride) containing phosphonic acid as anticorrosion coating for steel*. **ACS applied materials & interfaces**. 9 (2017) 6433-6443.
27. Chaudhari, A.B., P.D. Tatiya, R.K. Hedao, R.D. Kulkarni, and V.V. Gite, *Polyurethane prepared from neem oil polyesteramides for self-healing anticorrosive coatings*. **Industrial & Engineering Chemistry Research**. 52 (2013) 10189-10197.
28. Liu, Y. and J. Liu, *Design of multifunctional SiO<sub>2</sub>-TiO<sub>2</sub> composite coating materials for outdoor sandstone conservation*. **Ceramics International**. 42 (2016) 13470-13475.

29. Praveen, B., T. Venkatesha, Y.A. Naik, and K. Prashantha, *Corrosion studies of carbon nanotubes-Zn composite coating*. **Surface and Coatings Technology**. 201 (2007) 5836-5842.
30. Cecchetto, L., D. Delabouglise, and J.-P. Petit, *On the mechanism of the anodic protection of aluminium alloy AA5182 by emeraldine base coatings: Evidences of a galvanic coupling*. **Electrochimica Acta**. 52 (2007) 3485-3492.
31. Kim, D.-K., S. Muralidharan, T.-H. Ha, J.-H. Bae, Y.-C. Ha, H.-G. Lee, and J. Scantlebury, *Electrochemical studies on the alternating current corrosion of mild steel under cathodic protection condition in marine environments*. **Electrochimica Acta**. 51 (2006) 5259-5267.
32. Subasri, R., T. Shinohara, and K. Mori, *Modified TiO<sub>2</sub> coatings for cathodic protection applications*. **Science and Technology of Advanced Materials**. 6 (2005) 501.
33. Umoren, S., *Polymers as corrosion inhibitors for metals in different media-A review*. **The Open Corrosion Journal**. 2 (2009) 175-188.
34. Loto, R., C. Loto, and M. Ranyaoa, *Pyrimidine derivatives as environmentally-friendly corrosion inhibitors-A review*. **International Journal of Physical Sciences**. 7 (2012) 2697-2705.
35. Sastry, K., R. Narayanan, C. Shamantha, S. Sundaresan, S. Seshadri, V. Radhakrishnan, K. Iyer, and S. Sundararajan, *Stress corrosion cracking of maraging steel weldments*. **Materials Science and Technology**. 19 (2003) 375-381.
36. Mistry, B., N. Patel, S. Sahoo, and S. Jauhari, *Experimental and quantum chemical studies on corrosion inhibition performance of quinoline derivatives for MS in 1N HCl*. **Bulletin of Materials Science**. 35 (2012) 459-469.
37. El-Maksoud, S.A., *The influence of some Arylazobenzoyl acetonitrile derivatives on the behaviour of carbon steel in acidic media*. **Applied Surface Science**. 206 (2003) 129-136.
38. Wang, L., *Inhibition of mild steel corrosion in phosphoric acid solution by triazole derivatives*. **Corrosion Science**. 48 (2006) 608-616.
39. Koch, G.H., M.P. Brongers, N.G. Thompson, Y.P. Virmani, and J.H. Payer, *Corrosion cost and preventive strategies in the United States*. 2002.
40. Kesavan, D., M. Gopiraman, and N. Sulochana, *Green inhibitors for corrosion of metals: a review*. **Chemical Science Review and Letters**. 1 (2012) 1-8.
41. Olsson, C.A., P. Agarwal, M. Frey, and D. Landolt, *An XPS study of the adsorption of organic inhibitors on mild steel surfaces*. **Corrosion Science**. 42 (2000) 1197-1211.

42. McEwan, J. *Corrosion Control in Southern Africa*. in *Corrosion Institute of Southern Africa, Johannesburg, South Africa*. 2004.
43. Kamis, A., *Cost of corrosion, Bullet*. 1992, FKKKSA.
44. McConnell, R., *Volatile corrosion inhibitors offer effective protection for processing and shipment of metal-based products*. **Metal Finishing**. 106 (2008) 23-27.
45. Obi-Egbedi, N. and I. Obot, *Adsorption behavior and corrosion inhibitive potential of xanthene on mild steel/sulphuric acid interface*. **Arabian Journal of Chemistry**. 5 (2012) 121-133.
46. Senthilkumar, A., K. Tharini, and M. Sethuraman, *Studies on a few substituted piperidin-4-one oximes as corrosion inhibitor for mild steel in HCl*. **Journal of Materials Engineering and Performance**. 20 (2011) 969-977.
47. Umoren, S., I. Obot, E. Ebenso, P. Okafor, O. Ogbobe, and E. Oguzie, *Gum arabic as a potential corrosion inhibitor for aluminium in alkaline medium and its adsorption characteristics*. **Anti-Corrosion Methods And Materials**. 53 (2006) 277-282.
48. Hou, B., X. Li, X. Ma, C. Du, D. Zhang, M. Zheng, W. Xu, D. Lu, and F. Ma, *The cost of corrosion in China*. **NPJ Materials Degradation**. 1 (2017) 1-10.
49. Cardoso, M., S. Amaral, and E. Martini, *Temperature effect in the corrosion resistance of Ni-Fe-Cr alloy in chloride medium*. **Corrosion Science**. 50 (2008) 2429-2436.
50. Walsh, F., *Faraday and his laws of electrolysis*. **Bulletin of Electrochem**. 7 (1991) 481-489.
51. Fontana, M.G. and N.D. Greene, *Corrosion Engineering*. 1967: McGraw Hill.
52. Frumkin, A.N. *Proceedings of the symposium on rechargeable zinc batteries: Commemorating the 100th birthday of AN Frumkin*. 1996. The Electrochemical Society.
53. Pedefferri, P., *Corrosion Science and Engineering*. 2018: Springer International Publishing.
54. McCafferty, E., *Introduction to corrosion science*. 2010: Springer Science & Business Media.
55. Wagner, C. and W. Traud, *On the interpretation of corrosion processes by superimposing of Electro Chemical potential and the potential formation of mixed electrodes*. **Journal of Electrochemistry**. 44 (1938) 391-402.
56. Fontana, M.G., *Corrosion engineering*. 2005: Tata McGraw-Hill Education.
57. Sharma, A., G. Choudhary, A. Sharma, and S. Yadav, *Effect of temperature on inhibitory efficacy of Azadirachta indica fruit on acid corrosion of aluminum*.

- International Journal of Innovative Research in Science Engineering and Technology.** 2 (2013) 7982-7992.
58. Stansbury, E.E. and R.A. Buchanan, *Fundamentals of electrochemical corrosion*. 2000: ASM international.
59. Craig, B.D., R.A. Lane, and D.H. Rose, *Corrosion prevention and control: A program management guide for selecting materials*. 2006: Advanced Materials, Manufacturing, and Testing Information Analysis Center.
60. Mora, N., E. Cano, E. Mora, and J. Bastidas, *Influence of pH and oxygen on copper corrosion in simulated uterine fluid*. **Biomaterials**. 23 (2002) 667-671.
61. Roberge, P.R., *Handbook of Corrosion Engineering*. 2000: McGraw-Hill.
62. Shreir, L.L., G.T. Burstein, and R.A. Jarman, *Corrosion*. 1994: Butterworth Heinemann.
63. Berchmans, L.J., V. Sivan, and S.V. Iyer, *Eighth National Congress on Corrosion Control, in Kochi, Organised by NCCI*. 1998. p. 321-325.
64. Bonnel, A., F. Dabosi, C. Deslouis, M. Duprat, M. Keddou, and B. Tribollet, *Corrosion study of a carbon steel in neutral chloride solutions by impedance techniques*. **Journal of the Electrochemical Society**. 130 (1983) 753-761.
65. Nithya, A. and S. Rajendran, *Synergistic effect of ethylphosphonic acid-Zn<sup>2+</sup> system in controlling corrosion of carbon steel in chloride medium*. **Bulgarian Chemical Communications**. 42 (2010) 119-125.
66. Ouchrif, A., M. Zegmout, B. Hammouti, S. El-Kadiri, and A. Ramdani, *1,3-Bis (3-hydroxymethyl-5-methyl-1-pyrazole) propane as corrosion inhibitor for steel in 0.5 M H<sub>2</sub>SO<sub>4</sub> solution*. **Applied Surface Science**. 252 (2005) 339-344.
67. Perez, N., *Electrochemistry and corrosion science*. 2004: Springer.
68. Roberge, P.R., *Corrosion Engineering*. 2008: McGraw-Hill New York, NY, USA:.
69. Heidersbach, R., *Metallurgy and corrosion control in oil and gas production*. 2018: John Wiley & Sons.
70. Berchmans, L.J., V. Sivan, and S.V.K. Iyer, *Studies on triazole derivatives as inhibitors for the corrosion of muntz metal in acidic and neutral solutions*. **Materials Chemistry and Physics**. 98 (2006) 395-400.
71. Kalman, E., B. Varhegyi, I. Bako, I. Felhősi, F. Karman, and A. Shaban, *Corrosion Inhibition by 1-Hydroxy-ethane-1,1-diphosphonic acid-An electrochemical impedance spectroscopy study*. **Journal of the Electrochemical Society**. 141 (1994) 3357-3360.

72. Badiea, A. and K. Mohana, *Corrosion mechanism of low-carbon steel in industrial water and adsorption thermodynamics in the presence of some plant extracts*. **Journal of Materials Engineering and Performance**. 18 (2009) 1264-1271.
73. Lahhit, N., A. Bouyanzer, J.-M. Desjobert, B. Hammouti, R. Salghi, J. Costa, C. Jama, F. Bentiss, and L. Majidi, *Fennel (Foeniculum vulgare) essential oil as green corrosion inhibitor of carbon steel in hydrochloric acid solution*. **Portugaliae Electrochimica Acta**. 29 (2011) 127-138.
74. Obot, I. and N. Obi-Egbedi, *An interesting and efficient green corrosion inhibitor for aluminium from extracts of Chlomolaena odorata L. in acidic solution*. **Journal of Applied Electrochemistry**. 40 (2010) 1977-1984.
75. Obanijesu, E.O., V. Pareek, R. Gubner, and M.O. Tade, *Hydrate formation and its influence on natural gas pipeline internal corrosion*. **Nafta**. 62 (2011) 164-173.
76. Sherine, H.B. and A.J.A. Nasser, *Inhibition of corrosion of mild steel in well water by phenolic compounds*. (2014).
77. Munn, P., *Causes of copper corrosion in plumbing systems*. 2017: Foundation for Water Research.
78. Nazari, M.H., D. Bergner, X. Shi, and L. Fay, *Best practices for the prevention of corrosion of department of transportation equipment-A user's manual*. 2015.
79. McKay, R.J. and R. Worthington, *Corrosion resistance of metals and alloys*. 1936: Reinhold Publishing Corporation.
80. Fontana, M. and N. Greene, *Corrosion engineering, materials science and engineering series*. 1978: McGraw-Hill.
81. Lunder, O., J. Lein, S. Hesjevik, T.K. Aune, and K. Nişancioğlu, *Corrosion morphologies on magnesium alloy AZ91*. **Materials and Corrosion**. 45 (1994) 331-340.
82. Yamamoto, A., A. Watanabe, K. Sugahara, S. Fukumoto, and H. Tsubakino. *Applying a vapor deposition technique to improve corrosion resistance in magnesium alloys*. in *Proceedings of the second international conference on environment sensitive cracking and corrosion damage*. 2001. Nishiki Printing Ltd, ESCCD.
83. Andrews, N., L. Giourntas, A. Galloway, and A. Pearson, *Effect of impact angle on the slurry erosion-corrosion of Stellite 6 and SS316*. **Wear**. 320 (2014) 143-151.
84. Zeng, L., S. Shuang, X. Guo, and G. Zhang, *Erosion-corrosion of stainless steel at different locations of a 90° elbow*. **Corrosion Science**. 111 (2016) 72-83.

85. Islam, M.A., Z.N. Farhat, E.M. Ahmed, and A. Alfantazi, *Erosion enhanced corrosion and corrosion enhanced erosion of API X-70 pipeline steel*. **Wear**. 302 (2013) 1592-1601.
86. Wang, Y., Z. Xing, Q. Luo, A. Rahman, J. Jiao, S. Qu, Y. Zheng, and J. Shen, *Corrosion and erosion-corrosion behaviour of activated combustion high-velocity air fuel sprayed Fe-based amorphous coatings in chloride-containing solutions*. **Corrosion Science**. 98 (2015) 339-353.
87. Houghton, C.J. and R.V. Westermar, *Downhole corrosion mitigation in Ekofisk (North Sea) field*. **Materials Performance**. 22 (1983) 16-22.
88. McCoy, J.W., *The chemical treatment of cooling water*. 1974: Chemical Publishing Company New York.
89. Bardal, E., *Corrosion and protection*. 2007: Springer Science & Business Media.
90. Bill, R., *Review of factors that influence fretting wear*, in *Materials Evaluation Under Fretting Conditions*. 1982, ASTM International.
91. Bogaerts, W.F. and K. Agema, *Active library on corrosion*. 1994: Elsevier.
92. Frankel, G.S., *Pitting corrosion of metals: a review of critical factors*. **Journal of the Electrochemical Society**. 145 (1998) 2186-2198.
93. Pistorius, P.S. and G.T. Burstein, *Growth of corrosion pits on stainless steel in chloride solution containing dilute sulfate*. **Corrosion Science**. 33 (1992) 1885-1897.
94. Burstein, G.T., C. Liu, R.M. Souto, and S.P. Vines, *Origin of pitting corrosion*. **Corrosion Engineering Science and Technology**. 39 (2004) 25-30.
95. Eddy, N.O., S.R. Stoyanov, and E.E. Ebenso, *Fluoroquinolones as corrosion inhibitors for mild steel in acidic medium; experimental and theoretical studies*. **International Journal of Electrochemical Science**. 5 (2010) 1127-1150.
96. Dehri, I. and M. Özcan, *The effect of temperature on the corrosion of mild steel in acidic media in the presence of some sulphur-containing organic compounds*. **Materials Chemistry and Physics**. 98 (2006) 316-323.
97. Craig, B.D., *Fundamental aspects of corrosion films in corrosion science*. 2013: Springer Science & Business Media.
98. Ren, C., D. Liu, Z. Bai, and T. Li, *Corrosion behavior of oil tube steel in simulant solution with hydrogen sulfide and carbon dioxide*. **Materials Chemistry and Physics**. 93 (2005) 305-309.
99. Tang, L., G. Mu, and G. Liu, *The effect of neutral red on the corrosion inhibition of cold rolled steel in 1.0 M hydrochloric acid*. **Corrosion Science**. 45 (2003) 2251-2262.



100. Noor, E.A., *Temperature effects on the corrosion inhibition of mild steel in acidic solutions by aqueous extract of fenugreek leaves*. **International Journal of Electrochemical Science**. 2 (2007) 996-1017.
101. Singh, A., I. Ahamad, V. Singh, and M.A. Quraishi, *Inhibition effect of environmentally benign Karanj (Pongamia pinnata) seed extract on corrosion of mild steel in hydrochloric acid solution*. **Journal of Solid State Electrochemistry**. 15 (2011) 1087-1097.
102. Frandsen, F.J., *Utilizing biomass and waste for power production-A decade of contributing to the understanding, interpretation and analysis of deposits and corrosion products*. **Fuel**. 84 (2005) 1277-1294.
103. Nielsen, H., F. Frandsen, K. Dam-Johansen, and L. Baxter, *The implications of chlorine-associated corrosion on the operation of biomass-fired boilers*. **Progress in Energy and Combustion Science**. 26 (2000) 283-298.
104. Arya, C. and P. Vassie, *Influence of cathode-to-anode area ratio and separation distance on galvanic corrosion currents of steel in concrete containing chlorides*. **Cement and Concrete Research**. 25 (1995) 989-998.
105. Thirumoolan, D., V.A. Katkar, G. Gunasekaran, T. Kanai, and K.A. Basha, *Hyperbranched poly (cyanurateamine): a new corrosion inhibitor for mild steel in hydrochloric acid medium*. **Progress in Organic Coatings**. 77 (2014) 1253-1263.
106. Fahlman, M., S. Jasty, and A. Epstein, *Corrosion protection of iron/steel by emeraldine base polyaniline: an X-ray photoelectron spectroscopy study*. **Synthetic Metals**. 85 (1997) 1323-1326.
107. Ferreira, E., C. Giacomelli, F. Giacomelli, and A. Spinelli, *Evaluation of the inhibitor effect of L-ascorbic acid on the corrosion of mild steel*. **Materials Chemistry and Physics**. 83 (2004) 129-134.
108. Li, W.-h., Q. He, S.-t. Zhang, C.-l. Pei, and B.-r. Hou, *Some new triazole derivatives as inhibitors for mild steel corrosion in acidic medium*. **Journal of Applied Electrochemistry**. 38 (2008) 289-295.
109. Zarrok, H., H. Oudda, A. El Midaoui, A. Zarrouk, B. Hammouti, M.E. Touhami, A. Attayibat, S. Radi, and R. Touzani, *Some new bipyrazole derivatives as corrosion inhibitors for C38 steel in acidic medium*. **Research on Chemical Intermediates**. 38 (2012) 2051-2063.
110. Lomnitski, L., M. Bergman, A. Nyska, V. Ben-Shaul, and S. Grossman, *Composition, efficacy, and safety of spinach extracts*. **Nutrition and cancer**. 46 (2003) 222-231.

111. Jamil, S., N. Qudisia, and S. Mehboobus, *Centella asiatica (Linn.) urban-A review*. **Natural Product Radiance**. 6 (2007) 158-170.
112. Quraishi, M., M. Rafiquee, S. Khan, and N. Saxena, *Corrosion inhibition of aluminium in acid solutions by some imidazoline derivatives*. **Journal of Applied Electrochemistry**. 37 (2007) 1153-1162.
113. Singh, A. and M. Quraishi, *Piroxicam; A novel corrosion inhibitor for mild steel corrosion in HCl acid solution*. **Journal of Materials and Environmental Science**. 1 (2010) 101-110.
114. Ebenso, E.E., I.B. Obot, and L. Murulana, *Quinoline and its derivatives as effective corrosion inhibitors for mild steel in acidic medium*. **International Journal of Electrochemical Science**. 5 (2010) 1574-1586.
115. Umoren, S., I. Obot, E. Ebenso, and N. Obi-Egbedi, *The Inhibition of aluminium corrosion in hydrochloric acid solution by exudate gum from Raphia hookeri*. **Desalination**. 247 (2009) 561-572.
116. Garverick, L., *Corrosion in the petrochemical industry*. 1994: ASM international.
117. Butlin, K., W. Vernon, and L. Whiskin, *Investigations on underground corrosion; Special report*, in *Iron and Steel Institute*. 1952: London. p. 29.
118. Didei, I., *Geoelectrical and physicochemical investigation of corrosive nature of soil towards buried pipelines in koloand environs*. **IOSR Journal of Applied Geology and Geophysics**. 6 (2018) 1-9.
119. Ayeni, F., I. Madugu, P. Sukop, A. Ihom, O. Alabi, R. Okara, and M. Abdulwahab, *Effect of aqueous extracts of bitter leaf powder on the corrosion inhibition of Al-Si alloy in 0.5 M caustic soda solution*. **Journal of Minerals and Materials characterization and Engineering**. 11 (2012) 667-670.
120. Bouyanzer, A., B. Hammouti, and L. Majidi, *Pennyroyal oil from Mentha pulegium as corrosion inhibitor for steel in 1 M HCl*. **Materials Letters**. 60 (2006) 2840-2843.
121. El-Sayed, M., O.Y. Mansour, I.Z. Selim, and M.M. Ibrahim, *Identification and utilization of banana plant juice and its pulping liquor as anti-corrosive materials*. 60 (2001) 738-747.
122. Loto, C., *The effect of mango bark and leaf extract solution additives on the corrosion inhibition of mild steel in dilute sulphuric acid-part 1*. **Corrosion Prevention and Control**. 48 (2001) 38-41.

123. Okafor, P., M.E. Ikpi, I. Uwah, E. Ebenso, U. Ekpe, and S. Umoren, *Inhibitory action of Phyllanthus amarus extracts on the corrosion of mild steel in acidic media*. **Corrosion Science**. 50 (2008) 2310-2317.
124. Satapathy, A., G. Gunasekaran, S. Sahoo, K. Amit, and P. Rodrigues, *Corrosion inhibition by Justicia gendarussa plant extract in hydrochloric acid solution*. **Corrosion Science**. 51 (2009) 2848-2856.
125. Uhlig, H.H., *The cost of corrosion to the United States*. **Chemical and Engineering News**. 27 (1949) 2764.
126. Javaherdashti, R., *How corrosion affects industry and life*. **Anti-Corrosion Methods And Materials**. 47 (2000) 30-34.
127. Bennet, L.H., J. Kruger, R.I. Parker, E. Passiglia, C. Reimann, A.W. Ruff, H. Yakowitz, and E.B. Berman, *Economic effects of metallic corrosion in the United States*, in *National Bureau of Standards Special Publication*. 1978.
128. Narayan, R., *An introduction to metallic corrosion and its prevention*. 1990: Oxford Publishing Company.
129. Haque, J., V. Srivastava, C. Verma, and M. Quraishi, *Experimental and quantum chemical analysis of 2-amino-3-((4-((S)-2-amino-2-carboxyethyl)-1H-imidazol-2-yl)thio) propionic acid as new and green corrosion inhibitor for mild steel in 1 M hydrochloric acid solution*. **Journal of Molecular Liquids**. 225 (2017) 848-855.
130. Thirumangalam Karunanithi, B. and J. Chellappa, *Adsorption and inhibition properties of Tephrosia Purpurea as corrosion inhibitor for mild steel in sulphuric acid solution*. **Journal of Dispersion Science and Technology**. 40 (2019) 1-10.
131. Gerengi, H., H. Goksu, and P. Slepski, *The inhibition effect of mad honey on corrosion of 2007-type aluminium alloy in 3.5% NaCl solution*. **Materials Research**. 17 (2014) 255-264.
132. Al-Mhyawi, S.R., *Corrosion inhibition of aluminum in 0.5 M HCl by garlic aqueous extract*. **Oriental Journal of Chemistry**. 30 (2014) 541-552.
133. Fouda, A.E.-A.S., M.M. Farahat, and M. Abdallah, *Cephalosporin antibiotics as new corrosion inhibitors for nickel in HCl solution*. **Research on Chemical Intermediates**. 40 (2014) 1249-1266.
134. Oki, M., *Corrosion of Aluminium in Chloride Environments*. **International Research Journal of Pure and Applied Chemistry**. 3 (2013) 147.
135. Nisancioglu, K., *Corrosion of aluminium alloys*. **Norwegian Institute of Technology, SINTEF Metallurgy**. 3 (1992) 239-259.

136. Raju, P.V.K., K.A. Reddy, J.B. Rao, N. Bhargava, and M.I. Reddy, *Study of corrosion of Al-Cu hypoeutectic alloys and Al-Cu composite fabricated using stir casting technique. Materials Today: Proceedings.* 5 (2018) 1776-1784.
137. Abdulwahab, M., A. Popoola, O. Oladijo, C. Loto, and O. Oladijo, *Corrosion resistance of AA2036 and AA7075-T651 in contaminated acid chloride environments. Asian Journal of Chemistry.* 28 (2016) 1453.
138. Kciuk, M., A. Kurc, and J. Szewczenko, *Structure and corrosion resistance of aluminium AlMg2.5; AlMg5Mn and AlZn5Mg1 alloys. Journal of Achievements in Materials and Manufacturing Engineering.* 41 (2010) 74-81.
139. Kciuk, M. and S. Tkaczyk, *Structure, mechanical properties and corrosion resistance of AlMg5 and AlMg1Si1 alloys. Journal of Achievements in Materials and Manufacturing Engineering.* 21 (2007) 39-42.
140. Tkaczyk, S. and M. Kciuk. *The stress corrosion resistance investigations of aluminium AlMg5 alloy.* in *Proceedings of 12th International Scientific Conference: Achievements in Mechanical & Materials Engineering* 2003. Gliwice-Zakopane.
141. Ameer, M., A. Ghoneim, and A. Fekry, *Electrochemical corrosion inhibition of Al-Si alloy in phosphoric acid. International Journal of Electrochemical Science.* 7 (2012) 4418-4431.
142. Chaubey, N., M. Quraishi, and E.E. Ebenso, *Corrosion inhibition of aluminium alloy in alkaline media by Neolamarkia Cadamba Bark extract as a green inhibitor. International Journal of Electrochemical Science.* 10 (2015) 504 -518.
143. Hassan, R.M. and I.A. Zaafarany, *Kinetics of corrosion inhibition of aluminum in acidic media by water-soluble natural polymeric pectates as anionic polyelectrolyte inhibitors. Materials.* 6 (2013) 2436-2451.
144. Sangeetha, M., S. Rajendran, J. Sathiyabama, and A. Krishnavenic, *Inhibition of corrosion of aluminium and its alloys by extracts of green inhibitors. Portugaliae Electrochimica Acta.* 31 (2013) 41-52.
145. Szklarska-Smialowska, Z., *Pitting corrosion of aluminum. Corrosion Science.* 41 (1999) 1743-1767.
146. Salah, B.A., M.G. Abd-El-Nasser, and A.T. Kandil, *Evaluation of some synthesized compounds as corrosion inhibitors in oil fields. Global Journal of Science Frontier Research Chemistry.* 12 (2012) 1-49.

147. Hurley, B.L., *Characterization and growth analysis of two types of thin films formed on copper surfaces: an inorganic chromium containing film and an organic film formed via reduction of diazonium ions*. 2004, The Ohio State University.
148. Sulaiman, N. and M. Kassim, *Study of thermodynamic characterization and adsorption properties of stingless bee honey and honey bee honey in 1 M phosphoric acid*. 2016, University of Science, Malaysia.
149. Sangeetha, M., S. Rajendran, T. Muthumegala, and A. Krishnaveni, *Green corrosion inhibitors-An overview*. **Zastita Materijala**. 52 (2011) 3-19.
150. Kumar, H. and V. Yadav, *Corrosion characteristics of mild steel under different atmospheric conditions by vapour phase corrosion inhibitors*. **American Journal of Materials Science and Engineering**. 1 (2013) 34-39.
151. Boffardi, B., *Corrosion inhibitors in the water treatment industry*. **ASM Handbook**. 13 (2003) 891-906.
152. Zhao, X., P. Gong, G. Qiao, J. Lu, X. Lv, and J. Ou, *Brillouin corrosion expansion sensors for steel reinforced concrete structures using a fiber optic coil winding method*. **Sensors**. 11 (2011) 10798-10819.
153. Wilcox, G. and D. Gabe, *Electrodeposited zinc alloy coatings*. **Corrosion Science**. 35 (1993) 1251-1258.
154. Pistofidis, N., G. Vourlias, S. Konidaris, E. Pavlidou, A. Stergiou, and G. Stergioudis, *Microstructure of zinc hot-dip galvanized coatings used for corrosion protection*. **Materials Letters**. 60 (2006) 786-789.
155. Dake, L., D. Baer, and J. Zachara, *Auger parameter measurements of zinc compounds relevant to zinc transport in the environment*. **Surface and Interface Analysis**. 14 (1989) 71-75.
156. Cunningham, B.C., M.G. Mulkerrin, and J.A. Wells, *Dimerization of human growth hormone by zinc*. **Science**. 253 (1991) 545-548.
157. Hinton, B. and L. Wilson, *The corrosion inhibition of zinc with cerous chloride*. **Corrosion Science**. 29 (1989) 967-985.
158. Tracton, A.A., *Coatings materials and surface coatings*. 2006: CRC Press.
159. Qian, Y., Y. Li, S. Jungwirth, N. Seely, Y. Fang, and X. Shi, *The application of anti-corrosion coating for preserving the value of equipment asset in chloride-laden environments-A review*. **International Journal of Electrochemical Science**. 10 (2015) 10756-10780.

160. Rosenfeld, I.L., *Whitney award lecture: New data on the mechanism of metals protection with inhibitors*. **Corrosion**. 37 (1981) 371-377.
161. Gautam, M.K., *Study of some triazoles as corrosion inhibitors for mild steel in acidic medium*. (2012).
162. Davis, J., *Corrosion: understanding the basics*. 2000. Materials Park, Ohio: ASM International.
163. Lakshmi Prabha, K., *Influence of some plant leaves extracts on corrosion inhibition of aluminium in alkaline medium*. (2012).
164. Agrawal, Y., J. Talati, M. Shah, M. Desai, and N. Shah, *Schiff bases of ethylenediamine as corrosion inhibitors of zinc in sulphuric acid*. **Corrosion Science**. 46 (2004) 633-651.
165. Ehteshamzade, M., T. Shahrabi, and M. Hosseini, *Inhibition of copper corrosion by self-assembled films of new Schiff bases and their modification with alkanethiols in aqueous medium*. **Applied Surface Science**. 252 (2006) 2949-2959.
166. El Rehim, S.S.A., H.H. Hassan, and M.A. Amin, *Corrosion inhibition of aluminum by 1, 1 (lauryl amido) propyl ammonium chloride in HCl solution*. **Materials Chemistry and Physics**. 70 (2001) 64-72.
167. Migahed, M., *Electrochemical investigation of the corrosion behaviour of mild steel in 2 M HCl solution in presence of 1-dodecyl-4-methoxy pyridinium bromide*. **Materials Chemistry and Physics**. 93 (2005) 48-53.
168. Mathiazhagan, A. *Corrosion management for effective mitigation of corrosion in ships- Overview*. in *3rd international conference on information and financial engineering*. 2011. International Association of Computer Science and Information Technology.
169. Nalli, K., *Appendix VI: Corrosion and its mitigation in the oil and gas industries*. **Process Plant Equipment: Operation, Control, and Reliability**. (2012) 673-679.
170. Papavinasam, S., R.W. Revie, M. Attard, A. Demoz, J.C. Donini, and K. Michaelian. *Standardized methodology for inhibitor evaluation and qualification for pipeline applications*. in *2000 3rd international pipeline conference*. 2000. American Society of Mechanical Engineers.
171. Azim, S.S., S. Muralidharan, S.V. Iyer, B. Muralidharan, and T. Vasudevan, *Synergistic influence of iodide ions on inhibition of corrosion of mild steel in H<sub>2</sub>SO<sub>4</sub> by N-phenyl thiourea*. **British Corrosion Journal**. 33 (1998) 297-301.

172. Bentiss, F., M. Lagrenee, M. Traisnel, and J. Hornez, *Corrosion inhibition of mild steel in 1 M hydrochloric acid by 2,5-bis (2-aminophenyl)-1,3,4-oxadiazole*. **Corrosion**. 55 (1999) 968-976.
173. Bentiss, F., M. Traisnel, and M. Lagrenee, *The substituted 1,3,4-oxadiazoles-A new class of corrosion inhibitors of mild steel in acidic media*. **Corrosion Science**. 42 (2000) 127-146.
174. Boffardi, B.P., *Control of environmental variables in water-recirculating systems*. **ASM Handbook**. 13 (1987) 487-497.
175. Cisse, M., B. Zerga, F. El Kalai, M.E. Touhami, M. Sfaira, M. Taleb, B. Hammouti, N. Benchat, S. El Kadiri, and A.T. Benjelloun, *Two dipodal pyridin-pyrazol derivatives as efficient inhibitors of mild steel corrosion in HCl solution-part i: Electrochemical study*. **Surface Review and Letters**. 18 (2011) 303-313.
176. Hackerman, N. and E. Snavely, *Inhibitors corrosion basics*. 1984: NACE International.
177. Kemkhadze, V., S. Balezin, and V.J. Bregman, *Corrosion inhibitors*. 1963: MacMillans. 192.
178. Musa, A.Y., R.T. Jalgham, and A.B. Mohamad, *Molecular dynamic and quantum chemical calculations for phthalazine derivatives as corrosion inhibitors of mild steel in 1 M HCl*. **Corrosion Science**. 56 (2012) 176-183.
179. Nataraja, S., T. Venkatesha, and H. Tandon, *Computational and experimental evaluation of the acid corrosion inhibition of steel by tacrine*. **Corrosion Science**. 60 (2012) 214-223.
180. Sharma, S. and R. Chaudhary, *Inhibitive action of methyl red towards corrosion of mild steel in acids*. **Bulletin of Electrochemistry**. 16 (2000) 267-271.
181. Stone, P.J., *Corrosion inhibitors for oil and gas production*. **ASM Handbook**. 13 (1987) 478-484.
182. Thomas, J., *The mechanism of corrosion prevention by inhibitors*, in *Corrosion*. 1994, Elsevier. p. 17-40.
183. Yurt, A., A. Balaban, S.U. Kandemir, G. Bereket, and B. Erk, *Investigation on some Schiff bases as HCl corrosion inhibitors for carbon steel*. **Materials Chemistry and Physics**. 85 (2004) 420-426.
184. Al-Amoudi, O.S.B., M. Maslehuddin, A. Lashari, and A.A. Almusallam, *Effectiveness of corrosion inhibitors in contaminated concrete*. **Cement and Concrete Composites**. 25 (2003) 439-449.

185. Vasanth, K., *Corrosion inhibition in naval vessels*. **Corrosion/96, paper**. (1996).
186. Hamner, N. and C. Nathan, *Corrosion Inhibitors*. 1973: NACE Houston.
187. Nestle, A. and C. Nathan, *Corrosion inhibitors in petroleum production primary recovery, in Corrosion Inhibitors*. **NACE Publication**. 12 (1973) 61-75.
188. Alberty, R.A., *Physical chemistry*. 1987: John Wiley & Sons.
189. Cotton, A.F., G. Wilkinson, M. Bochmann, and C.A. Murillo, *Advanced inorganic chemistry*. 1999: Wiley.
190. Beaunier, L., *Corrosion of grain boundaries: initiation processes and testing*. **Le Journal de Physique Colloques**. 43 (1982) 271-282.
191. Aziz, P., *Application of the statistical theory of extreme values to the analysis of maximum pit depth data for aluminum*. **Corrosion**. 12 (1956) 35-46.
192. Bailey, J., F. Porter, and A. Pearson, *Aluminum and aluminum alloys, in corrosion*. **Newnes-Butterworths**. 1 (1976) 43-433.
193. Bockris, J.O.M., B.E. Conway, and R.E. White, *Modern aspects of electrochemistry*. 2012: Springer Science & Business Media.
194. Conway, B.E. and R. Greef, *Theory and principles of electrode processes*. 1966: The Electrochemical Society.
195. Foley, R., *Role of the chloride ion in iron corrosion*. **Corrosion**. 26 (1970) 58-70.
196. Bouklah, M., B. Hammouti, M. Lagrenee, and F. Bentiss, *Thermodynamic properties of 2,5-bis (4-methoxyphenyl)-1,3,4-oxadiazole as a corrosion inhibitor for mild steel in normal sulfuric acid medium*. **Corrosion Science**. 48 (2006) 2831-2842.
197. Durnie, W., R. De Marco, A. Jefferson, and B. Kinsella, *Development of a structure-activity relationship for oil field corrosion inhibitors*. **Journal of the Electrochemical Society**. 146 (1999) 1751-1756.
198. Kairi, N.I. and J. Kassim, *The effect of temperature on the corrosion inhibition of mild steel in 1 M HCl solution by curcuma longa extract*. **International Journal of Electrochemical Science**. 8 (2013) 7138-7155.
199. Ita, B. and O. Offiong, *Corrosion inhibitory properties of 4-phenylsemicarbazide and semicarbazide on mild steel in hydrochloric acid*. **Materials Chemistry and Physics**. 59 (1999) 179-184.
200. Bastidas, J., J. Polo, E. Cano, and C. Torres, *Tributylamine as corrosion inhibitor for mild steel in hydrochloric acid*. **Journal of materials science**. 35 (2000) 2637-2642.
201. El Rehim, A., *Corrosion inhibition and adsorption behaviour of 4-aminoantipyrine on mild steel in H<sub>2</sub>SO<sub>4</sub>*. **Corrosion Prevention and Control**. 46 (1999) 157-62.



202. El-Rehim, S.A., M.A. Ibrahim, and K. Khaled, *4-Aminoantipyrine as an inhibitor of mild steel corrosion in HCl solution*. **Journal of Applied Electrochemistry**. 29 (1999) 593-599.
203. Hariharaputhran, R., A. Subramanian, A. Antony, P. Sankar, A. Gopalan, T. Vasudevan, and S.V. Iyer, *Influence of substituent groups on performance of N-benzylidene phenylamine-N-oxide as corrosion inhibitor of mild steel in acidic solutions*. **British Corrosion Journal**. 33 (1998) 214-218.
204. Muralidharan, S. and S. Iyer, *Pyrrrole and its derivatives as inhibitors for the corrosion of mild steel in acidic solutions*. **Journal of Electrochemical Society of India**. 48 (1999) 113-120.
205. Quraishi, M., J. Rawat, and M. Ajmal, *Dithiobiurets: a novel class of acid corrosion inhibitors for mild steel*. **Journal of Applied Electrochemistry**. 30 (2000) 745-751.
206. Al-Mayout, A., A. Al-Suhybani, and A. Al-Ameery, *Corrosion inhibition of 304SS in sulfuric acid solutions by 2-methyl benzoazole derivatives*. **Desalination**. 116 (1998) 25-33.
207. Lazarova, E., T. Yankova, and G. Neykov, *Electrochemical study of the adsorption of n-phenylmaleimide and its p-substituted derivatives on iron in sulfuric acid solutions*. **Bulgarian Chemical Communications**. 28 (1995) 647-660.
208. Touham, F., A. Aouniti, Y. Abed, B. Hammouti, S. Kertit, and A. Ramdani, *New pyrazolic compounds as corrosion inhibitors for Iron Armco in HCl media*. **Bulletin of Electrochemistry**. 16 (2000) 245-249.
209. Jiajian, C., C. Dianzhen, and C. Chu'nan, *Inhibition and desorption behaviour of N, N-dipropoxy methyl amine trimethyl phosphonate in hydrochloric acid*. **Bulletin of Electrochemistry**. 13 (1997) 13-17.
210. Anbarasi, M., S. Rajendran, M. Pandiarajan, and A. Krishnaveni, *An encounter with corrosion inhibitors*. **European Chemical Bulletin**. 2 (2013) 197-207.
211. Kar, B., *Study of mitigation of corrosion rate of mild steel using green inhibitors*. 2010.
212. West, J.M., *Basic corrosion and oxidation*. 1986: John Wiley & Sons.
213. Leng, A. and M. Stratmann, *The inhibition of the atmospheric corrosion of iron by vapour-phase-inhibitors*. **Corrosion Science**. 34 (1993) 1657-1683.
214. Desimone, M., G. Grundmeier, G. Gordillo, and S. Simison, *Amphiphilic amido-amine as an effective corrosion inhibitor for mild steel exposed to CO<sub>2</sub> saturated solution: polarization, EIS and PM-IRRAS studies*. **Electrochimica Acta**. 56 (2011) 2990-2998.

215. Ash, M. and I. Ash, *Handbook of corrosion inhibitors*. 2001: Synapse Information Resources Incorporated.
216. Bentiss, F., M. Lebrini, and M. Lagrenée, *Thermodynamic characterization of metal dissolution and inhibitor adsorption processes in mild steel/2, 5-bis (n-thienyl)-1, 3, 4-thiadiazoles/hydrochloric acid system*. **Corrosion Science**. 47 (2005) 2915-2931.
217. Mercer, A., *Corrosion inhibition: Principles and practice*. 1994: Butterworths-Heinemann.
218. Osokogwu, U. and E. Oghenekaro, *Evaluation of corrosion inhibitors effectiveness in oilfield production operations*. **international journal of scientific & technology research**. 1 (2012) 19-23.
219. Roberge, P.R., K. Szklarz, and V. Sastri. *Materials performance: sulphur and energy: Proceedings of the international symposium on materials performance*. in *Sulphur and energy*. 1992. Canadian Institute of Mining, Metallurgy and Petroleum.
220. Schweitzer, P.A., *Fundamentals of metallic corrosion: atmospheric and media corrosion of metals*. 2006: CRC press.
221. Vatsala, S., V. Bansal, D. Tuli, M. Rai, S. Jain, S. Srivastava, and A. Bhatnagar, *Gas chromatographic determination of residual hydrazine and morpholine in boiler feed water and steam condensates*. **Chromatographia**. 38 (1994) 456-460.
222. Koehan, F.L., D.E. Cole, and B.G. Dixon. *New low toxicity, multi-metal active vapor phase corrosion inhibitors*. in *Corrosion 99*. 1999. NACE International.
223. Jevremović, I., A. Debeljković, M. Singer, M. Achour, S. Nešić, and V. Misković-Stanković, *The mixture of dicyclohexylamine and oleylamine as corrosion inhibitor for mild steel in NaCl solution saturated with CO<sub>2</sub> under both continual immersion and top of the line corrosion*. **Journal of the Serbian Chemical Society**. 77 (2012) 1047-1061.
224. Poongothai, N., P. Rajendran, M. Natesan, and N. Palaniswamy, *Wood bark oils as vapour phase corrosion inhibitors for metals in NaCl and SO<sub>2</sub> environments*. **Indian Journal of Chemical Technology**. 12 (2005) 641-647.
225. Amira, W.E., A. Rahim, H. Osman, K. Awang, and P.B. Raja, *Corrosion inhibition of mild steel in 1 M HCl solution by Xylopiya ferruginea leaves from different extract and partitions*. **International Journal of Electrochemical Science**. 6 (2011) 2998-3016.
226. Abiola, O.K., N. Oforka, and E. Ebenso, *The inhibition of mild steel corrosion in an acidic medium by fruit juice of citrus paradisi*. **Journal of Corrosion Science and Engineering**. 1 (2004) 75-78.

227. Karthik, R., P. Muthukrishnan, S.-M. Chen, B. Jeyaprabha, and P. Prakash, *Anti-corrosion inhibition of mild steel in 1M hydrochloric acid solution by using Tiliacora acuminate leaves extract*. **International Journal of Electrochemical Science**. 10 (2015) 3707-3725.
228. Idowu, P.A.P. and F.O.S. Isaac, *Environmental failure of 2 M acid strength on zinc electroplated mild steel in the presence of Nicotiana glauca*. **International Journal of Electrochemical Science**. 6 (2011) 4798-4810.
229. Muhamath, B.M.A. and K. Kulanthai, *Inhibition effect of Parthenium hysterophorus L extracts on the corrosion of mild steel in sulphuric acid*. **Journal of Applied Sciences and Environmental Management**. 13 (2009) 27-36.
230. Subhashini, S., R. Rajalakshmi, A. Prithiba, and A. Mathina, *Corrosion mitigating effect of Cyamopsis Tetragonoloba seed extract on mild steel in acid medium*. **Journal of Chemistry**. 7 (2010) 1133-1137.
231. Dahmani, M., A. Et-Touhami, S. Al-Deyab, B. Hammouti, and A. Bouyanzer, *Corrosion inhibition of C38 steel in 1M HCl: A comparative study of Black pepper extract and its isolated piperine*. **International Journal of Electrochemical Science**. 5 (2010) 1060-1069.
232. Rajendran, A., *Isolation, characterization, pharmacological and corrosion inhibition studies of flavonoids obtained from nerium oleander and tecoma stans*. **International Journal of PharmTech Research**. 3 (2011) 1005-1013.
233. Bregman, J., *Metallic Corrosion Inhibitors*. 1963, Pergamon Press, New York.
234. Antonijevic, M. and M. Petrovic, *Copper corrosion inhibitors-A review*. **International Journal of Electrochemical Science**. 3 (2008) 1-28.
235. Tomashov, N.D., *Passivity and protection of metals against corrosion*. 2012: Springer Science & Business Media.
236. Levy, M., *Anodic behavior of titanium and commercial alloys in sulfuric acid*. **Corrosion**. 23 (1967) 236-244.
237. Sedriks, A., J. Green, and D. Novak, *Electrochemical behavior of Ti-Ni alloys in acidic chloride solutions*. **Corrosion**. 28 (1972) 137-142.
238. Chirkunov, A. and Y. Kuznetsov, *Corrosion inhibitors in cooling water systems*. Mineral Scales and Deposits. 2015: Elsevier. 85-105.
239. Hartwick, D., *Water treatment in closed systems*. **ASHRAE Journal**. 43 (2001) 30-43.
240. Meng, Y., W. Ning, B. Xu, W. Yang, K. Zhang, Y. Chen, L. Li, X. Liu, J. Zheng, and Y. Zhang, *Inhibition of mild steel corrosion in hydrochloric acid using two novel*

- pyridine Schiff base derivatives-A comparative study of experimental and theoretical results.* **RSC Advances.** 7 (2017) 43014-43029.
241. Krim, O., A. Elidrissi, B. Hammouti, A. Ouslim, and M. Benkaddour, *Synthesis, characterization, and comparative study of pyridine derivatives as corrosion inhibitors of mild steel in HCl medium.* **Chemical Engineering Communications.** 196 (2009) 1536-1546.
242. Oguzie, E.E., Y. Li, S.G. Wang, and F. Wang, *Understanding corrosion inhibition mechanisms-experimental and theoretical approach.* **Rsc Advances.** 1 (2011) 866-873.
243. Brycki, B.E., I.H. Kowalczyk, A. Szulc, O. Kaczerewska, and M. Pakiet, *Organic corrosion inhibitors.* Corrosion inhibitors, principles and recent applications. 2017: IntechOpen.
244. Likhanova, N.V., M.A. Domínguez-Aguilar, O. Olivares-Xometl, N. Nava-Entzana, E. Arce, and H. Dorantes, *The effect of ionic liquids with imidazolium and pyridinium cations on the corrosion inhibition of mild steel in acidic environment.* **Corrosion Science.** 52 (2010) 2088-2097.
245. Lin, P.-C., I.-W. Sun, J.-K. Chang, C.-J. Su, and J.-C. Lin, *Corrosion characteristics of nickel, copper, and stainless steel in a Lewis neutral chloroaluminate ionic liquid.* **Corrosion Science.** 53 (2011) 4318-4323.
246. Atta, A., G. El-Mahdy, H. Al-Lohedan, and A. Ezzat, *A new green ionic liquid-based corrosion inhibitor for steel in acidic environments.* **Molecules.** 20 (2015) 11131-11153.
247. Zhang, Q. and Y. Hua, *Corrosion inhibition of mild steel by alkylimidazolium ionic liquids in hydrochloric acid.* **Electrochimica Acta.** 54 (2009) 1881-1887.
248. Tüken, T., F. Demir, N. Kıcır, G. Sığırcık, and M. Erbil, *Inhibition effect of 1-ethyl-3-methylimidazolium dicyanamide against steel corrosion.* **Corrosion Science.** 59 (2012) 110-118.
249. Ali, A., O. Abdel Salam, A. Waheed, and R. Abdel-Karim. *Corrosion inhibition of carbon steel in cooling system media by non-toxic linear sodium octanoate.* in *17th international conference on nuclear engineering.* 2010. American Society of Mechanical Engineers Digital Collection.
250. McMurry, J.E., *Organic chemistry.* 2016: Cengage Learning.
251. Spek, A.L., *Structure validation in chemical crystallography.* **Acta Crystallographica Section D: Biological Crystallography.** 65 (2009) 148-155.

252. Fujita, M., *Molecular self-assembly: organic versus inorganic approaches*. 2003: Springer.
253. Meyer, R., T.-k. Ha, H. Frei, and H. Günthard, *Acetic acid monomer: Ab initio study, barrier to proton tunnelling, and infrared assignment*. **Chemical Physics**. 9 (1975) 393-402.
254. Vishwanatham, S. and A. Kumar, *Corrosion inhibition of mild steel in binary acid mixture*. **Corrosion Reviews**. 23 (2005) 181-194.
255. Shivakumar, S.S. and K.N. Mohana, *Corrosion inhibition character of Azure B for mild steel in hydrochloric acid solution*. **International Journal of Electrochemical Science**. 7 (2012) 1620-1638.
256. Shaker, N., E. Badr, and E. Kandeel, *Adsorption and inhibitive properties of fatty imidazoline surfactants on mild steel*. **Pelagia Research Library. Der Chemica Sinica**. 2 (2011) 26-35.
257. Quraishi, M. and D. Jamal, *Inhibition of mild steel corrosion in the presence of fatty acid triazoles*. **Journal of Applied Electrochemistry**. 32 (2002) 425-430.
258. Popova, A., M. Christov, S. Raicheva, and E. Sokolova, *Adsorption and inhibitive properties of benzimidazole derivatives in acid mild steel corrosion*. **Corrosion Science**. 46 (2004) 1333-1350.
259. Mohana, K., S. Shivakumar, and A. Badiea, *Inhibition of mild steel corrosion in 0.25 M Sulphuric acid solution by Imatinib Mesylate*. **Journal of the Korean Chemical Society**. 55 (2011) 364-372.
260. Hart, K., N. Oforika, and A. James, *N-[[2-Pyridine-2-azo)-5-Hydroxyl] Phenyl]-4-Methoxy benzilidenimine (LPYA) as a corrosion inhibitor of mild steel in 0.5 M HCl*. **Advances in Applied Science Research**. 2 (2011) 14-20.
261. Singh, A.K. and M. Quraishi, *Effect of Cefazolin on the corrosion of mild steel in HCl solution*. **Corrosion Science**. 52 (2010) 152-160.
262. Raman, A. and P. Labine, *Reviews on corrosion inhibitor science and technology*. **National Association of Corrosion Engineers** (1993).
263. Hosseini, M., S.F. Mertens, M. Ghorbani, and M.R. Arshadi, *Asymmetrical Schiff bases as inhibitors of mild steel corrosion in sulphuric acid media*. **Materials Chemistry and Physics**. 78 (2003) 800-808.
264. Malik, M.A., M.A. Hashim, F. Nabi, S.A. Al-Thabaiti, and Z. Khan, *Anti-corrosion ability of surfactants-A review*. **International Journal of Electrochemical Science**. 6 (2011) 1927-1948.

265. Bouklah, M., N. Benchat, B. Hammouti, A. Aouniti, and S. Kertit, *Thermodynamic characterisation of steel corrosion and inhibitor adsorption of pyridazine compounds in 0.5 M H<sub>2</sub>SO<sub>4</sub>*. **Materials Letters**. 60 (2006) 1901-1905.
266. Ormellese, M., L. Lazzari, S. Goidanich, G. Fumagalli, and A. Brenna, *A study of organic substances as inhibitors for chloride-induced corrosion in concrete*. **Corrosion Science**. 51 (2009) 2959-2968.
267. Wombacher, F., U. Maeder, and B. Marazzani, *Aminoalcohol based mixed corrosion inhibitors*. **Cement and Concrete Composites**. 26 (2004) 209-216.
268. Söylev, T.A. and M. Richardson, *Corrosion inhibitors for steel in concrete: State-of-the-art report*. **Construction and Building Materials**. 22 (2008) 609-622.
269. Gaidis, J.M., *Chemistry of corrosion inhibitors*. **Cement and Concrete Composites**. 26 (2004) 181-189.
270. Kern, P. and D. Landolt, *Adsorption of organic corrosion inhibitors on iron in the active and passive state. A replacement reaction between inhibitor and water studied with the rotating quartz crystal microbalance*. **Electrochimica Acta**. 47 (2001) 589-598.
271. Bobina, M., A. Kellenberger, J.-P. Millet, C. Muntean, and N. Vaszilcsin, *Corrosion resistance of carbon steel in weak acid solutions in the presence of l-histidine as corrosion inhibitor*. **Corrosion Science**. 69 (2013) 389-395.
272. Amin, M.A., K. Khaled, Q. Mohsen, and H. Arida, *A study of the inhibition of iron corrosion in HCl solutions by some amino acids*. **Corrosion Science**. 52 (2010) 1684-1695.
273. Bastidas, D.M., E. Cano, and E. Mora, *Volatile corrosion inhibitors: a review*. **Anti-Corrosion Methods And Materials**. 52 (2005) 71-77.
274. Kondo, H., *Protic ionic liquids with ammonium salts as lubricants for magnetic thin film media*. **Tribology Letters**. 31 (2008) 211-218.
275. Rammelt, U., S. Koehler, and G. Reinhard, *Use of vapour phase corrosion inhibitors in packages for protecting mild steel against corrosion*. **Corrosion Science**. 51 (2009) 921-925.
276. Vuorinen, E. and W. Skinner, *Amine carboxylates as vapour phase corrosion inhibitors*. **British Corrosion Journal**. 37 (2002) 159-160.
277. Bommersbach, P., C. Alemany-Dumont, J.-P. Millet, and B. Normand, *Formation and behaviour study of an environment-friendly corrosion inhibitor by electrochemical methods*. **Electrochimica Acta**. 51 (2005) 1076-1084.

278. Kohler, F., H. Atrops, H. Kalali, E. Liebermann, E. Wilhelm, F. Ratkovics, and T. Salamon, *Molecular interactions in mixtures of carboxylic acids with amines. 1. Melting curves and viscosities*. **The Journal of Physical Chemistry**. 85 (1981) 2520-2524.
279. Kohler, F., R. Gopal, G. Goetze, H. Atrops, M. Demeriz, E. Liebermann, E. Wilhelm, F. Ratkovics, and B. Palagyi, *Molecular interactions in mixtures of carboxylic acids with amines. 2. Volumetric, conductimetric, and NMR properties*. **The Journal of Physical Chemistry**. 85 (1981) 2524-2529.
280. Wranglen, G., *An introduction to corrosion and protection of metals*. 1985: Chapman and Hall.
281. Soeda, K. and T. Ichimura, *Present state of corrosion inhibitors in Japan*. **Cement and Concrete Composites**. 25 (2003) 117-122.
282. Sagoe-Crentsil, K., V. Yilmaz, and F.P. Glasser, *Corrosion inhibition of steel in concrete by carboxylic acids*. **Cement and Concrete Research**. 23 (1993) 1380-1388.
283. Gouda, V. and W. Halaka, *Corrosion and corrosion inhibition of reinforcing steel: II. Embedded in concrete*. **British Corrosion Journal**. 5 (1970) 204-208.
284. Andreev, N., E. Starovoitova, and N. Lebedeva, *Steel corrosion inhibition by benzoic acid salts in calcium hydroxide solutions*. **Protection of Metals**. 44 (2008) 688-691.
285. Žerjav, G. and I. Milošev, *Carboxylic acids as corrosion inhibitors for Cu, Zn and brasses in simulated urban rain*. **International Journal of Electrochemical Science**. 9 (2014) 2696-2715.
286. Khaled, K., N. Abdel-Shafi, and N. Al-Mobarak, *Understanding corrosion inhibition of iron by 2-thiophenecarboxylic acid methyl ester: Electrochemical and computational study*. **International Journal of Electrochemical Science**. 7 (2012) 1027-1044.
287. Bouzidi, D., A. Chetouani, B. Hammouti, S. Kertit, M. Taleb, and S. Al-Deyab, *Electrochemical corrosion behaviour of iron rotating disc electrode in physiological medium containing amino acids and amino esters as an inhibitors*. **International Journal of Electrochemical Science**. 7 (2012) 2334-2348.
288. Madram, A.R., F. Shokri, M.R. Sovizi, and H. Kalhor, *Aromatic carboxylic acids as corrosion inhibitors for aluminium in alkaline solution*. **Portugaliae Electrochimica Acta**. 34 (2016) 395-405.
289. Agarwal, P. and D. Landolt, *Effect of anions on the efficiency of aromatic carboxylic acid corrosion inhibitors in near neutral media: Experimental investigation and theoretical modeling*. **Corrosion Science**. 40 (1998) 673-691.

290. Ashassi-Sorkhabi, H. and M. Es'haghi, *Corrosion inhibition of mild steel in acidic media by [BMIm] Br Ionic liquid*. **Materials Chemistry and Physics**. 114 (2009) 267-271.
291. Belfilali, I., A. Chetouani, B. Hammouti, S. Louhibi, A. Aouniti, and S. Al-Deyab, *Quantum chemical study of inhibition of the corrosion of mild steel in 1 M hydrochloric acid solution by newly synthesized benzamide derivatives*. **Research on Chemical Intermediates**. 40 (2014) 1069-1088.
292. Hassan, H.M., A. Eldesoky, R. Younis, and W.A. Zordok, *Density Functional Theory (DFT) Studies on sulfa dimedine azo derivatives as green inhibitors for C-steel in 0.5 MH<sub>3</sub>PO<sub>4</sub> Solutions*. **International Journal**. 2 (2014) 550-568.
293. Manamela, K.M., L.C. Murulana, M.M. Kabanda, and E.E. Ebenso, *Adsorptive and DFT studies of some imidazolium based ionic liquids as corrosion inhibitors for zinc in acidic medium*. **International Journal of Electrochemical Science**. 9 (2014) 3029-3046.
294. Helen, L., A. Rahim, B. Saad, M. Saleh, and P.B. Raja, *Aquilaria crassna leaves extracts-a green corrosion inhibitor for mild steel in 1 M HCl medium*. **Int. J. Electrochem. Sci**. 9 (2014) 830-846.
295. Rajam, K., S. Rajendran, M. Manivannan, and R. Saranya, *Corrosion inhibition by Allium sativum (garlic) extract*. **Journal of chemical, Biological and physical sciences**. 2 (2012) 1223-1233.
296. Zhou, W., R. Apkarian, Z.L. Wang, and D. Joy, *Fundamentals of scanning electron microscopy (SEM)*, in *Scanning microscopy for nanotechnology*. 2006, Springer. p. 1-40.
297. Christensen, B.J., T. Coverdale, R.A. Olson, S.J. Ford, E.J. Garboczi, H.M. Jennings, and T.O. Mason, *Impedance Spectroscopy of Hydrating Cement-Based Materials: Measurement, Interpretation, and Application*. **Journal of the American Ceramic Society**. 77 (1994) 2789-2804.
298. Kelly, R.G., J.R. Scully, D. Shoesmith, and R.G. Buchheit, *The polarization resistance method for determination of instantaneous corrosion rates*, in *Electrochemical Techniques in Corrosion Science and Engineering*. 2002, CRC Press. p. 135-160.
299. Kelly, R.G., J.R. Scully, D. Shoesmith, and R.G. Buchheit, *Electrochemical techniques in corrosion science and engineering*. 2002: CRC Press.
300. Enegele, O., *Ageing of Overhead Conductors*. (2013).



301. Chetouani, A., B. Hammouti, A. Aouniti, N. Benchat, and T. Benhadda, *New synthesised pyridazine derivatives as effective inhibitors for the corrosion of pure iron in HCl medium*. **Progress in Organic Coatings**. 45 (2002) 373-378.
302. Mu, G., X. Li, Q. Qu, and J. Zhou, *Molybdate and tungstate as corrosion inhibitors for cold rolling steel in hydrochloric acid solution*. **Corrosion Science**. 48 (2006) 445-459.
303. Popova, A., E. Sokolova, S. Raicheva, and M. Christov, *AC and DC study of the temperature effect on mild steel corrosion in acid media in the presence of benzimidazole derivatives*. **Corrosion Science**. 45 (2003) 33-58.
304. Prabhu, R., A. Shanbhag, and T. Venkatesha, *Influence of tramadol [2-[(dimethylamino) methyl]-1-(3-methoxyphenyl) cyclohexanol hydrate] on corrosion inhibition of mild steel in acidic media*. **Journal of Applied Electrochemistry**. 37 (2007) 491-497.
305. Umoren, S. and I. Obot, *Polyvinylpyrrolidone and polyacrylamide as corrosion inhibitors for mild steel in acidic medium*. **Surface Review and Letters**. 15 (2008) 277-286.
306. Obot, I., N. Obi-Egbedi, and S. Umoren, *The synergistic inhibitive effect and some quantum chemical parameters of 2,3-diaminonaphthalene and iodide ions on the hydrochloric acid corrosion of aluminium*. **Corrosion Science**. 51 (2009) 276-282.
307. Solomon, M., S. Umoren, I. Udosoro, and A. Udoh, *Inhibitive and adsorption behaviour of carboxymethyl cellulose on mild steel corrosion in sulphuric acid solution*. **Corrosion Science**. 52 (2010) 1317-1325.
308. Poornima, T., J. Nayak, and A. Shetty, *Corrosion inhibition of the annealed 18 Ni 250 grade maraging steel in 0.67 M phosphoric acid by 3,4-dimethoxybenzaldehydethiosemicarbazone*. **Chemical Sciences Journal**. (2012).
309. Umoren, S., M. Solomon, I. Udosoro, and A. Udoh, *Synergistic and antagonistic effects between halide ions and carboxymethyl cellulose for the corrosion inhibition of mild steel in sulphuric acid solution*. **Cellulose**. 17 (2010) 635-648.
310. Korde, R., C.B. Verma, E. Ebenso, and M. Quraishi, *Electrochemical and Thermo Dynamical Investigation of 5-ethyl 4-(4-methoxyphenyl)-6-methyl-2-thioxo-1,2,3,4-tetrahydropyrimidine-5-carboxylate on corrosion inhibition behavior of aluminium in 1M hydrochloric acid medium*. **International Journal of Electrochemical Science**. 10 (2015) 1081-1093.
311. Yadav, M., S. Kumar, R. Sinha, I. Bahadur, and E. Ebenso, *New pyrimidine derivatives as efficient organic inhibitors on mild steel corrosion in acidic medium:*

- electrochemical, SEM, EDX, AFM and DFT studies. Journal of Molecular Liquids.* 211 (2015) 135-145.
312. Mu, G.N., X. Li, and F. Li, *Synergistic inhibition between o-phenanthroline and chloride ion on cold rolled steel corrosion in phosphoric acid. Materials Chemistry and Physics.* 86 (2004) 59-68.
313. Zarrouk, A., B. Hammouti, T. Lakhliifi, M. Traisnel, H. Vezin, and F. Bentiss, *New 1H-pyrrole-2, 5-dione derivatives as efficient organic inhibitors of carbon steel corrosion in hydrochloric acid medium: electrochemical, XPS and DFT studies. Corrosion Science.* 90 (2015) 572-584.
314. Gomma, G.K. and M.H. Wahdan, *Schiff bases as corrosion inhibitors for aluminium in hydrochloric acid solution. Materials Chemistry and Physics.* 39 (1995) 209-213.
315. Tang, L., X. Li, L. Li, Q. Qu, G. Mu, and G. Liu, *The effect of 1-(2-pyridylazo)-2-naphthol on the corrosion of cold rolled steel in acid media: Part 1: Inhibitive action in 1.0 M hydrochloric acid. Materials Chemistry and Physics.* 94 (2005) 353-359.
316. Ghasemi, O., I. Danaee, G. Rashed, M. RashvandAvei, and M. Maddahy, *Inhibition effect of a synthesized N, N'-bis (2-hydroxybenzaldehyde)-1, 3-propandiimine on corrosion of mild steel in HCl. Journal of Central South University.* 20 (2013) 301-311.
317. Musa, A.Y., A.A.H. Kadhum, A.B. Mohamad, A.R. Daud, M.S. Takriff, S.K. Kamarudin, and N. Muhamad, *Stability of layer forming for corrosion inhibitor on mild steel surface under hydrodynamic conditions. International Journal of Electrochemical Science.* 4 (2009) 707-716.
318. Popova, A., M. Christov, and A. Vasilev, *Mono-and dicationic benzothiazolic quaternary ammonium bromides as mild steel corrosion inhibitors. Part III: influence of the temperature on the inhibition process. Corrosion Science.* 94 (2015) 70-78.
319. Morad, M. and A.K. El-Dean, *2,2'-Dithiobis (3-cyano-4,6-dimethylpyridine): A new class of acid corrosion inhibitors for mild steel. Corrosion Science.* 48 (2006) 3398-3412.
320. Qu, Q., Z. Hao, L. Li, W. Bai, Y. Liu, and Z. Ding, *Synthesis and evaluation of Tris-hydroxymethyl-(2-hydroxybenzylidenamino)-methane as a corrosion inhibitor for cold rolled steel in hydrochloric acid. Corrosion Science.* 51 (2009) 569-574.
321. Hegazy, M., H. Ahmed, and A. El-Tabei, *Investigation of the inhibitive effect of p-substituted 4-(N, N, N-dimethyldodecylammonium bromide) benzylidene-benzene-2-yl-*

- amine on corrosion of carbon steel pipelines in acidic medium. Corrosion Science.* 53 (2011) 671-678.
322. Kern, P. and D. Landolt, *Adsorption of an organic corrosion inhibitor on iron and gold studied with a rotating EQCM. Journal of the Electrochemical Society.* 148 (2001) B228-B235.
323. Sastri, V.S., *Corrosion inhibitors. Principles and applications.* 1998: John Wiley & Sons
324. El-Awady, A., B. Abd-El-Nabey, and S. Aziz, *Kinetic-thermodynamic and adsorption isotherms analyses for the inhibition of the acid corrosion of steel by cyclic and open-chain amines. Journal of the Electrochemical Society.* 139 (1992) 2149-2154.
325. Obot, I., N. Obi-Egbedi, and S. Umoren, *Adsorption characteristics and corrosion inhibitive properties of clotrimazole for aluminium corrosion in hydrochloric acid. International Journal of Electrochemical Science.* 4 (2009) 863-877.
326. OZA, B. and R. SINHA, *Study of corrosion behaviour of high strength Al-Mg alloy in chloride containing electrolytes. Transactions of the Indian Institute of Metals.* 36 (1983) 216-218.
327. Oguzie, E., B. Okolue, E. Ebenso, G. Onuoha, and A. Onuchukwu, *Evaluation of the inhibitory effect of methylene blue dye on the corrosion of aluminium in hydrochloric acid. Materials Chemistry and Physics.* 87 (2004) 394-401.
328. Thiraviyam, P. and K. Kannan, *Inhibition of aminocyclohexane derivative on mild steel corrosion in 1 N HCl. Arabian Journal for Science and Engineering.* 38 (2013) 1757-1767.
329. Mertens, S., C. Xhoffer, B. De Cooman, and E. Temmerman, *Short-term deterioration of polymer-coated 55% Al-Zn-part 1: behavior of thin polymer films. Corrosion.* 53 (1997) 381-388.
330. Li, X., S. Deng, and H. Fu, *Inhibition of the corrosion of steel in HCl, H<sub>2</sub>SO<sub>4</sub> solutions by bamboo leaf extract. Corrosion Science.* 62 (2012) 163-175.
331. Noor, E.A. and A.H. Al-Moubaraki, *Thermodynamic study of metal corrosion and inhibitor adsorption processes in mild steel/1-methyl-4 [4'(-X)-styryl pyridinium iodides/hydrochloric acid systems. Materials Chemistry and Physics.* 110 (2008) 145-154.
332. Bentiss, F., M. Lagrenee, M. Traisnel, and J. Hornez, *The corrosion inhibition of mild steel in acidic media by a new triazole derivative. Corrosion Science.* 41 (1999) 789-803.

333. Avci, G., *Corrosion inhibition of indole-3-acetic acid on mild steel in 0.5 M HCl. Colloids and Surfaces A: Physicochemical and Engineering Aspects.* 317 (2008) 730-736.
334. Li, X. and G. Mu, *Tween-40 as corrosion inhibitor for cold rolled steel in sulphuric acid: weight loss study, electrochemical characterization, and AFM. Applied Surface Science.* 252 (2005) 1254-1265.
335. Li, X., S. Deng, and H. Fu, *Adsorption and inhibition effect of vanillin on cold rolled steel in 3.0 M H<sub>3</sub>PO<sub>4</sub>. Progress in Organic Coatings.* 67 (2010) 420-426.
336. Mu, G., X. Li, and G. Liu, *Synergistic inhibition between tween 60 and NaCl on the corrosion of cold rolled steel in 0.5 M sulfuric acid. Corrosion Science.* 47 (2005) 1932-1952.
337. Naderi, E., A. Jafari, M. Ehteshamzadeh, and M. Hosseini, *Effect of carbon steel microstructures and molecular structure of two new Schiff base compounds on inhibition performance in 1 M HCl solution by EIS. Materials Chemistry and Physics.* 115 (2009) 852-858.
338. Khadiri, A., A. Ousslim, K. Bekkouche, A. Aouniti, A. Elidrissi, and B. Hammouti, *Inhibition Effects on the Corrosion of Mild Steel in 1 M HCl by 1,1'-(2,2'-(2,2'-oxybis (ethane-2,1-diyl) bis (sulfanediyl)) bis (ethane-2,1-diyl)) diazepam-2-one. Portugaliae Electrochimica Acta.* 32 (2014) 35-50.
339. Renita, D., T. Sanish, Dwivedi, and C. Amit, *Green Approach to Corrosion Inhibition by Emblica Officinalis (NA-7) Leaves Extract. International Journal of Nano Corrosion Science Engineering.* 2 (2015) 29-45.
340. Abu-Dalo, M.A., N.A. Al-Rawashdeh, and A. Ababneh, *Evaluating the performance of sulfonated Kraft lignin agent as corrosion inhibitor for iron-based materials in water distribution systems. Desalination.* 313 (2013) 105-114.
341. Mashuga, M., L. Olasunkanmi, A. Adekunle, S. Yesudass, M. Kabanda, and E. Ebenso, *Adsorption, thermodynamic and quantum chemical studies of 1-hexyl-3-methylimidazolium based ionic liquids as corrosion inhibitors for mild steel in HCl. Materials.* 8 (2015) 3607-3632.
342. Ahamad, I., R. Prasad, and M. Quraishi, *Thermodynamic, electrochemical and quantum chemical investigation of some Schiff bases as corrosion inhibitors for mild steel in hydrochloric acid solutions. Corrosion Science.* 52 (2010) 933-942.
343. Tourabi, M., K. Nohair, M. Traisnel, C. Jama, and F. Bentiss, *Electrochemical and XPS studies of the corrosion inhibition of carbon steel in hydrochloric acid pickling*

- solutions by 3,5-bis (2-thienylmethyl)-4-amino-1,2,4-triazole. Corrosion Science. 75 (2013) 123-133.*
344. Thanapackiam, P., S. Rameshkumar, S. Subramanian, and K. Mallaiya, *Electrochemical evaluation of inhibition efficiency of ciprofloxacin on the corrosion of copper in acid media. Materials Chemistry and Physics. 174 (2016) 129-137.*
345. El-Deeb, M., S. Sayyah, S.A. El-Rehim, and S. Mohamed, *Corrosion inhibition of aluminum with a series of aniline monomeric surfactants and their analog polymers in 0.5 M HCl solution: Part II: 3-(12-sodiumsulfonate dodecyloxy) aniline and its analog polymer. Arabian Journal of Chemistry. 8 (2015) 527-537.*
346. Abdel-Rehim, S., K. Khaled, and N. Al-Mobarak, *Corrosion inhibition of iron in hydrochloric acid using pyrazole. Arabian Journal of Chemistry. 4 (2011) 333-337.*
347. Macdonald, J.R., *Impedance spectroscopy. Annals of Biomedical Engineering. 20 (1992) 289-305.*
348. Jacob, K.S. and G. Parameswaran, *Corrosion inhibition of mild steel in hydrochloric acid solution by Schiff base furoin thiosemicarbazone. Corrosion Science. 52 (2010) 224-228.*
349. Ehsani, A., M. Nasrollahzadeh, M.G. Mahjani, R. Moshrefi, and H. Mostanzadeh, *Electrochemical and quantum chemical investigation of inhibitory of 1, 4-Ph (OX) 2 (Ts) 2 on corrosion of 1005 aluminum alloy in acidic medium. Journal of Industrial and Engineering Chemistry. 20 (2014) 4363-4370.*
350. Ehsani, A., M. Ghasem Mahjani, M. Nasser, and M. Jafarian, *Influence of electrosynthesis conditions and Al<sub>2</sub>O<sub>3</sub> nanoparticles on corrosion protection effect of polypyrrole films. Anti-Corrosion Methods And Materials. 61 (2014) 146-152.*
351. Yadav, D.K., M. Quraishi, and B. Maiti, *Inhibition effect of some benzylidenes on mild steel in 1 M HCl: an experimental and theoretical correlation. Corrosion Science. 55 (2012) 254-266.*
352. Yadav, M., D. Behera, S. Kumar, and R.R. Sinha, *Experimental and quantum chemical studies on the corrosion inhibition performance of benzimidazole derivatives for mild steel in HCl. Industrial & Engineering Chemistry Research. 52 (2013) 6318-6328.*
353. Hassan, M., H. Barker, and S. Collie, *Enhanced corrosion inhibition of mild steel by cross-linked lanolin-coatings. Progress in Organic Coatings. 78 (2015) 249-255.*
354. Loveday, D., P. Peterson, and B. Rodgers, *Evaluation of organic coatings with electrochemical impedance spectroscopy. Part 3: Protocols for testing coatings with EIS. JCT Coatingstech. 2 (2005) 22-27.*

355. Krishnegowda, P.M., V.T. Venkatesha, P.K.M. Krishnegowda, and S.B. Shivayogiraju, *Acalypha torta leaf extract as green corrosion inhibitor for mild steel in hydrochloric acid solution*. **Industrial & Engineering Chemistry Research**. 52 (2013) 722-728.
356. Pavithra, M., T. Venkatesha, K. Vathsala, and K. Nayana, *Synergistic effect of halide ions on improving corrosion inhibition behaviour of benzisothiazole-3-piperazine hydrochloride on mild steel in 0.5 M H<sub>2</sub>SO<sub>4</sub> medium*. **Corrosion Science**. 52 (2010) 3811-3819.
357. Stupnisek-Lisac, E., A. Brnada, and A.D. Mance, *Secondary amines as copper corrosion inhibitors in acid media*. **Corrosion Science**. 42 (2000) 243-257.
358. Loto, R.T., *Corrosion inhibition effect of non-toxic  $\alpha$ -amino acid compound on high carbon steel in low molar concentration of hydrochloric acid*. **Journal of Materials Research and Technology**. (2017).
359. Amin, M.A., S.S.A. El-Rehim, E. El-Sherbini, and R.S. Bayoumi, *The inhibition of low carbon steel corrosion in hydrochloric acid solutions by succinic acid: Part I. Weight loss, polarization, EIS, PZC, EDX and SEM studies*. **Electrochimica Acta**. 52 (2007) 3588-3600.
360. Yadav, D.K., B. Maiti, and M. Quraishi, *Electrochemical and quantum chemical studies of 3, 4-dihydropyrimidin-2 (1H)-ones as corrosion inhibitors for mild steel in hydrochloric acid solution*. **Corrosion Science**. 52 (2010) 3586-3598.
361. Ezeoke, A.U., O.G. Adeyemi, O.A. Akerele, and N.O. Obi-Egbedi, *Computational and experimental studies of 4-aminoantipyrine as corrosion inhibitor for mild steel in sulphuric acid solution*. **International Journal of Electrochemical Science**. 7 (2012) 534-553.
362. Abood, H.A., *The study of the inhibitory properties of Omeprazole on the corrosion of Aluminum 6063 in alkaline media*. **Basrah Journal of Science**. 29 (2011) 74-93.
363. Chaubey, N., Savita, V.K. Singh, and M. Quraishi, *Corrosion inhibition performance of different bark extracts on aluminium in alkaline solution*. **Journal of the Association of Arab Universities for Basic and Applied Sciences**. 22 (2017) 38-44.
364. Santhini, N. and T. Jeyaraj, *The inhibition effect of [3-(4-hydroxy-3-methoxy-phenyl)-1-phenyl-propenone] on the corrosion of the aluminium in alkaline medium*. **Journal of Chemical and Pharmaceutical Research**. 4 (2012) 3550-3556.
365. Ebenso, E., H. Alemu, S. Umoren, and I. Obot, *Inhibition of mild steel corrosion in sulphuric acid using alizarin yellow GG dye and synergistic iodide additive*. **International Journal of Electrochemical Science**. 3 (2008) 1325-1339.

366. Obot, I. and N. Obi-Egbedi, *Fluconazole as an inhibitor for aluminium corrosion in 0.1 M HCl*. **Colloids and Surfaces A: Physicochemical and Engineering Aspects**. 330 (2008) 207-212.
367. Negm, N.A. and M.F. Zaki, *Corrosion inhibition efficiency of nonionic Schiff base amphiphiles of p-aminobenzoic acid for aluminum in 4N HCL*. **Colloids and Surfaces A: Physicochemical and Engineering Aspects**. 322 (2008) 97-102.
368. Zhang, D.-Q., Q.-R. Cai, X.-M. He, L.-X. Gao, and G.-D. Zhou, *Inhibition effect of some amino acids on copper corrosion in HCl solution*. **Materials Chemistry and Physics**. 112 (2008) 353-358.
369. Finšgar, M., A. Lesar, A. Kokalj, and I. Milošev, *A comparative electrochemical and quantum chemical calculation study of BTAH and BTAOH as copper corrosion inhibitors in near neutral chloride solution*. **Electrochimica Acta**. 53 (2008) 8287-8297.
370. Fekry, A. and R.R. Mohamed, *Acetyl thiourea chitosan as an eco-friendly inhibitor for mild steel in sulphuric acid medium*. **Electrochimica Acta**. 55 (2010) 1933-1939.
371. Popova, A., *Temperature effect on mild steel corrosion in acid media in presence of azoles*. **Corrosion Science**. 49 (2007) 2144-2158.
372. El-Rehim, S.A., S. Refaey, F. Taha, M. Saleh, and R. Ahmed, *Corrosion inhibition of mild steel in acidic medium using 2-amino thiophenol and 2-cyanomethyl benzothiazole*. **Journal of Applied Electrochemistry**. 31 (2001) 429-435.
373. Tang, L., X. Li, Y. Si, G. Mu, and G. Liu, *The synergistic inhibition between 8-hydroxyquinoline and chloride ion for the corrosion of cold rolled steel in 0.5 M sulfuric acid*. **Materials Chemistry and Physics**. 95 (2006) 29-38.
374. Maayta, A. and N. Al-Rawashdeh, *Inhibition of acidic corrosion of pure aluminum by some organic compounds*. **Corrosion Science**. 46 (2004) 1129-1140.
375. Cheng, S., S. Chen, T. Liu, X. Chang, and Y. Yin, *Carboxymethylchitosan as an ecofriendly inhibitor for mild steel in 1 M HCl*. **Materials Letters**. 61 (2007) 3276-3280.
376. Ghali, E., V.S. Sastri, and M. Elboudjaini, *Corrosion prevention and protection: practical solutions*. 2007: John Wiley & Sons.
377. El-Etre, A., M. Abdallah, and Z. El-Tantawy, *Corrosion inhibition of some metals using lawsonia extract*. **Corrosion Science**. 47 (2005) 385-395.
378. Langmuir, I., *The constitution and fundamental properties of solids and liquids. Part I. Solids*. **Journal of the American Chemical Society**. 38 (1916) 2221-2295.

379. Liu, L., X.-B. Luo, L. Ding, and S.-L. Luo, *Application of nanotechnology in the removal of heavy metal from water*. Nanomaterials for the Removal of Pollutants and Resource Reutilization. 2019: Elsevier. 83-147.
380. Shaban, S.M., I. Aiad, M.M. El-Sukkary, E. Soliman, and M.Y. El-Awady, *Inhibition of mild steel corrosion in acidic medium by vanillin cationic surfactants*. **Journal of Molecular Liquids**. 203 (2015) 20-28.
381. Villamil, R.F., P. Corio, S.M. Agostinho, and J.C. Rubim, *Effect of sodium dodecylsulfate on copper corrosion in sulfuric acid media in the absence and presence of benzotriazole*. **Journal of Electroanalytical Chemistry**. 472 (1999) 112-119.
382. Emregül, K.C. and M. Hayvali, *Studies on the effect of a newly synthesized Schiff base compound from phenazone and vanillin on the corrosion of steel in 2 M HCl*. **Corrosion Science**. 48 (2006) 797-812.
383. Ituen, E. and U. Udo, *Phytochemical profile, adsorptive and inhibitive behaviour of Costus afer extracts on aluminium corrosion in hydrochloric acid*. **Der Chemica Sinica**. 3 (2012) 1394-1405.
384. Mahdavian, M. and M. Attar, *Electrochemical behaviour of some transition metal acetylacetonate complexes as corrosion inhibitors for mild steel*. **Corrosion Science**. 51 (2009) 409-414.
385. Oguzie, E., S. Wang, Y. Li, and F.H. Wang, *Corrosion and corrosion inhibition characteristics of bulk nanocrystalline ingot iron in sulphuric acid*. **Journal of Solid State Electrochemistry**. 12 (2008) 721-728.
386. Potdar, H., K.-W. Jun, J.W. Bae, S.-M. Kim, and Y.-J. Lee, *Synthesis of nano-sized porous  $\gamma$ -alumina powder via a precipitation/digestion route*. **Applied Catalysis A: General**. 321 (2007) 109-116.
387. Musa, A.Y., A.A.H. Kadhum, A.B. Mohamad, and M.S. Takriff, *Experimental and theoretical study on the inhibition performance of triazole compounds for mild steel corrosion*. **Corrosion Science**. 52 (2010) 3331-3340.
388. Li, L., X. Zhang, J. Lei, J. He, S. Zhang, and F. Pan, *Adsorption and corrosion inhibition of Osmanthus fragran leaves extract on carbon steel*. **Corrosion Science**. 63 (2012) 82-90.
389. Abouchane, M., M. El Bakri, R. Touir, A. Rochdi, O. Elkhatabi, M.E. Touhami, I. Forssal, and B. Mernari, *Corrosion inhibition and adsorption behavior of triazoles derivatives on mild steel in 1 M  $H_3PO_4$  and synergistic effect of iodide ions*. **Research on Chemical Intermediates**. 41 (2015) 1907-1923.



390. Yadav, M., S. Kumar, N. Kumari, I. Bahadur, and E.E. Ebenso, *Experimental and theoretical studies on corrosion inhibition effect of synthesized benzothiazole derivatives on mild steel in 15% HCl solution*. **International Journal of Electrochemical Science**. 10 (2015) 602-624.
391. Khaled, K., *New synthesized guanidine derivative as a green corrosion inhibitor for mild steel in acidic solutions*. **International Journal of Electrochemical Science**. 3 (2008) 462-475.
392. Frers, S., M. Stefenel, C. Mayer, and T. Chierchie, *AC-Impedance measurements on aluminium in chloride containing solutions and below the pitting potential*. **Journal of Applied Electrochemistry**. 20 (1990) 996-999.
393. Cinderey, R. and G. Burstein, *The repassivation potential of aluminium in water*. **Corrosion Science**. 33 (1992) 499-502.
394. Ladha, D., P. Wadhvani, S. Kumar, and N. Shah, *Evaluation of corrosion inhibitive properties of trigonellafoenum-graecum for pure aluminium in hydrochloric acid*. **Journal of Materials and Environmental Science**. 6 (2015) 1200-1207.
395. Yurt, A., S. Ulutas, and H. Dal, *Electrochemical and theoretical investigation on the corrosion of aluminium in acidic solution containing some Schiff bases*. **Applied Surface Science**. 253 (2006) 919-925.
396. Ashassi-Sorkhabi, H. and E. Asghari, *Electrochemical corrosion behavior of Al7075 rotating disc electrode in neutral solution containing l-glutamine as a green inhibitor*. **Journal of Applied Electrochemistry**. 40 (2010) 631-637.
397. Khaled, K. and M. Al-Qahtani, *The inhibitive effect of some tetrazole derivatives towards Al corrosion in acid solution: Chemical, electrochemical and theoretical studies*. **Materials Chemistry and Physics**. 113 (2009) 150-158.
398. Gonçalves, R.S., D.S. Azambuja, and A.M.S. Lucho, *Electrochemical studies of propargyl alcohol as corrosion inhibitor for nickel, copper, and copper/nickel (55/45) alloy*. **Corrosion Science**. 44 (2002) 467-479.
399. Tsuru, T., S. Haruyama, and B. Gijutsu, *Corrosion inhibition of iron by amphoteric surfactants in 2 M HCl*. **Japan Society of Corrosion Engineering**. 27 (1978) 573-581.
400. Ogundele, G. and W. White, *Some observations on corrosion of carbon steel in aqueous environments containing carbon dioxide*. **Corrosion**. 42 (1986) 71-78.
401. Curkovic, H.O., E. Stupnisek-Lisac, and H. Takenouti, *The influence of pH value on the efficiency of imidazole based corrosion inhibitors of copper*. **Corrosion Science**. 52 (2010) 398-405.

402. Schweinsberg, D.P., G.A. George, A.K. Nanayakkara, and D.A. Steinert, *The protective action of epoxy resins and curing agents-inhibitive effects on the aqueous acid corrosion of iron and steel*. **Corrosion Science**. 28 (1988) 33-42.
403. Desai, M., *Corrosion Inhibitors for Aluminium Alloys*. **Materials and Corrosion**. 23 (1972) 475-482.